ISSN: 2153-1196 Volume 10, Number 3, March 2019

Scientific Research Publishing

Journal of Modern Physics

Special Issue on Astrophysics, Cosmology and Gravitation

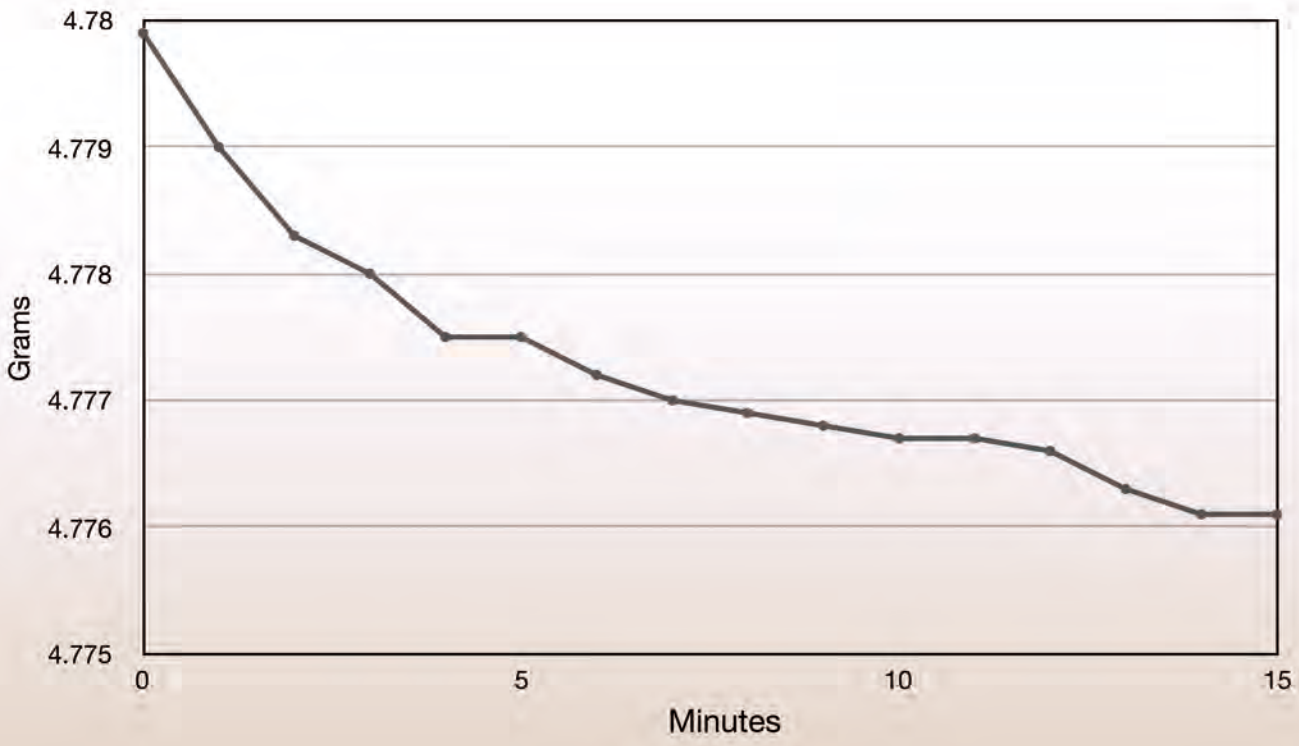

ISSN: 2153-1196
9 772153 119007 03

www.scirp.org/journal/jmp

Journal Editorial Board

ISSN: 2153-1196 (Print) ISSN: 2153-120X (Online)
http://www.scirp.org/journal/jmp

Editor-in-Chief

Editorial Board

Journal of Modern Physics, 2019, 10, 195-421
http://www.scirp.org/journal/jmp
ISSN Online: 2153-120X
ISSN Print: 2153-1196

Table of Contents

Volume 10 Number 3 March 2019

Journal of Modern Physics, 2019, 10, 195-421
http://www.scirp.org/journal/jmp
ISSN Online: 2153-120X
ISSN Print: 2153-1196

The figure on the front cover is from the article published in Journal of Modern Physics, 2019, Vol. 10, No. 3, pp. 195-213 by W. John Martin.

Journal of Modern Physics (JMP)
Journal Information

SUBSCRIPTIONS

The *Journal of Modern Physics* (Online at Scientific Research Publishing, www.SciRP.org) is published monthly by Scientific Research Publishing, Inc., USA.

Subscription rates:
Print: $89 per issue.
To subscribe, please contact Journals Subscriptions Department, E-mail: sub@scirp.org

SERVICES

Advertisements
Advertisement Sales Department, E-mail: service@scirp.org

Reprints (minimum quantity 100 copies)
Reprints Co-ordinator, Scientific Research Publishing, Inc., USA.
E-mail: sub@scirp.org

COPYRIGHT

PRODUCTION INFORMATION

For manuscripts that have been accepted for publication, please contact:
E-mail: jmp@scirp.org

Journal of Modern Physics, 2019, 10, 195-213
http://www.scirp.org/journal/jmp
ISSN Online: 2153-120X
ISSN Print: 2153-1196

Electromagnetic Radiation Causes Weight Loss and Weight Destabilization of Objects with Presumed Elevated Levels of KELEA (Kinetic Energy Limiting Electrostatic Attraction), Relevance to Human Health and to Global Warming

W. John Martin

Institute of Progressive Medicine, South Pasadena CA, USA
Email: wjohnmartin@ccid.org

How to cite this paper: Martin, W.J. (2019) Electromagnetic Radiation Causes Weight Loss and Weight Destabilization of Objects with Presumed Elevated Levels of KELEA (Kinetic Energy Limiting Electrostatic Attraction), Relevance to Human Health and to Global Warming. *Journal of Modern Physics*, **10**, 195-213.
https://doi.org/10.4236/jmp.2019.103015

Received: February 1, 2019
Accepted: February 25, 2019
Published: February 28, 2019

Abstract

A natural force has been proposed, which is required to prevent the fusion and disappearance of the discrete electrical charges that are present on electrostatically attached opposing electrical charges. This force may also explain the repulsion between objects with either matching positive or negative electrical charges. The energy of this force is referred to as KELEA (kinetic energy limiting electrostatic attraction). KELEA is especially attracted to dipolar compounds and to other materials with spatially separated opposite electrical charges. These compounds can be used to increase the level of KELEA in water. KELEA activated water can become an added source of KELEA for objects that are placed in close proximity to the water. It is generally held that the weight of an object is solely determined by its mass in relation to that of the earth. Yet, it was previously reported that the measured weight of certain KELEA attracting objects can undergo considerable variability over time. This observation is consistent with the concept that KELEA can contribute to the measured weight of certain objects. The present study strengthens this concept by demonstrating that the weight of cellulose containing materials, including paper, cotton fabrics, and wood, is increased if the materials are placed close to containers of KELEA activated water. It is further shown that electromagnetic radiation can significantly reduce the added weight of the KELEA exposed cellulose containing materials. Moreover, the previously added weight of the materials can be regained by replacing the materials back

into the KELEA enhanced environment. It is proposed that the electrical charges that accompany electromagnetic radiation are able to competitively withdraw some of the KELEA from certain KELEA-enhanced objects. This effect can be reliably demonstrated using single sheets of writing paper, which are primarily composed of mechanically-bonded, branched cellulose fibers. There can be considerable fluctuations of the weight of the materials exposed to electromagnetic radiation after having been placed nearby to KELEA activated water. The weight instability is interpreted as being due to the electromagnetic radiation also triggering a dynamic process of rapid additions and removals of significant quantities of KELEA to and from objects. These observations are relevant to the further understanding of KELEA and to the potential health and climate consequences of manmade electromagnetic radiation causing a reduction in the environmental levels of KELEA.

Keywords

KELEA, Alternative Cellular Energy, Paper, Cotton, Wood, Cellulose, Activated Water, Weight, Gravity, Weather, Global Warming, Clouds, Electrostatic, Electromagnetic Radiation, Radio Waves, Microwaves, Cosmic Waves, Inkjet Printing, Electropollution

1. Introduction

As previously reported, there can be fluctuations in the measured weights of certain objects when the objects are repeatedly weighed over a period of several days [1]. It was proposed that the increases in weight were due to the involvement of a natural force termed KELEA (kinetic energy limiting electrostatic attraction). The primary function of KELEA is presumably to prevent electrostatically attracted opposite electrical charges from being eliminated by fusion with one another [2] [3].

Dipolar compounds with separated electrical charges are able to attract KELEA from the environment [4]. Certain of these compounds can transfer some of the attracted KELEA to nearby fluids, including water; possibly in an oscillatory manner. When absorbed into fluids, KELEA can lead to a loosening of the intermolecular hydrogen bonding, with a lowering of surface tension and an increase in volatility [5]. The increased volatility of KELEA activated water can be measured as a faster loss of weight of the activated water when compared with control water, when the water samples are placed into caped, but not completely sealed, containers [4].

Similar to KELEA attracting and releasing dipolar compounds, KELEA activated water can lead to the increased volatility of added regular water [6]. It can also activate regular water, which is positioned nearby to KELEA activated water [7] [8]. Presumably, the loosened hydrogen bonding in the KELEA activated water adds to the level of electrical charges on the water molecules. This would result in a greater attraction of KELEA from the environment. Again, possibly in

an oscillatory manner, much of the additionally attracted KELEA could be radiated from the activated water. KELEA activated water can, thereby, establish a heightened KELEA enriched environment.

Approximately two gallons of KELEA activated water in numerous 2 oz bottles and in several larger containers are routinely stored in the same room as an electronic balance. Various items were selected to be placed near the containers of KELEA activated water to see if their weight would show a discernable increase. Individual sheets of typing paper were among the items tested. The initial reasoning for using typing paper was to see if inkjet-printing of multiple lines of text onto the paper would create linear arrays of negatively charged ink against a background of essentially neutral or induced slightly positively charged blank regions of the paper [9]. The multiple charges on the printed sheets of paper could potentially attract KELEA onto the paper and this would be seen as an increase in the weight of paper from being placed in the KELEA-enriched environment. This predicted increase in the weight of printed sheets of paper was confirmed, but this was also shown, to a somewhat lesser extent, for blank sheets of paper on which there was no printed text. More surprising was the relatively rapid decreasing of the weight of the KELEA exposed paper during the time it was being weighed in an electronic balance. Similar measurable weight gains from a KELEA enriched environment and the subsequent weight losses when placed onto the balance were made with both printed and non-printed cotton fabrics and with unprocessed wood. The tentative interpretation of the findings is that KELEA activated water can transfer KELEA to cellulose containing and certain other materials and that electromagnetic radiation emitted by the electronic balance is able to remove the added KELEA from these materials. This article outlines the experiments leading to this interpretation. The article also discusses some of the likely health and climate related implications of the findings.

2. Materials and Methods

KELEA-enriched environment. Water is routinely being activated by the addition of small amounts of various dipolar compounds, followed by several 10-fold dilutions and filtration through a zero-residue filter. Occasionally other procedures are used such as electrolysis of copper and silver in a potassium citrate solution. About two gallons of KELEA activated water are routinely stored in the same room that has the electronic balance. Bringing regular distilled water into the room will lead to the water becoming activated, as shown by its increased volatility and the linear dissolving pattern and surface breaking ability of sprinkled particles of neutral red dye [4]. The volatility of water is also assessed by the rate of weight loss in closed but not completely sealed containers [4].

Weighing. A Sartorius electronic balance (Type 1702) is located in the same room as the stored KELEA activated water. The balance is used to obtain weight measurements up to 200 grams with a sensitivity level of 0.1 milligram. The balance was originally purchased from Brinkman Instruments, New York. In some

studies, a non-electronic beam balance (OHAUS Dial-O-Gram 310 gm weight) was used.

Weight-standards. Salter Brass Weights Set (Imperial) Model 063, Salter Hardwares Ltd., Tonbridge Kent UK, was used to confirm the accuracy and stability of routine weighing measurements using the electronic balance. The weight standards used to confirm the accuracy of the balance were 0.25, 0.5, 1 and 2 oz.

Paper. Individual sheets of regular 8" × 11" white paper (Basis weight of 20 lb) were used in most experiments. The sheet of paper was either repeatedly folded into approximately 2" × 2" size or rolled into a cylinder shape. The folded or rolled paper was held in place using either a staple or more commonly a small strip of adhesive tape. The sheets of paper were either left blank (unprinted) or printed with various texts prior to being tested. An Epson XP-820 Inkjet printer was programmed from a computer running Microsoft Word software. To maximize the amount of printing, 5 point, Times New Roman font style, was employed with printing on both sides of the page with minimal margins. The printed pages were allowed to dry for several hours before being tested.

Cotton fabric. Several yards of different colored cotton material were purchased from a local fabric store. The cotton materials were cut into rectangular shapes, the edges of which could be placed within the margins of an "8 × 11" sheet of paper. For printing, the edges of the cotton were adhered to the paper using transparent tape. The paper sheet could then be fed into the printer so that the printing occurred onto the cotton material. The cotton material could then be turned over to achieve double-sided printing. Several tee shirts with either an adhesive applied image or direct to garment (DTG) printed image were obtained from a local thrift store. The area with the image was cut from the tee shirt and compared with a similar sized non-printed area from the same tee shirt. The printed and unprinted cotton materials were either folded into square to rectangular shapes or measured after being added to a plastic cup, whose weight could be tarred if necessary or simply subtracted from the total weight.

Wood. Store purchased smokehouse wood chips of several individual varieties of wood including cherry, hickory, pecan, oak, apple, etc., were purchased from a local store. Either individual chips or a grouping of several pieces of wood were tested.

Radio. A Nicetex Electronics Ltd., Model NE-368-R, radio with two 5 1/2 square side speakers was used. The radio is powered by 12 Watts delivered from a 120-volt, 60 Hz household electrical supply. It was manufactured at HiTech Industrial Park, Hong Kong.

Electromagnetic Field (EMF) Detector, An EMF Detector App was downloaded onto an Apple iphone-6 from the Apple Store. The seller of the App is Ngoc Que Nguyen. EMF values are measured in microTeslars (μT).

Photos and videos were obtained using a hand-held iphone-6 or either a Sony or a Cannon camera mounted onto a tripod. The images were captured onto a

128 gigabyte Scandisk. In some experiments, a digital timer was placed near the weight display panel of the balance so that photos and videos could be taken of both the displayed weight of the balance and the elapsed time.

3. Results

After some initial minor fluctuations, the digital displays of the weight of most items placed onto the weighing pan of the electronic balance become stable. The reaching of a stable weight generally occurs within 10 seconds. The displayed digital reading is then followed by the letter "g" for grams. Unless there are undue movements within the room, the displayed weight of the item will not generally vary by more than ± 0.2 mg over a 30 minutes period. Moreover, the measurements are consistent upon reweighing the same object and are not affected by leaving the object in the weighing room. This is noted because the weighing room is where approximately two gallons of KELEA activated water in multiple 2 oz bottles and in several larger containers are regularly stored. The multiple samples of water had previously been tested for increased volatility based on the measured reductions in weight.

The weighing results obtained using single sheets of regular typing paper were quite different. Rolled or folded paper brought directly into the weighing room and placed onto the balance would regularly show more minor fluctuations than did most other objects. This occurred with paper that had either been printed with text or left blank. The results over the first 40 minutes of such an experiment are shown in Figure 1. The beginning weight of the rolled blank sheet of paper was 4.7752 gm. At 40 minutes the weight was 4.7751 gm. The maximum and minimum recorded weights over the 40-minute period were 4.7764 gm and 4.7748 gm, respectively. The variability in weight, therefore, amounted to 0.0016 gm (1.6 mg). The sheet of paper was left on the balance for an additional 35 minutes for a total time of 75 minutes. There was some continuing minor variability as subsequently recorded in 5-minute intervals, but at 50, 60 minutes and 75

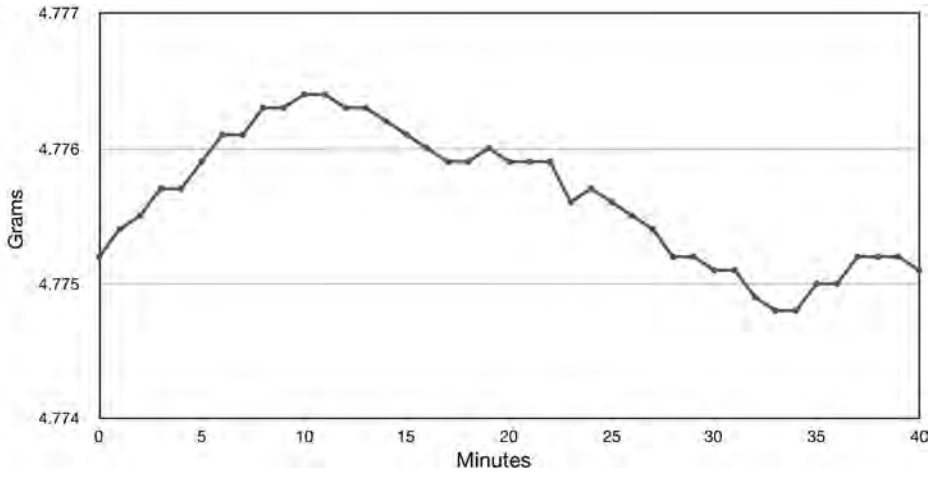

Figure 1. Minor variability over a 40-minute period in the weight of a Non-KELEA exposed sheet of paper.

minutes, the weight was the same as the initial weight (4.7752 gm). The rolled sheet of paper was removed from the balance at 75 minutes.

It was noted that the reweighing individual rolled or folded sheets of paper after they had been left in the weighing room, would yield values higher than were initially recorded. This observation was consistent with the paper being able to obtain additional KELEA from the KELEA activated water being stored in the room. The increase in weight occurred regardless of whether the paper was printed or blank. For example, the same sheet of paper on which the weight measurements are recorded in Figure 1 was removed from the balance after the 75-minute period of weighing. It was then placed near to the containers of KELEA activated water for 30 minutes before being reweighed. As noted above, the final reading before removing the paper from the balance was 4.7752 gm. During the 30-minute period near the KELEA activated water, the weight of the sheet of rolled paper had increased by 4.7 mg to 4.7799 gm.

Leaving this sheet of paper on the electronic balance during the reweighing process led to a progressive reduction of the weight back to the value at which it was initially weighed. The loss of weight over the first 15 minutes of the reweighing process is depicted in Figure 2. During this 15-minute period, the weight of the paper had dropped by 3.8 mg from 4.7799 gm to 4.7761 gm. The weight continued to slowly fall during the next 15 minutes at which time the weight was 4.7756 gm, nearly the same as when it was initially weighed (4.7752 gm).

Similar findings have been repeatedly obtained with either rolled or folded single sheets of typing paper. Figure 3 shows the marked reduction in weight over a 20-minute period of a rolled printed sheet of paper that was weighed after it had been left overnight in the weighing room. The weight had dropped from 4.6819 gm to 4.6703 gm, a difference of 11.6 mg. Some of the recorded weights of this sheet of paper at later time points in this experiment are included in the

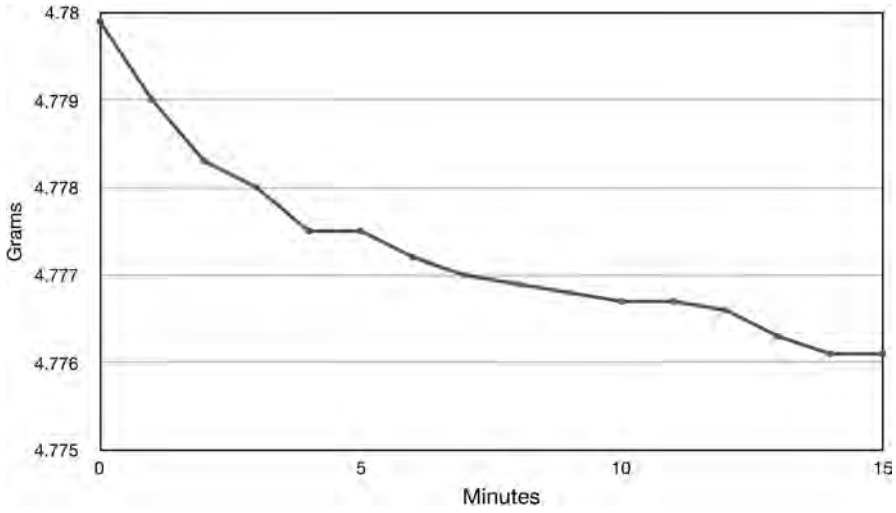

Figure 2. Weight loss during the weighing of paper that had been earlier exposed to containers of KELEA activated water.

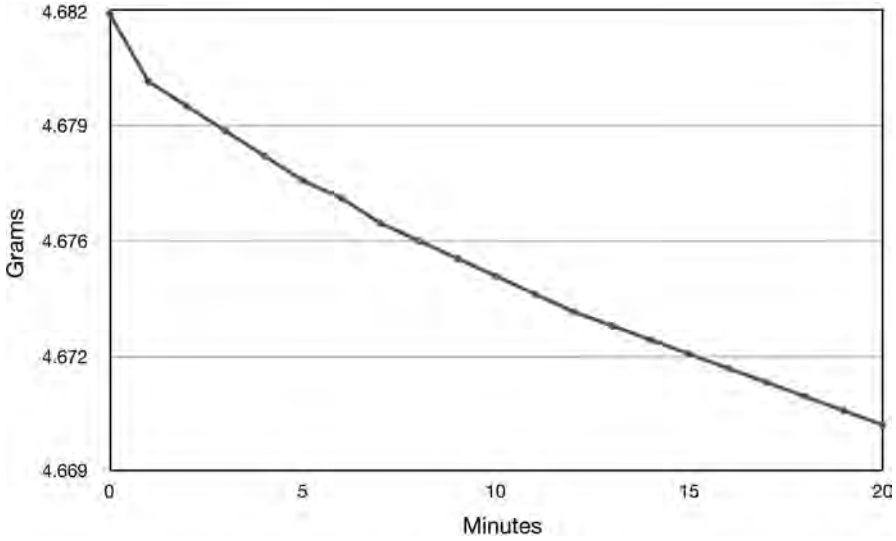

The weight was recorded at various time intervals thereafter. The weights recorded as 40, 50, 60, 90 and 100 minutes on the balance were 4.6634, 4.6611, 4.6591, 4.6586 and 4.6561 grams respectively. Later after the balance had been turned off and the paper sheet left in the weighing room, its weight increased to 4.6685 gm.

Figure 3. Weight loss during the weighing of a KELEA exposed sheet of paper.

Legend to **Figure 3**. Overall, there was a reduction of 25.8 mg from 4.6819 gm to 4.6561 gm. The sheet of paper rapidly regained some of the lost weight by being placed near to the containers of KELEA activated water. In other experiments, it was clear that the gain in weight of the paper would not occur if the paper was taken from the balance and placed in a different room. On the other hand, a sheet of paper that had shown an increase in weight from being left near the containers of KELEA activated water would not noticeably lose the added weight when taken to a different room. The gain and loss in weight of a sheet of paper are, therefore, dependent upon the presence of KELEA activated water and the use of the electronic balance, respectively.

An arbitrary criterion was used to establish whether the weight losses during the weighing of a rolled or folded sheet of paper were to be regarded as meaningful. The criterion was that the losses over a 30-minute period had to be >1 mg per gram of the beginning weight of the paper. Over several months of experiments, this criterion was consistently met with paper that had been left in the room with the activated water. There were many examples of weight losses during the first 30 minutes of weighing being >4 mg/gram. The 1 mg/gm criterion was not met for the weighing of freshly prepared rolled or folded sheets of paper, which had not previously been in the weighing room or, which had immediately been located outside of the weighing room, after having been weighed for a prolonged period of time. Exceptions included paper that had been placed in an outside garden setting or had been exposed to other presumed KELEA rich environment (unpublished data). Several individual sheets of rolled paper were subjected to repeated experiments. These items showed recurring meaningful gains and losses of weight by being placed near KELEA activated water and then

being weighed in the electronic balance, respectively. The quantitative results from individual experiments varied, however, even when performed using the same paper item. In spite of indications of an increased sensitivity of printed paper, the use of blank paper has advantages of convenience and better standardization.

A series of experiments were performed using printed and non-printed cotton fabrics, which have been weighed directly upon being brought into the weighing room and/or have been weighed after being stored for some time in the weighing room near the containers of KELEA activated water. Cotton fabric brought directly into the weighing room for immediate weighing would generally show no weight loss if left on the balance for several hours. A slight gain in weight was occasionally noted. Considerable weight gain would progressively occur in pieces of cotton fabric, which were placed nearby to the containers of KELEA activated water. This is illustrated in Figure 4. It shows the increasing weight of a piece of cotton fabric over the first 6 hours after it was brought into the weighing room. During this time, the weight increased from 54.2593 gm to 54.3070 gm, an increase of 47.7 mg.

As anticipated from the studies with paper, there was a significant reversal of the added weight of cotton fabrics left in the weighing room when the cotton fabrics were subsequently continually weighed in the electronic balance. An example of weight loss upon weighing a piece of cotton fabric that had been left in the weighing room for several days is shown in Figure 5. Over the first 60 minutes its weight dropped by 25.3 mg from 13.5392 gm to 13.5139 gm. The weight loss continued over the next several hours with the weight at 2 and 9 hours after the start of the weighing being recorded at 13.5076 gm and 13.4905 gm, respectively. There was no further weight loss over the next hour and, in fact, a slight increase in weight to 13.4914 gm. The experiment was then terminated by removing the fabric from the balance.

Similar to the studies on paper, the gains and losses in weight for the cotton

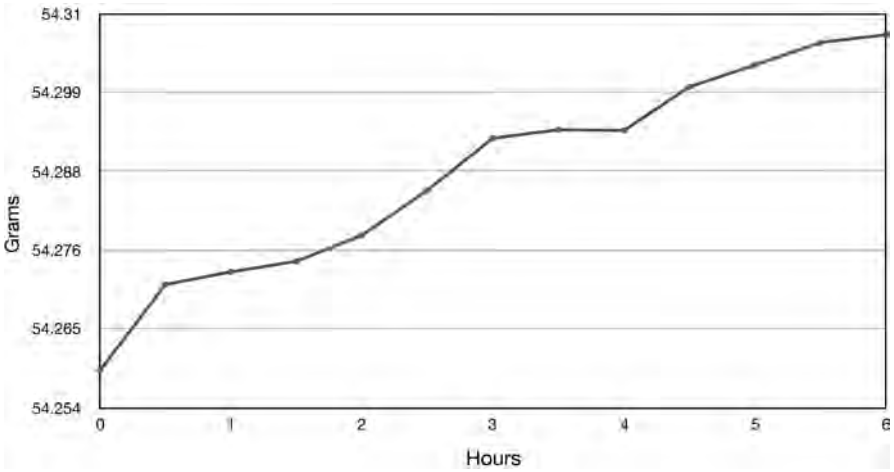

Figure 4. Gain in weight of cotton fabric placed near to containers of KELEA activated water.

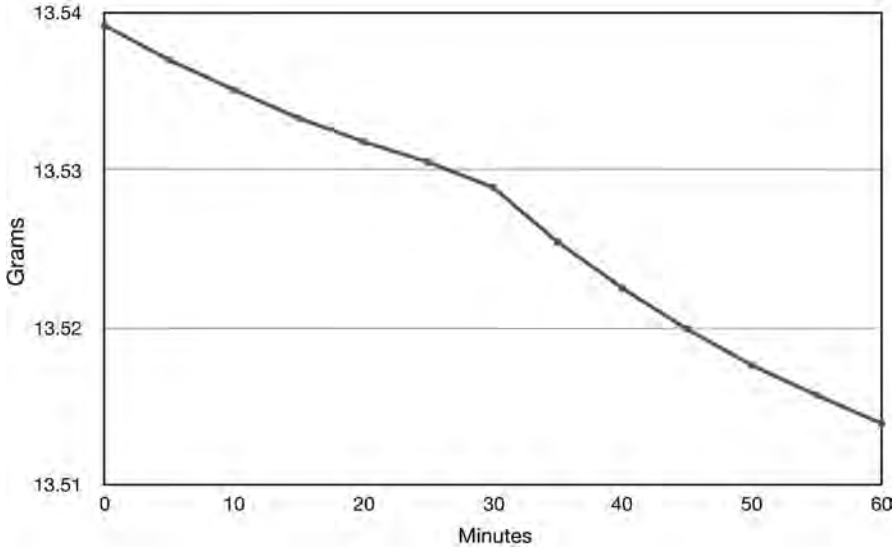

Figure 5. Loss of weight during the weighing of KELEA exposed cotton fabric.

fabrics have been in the range of several mg per gm. Unlike with paper, the weight changes have continued over much longer periods of time, even up to 36 hours. Another difference is that with some of the tested cotton fabrics, there have been several minutes of delay prior to the beginning of a meaningful decline in the measured weight. Moreover, the rates of weight loss of many of the tested cotton fabrics have been irregular and sometimes temporarily stalled. Not infrequently, the decline in weight is temporarily reversed with either slow or occasionally quite abrupt gains of weight of several mg or even more. Significant weight fluctuations are especially noticeable towards the lowest recorded weight and are usually followed by small but significant increases in weight. The rate of increase in the weight proceeds more rapidly after the cotton fabric is removed from the balance and placed near the KELEA activated water. The weight of the cotton fabric only marginally increases when it is removed from the balance and placed in another room for storage. Again, there was a general sense of increased sensitivity of printed cotton fabric.

Cotton fabric materials have allowed for some additional experiments. These included the following. 1) Leaving a relatively large piece of KELEA exposed cotton fabric inside the balance but away from the weighing pan in the balance did not affect the weighting of an unrelated item, the weight of which would remain unchanged. 2) Reweighing the cotton fabric, which had been placed in the active balance, but not on the weighing pan, showed a loss of its measured weight. 3) A cotton fabric, which showed a marked reduction in its weight in the electronic balance after it had been stored overnight in the weighing room, did not show any discernable weight loss when, after it was again stored overnight in the weighing room, it was subsequently weighed using a beam balance located in a different room. 4) Significant weight loss of a cotton fabric was achieved by placing the cotton fabric onto the speaker of a radio in which the volume of sound was set to zero. The overall weight loss of KELEA weight-enhanced cotton

fabrics placed onto the radio speaker was generally greater than that achieved by the electronic balance. Figure 6 provides an example of the weight loss seen with a piece of cotton fabric placed onto the speaker of the radio. Similar results were seen with other active electronic devices including a television set, cell phone and 120-volt electrical wiring.

An EMF meter was used to confirm that the electronic balance and the radio speaker would establish an electromagnetic field. High EMF levels were seen within the electronic balance, which varied from 155 to 578 μT depending upon the placement of the meter within the balance. Only low levels (<30 μT) were recorded away from the balance and elsewhere in the room, even when the balance was operating. The EMF level recorded on the speaker of the radio was higher than that recorded on the electronic balance and ranged from 1453 to 1667 μT. Other EMF emitting devices that could also reverse the KELEA acquired weight gain of cotton fabric included a television, an operating cell phone, and various electrical outlets. These EMF sources could also reduce the weight of KELEA exposed paper.

The results obtained with wood chips were similar, although less pronounced than those seen with the cotton fabric. Small pieces of cherry, hickory and pecan wood were weighed and then placed close to the containers of KELEA activated water in the weighing room. They were reweighed at approximately 1, 4, 9 and 21 hours later. Increases in weight occurred within the first hour with additional comparable increases occurring by 4 hours. The before and after readings of the three pieces of wood are recorded in Table 1. There were little subsequent changes in the weight measurements taken at 9 and 21 hours. The weight gains were not strikingly different for the three types of wood.

The three pieces of wood were collectedly placed onto the weighing pan of the electronic balance giving a combined initial recorded weight of 7.6462 gm. The weight of the wood chips was recorded at minute intervals for 40 minutes and

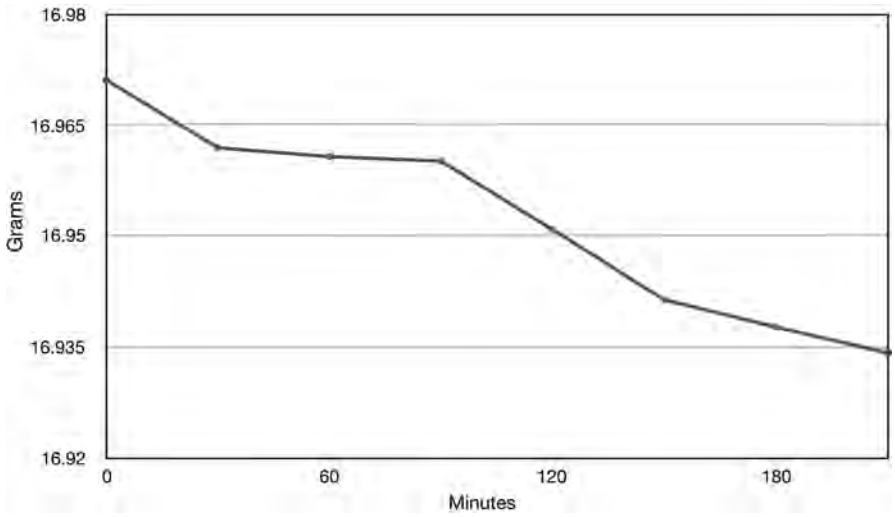

Figure 6. Loss of weight of KELEA exposed cotton fabric that was placed on the speaker of a radio.

less frequently, thereafter, till 5 hours and 35 minutes had elapsed. The results over the first 40 minutes are shown in Figure 7. During this time there was a weight loss of 6.4 mg. The reductions in weight were interspersed with short periods of actual increases in weight. This fluctuation in weight was similar to that seen with the weighing of cotton fabrics. The overall weight loss of the wood is recorded in Table 2. At 5 hours and 35 minutes (335 minutes), the weight loss was 15.3 mg. The wood items were then taken out of the balance and placed near the containers of KELEA activated water. Seven minutes later the weight had increased by 3.6 mg to 7.6345 gm. After an additional seventy-seven minutes, the weight had increased by an additional 4.3 mg to 7.6388 gm. Thereafter, the weight remained essentially unchanged with a reading of 7.6689 gm at 6 hours after the wood was taken out of the balance.

4. Discussion

Evidence was obtained in an earlier study for the weights of pieces of aluminum foil to fluctuate over time, with overall increases in the measured weights [1]. It was suggested that the added weight was due to the attraction of KELEA by areas of separated electrical charges, which were presumably present on the aluminum

Table 1. Gain in weight of wood chips placed near to containers of KELEA activated water.

Duration of Exposure Hours	Cherry		Hickory		Pecan	
	Weight gm	Gain in Weight	Weight gm	Gain in Weight	Weight gm	Gain in Weight
0	2.5540	-	2.5064	-	2.5546	-
1	2.5588	4.8 mg	2.5102	3.8 mg	2.5588	4.2 mg
4	2.5667	12.7 mg	2.5164	10.0 mg	2.5647	10.1 mg
9	2.5660	12.0 mg	2.5164	10.0 mg	2.5644	9.8 mg
21	2.5662	12.2 mg	2.5164	10.0 mg	2.5647	10.1 mg

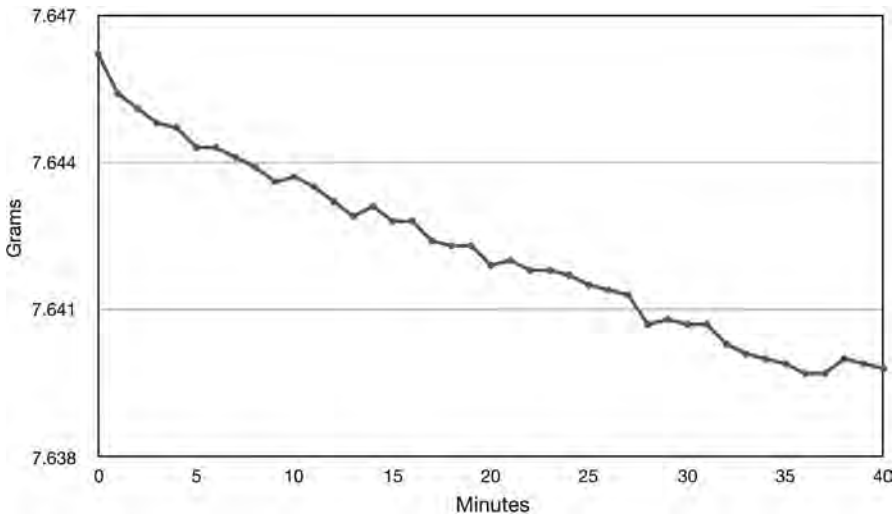

Figure 7. Loss of weight during the weighing of KELEA exposed wood.

Table 2. Continuing weight loss of KELEA exposed wood at longer times of weighing.

Minutes in the Balance	Weight (gm)	Weight Loss (mg)
-	7.6462	-
40	7.6398	6.4
72	7.6369	9.3
83	7.6358	10.4
98	7.6351	11.1
130	7.6339	12.3
153	7.6331	13.1
200	7.6325	13.7
270	7.6310	15.2
335	7.6309	15.3

foil as a result of partial oxidation. The attraction of KELEA was probably also facilitated by the increased overall environmental level of KELEA in the room where the testing was performed. This is explainable because the room was and is still used to store containers of KELEA activated water.

Preliminary experiments showed variable increases in the weights of small pieces of humates and related water activating solid materials when they were simply stored adjacent to KELEA activated water. Inkjet-printed typing paper was viewed as possibly providing a more easily standardized KELEA detection system. Inkjet printing is based on the electrostatic binding of negatively charged ink onto paper or other surfaces [9]. The individual letters on the printed paper would presumably display the negative charge provided to the ink by the printer, in comparison to the non-printed regions of the paper. The separated electrical charges could, therefore, be expected to attract KELEA. Electrostatic painting onto metals would work similarly, except that the paint is positively charged and the surface to be painted has a temporarily induced negative electrical charge [10]. It was, therefore, also intended to test electrostatically painted metals with discrete fine droplets of positively charged paint for KELEA attracting capacity. In both study models, the presumptive attraction of KELEA was to be measured as weight gain. The somewhat surprising result from the first study model was the variability in weight measurements of regular paper, whether printed or not. This variability contrasted with the steady and reproducible weight measurements of most items. Along with certain other tested materials, it became clear that locating even a blank sheet of regular typing paper near KELEA activated water will lead to an increase in weight, as shown when the sheet of paper is subsequently reweighed. Moreover, continuing to weigh the slightly heavier sheet of paper in the electronic balance leads to the relatively rapid reversal of the prior weight gain. In other words, the added weight of the KELEA exposed paper was readily reversed during the subsequent continuing weighing of the paper in the electronic balance. As was predicted, KELEA induced weight gains

followed by the electronic balance mediated reversal of the weight gain were also observed with other cellulose containing materials, including cotton fabrics and wood chips. The use of blank paper provided better standardization than using paper with printed text or using either cotton fabrics or wood. Overall, the findings suggest that, similar to humates, zeolites, and metal oxides [3], cellulose can acquire additional KELEA. Furthermore, the added KELEA can be readily removed or stripped from the energized cellulose by electromagnetic radiation. The various experiments reported in this article are consistent with this interpretation.

Before elaborating on this interpretation, it is helpful to summarize some of the recently proposed aspects of KELEA. These aspects extend beyond the presumed primary function of KELEA to prevent the fusion and elimination of electrostatically attracted opposite electrical charges [2] [3]. For example, it is likely that the combined level of KELEA on opposing electrical charges is inversely related to the closeness of the charges; with sufficient repulsive force remaining to prevent the annihilation of the finally juxtaposed opposite electrical charges. The proposed loss and gain of KELEA by approaching and separating electrical charges, respectively, on interacting chemical compounds may be the equivalent of what chemists refer to as the exchangeable chemical energy in linked chemical reactions. In other words, KELEA can be a source of chemical energy [11]. Consistent with this concept is the observation that KELEA emitting devices can increase the energy yield from the combustion of gasoline and diesel fuels [12] [13]. Also consistent with KELEA being a net source of chemical energy, is the abiotic production of lipids and aromatic chemicals in tubes that were previously used to culture stealth adapted viruses. The infected cells produce alternative cellular energy (ACE) pigments, which persist long after the cells have died [14]. KELEA attracting ACE pigments can lead to the synthesis of a wide range of organic compounds including hydrocarbons [14] [15]. Bacteria can also produce ACE pigments [16].

In addition to KELEA being an alternative (non-food calorie) source of cellular energy, it is likely to be directly involved in normal electrical functioning of the brain, sensory organs, and muscles, including the heart [17] [18] [19] [20]. It can add resilience to the unwarranted triggering of tissue-destructive and scaring inflammatory responses [21]. It can also lead to the regression of cancer through apoptosis [22] [23]. Indeed, many illnesses can be viewed as resulting from an insufficiency of cellular energy [24]. On the basis that KELEA provides life-enhancing benefits, the reductions in KELEA by the increasing manmade levels of electromagnetic radiation have undoubtedly had serious health consequences.

The environmental levels of manmade electromagnetic radiation have progressively increased in the 20th and 21st centuries [25] [26] [27] [28]. The enormous increase is estimated to be several million-fold. The major examples of increases in electromagnetic radiation have been the widespread uses of mi-

crowaves and radio waves in local and distant communications; light pollution; the requirements for electrical power by numerous machines and other devices; and electrical energy transmissions, some of which occur within the ground (dirty electricity) [29]. By evoking the local formation of electrical charges, the increasing electromagnetic radiation has presumably reduced the availability of KELEA for various life forms, including humans, animals and plants. As noted above, given the many important biological functions attributed to KELEA, this will likely have many consequences. Indeed, a significant number of individuals attribute symptoms of their chronic illnesses to electropollution [26] [27] [28]. The findings in this paper imply that symptomatic relief for these individuals will likely be achievable through the consumption, inhalation, and both the direct and indirect exposure of the skin to KELEA activated water [30] [31] [32] [33] [34]. Clinical benefits should also come from various devices able to create a KELEA enhanced environment.

The current study raises interesting new topics for further study. Cellulose can now be added to the increasing array of natural products, which appear to have the capacity to variably attract KELEA. This is interesting since cellulose is one of the most abundant organic compounds on earth [35]. It is a polymer formed by the beta glycosidic covalent linkage of glucose molecules. The glucose molecules in cellulose retain separated electrical charges, which can engage in hydrogen bonding. Cellulose is the major component of plant cell walls, including the wood in trees. It also comprises much of the fibrous tissue in plants. Cotton is almost pure cellulose that provides a protective and dispersal mechanism for the seeds of the cotton plant [36] [37]. Paper and cotton fabrics are manufactured from the cellulose of trees and of cotton plants, respectively. In the formation of paper, the longer tree-derived cellulose polymers are disrupted into smaller units [38] [39] [40]. These units recombine to form mechanically interacting branched polymers. This would, presumably, lead to more exposure of free electrical charges and could explain why paper responds more quickly to the KELEA enriching and KELEA stripping environments than do wood and cotton fabrics. More so than with paper, wood and cotton fabrics can show brief periods of increasing weight while in the electronic balance. These weight increasing periods are interspersed with the more prolonged periods of declining weight and tend also to occur after the lowest weight is recorded. The findings are suggestive of competing KELEA addition and removal processes. The rather abrupt increases of several milligrams over 1 - 2 seconds in the weight of some cotton fabrics are also consistent with competing processes. It is reasonable to assume that different materials can variously attract and/or be stripped of added KELEA. Indeed, preliminary data support the idea that certain materials may actually be able to capture some of the KELEA, which is presumably normally associated with electromagnetic radiation. It will be interesting to compare the KELEA-delivering and removing capacities of various frequencies of electromagnetic radiation on different materials.

It is generally assumed that photosynthesis is the primary source of energy for plants [41]. The apparent attraction of KELEA by cellulose can be viewed as a potential additional primary source of energy for plants. For example, it could be that increasing natural electromagnetic radiation from the sun in early spring could help in the release of some of the KELEA attracted to the cellulose of deciduous trees. The suggested release of KELEA from the tree cellulose into the tree's fluid compartments may contribute to the energy required for the rather spectacular rapid springtime formation of leaves by deciduous trees. Specifically, the released KELEA could possibly increase the permeability of the circulating fluids that supply nutrients and remove metabolic waste products from the tree. A natural energy augmenting function can similarly be envisioned for cellulose polymers in cotton. The widespread use of cotton in clothing and even as prayer cloths [42] is of further interest.

It is postulated that KELEA is being delivered to the earth in association with the charged particles comprising cosmic rays [43]. KELEA may, thereby, contribute to the ionization of atmospheric aerosols, leading to the formation of cloud condensation nuclei (CCN). Partial stripping of incoming KELEA by electromagnetic waves in the upper atmosphere could, therefore, potentially lead to a reduction in cloud formation. Lower level clouds are known to reflect some of the sun's thermal energy back into space. A reduction in cloud formation can, therefore, potentially lead to global warming. Some climatologists have argued that the intensities of cyclones, which are referred to in some locations as hurricanes, and of tornadoes, have increased over recent decades. There are still uncertainties as to the precise triggering of these events. The observed episodes of abrupt changes in the measured weights of certain objects could reflect similar phenomena occurring in Nature. It is not unreasonable, therefore, to suggest a linkage of rapidly changing atmospheric levels of KELEA with the local formation of cyclones and tornadoes. Wilhelm Reich advanced the idea that an energy, which he referred to as orgone and which is probably the same as KELEA, was able to alter the path of a hurricane [44].

The increases in weight of certain compounds from non-contact exposure to activated water and the progressive reductions in the added weight when the objects are being weighed in an electronic balance, require a rethinking of the concepts of weight and gravity. According to current theory as proposed by Einstein, weight is simply a passive reflection of the relative distortion of spacetime by the objects with that caused by the earth [45]. Objects are supposedly attracted to one another solely by the resulting curvature of the spacetime between the objects, and not as presumed by Isaac Newton to an unknown external or emitted force, which attracts distant objects. Nicolas Fatio in the 17th century and Georges-Louis Le Sage in the 18th century proposed an external pushing force coming from every direction [46]. Objects could potentially partially shield one another from the force acting in the area between the objects. The objects would, therefore, be pushed towards one another. This theory was abandoned

mainly because it was wrongly assumed that the shielding would be a reflection of surface area rather than the mass of an object. The observed reversible reductions in the displayed weight of certain objects, together with periods of rapid and seemingly erratic fluctuations in the displayed weight, are clearly indicative of an additional component to weight beyond the distortion of spacetime. It may be time to revive some of the earlier considerations of Fatio and Le Sage [46].

As noted above, the results have major implications for the possibility of an overall decline in the health and vitality of all life forms. This decline may be corrected by the more widespread, routine use of KELEA activated water in humans, animals, and agriculture [30] [31] [32] [33] [34]. Efforts to achieve this goal are underway.

5. Conclusion

The results and discussion in this paper add to a better understanding of a natural force termed KELEA (kinetic energy limiting electrostatic attraction). Specifically, it supports an earlier notion that KELEA can add to the measured weight of certain materials. It also confirms that KELEA activated water can transfer energy to certain nearby objects. Increases in weight were shown for cellulose containing materials, including paper, cotton fabrics, and unprocessed wood, by simply being placed near KELEA activated water. The increases in weight were reversed by exposing the materials with the added weight to electromagnetic radiation, including that resulting from the use of an electronic balance. KELEA can be a source of chemical energy, as well as a means of increasing the permeability and nutrient delivery of the intra- and extracellular fluids in all life forms. Levels of manmade electromagnetic radiations are continuing to greatly increase. This has likely lowered the availability of the life promoting benefits of KELEA to humans, animals, and plants. This deficiency is potentially correctable by increasing the input of KELEA, including through the use of KELEA activated water. The article also postulates that, because of increased manmade electromagnetic radiation that a reduction has occurred in the cosmic rays delivery of KELEA to the lower atmosphere. This would likely reduce the amount of cloud formation contributing to global warming. The rate of decline in the weight of cotton fabrics while on an electronic balance was irregular and frequently interrupted by periods of partial and sometimes abrupt reversals. This suggested a dynamic and somewhat erratic KELEA addition and withdrawal process, which could also contribute to climate change. Another basic science implication of the results is a revival of the idea of a pushing gravity as previously proposed by Fatio and Le Sage. The article provides a simple approach to explore many of these interesting and important topics.

Acknowledgements

The research has been supported by MI Hope Inc., a non-profit public charity based in Los Angeles, CA, USA.

Conflicts of Interest

The author declares no conflicts of interest regarding the publication of this paper.

References

[1] Martin, W.J. (2016) *Journal of Modern Physics*, **7**, 461-472. https://doi.org/10.4236/jmp.2016.76048

[2] Martin, W.J. (2014) Stealth Adapted Viruses; Alternative Cellular Energy (ACE) & KELEA Activated Water. Author House, Bloomingdale, IN, 321.

[3] Martin, W.J. (2016) *Journal of Modern Physics*, **7**, 1995-2007. https://doi.org/10.4236/jmp.2016.715176

[4] Martin, W.J. (2016) *International Journal of Complementary & Alternative Medicine*, **3**, 00059.

[5] Martin, W.J. (2015) *Open Journal of Biophysics*, **5**, 69-79. https://doi.org/10.4236/ojbiphy.2015.53006

[6] Martin, W.J. and Laurent, D. (2015) *International Journal of Complementary & Alternative Medicine*, **2**, 00045.

[7] Martin, W.J. (2015) *Open Journal of Biophysics*, **5**, 115-121. https://doi.org/10.4236/ojbiphy.2015.54010

[8] Martin, W.J. (2015) *International Journal of Complementary & Alternative Medicine*, **1**, 00034.

[9] Hoath, S.D. (2016) Fundamentals of Inkjet Printing, The Science of Inkjet and Droplets. Wiley-VCH, Weinheim, Germany, 472. https://doi.org/10.1002/9783527684724

[10] Lutes, R.S. (1948) Electrostatic Painting Process. University of Cincinnati, Cincinnati, OH, 60.

[11] Martin, W.J. (2017) *MOJ Bioorganic & Organic Chemistry*, **1**, 54‒58.

[12] Martin, W.J. (2016) *Journal of Transportation Technologies*, **6**, 148-154. https://doi.org/10.4236/jtts.2016.63014

[13] Martin, W.J. (2017) *Open Journal of Air Pollution*, **6**, 103-116. https://doi.org/10.4236/ojap.2017.63009

[14] Martin, W.J. (2003) *Experimental and Molecular Pathology*, **74**, 210-223. https://doi.org/10.1016/S0014-4800(03)00037-6

[15] Martin, W.J. (2014) The Alternative Cellular Energy (ACE) Pathway in the Repair of the Cytopathic Effect (CPE) Caused by Stealth Adapted Viruses, *in Vitro* and *in Vivo* Evidence Supporting a New Therapeutic Paradigm. *In Stealth Adapted Viruses; Alternative Cellular Energy* (*ACE*) *& KELEA Activated Water*, Author House, Bloomington, IN, 31-70.

[16] Martin, W.J. (2005) *Experimental Molecular Pathology*, **78**, 215-217. https://doi.org/10.1016/j.yexmp.2005.01.008

[17] Martin, W.J. (2016) *Advances in Alzheimer's Disease*, **6**, 1-12. https://doi.org/10.4236/aad.2017.61001

[18] Martin, W.J. (2017) *International Journal of Complementary & Alternative Medicine*, **4**, Article ID: 00112.

[19] Martin, W.J. (2016) *International Journal Complementary Alternative Medicine*, **4**, Article ID: 00118.

[20] Martin, W.J. (2017) *World Journal of Neuroscience*, **7**, 257-266.

https://doi.org/10.4236/wjns.2017.73021

[21] Martin, W.J. (2017) *Journal of Cosmetics, Dermatological Sciences and Applications*, **7**, 82-98. https://doi.org/10.4236/jcdsa.2017.71009

[22] Martin, W.J. (2016) *International Journal of Complementary & Alternative Medicine*, **3**, Article ID: 00074. https://doi.org/10.15406/ijcam.2016.03.00074

[23] Martin, W.J. (2017) *Journal of Cancer Therapy*, **8**, 1279-1290. https://doi.org/10.4236/jct.2017.813106

[24] Martin, W.J. (2016) *International Journal of Complementary & Alternative Medicine*, **4**, 00106.

[25] Global Electricity Transmission Report and Database 2016-2025. Global Transmission Reports, 3rd Edition, New Delhi.

[26] Bak, M. and Zmyślony, M. (2010) *Medycyna Pracy*, **61**, 671-683.

[27] DeBaun, D.T. and DeBaun, R.P. (2017) Radiation Nation, Fallout of Modern Technology—Your Complete Guide to EMF Protection & Safety, The Proven Health Risks of Electromagnetic Radiation (EMF) & What to Do Protect Yourself & Family. Icaro Publishing, St. Petersburg, FL.

[28] Becker, R.O. (1960) The Promise of Electromedicine: The Perils of Electropollution. JP Tarcher, New York, 326.

[29] Milham, S. (2012) Dirty Electricity, Electrification and the Diseases of Civilization. 2nd Edition, iUniverse Inc., Bloomington, 128.

[30] Martin, W.J. (2014) KELEA Activated Water—Enhancing the Alternative Cellular Energy (ACE) Pathway. In: *Stealth Adapted Viruses*; *Alternative Cellular Energy* (*ACE*) *& KELEA Activated Water*, Author House, Bloomington, 115-144.

[31] Martin, W.J. (2015) *Journal of Water Resource and Protection*, **7**, 1331-1344. https://doi.org/10.4236/jwarp.2015.716108

[32] Martin, W.J. (2014) *Advances in Plants & Agriculture Research*, **2**, Article ID: 00033. https://doi.org/10.15406/apar.2015.02.00033

[33] Martin, W.J. (2015) *International Journal of Complementary & Alternative Medicine*, **1**, Article ID: 00001. https://doi.org/10.15406/ijcam.2015.01.00001

[34] Martin, W.J. (2015) *International Journal of Complementary & Alternative Medicine*, **2**, Article ID: 00051. https://doi.org/10.15406/ijcam.2015.02.00051

[35] Brown, R.M. and Saxena, I.M. (2007) Cellulose Molecular and Structural Biology. Springer, The Netherlands, 379. https://doi.org/10.1007/978-1-4020-5380-1

[36] Hall, A.J. (1924) Cotton Cellulose, Its Chemistry and Technology. Ernest Benn Ltd., London, 228.

[37] Mahood, S.A. and Cable, D.E. (1922) *Industrial & Engineering Chemistry*, **14**, 727-730. https://doi.org/10.1021/ie50152a018

[38] Rolland, J.P. and Mourey, D.A. (2013) *MRS Bulletin*, **38**, 299-333. https://doi.org/10.1557/mrs.2013.58

[39] Schmied, F.J., Teichert, C., Kappel, L., Hirn, U., Bauer, W. and Schennach, R. (2013) *Scientific Reports*, **3**, Article No. 2432. https://doi.org/10.1038/srep02432

[40] Persson, B.N., Ganser, C., Schmied, F., Teichert, C., Schennach, R., Gilli, E. and Hirn, U. (2013) *Journal of Physics*: *Condensed Matter*, **25**, Article ID: 045002. https://doi.org/10.1088/0953-8984/25/4/045002

[41] Pessarakli, M. (2016) Handbook of Photosynthesis. 3rd Edition, CRC Press, Boca Raton, 846. https://doi.org/10.1201/b19498

[42] Eckhardt, J. (2010) Prayers That Bring Healing. Charisma Media, Lake Mary, 117.

[43] Martin, W.J. (2016) *Atmospheric and Climate Sciences*, **6**, 174-179. https://doi.org/10.4236/acs.2016.62015

[44] Reich, W. (1942) The Discovery of the Orgone. Vol. 1, Orgone Institute Press, New York, 358.

[45] Einstein, A. (1920) Relativity: The Special and the General Theory. Henry Holt & Co., New York, 168.

[46] Edwards, M.R. (2002) Pushing Gravity. New Perspective on Le Sage's Theory of Gravitation. C. Roy Keys Inc., Montreal, 316.

Abbreviations

KELEA—kinetic energy limiting electrostatic attraction,
ACE—alternative cellular energy,
EMF—Electromagnetic Field,
mg—milligram,
μT—microTeslars,
Hz—Hertz,
oz—ounce,
lb—pound,
”—inches.

Journal of Modern Physics, 2019, 10, 214-224
http://www.scirp.org/journal/jmp
ISSN Online: 2153-120X
ISSN Print: 2153-1196

Formation of Galaxies in the Context of Gravitational Waves and Primordial Black Holes

Shawqi Al Dallal[1], Walid J. Azzam[2*]

[1]College of Graduate Studies and Research, Ahlia University, Manama, Bahrain
[2]Department of Physics, College of Science, University of Bahrain, Sakhir, Bahrain
Email: *wjazzam@gmail.com

How to cite this paper: Al Dallal, S. and Azzam, W.J. (2019) Formation of Galaxies in the Context of Gravitational Waves and Primordial Black Holes. *Journal of Modern Physics*, **10**, 214-224.
https://doi.org/10.4236/jmp.2019.103016

Received: January 23, 2019
Accepted: March 1, 2019
Published: March 4, 2019

Abstract

The recent discovery of gravitational waves has revolutionized our understanding of many aspects regarding how the universe works. The formation of galaxies stands as one of the most challenging problems in astrophysics. Regardless of how far back we look in the early universe, we keep discovering galaxies with supermassive black holes lurking at their centers. Many models have been proposed to explain the rapid formation of supermassive black holes, including the massive accretion of material, the collapse of type III stars, and the merger of stellar mass black holes. Some of these events give rise to the production of gravitational waves that could be detected by future generations of more sensitive detectors. Alternatively, the existence of these supermassive black holes can be explained in the context of primordial black holes. In this paper we discuss the various models of galaxy formation shedding light on the role that gravitational waves can play to test of the validity of some of these models. We also discuss the prospect of primordial black holes as a seeding constituent for galaxy formation.

Keywords

Gravitational Waves, Galaxy Formation, Primordial Black Holes, Supermassive Black Holes

1. Introduction

The formation of galaxies has been the subject of intensive theoretical and observational work during the past few decades. Observational data reveal the existence of supermassive black holes lurking at the centers of galaxies formed at a

period very close to the recombination era. However, current observations remain incapable of providing a decisive answer as to the origin of these supermassive black holes. Recent development in the detection techniques of gravitational waves may provide a clue to the processes leading to the formation of supermassive black holes at the center of galaxies. Gravitational waves emanating from these processes in the early universe are extremely weak. Nevertheless, future generations of gravitational wave detectors may shed light on the formation of supermassive black holes in the early universe.

The demography of black holes at the center of galaxies is a promising channel for a better understanding of galaxy formation [1]. The Hubble Space Telescope and the Chandra X-ray Observatory detected supermassive black holes with masses in excess of one billion solar masses in quasars at redshifts corresponding to only a few hundred million years after the Big Bang [2]. The existence of supermassive black holes imposes important constraints on the formation mechanism of galaxies [3]. Furthermore, the gas physics involved in the formation of supermassive black holes is not fully understood yet [4]. So far there is no decisive answer concerning the formation of the earliest black holes, primarily because their growth process masks the origin and properties of the initial progenitor. The logical question that might arise is to what extent modern astronomical observations can set the stage for probing the evolutionary phase of galaxy formation. In this paper, we review some theoretical and observational studies of black holes in the early universe, their possible origin, formation, and fate. In the first part we outline the observational evidence connecting the existence of supermassive black holes in the early universe, followed by a brief introduction to the technique employed in the determination of their masses. In the second part, we present the various models for the formation of supermassive black holes in the early universe, including the collapse of population III stars, dynamical instabilities, the collapse of gas due to dynamical instabilities, the collapse of supermassive stars, the dynamical processes in enriched halos, and the formation and fate of primordial black holes.

2. Masses of Supermassive Black Holes

The determination of the masses of black holes is an essential requirement in verifying the degree of accuracy of various galactic formation and black hole growth models and the extent of their adherence to observations. Two important approaches are used to estimate the masses of black holes lurking at the centers of galaxies. The first technique is known as reverberation mapping. It involves the measurement of the structure of the broad emission line region (BLR) around a supermassive black hole. The equation describing this process is given by [5]

$$GM = fR_{BLR}\left(\Delta V\right)^2 \tag{1}$$

where G is the gravitational constant, ΔV is the rms velocity of gas moving near the black hole as determined from the Doppler broadening of the gaseous

emission lines, R_{BLR} is the radius of the broad line region, and f is a form factor that depends on the shape of the BLR. The measurement of R_{BLR} is considered a serious challenge [6], and the measurement of the f factor is also difficult [5].

The other technique to estimate the masses of supermassive black holes is the use of the M-sigma relation. It represents the correlation between the mass of the supermassive black hole and the velocity dispersion of its host galaxy's bulge [7]. It is used to estimate black hole masses in faraway galaxies, and is given by:

$$\frac{M}{10^8 M_o} \approx A\left[\frac{\sigma}{200\ \text{km/s}}\right]^{\alpha} \tag{2}$$

where A is a constant of order 3, σ is the stellar velocity dispersion of the galaxy's bulge, and α is a constant of order 5 representing the slope of the M-σ relation. Ferrarese and Merritt [8] found A = 3.1 and α = 4.8 ± 0.5. Other studies gave values very close to the above results [9]. The tight nature of the M-σ relation suggests that a feedback mechanism is operating between the growth of supermassive black holes and the growth of the galaxy's bulge.

3. Processes in Black Hole Formation

In this section we introduce some basic processes leading to the formation of supermassive black holes. Accretion around a black hole is one of the key ingredients of its growth. The second element is the existence of a dark matter halo that forms and grows from primordial density fluctuations characterized by a virial radius, a mass over-density, and a virial temperature. This halo serves as a host for the pre-galactic disk, which usually grows via gas dynamic processes.

3.1. Accretion around Supermassive Black Holes

Accretion around supermassive black holes is considered the only mechanism capable of producing the observed luminosities produced by supermassive black holes in quasars [10]. If accretion is an acceptable mechanism for black hole growth, the progenitor remains controversial, with primordial black holes [11], dark stars [12], and collapsing clouds of gas [13] being the main candidates. The existence of an efficient mechanism for transporting angular momentum outward will enable the accretion material to approach a marginally stable orbit. The existence of magnetic fields in the matter flowing into the disk, as well as turbulent motions, is one such mechanism, since it leads to the transfer of angular momentum outward [14]. The Eddington accretion rate is a characteristic scale for accretion, and is given by [15]

$$\dot{M}_E = 3\times 10^{-8}\frac{0.06}{\eta}\frac{M}{M_O}. \tag{3}$$

The total energy released in the disk is equal to the Eddington luminosity

$$L_E = \eta \dot{M} c^2. \tag{4}$$

This is a critical luminosity for any given mass M, beyond which the radiation force overcomes gravity. Luminosities ranging from 10^{42} to 10^{48} erg/s have been

observed for active galactic nuclei (AGNs), corresponding to black hole masses ranging from 10^5 to 10^9 solar masses [16]. Even though a good agreement has been found between the observation and the theory of the spectral distribution of radiation, these theories are mainly concerned with mass accretion rates and the luminosity of the accretion disk irrespective of the origin of the accreting supermassive black hole.

3.2. Primordial Dark Matter Halos

Galaxies are thought to be formed from baryonic matter in dark matter halos born out of small primordial density fluctuations [17]. There are three important parameters that can be inferred from these halos. The first is the virial mass M_{vir} that can be calculated directly from the virial theorem. The second is the circular velocity V_c which can be calculated from the relation

$$V_c = \left(GM_{vir}/r_{vir}\right)^{1/2} \tag{5}$$

where r_{vir} is the virial radius. The third parameter is the virial temperature, which is given by

$$T_{vir} = \mu m_p V_c^2 / 2k_B \tag{6}$$

where m_p is the proton mass, μ is the mean molecular weight, and k_B is the Boltzmann constant. The gravitational collapse of the baryon component can proceed when the mass of the over dense region reaches the Jeans mass M_J. At masses in excess of M_J, baryons are captured and are then shock-heated by the subsequent collapse and virilization of dark matter. Gas dynamics processes predict that low-mass objects are less efficient in dissipating energy and cool rather slowly, whereas more massive objects can cool at a faster rate [18]. The collapsing halos in the early universe exhibit a virial temperature smaller than 10^4 K and are referred to as mini-halos. A necessary condition for the gas to cool down and form the first stars is that the halos should rely on the less efficient H_2 cooling [17].

4. Formation of Supermassive Black Holes

During the past few decades, several models have been proposed to explain the presence of massive black holes (MBHs) at redshifts corresponding to the era when the universe was less than one billion years old. Important questions to answer are when did the seeding black holes at the center of galaxies form and what mechanism was involved in their growth? Several possible formation channels have been investigated to understand the MBH seed, as outlined below.

4.1. Collapse of Population III Stars

Population III stars are massive metal-free objects comprising the first generation of stars after the Big Bang. These stars are postulated to have formed in mini-halos with masses of the order 10^6 solar masses and to have collapsed from the highest primordial density field. For $T_{vir} > 10^3$ K, the cooling process is mediated by molecular hydrogen [18]. Atomic hydrogen cooling takes place in the

larger halos with a total mass of 10^8 solar masses and $T_{vir} \geq 10^4$. Simulation of the collapse of molecular clouds suggests that massive stars with $M > 100$ solar masses can form [19]. The fate of population III stars depends primarily on their masses. The collapse of 40 - 140 solar masses low metallicity stars is predicted to directly form a black hole. When the mass of the population III star is in the range 140 to 260 solar masses, the fate of the star is determined by the electron-positron pair production instability that leads to supernova explosions. Supernovae predicted by this model for certain ranges of massive stars will release a colossal amount of energy that can be detected by current observatories. No such events have been recorded so far. On the other hand, the above model has large uncertainties concerning the final mass of the population III stars.

4.2. Gas Dynamic Instabilities

Metal-free or metal-poor proto-galaxies are efficient nurseries where black holes can for and grow. In these systems, supermassive black holes can also be formed directly out of a dense gas cloud [20]. On the other hand, enriched halos exhibit an efficient cooling process which favors fragmentation and star formation rather than direct black hole formation. In metal-free gas clouds that characterize the very first proto-galaxies, the collapse is expected to occur only in massive halos with virial temperatures $T_{vir} > 10^4$ K, where the formation of molecular hydrogen is inhibited [21]. At these temperatures H_2 formation is inhibited and atomic hydrogen becomes an efficient agent for cooling down the tenuous gas until it reaches 4000 K [17]. At $T_{vir} > 10^4$ K, the line-trapping of Lyman-α photons in isothermally collapsing gas causes the equation of state to stiffen with the consequence that fragmentation becomes harder to achieve provided that the metallicity does not exceed about 10^{-4} of the solar metallicity [22]. The dissociation of H_2 in these systems is brought about by Lyman-α trapping. In such halos, gas cooling and contraction proceed gradually with no fragmentation until rotational support halts the collapse, which usually occurs before reaching densities that allow the formation of a massive black hole (MBH).

Local, rather than global, instabilities in a self-gravitating galactic disk can be calculated using the Toomre stability parameter formalism. The Toomre parameter Q is defined as

$$Q = \frac{c_s \kappa}{\pi G \Sigma} \tag{7}$$

where Σ is the surface mass density, c_s is the speed of sound, and $\kappa = \sqrt{2}V/R$ is the epicyclical frequency, and V is the circular velocity of the disk. Gravitational instabilities occur when Q approaches a critical value Q_C. Instabilities might lead to mass in-fall rather than fragmentation and star formation, provided that the destabilization of the system is kept below a threshold value. This happens when the inflow rate is below a critical threshold

$$\dot{M}_{\max} = 2\alpha_c c_s^3 / G \tag{8}$$

where α_c is the viscosity parameter. This process continues until the mass accu-

mulated at the center (M_a) is enough to make the disk marginally stable. The upper limit of the mass that can contribute to MBH formation is determined by the mass and spin parameter of the halo.

4.3. Collapse of Supermassive Stars

Gas dynamical processes can also lead to the formation of supermassive stars (SMS) that may collapse, under certain conditions, to form an MBH. Gas accumulated at the few parsecs around the center of the halo, by processes described in the previous section, can reach 10^4 to 10^6 solar masses. For efficient gas accumulation, an SMS ($M \approx 5\times10^4 M_O$) may form, which eventually collapses to form a black hole [17]. In systems where mass accumulation is fast enough, the outer layers of the SMS are not thermally relaxed during much of the lifetime of a main sequence star [23]. These stars exhibit complex structures with a convective core surrounded by a convectively stable envelope containing most of the star's mass. Hydrogen burning in the core of these stars is relatively low and continues throughout most of its massive stages. When hydrogen is exhausted, the SMS will contract and suffer catastrophic neutrino losses that lead to its collapse to an initial black hole with a mass of a few solar masses that grows subsequently via accretion from the resulting bloated envelope. This object is referred to as a quasistar [24], and it consists of a low-mass central black hole surrounded by a massive radiation-pressure-supported envelope. The black hole grows gradually at the expense of the massive envelope until the resulting MBH is unveiled.

4.4. Dynamical Processes in Enriched Halos

Star formation can proceed in mini-halos characterized by a virial temperature $T_{vir} < 10^4$ K [21] [25]. The halos will be enriched with metals by the first generation of population III stars, and thus fragmentation and formation of low mass stars will be a natural outcome of this enrichment [26]. This process sets the stage for new horizons of MBH formation. Stellar dynamical processes may lead to the formation of compact star clusters [10] [27], resulting from collisions. These collisions arise from dynamical interactions and may play a major role in the formation of very massive stars (VMS) leading to the formation of MBH remnants in the range 10^2 - 10^4 solar masses [28]. In an attempt to reach equilibrium, the compact core cluster initially contracts and then starts to decouple thermally from its outer region. Energy transfer from the central dense core will cause a rapid core collapse [29]. Dynamical friction causes a segregation of more massive stars in the center. If these massive stars remain in the main sequence stage, then a subsystem will be developed and will decouple from the cluster. In this subsystem, star collisions can proceed in a runaway manner eventually leading to the growth of VMSs [30]. The fate of VMSs depends essentially on their metal enrichment. Metal enriched VMSs will lose much of their mass and end their life as less massive objects (≈150 M_O) [31]. The final fate is either a

low-mass black hole or a pair-instability supernova. For low metallicity, VMSs may have a different fate. Stars with masses $\geq 40M_O$ and sub-solar metallicity may collapse directly into a black hole without a supernova explosion.

4.5. Dark Stars in the Early Universe

Dark stars are a new line of research that proposes that the first stars in the universe were fueled by dark matter heating rather than by nuclear fusion [32]. Weakly interacting massive particles (WIMPs) are considered among the best dark matter candidates [33]. It is assumed that in the early universe the density of dark matter was sufficiently high to trigger dark matter annihilation [34]. The annihilation products of WIMPs inside a star can be trapped to produce enough energy to heat its core and prevent its collapse. The first stars are postulated to form inside dark matter halos of masses of the order of 106 solar masses [35], with one single star per halo. It is also argued that these stars set the stage for many important processes like reionization, the seeding of supermassive black holes, and the production of heavy elements in subsequent generations of stars. The lightest neutralino is motivated by supersymmetry (SUSY) arguments and is considered the best WIMP candidate in the Minimal Supersymmetric Standard Model [36].

In the dark star model, authors assumed a mass of 100 GeV for the annihilating WIMPS. So far, WIMPs in general and neutralinos in particular have not been detected despite intensive searches over the past few decades. Furthermore, no trace of supersymmetric particles has been found in the Large Hadron Collider (LHC), even though it attains energies of seven tera-electron volts, which is far in excess of the 100 GeV postulated for annihilating DM particles in dark stars.

5. Primordial Black Holes

Theoretical studies of the possibility of formation of primordial black holes (PBH) in the early universe date back to the original work of Hawking [37]. He argued that extreme densities and inhomogeneities in the early universe can lead to the local collapse of matter resulting in the formation of black holes. More recently, Choptuik [37] and Kim [38] demonstrated the formation of PBHs in the inflationary era, during which the energy density of the universe experienced a dramatic decrease leading to a cosmological phase transition. Hawking [37] argues that PBHs formed in a wide spectrum of masses in the early universe ranging from 10^{-5} g, corresponding to the Planck mass, to 10^{17} solar masses. His upper limit for mass exceeds, by many orders of magnitude, even the greatest masses of supermassive black holes observed today in galactic centers. On the other hand, the formation of very small black holes may arise either from the softening of the equation of state, phase transitions, or from the collapse of hypothetical cosmic strings.

Over dense regions in the early universe may collapse to a black hole if the

gravitational attraction overcomes the pressure forces and the velocity of expansion [33]. This condition is fulfilled when the potential energy for self-gravitation

$$\Omega \sim -\mu^2 R^5 \tag{9}$$

exceeds the kinetic energy of expansion

$$T \sim -\mu R^3 \dot{R}^2 \tag{10}$$

where R is the radius of a region in the early universe, and μ is the energy density. The units are such that $G = c = 1$. In a $k = 0$ Friedman universe the sum of these energies is zero, therefore

$$\left(\frac{\dot{R}}{R}\right)^2 \sim \mu . \tag{11}$$

Furthermore, Hawking assumed that the equation of state relating the pressure P and the energy density μ has the form $P = \mu/3$, and that μ is proportional to R^{-4}. Thus,

$$\mu \sim t^{-2} \text{ and } R \propto\sim t^{-1/2} . \tag{12}$$

A necessary condition for the collapse to occur is that the gravitational energy, μ, should exceed the internal energy U. Taking $P = \mu/3$ and $U \sim \mu \sim R^3$, the condition for collapse to occur becomes

$$\mu R^2 > 1 \tag{13}$$

for $P \sim \mu_{\tilde{o}} \log \mu/\mu_o$, and $U \sim \mu_o R^3 \log \mu/\mu_o$, the condition for collapse reduces to

$$\mu R^2 > \frac{\mu}{\mu_o} \log \frac{\mu}{\mu_o} . \tag{14}$$

Once a black hole is formed, it will grow by accreting nearby matter. The rate of accretion was calculated by Zeldovitch and Navikov [39]

$$\frac{\mathrm{d}M}{\mathrm{d}t} \sim \mu \sim R_g^2 \sim \mu \sim M^2 \tag{15}$$

where μ here is the density of the background universe. But since $\mu = t^{-2}$ (see above), then

$$M \sim \frac{t}{1 + \frac{t}{t_o}\left(\frac{t_o}{M_o} - 1\right)} \tag{16}$$

where M_o is the initial mass of the black hole and t_o is the time of its formation. Thus, if M_o is small compared to t_o, that is, if the black hole is small compared to the particle horizon, then $M - M_o$ remains small and there would be almost no accretion. However, if M_o is of the same order as t_o, then the Zeldovitch-Navikov argument leads to $M \sim t_o$. In this case, the accretion would cause the black hole to grow at the same rate as the particle horizon, producing black holes of the order of the Hubble radius if the growth continued to the present time, or it would reach a mass of 10^{15} to 10^{17} solar masses if the growth

was at the same rate as that of the particle horizon.

6. Gravitational Waves from the Relic of Galaxy Formation

Gravitational waves may be produced extensively during the initial phase of galaxy formation in the early universe. Several models have been proposed to explain the formation of massive black holes at the center of galaxies at redshifts corresponding to the era when the universe was less than one billion years old. Masses of black holes at the center of faraway galaxies can be estimated using the M-sigma relation [8]. An important question to answer is at what epoch the seeding black holes at the center of galaxies were formed, and what are the possible mechanisms involved in their growth. Many hypotheses have been advanced to elucidate the origin of the formation of massive or supermassive black holes at the center of galaxies. As mentioned earlier, several possible formation channels have been proposed for the formation of massive black holes seed [40], collapse of supermassive stars [17], merger of small and intermediate mass black holes. The collision of massive or supermassive black holes at the center of these galaxies will produce energetic GWs that may lie within a sphere of radius again corresponding to the sensitivity of the actual or future GWs detectors [37]. As the sensitivity of gravitational wave detectors improves, they will be capable of detecting GW events at redshifts beyond the era of star formation, and it is highly probable that these detections will provide evidence to support that primordial black holes are involved [41] [42].

7. Conclusion

The formation of supermassive black holes at the centers of galaxies in the early universe is one of the most challenging problems in astrophysics. In this paper we introduced the various models of supermassive black hole formation and we compared these models with observational findings. This approach reveals a gap in our understanding of the most efficient processes leading to the formation of supermassive black holes. Gravitational waves may be associated with the formation of supermassive black holes that can be detected by future generations of gravitational waves detectors. Alternatively, primordial black holes could be considered as a good candidate for seeding new born galaxies in the very early universe and in an era when no supermassive black holes could have had the time to form. An analysis of the cosmic background radiation may give a clue about the existence of primordial black holes. Future missions such as the James Webb Space Telescope will reveal the structure of new born galaxies in the very early universe and will provide a wealth of information regarding the nature of the initial seeding black holes at the centers of galaxies.

Conflicts of Interest

The authors declare no conflicts of interest regarding the publication of this paper.

References

[1] Tremaine, S., *et al.* (2002) *The Astrophysical Journal*, **574**, 740-753. https://doi.org/10.1086/341002

[2] Barth, A.J., *et al.* (2003) *Astrophysical Journal Letters*, **594**, L95-L98. https://doi.org/10.1086/378735

[3] Haimian, Z. (2004) *The Astrophysical Journal*, **613**, 36-40. https://doi.org/10.1086/422910

[4] Barakana, R. and Loeb, A. (2001) *Physics Reports*, **349**, 125-238. https://doi.org/10.1016/S0370-1573(01)00019-9

[5] Merritt, D. (2013) Dynamics and Evolution of Galactic Nuclei. Princeton University Press, Princeton, NJ.

[6] Peterson, B.M. and Horne, K. (2006) Reverberation on Mapping of Active Galactic Nuclei. In: Livio, M. and Casertano, S., Eds., *Planets to Cosmology*: *Essential Science in the Final Years of the Hubble Space Telescope*, Cambridge University Press, Cambridge, UK.

[7] Merritt, D. (1999) Black Holes and Galaxy Evolution. In: Combes, F., Mamon, G.A. and Charmandaris, V., Eds., *Dynamics of Galaxies*: *From the Early Universe to the Present*, Astronomical Society of the Pacific, 221-232.

[8] Ferrarese, F. and Merritt, D. (2000) *The Astrophysical Journal*, **539**, L9-L12. https://doi.org/10.1086/312838

[9] Merritt, D. and Ferrarese, F. (2001) *The Astrophysical Journal*, **547**, 140-145. https://doi.org/10.1086/318372

[10] Schneider, P. (2006) Extragalactic Astronomy and Cosmology: An Introduction. Springer-Verlag, Heidenberg.

[11] Barrau, A. (2000) *Astroparticle Physics*, **12**, 269-275. https://doi.org/10.1016/S0927-6505(99)00103-6

[12] Freese, K., Gondolo, P. and Spolyar, D. (2007) The Effect of Dark Matter on the First Stars: A New Phase of Stellar Evolution. Proceedings of *First Stars III*, Santa Fe, New Mexico, 16-20 July 2007.

[13] Koushiappas, S.M., Bullock, J.S.B. and Dekel, A. (2004) *Monthly Notices of the Royal Astronomical Society*, **354**, 292-304. https://doi.org/10.1111/j.1365-2966.2004.08190.x

[14] Jovanovic, P. and Popovoc, L.C. (2010) X-Ray Emission from Accretion Disks of AGN. In: Wacher, A.D. and Propst, R.J., Eds., *Black Holes and Galaxy Formation*.

[15] Shakura, N.I. and Sunyaev, R.A. (1973) *Astronomy and Astrophysics*, **24**, 337-355.

[16] Krolik, J.H. (1999) Active Galactic Nuclei. Princeton University Press, Princeton.

[17] Volonteri, M. (2010) *The Astronomy and Astrophysics Review*, **18**, 279-315. https://doi.org/10.1007/s00159-010-0029-x

[18] Tegmark, M., *et al.* (1997) *The Astrophysical Journal*, **474**, 1.

[19] Bromm, V., Coppi, P.S. and Larson, R.B. (1999) *The Astrophysical Journal Letters*, **527**, L5-L8. https://doi.org/10.1086/312385

[20] Haehnelt, M.G. and Rees, M.J. (1993) *Monthly Notices of the Royal Astronomical Society*, **263**, 168-178. https://doi.org/10.1093/mnras/263.1.168

[21] Bromm, V. and Loeb, A. (2003) *The Astrophysical Journal*, **596**, 34-46. https://doi.org/10.1086/377529

[22] Santoro, F. and Shull, J.M. (2006) *The Astrophysical Journal*, **643**, 26-37.

https://doi.org/10.1086/501518

[23] Begelman, M.C. (2009) *Monthly Notices of the Royal Astronomical Society*, **402**, 673-681. https://doi.org/10.1111/j.1365-2966.2009.15916.x

[24] Begelman, M.C., Volonteri, M. and Rees, M.J. (2006) *Monthly Notices of the Royal Astronomical Society*, **370**, 289-298.

[25] Abel, T., Bryan, G.L. and Norman, M.L. (2000) *The Astrophysical Journal*, **540**, 39-44. https://doi.org/10.1086/309295

[26] Omukai, K., Schneider, R. and Haiman, Z. (2008) *The Astrophysical Journal*, **686**, 801-814. https://doi.org/10.1086/591636

[27] Clark, P.C., Glover, S.C.O. and Klessen, R.S. (2008) *The Astrophysical Journal*, **672**, 757-764. https://doi.org/10.1086/524187

[28] Devecchi, B. and Volonteri, M. (2009) *The Astrophysical Journal*, **694**, 302-313. https://doi.org/10.1088/0004-637X/694/1/302

[29] Spitzer, L. (1987) Dynamical Evolution of Globular Clusters. Princeton University Press, Princeton.

[30] Portegies, Z.S.F., *et al.* (1999) *Astronomy & Astrophysics*, **348**, 117-126.

[31] Gaburov, E., Lombardi, J. and Portegies, Z.S. (2009) *Monthly Notices of the Royal Astronomical Society*, **402**, 105-126.

[32] Spolyar, D., Freese, K. and Gondolo, P. (2008) *Physical Review Letters*, **100**, Article ID: 051101.

[33] Feng, J.L. (2010) *Annual Review of Astronomy and Astrophysics*, **48**, 495-545. https://doi.org/10.1146/annurev-astro-082708-101659

[34] Krauss, L., *et al.* (1985) *The Astrophysical Journal*, **299**, 1001. https://doi.org/10.1086/163767

[35] Freese, K., *et al.* (2008) Dark Stars: The First Stars in the Universe May Be Powered by Dark Matter Heating. arXiv:0812.4844v1

[36] Primack, J., Seckel, D. and Sadoulet, B. (1988) *Annual Review of Nuclear and Particle Science*, **38**, 751-807. https://doi.org/10.1146/annurev.ns.38.120188.003535

[37] Hawking, S.W. (1971) *Monthly Notices of the Royal Astronomical Society*, **152**, 75. https://doi.org/10.1093/mnras/152.1.75

[38] Kim, H.I. (2000) *Physical Review D*, **62**, Article ID: 063504. https://doi.org/10.1103/PhysRevD.62.063504

[39] Zel'dovich, Y. and Navikov, I.D. (1971) Relativistic Astrophysics. Vol. 1: Stars and Relativity. University of Chicago Press, Chicago.

[40] Haehnelt, M.G. and Rees, M.J. (1993) *Monthly Notices of the Royal Astronomical Society*, **263**, 168-178. https://doi.org/10.1093/mnras/263.1.168

[41] Choptuik, M.W. (1993) *Physical Review Letters*, **70**, 9-12. https://doi.org/10.1103/PhysRevLett.70.9

[42] Koushiappas, S.M. and Loeb, A. (2017) *Physical Review Letters*, **119**, Article ID: 221104.

Journal of Modern Physics, 2019, 10, 225-255
http://www.scirp.org/journal/jmp
ISSN Online: 2153-120X
ISSN Print: 2153-1196

Completely New Gravitational Physics: The Ingenious Outside-Inside Centrifuge Mechanism of Gravity Clarified

Jacob Schaf

Universidade Federal do Rio Grande do Sul (UFRGS), Instituto de Fsica, Porto Alegre-RS, Brazil
Email: schaf@if.ufrgs.br

How to cite this paper: Schaf, J. (2019) Completely New Gravitational Physics: The Ingenious Outside-Inside Centrifuge Mechanism of Gravity Clarified. *Journal of Modern Physics*, **10**, 225-255.
https://doi.org/10.4236/jmp.2019.103017

Received: November 7, 2018
Accepted: March 4, 2019
Published: March 7, 2019

Abstract

The present work implements the idea that gravity is not a fundamental force and that the observed gravitational dynamics is the result of inertial motions within a Keplerian velocity field of the Higgs Quantum Space (HQS), giving mass and ruling the inertial motions of matter-energy. The Higgs theory introduces profound changes in the current view about the nature of empty space. It introduces the idea that a real quantum fluid medium, filling up the whole of space, gives mass to the elementary particles by the Higgs mechanism, an effect analogous to the Meissner effect, giving mass to the photons within superconductors. This HQS necessarily governs the inertial motion of matter-energy and is the *locally ultimate reference for rest and for motions*. The HQS materializes the local Lorentz frames (LFs), turning them into local proper LFs, *intrinsically stationary with respect to the local moving* HQS. This HQS also necessarily is responsible for the gravitational dynamics; because it is mass that creates the gravitational fields. The observed absence of the gravitational slowing of the GPS clocks by the solar field and the absence of light anisotropy with respect to the moving earth are both obvious signatures of the true physical mechanism of gravity. These observations demonstrate that the HQS is circulating round the sun and round earth according to Keplerian velocity fields $(GM/r)^{1/2}$, closely consistent respectively with the planetary motions and the orbital motion of the Moon. In this Keplerian velocity field *the planets are closely stationary with respect to the local HQS* and carried by the moving HQS round the sun *without the need of a central force field*. The Keplerian velocity field of the HQS *is the only possible imaginable mechanism able to give rise to the ingenious outside-inside centrifuge mechanism of gravity* that creates a central field of *centrifugal forces* toward the gravitational center on all matter bodies *not moving strictly along direct circular equatorial orbits*. The Keplerian velocity field of the HQS is shown to

appropriately create all the observed effects of the gravitational fields on matter, on light and on clocks.

Keywords

Fundamental Physics, Higgs Theory, Gravitational Physics, Gravitational Dynamics, Gravitational Effects

1. Introduction

In his General Theory of Relativity (GR) [1] [2] Einstein has replaced the Newtonian gravitation by a completely new theory of gravitation, in which *no gravitational forces are needed*. In order to explain the observed gravitational dynamics, he assumed that the gravitational sources curve the geometry of the four-dimensional spacetime in their neighborhood and that, in this curved spacetime, the orbital motion of the matter bodies follows geodesic paths, governed by a generalized principle of inertia. According to this principle, the gravitational pull on earth is equivalent to an inertial pull and any locally non-accelerated body is a proper reference. He described this spacetime curvature by his famous field equations for the four-dimensional metric tensor $g_{\mu\nu}$:

$$G_{\mu\nu} \equiv R_{\mu\nu} - \frac{1}{2} g_{\mu\nu} R = 8\pi G T_{\mu\nu}, \tag{1}$$

where $R_{\mu\nu}$ is the Ricci curvature tensor, R is the scalar curvature, G is the gravitational constant and $T_{\mu\nu}$ is the stress-energy tensor of the gravitatonal source. In the neighborhood of a spherically symmetric gravitational source, the metric of this curved spacetime is characterized by the invariant length of the four-dimensional line element ds. For sufficiently weak gravitational fields, it is described by:

$$\mathrm{d}s^2 \approx \left[1 - \frac{2U}{c^2}\right]^{-1} \mathrm{d}r_0^2 + r^2 \mathrm{d}w^2 - c^2 \left[1 - \frac{2U}{c^2}\right] \mathrm{d}t_0^2 \tag{2}$$

The coefficients $\left(1 - \frac{2U}{c^2}\right)^{-1}$ and $-c^2\left(1 - 2U/c^2\right)$ are respectively the diagonal g_{11} and g_{44} components of the Schwarzschild metric tensor, where c is the velocity of light in free empty space and $2U = 2GM/r$ is the square of the local escape velocity from the gravitational field.

The last term in Equation (2) expresses the gravitational time dilation as viewed by an external observer. There $\mathrm{d}t_0$ is an infinitesimal time interval in the absence of gravity. From the view of an external observer, the rate of a clock within a gravitational field runs slowly, which can be expressed as a slower effective velocity $\left(c^2 - 2GM/r\right)^{1/2}$ along the time axis. In the first term of Equation (2), $\mathrm{d}r_0$ is a radial distance in the absence of gravity. The time interval dt for a light pulse to travel a distance dr along the radial coordinate can be written as $\mathrm{d}t = \mathrm{d}r/c = \mathrm{d}r_0 \Big/ \left(c^2 - 2U\right)^{1/2}$, where $c' = \left(c^2 - 2GM/r\right)^{1/2}$ again is the effective

velocity of light, however along the radial coordinate. From the view of an external observer, the effective velocity of light c' and the rate of a clock both gradually reduce toward the gravitational center and fall to zero at the event horizon of a black hole.

According to the last term in Equation (2), clocks, stationary within a gravitational field, run slowly because the period of the time standard T, by which the clock counts time, is longer by a factor $\left(1-2U/c^2\right)^{-1/2}$, given by:

$$T(r)=T_0\left(1-2U/c^2\right)^{-1/2} \tag{3}$$

where T_0 is the time period for ($U=0$).

2. Actually Several Predictions of GR Discord from Observations

Atomic clocks, stationary within the earth's gravitational field, confirm exactly the gravitational slowing predicted by GR. However, recent experimental observations have revealed that the GPS clocks, moving with earth round the sun, do not show the gravitational slowing by the solar field. As the escape velocity (from the solar field) does not depend on the orbital velocity, this observation runs into conflict with Equation (3). It demonstrates that the orbital velocity of earth cancels locally the effects of the solar gravitational field, restoring locally the conditions of a proper reference.

Current theories [3] explain the absence of the gravitational slowing of the GPS clocks by the solar field in terms of the principle of equivalence. Accordingly, the local Lorentz frame (LF) of earth is a local proper LF in which the orbiting earth as well as the GPS clocks, moving with it, are stationary. It is alleged that these clocks are free-falling with earth in the solar field and that this orbital motion cancels locally all the effects of the solar gravitational field. According to Einstein, in a free-falling elevator the effects of gravity are locally canceled and the conditions of a proper reference are locally restored. However, consider elevators falling from all different altitudes, at velocities from zero to the local escape velocity. How can all these mutually moving elevators at a same given point be proper references? Moreover, according to this view, if the free-fall of the references is stopped, all clocks in them begin to run slow according to Equation (3) and the path of light becomes bent. The upward force, stopping the free-fall, seems to be the cause of the gravitational slowing. However, Muon decay in Cyclotrons [4] demonstrates that accelerations up to 10^{19} m/sec^2 do not give rise to any effect on the mean life-time of Muons. Only velocity causes the time dilation. In fact, the same GPS clocks too are moving with the GPS satellites along circular orbits round earth, which, according to the above interpretation of the principle of equivalence, too should cancel the gravitational slowing by the earth's field on them. Nevertheless, these same theories [3] include, for the time rate of the GPS clocks, the gravitational slowing by the earth's field of 1.67×10^{-10} sec/sec, which clearly is at odds with the previous assumptions in the

case of motions round the sun.

The fundamental question to be answered here is: Are all these relativistic effects simply perspectives, depending on the relative velocity of the observer as assumed in the theory of relativity, or are they real and do not depend on the observer's kinematical state? The present work will take the second alternative. The Higgs theory introduces fundamental changes in Einstein's view about the nature of empty space. It introduces the idea that a real quantum fluid medium, filling up the whole of space, gives mass to the elementary particles by the Higgs mechanism. This Higgs Quantum Space (HQS) is much more than simply a local reference for rest and for motions. It necessarily rules and governs the inertial motions of matter-energy and is the local ultimate (local absolute) reference for rest and for motions.

The present work adopts the view of the Higgs theory. The Higgs theory, besides disclosing the origin of the inertial mass, opens the new way to understand the origin of the gravitational dynamics. The HQS materializes the local Lorentz Frames (LFs), turning them into local proper LFs, intrinsically stationary with respect to the local HQS. Only *motions with respect to the local HQS* (*proper LFs*) and not relative velocities are the origin of all the effects of motion. From this viewpoint the effects of motion are real, depending on the velocity with respect to the local HQS and not on the relative velocity of the observer. Within this new scenario, the absence of the solar gravitational slowing of the GPS clocks and the absence of the light anisotropy with respect to earth demonstrate that earth is stationary with respect to the local HQS (proper LFs). This can make a sense only if the HQS is moving round the sun consistently with the orbital motion of the planets. From this viewpoint, the only possible and sensible conclusion from the observations is that *not every circular orbital motion cancels locally all the effects of the gravitational field*. Only motions *along direct circular equatorial orbits* (*planetary motions*) *cancel all the effects of the solar gravitational field*. All the other orbital motions, including *retrograde circular equatorial orbital motions and free-falling references* are not proper LFs and *do not cancel locally all the effects of the gravitational field*. They cancel only the gravitational pull. The point here is not putting in doubt the correctness of the estimate of the gravitational slowing of the GPS clocks by the current theories, however showing that the explanation in terms of the principle of equivalence in the case of the solar field and in the case of the earth's field are not consistent with each other. They hence cannot be true explanations.

The explanation in terms of the free-falling inertial references is an Aristotelian like explanation, according to which bodies fall because their inertial references fall (they fall because they fall). However, why do the local inertial references fall? The model of the free-falling inertial references has another much more serious shortcoming. It cannot give rise to a gravitational pull on a stationary body. It cannot because the velocity of Einstein's free-falling inertial references at the local escape velocity is fixed at each point $\left(r_0, \theta_0, \phi_0\right)$ of space.

Moreover, any such inertial reference is valid at only one spatial point. Locally, *the acceleration of the free-fall velocity*, seen by a stationary body, is zero ($\mathrm{d}v/\mathrm{d}t\big|_{r_0} = 0$). Obviously, a velocity constant in time and direction fixed in space cannot give rise to an inertial pull. Therefore, a matter body, brought to rest at any fixed point in a gravitational field and then released, should stay in equilibrium there. Any perturbation however would initiate a runaway departure, *upward or downward*. In order to enable Einstein's model of the free-falling inertial references to produce a gravitational pull, it would be necessary that *the local free-fall velocity*, *at any fixed position* r_0, *be given by* $\mathrm{d}v/\mathrm{d}t\big|_{r_0} = g(r_0)$. However, then the free-fall velocity would rapidly increase beyond the velocity of light, which clearly cannot be reasonable.

In a gravitational field, in which the gravitational dynamics is the result of purely inertial motions (as required by GR), all matter bodies, not acted on by an external force, are free bodies. Hence, the *real vertically upward forces* on such free bodies, necessary to prevent their free-fall on earth and acting *without producing any vertically upward velocity*, *can obviously be only of a centripetal nature.* Centripetal forces are real and act in a direction *normal to the instantaneous velocity vector of the moving body*. If the velocity of such a body is zero, the necessary centripetal force too is zero. Centripetal forces cause only a continuous change of the direction of the body's velocity vector, letting its magnitude perfectly constant. They produce *no velocity along their instantaneous direction*. In a gravitational field, the reaction force, opposite to the real (upward) centripetal force, is a downward centrifugal pull, *which is a fictitious force* exactly as Einstein wanted.

In order to implement, on earth, the scenario of the centrifugal pull toward the earth's gravitational center on *stationary matter bodies*, it is necessary that each stationary matter particle be *implicitly* moving along a circular path round an over-head axis. Such an implicit motion can be created only if a local spatial medium, *ruling the inertial motion of matter-energy and being the local ultimate* (*local absolute*) *reference for rest and for motions* is moving *non-uniformly* in the ordinary space along the horizontal direction oppositely to the implicit velocity of the body. The Higgs theory introduces exactly such a physical space, a quantum fluid medium, giving inertial mass to the elementary particles and thus governing their inertial motion. If the horizontal velocity of this spatial medium *increases toward the gravitational center*, *the distribution of velocity through any infinitesimal region in the plane normal to the implicit velocity of the particle* (*plane of the wave fronts of its matter wave*) *corresponds to rotation round an over-head axis.* In this scenario, the local inertial reference too will be rotating synchronously round the same over-head axis. The idea of a rotating reference being an IR may seem stupid. However, if it is this physical space, governing the inertial motion of matter-energy that is itself locally so rotating, *this is all what is real and senseful*. In this scenario, any local reference, not rotating in the ordinary space, is physically a non-inertial reference implicitly rotating oppositely

round the same overhead axis. A body, stationary in the ordinary space within the velocity field (gravitational field) will *implicitly* be moving, within the local true IR, along a circular path round the same over-head axis. However, this it can do only under an adequate upward centripetal force. The motion of such a body is implicit, because it cannot be described in the ordinary space. It however is physically real and has all the usual consequences of motion.

The next **Section 3** briefly discusses the nature of the quantum fluids, their relevant physical properties, the Higgs mechanism giving mass to the elementary particles, the coupling of quantum fluids with certain fields giving rise to dynamics etc. **Section 4** describes details of the ingenious physical mechanism of gravity. **Section 5** discusses the predictions of the Special and General theories of relativity within the scenario of the HQS dynamics. **Section 6** sets up and solves the differential equation describing the gravitational dynamics in the solar system and on earth. **Section 7** highlights the symmetry with orbital motions. Finally **Section 8** describes a large number of experimental observations that all are perfectly and adequately produced by the HQS dynamics gravitational mechanism.

3. The Higgs Quantum Space and the Foundations of the Gravitational Physics

According to the gauge theories, all the elementary particles (field quanta) are originally massless and moving at the velocity of light. However, in fact most elementary particles are observed to have rest masses. Explaining the origin of this rest mass was one of the hardest problems of fundamental physics to solve. The first clue of the physical origin of the inertial mass was found 1963 by Anderson in superconductivity. [5] The superconducting condensate is a charged quantum fluid of paired conduction electrons (zero spin) condensed into a phase coherent quantum state. Electromagnetic (EM) fields couple to the superconducting (SC) condensate and the vector potential, associated with a changing magnetic field, creates electric fields that cause phase displacements (phase gradients), generating screening velocity fields of the SC-condensate. The created phase disorder elevates the energy of the SC-condensate. These screening currents confine the magnetic field into quantized fluxons or expel it out from the superconductor, which is the Meissner effect. [6] The Meissner effect takes place, because the confinement and expulsion of the field lowers the energy of the SC-condensate. Anderson discovered that gauge transformations of the SC order parameter, in the presence of a magnetic field, reveal mass terms of the EM field quanta (photons). However, the gauge transformations obviously do not create the mass of the photons. They only reveal it on testing the mobility of the photons within the superconductor. Hypothetically, accelerating a photon within a superconductor (by an external force) involves the creation of additional phase gradients and an additional velocity field of the SC-condensate. This additional velocity field too is perfectly persistent, which adds additional inertial mass to

the photon.

Condensation of bosons (or pseudo-bosons He_4 and or Cooper electron pairs) into a phase coherent state takes place at low temperatures, when the Bose-Einstein (BE) phase correlation between the boson wave-functions is sufficiently strong to overcome the thermal fluctuations and cause breakdown of the $U(1)$ symmetry of the bosons. Along a second order phase transition the bosons can lower their energy by condensing into a phase coherent macroscopic quantum state, liberating the corresponding amount of energy. This second order phase transition involves no latent heat and the energy is liberated gradually until zero temperature. In the macroscopic quantum state, the bosons become identical, completely entangled and indistinguishable. Their uncertainty in momentum and energy tend to zero, while the uncertainty in position and in time tend to be large (very large in the Higgs condensate). The condensate usually is described by the complex macroscopic Ginsburg-Landau like order parameter $\Phi(r,\theta)=\phi(r)\mathrm{e}^{i\theta}$, where $\phi(r)$ is an amplitude and $\mathrm{e}^{i\theta}$ is a phase factor. [7] The condensate responds only to specific fields and the response always is coollective, involving all the bosons of the condensate, through the order parameter.

The BE correlation gives rise to a *negative* potential energy (bonding) term, the value of which increases linearly with the condensate density $\rho=\Phi^*\Phi$. BE phase correlation leads to phase coherence of the boson wave-functions, lowering their energy, an effect analogous to the phase correlation between atomic orbitals forming the molecular bonds. Another positive potential energy (anti-bonding) term arises from repulsive core interaction between the bosons, that increases with the squared density ρ^2 and prevents collapse of the boson system. The effective potential $U(\rho)$ is mainly the sum of these two terms that has the form:

$$U(\rho)=-n\left(\Phi^*\Phi\right)+m\left(\Phi^*\Phi\right)^2 \tag{4}$$

where the value of the negative coefficient $(-n)$ of the bonding term is considerably larger than the positive coefficient $(+m)$ of the anti-bonding term. Therefore the minimum of the effective potential energy occurs, not as usually for $\rho=0$, however for a finite value $\Phi^*\Phi=n/2m$, which is known as a non-zero vacuum expectation value. This effective potential *is intrinsically highly homogeneous throughout the volume of the condensate*. Quantum fluids have zero viscosity, are totally frictionless and perfectly conservative up to a well-defined velocity gradient. They couple only to very specific fields, which turns their presence extremely difficult to perceive.

The behavior of quantum fluids differs radically from classical fluids and even from perfect classical fluids. They really challenge commonsense. The fundamental characteristic of the quantum fluids is that their flow cannot be described in terms of positions as a function of time, because the wave function of each boson of the condensate already has non-zero amplitude in the whole volume. This makes their presence practically imperceptible. Consider a river of super-fluid

helium. Like any river, let it not move from place. All possible physical tests to detect motion of the fluid in the river would fail. Imagine the river reaches a power station. The super-fluid would flow through the turbines without driving them at all.

The Higgs theory [8] [9] introduces fundamental changes in Einstein's view about the nature of empty space (vacuum), about the meaning of motions and about the nature of the gravitational physics. It introduces the idea that a scalar field, a real quantum fluid medium of zero spin particles, with properties closely analogous to the SC-condensate, fills up the whole of space. Breakdown of the electroweak symmetry and subsequent spontaneous breakdown to the $U(1)$ symmetry of the weak force doublet results in the Higgs quantum condensate. In the actual low temperature of the universe, this Higgs Quantum Space (HQS) is an extremely stable, rigid and powerful quantum fluid medium, ruled by the principles of quantum physics and, likewise the SC-condensate, it can be described by a complex Ginsburg-Landau like order parameter $\Phi(r,\theta)=\phi(r)\mathrm{e}^{i\theta}$. However, while the SC-condensate is stabilized by an energy gap of only about 1 meV per particle and condenses only at very low temperatures, the HQS is stabilized by a huge energy gap. According to the Glashow-Weinberg-Salam electroweak model, [10] [11] the energy gap achieves 200 GeV, (10^{14} times larger than the energy gap of the usual superfluids and superconducting condensates) and condenses at 10^{15} K. This enormous energy gap very strongly suppresses the quantum fluctuations and the zero-point energies of the various nuclear force fields, thereby leading to vacuum energy densities consistent with the observed values [12].

The HQS is much more than simply a local reference for rest and for motions. It is responsible for the mechanical properties of matter-energy and hence necessarily governs the inertial motion of the elementary particles. It also necessarily is the *locally* ultimate (local absolute) reference for rest and for motions of matter-energy. However, if the HQS is responsible for the mass and the mechanical properties of the elementary particles, it necessarily too is responsible for the gravitational fields, because it is mass that creates the gravitational fields.

Likewise the SC-condensate confines the EM field by the Meissner effect [6] down to 10^{-7}m, quantizing it and giving inertial mass to the photons within superconductors, the Higgs quantum condensate or Higgs Quantum Space (HQS) confines the weak and strong nuclear foce fields down to 10^{-19}m, giving large inertial masses to the vector bosons of the weak force field by the Higgs mechanism as well as to all the elementary particles, porting hyper-charges, by an indirect Higgs mechanism. [8] [9] Also, analogously as the motion of the EM field quanta within the SC-condensate involves additional mass, motion of the elementary particles within the local HQS, too involves additional phase perturbation of the Higgs order parameter, additional velocity fields of the HQS, additional excitation energy, additional mass-energy and additional elevation of the energy of the Higgs condensate. The role of the HQS in the life of our universe is

absolutely vital. Without it, no laws of motion would exist and the universe, as we know it, simply could not exist.

Many authors insist that coupling of the nuclear fields to the HQS creates only a small part of the inertial mass of the elementary particles. This may well be true *in a static situation*. They justify this by saying that most of the mass of the elementary particles is relativistic mass, created by the high velocities of the internal confined constituents (quarks) of the real particles. This too can be true. It however is not relative velocity that causes this additional mass, but *the velocity of these constituents with respect to the local HQS*. Analogously as in the case of EM field quanta in superconductors, the motion of these constituents involves additional phase displacements, additional screening velocity fields of the Higgs condensate and additional energy. Moreover, all these additional are perfectly persistent.

In the case of the empty space, which is essentially the Higgs condensate in its ground state (without excitations), no external action can be invoked to explain the origin of the motions or changes of motion of isolated matter particles. Usual quantum fluids are well known to be totally in viscid, non-dissipative and intrinsically perfectly conservative. It also is well-known that the total momentum of any isolated particle or system of interacting particles is rigorously conserved. This demonstrates that the HQS does not itself manifest inertial mass and momentum effects. Therefore, any motion, once excited, becomes indefinitely persistent and can only be stopped by an opposite action of the same mechanism (field) creating the motion. This indefinite persistence is the very origin of the inertial behavior and the conservation of the momentum of isolated particles or particle systems. Also, due to the very high energy gap, the HQS too strongly suppresses quantum fluctuations, the creation of virtual particles and zero-point energies. It only intermediates, without loss, the effects of the various force fields between the elementary particles or particle systems. If the HQS itself could exhibit mass effects, the momentum as well as the other characteristic parameters of an isolated particle would not be conserved. However, in the real world, particles truly isolated from other particles do not exist. The fundamental requisite to create an elementary particle is a sufficient amount of energy. All the other characteristic parameters of the elementary particles were created from nothing but energy in the beginning of the universe, according to symmetries and laws of conservation. All together these parameters add up to zero, liberating the energy consumed in their creation. The amount of energy, liberated in the creation of the Higgs condensate (HQS) is much more than sufficient to create all the particles of the universe.

It also is often alleged that the Higgs field or HQS has no relation with gravity. This can well be true *in a static situation*. However, likewise superfluids and SC-condensates, the HQS certainly too can locally move. In a superconductor (SC), a constant applied electromotive force (emf) causes an increasing phase gradient along the conductor and flow of the SC-condensate at an increasing

velocity, proportional to the magnitude of the phase gradient. Once excited, this current is perfectly and perpetually persistent, as demonstrated by numerous experiments. The current can be stopped only by an opposite emf. Applying a magnetic field on the SC, the changing vector potential creates an electric field, causing phase displacements and hence phase disorder, elevating the energy of the SC-condensate. The phase displacements generate screening currents that are associated with a Lorentz force field that usually expel the magnetic field out from the superconductor and thereby lowering the energy of the SC-condensate. The Higgs mechanism [8] [9] is the perfect HQS analog of the Meissner effect. Apparently, the nuclear fields are associated with an HQS analog of the EM vector potential that too causes phase gradients and phase disorder, elevating the energy of the Higgs condensate. The corresponding phase gradients create a screening velocity field of the HQS in the space round the matter bodies. If these screening velocity fields are non-uniform, they refract mutually the matter waves of the interacting particles, generating an inertial dynamics (with conservation of the total linear and angular momenta). This inertial dynamics is, according to Einstein's principle of equivalence, gravitational dynamics.

In his Special Theory of Relativity (STR), Einstein has abolished the idea of an absolute reference and absolute motions. In this scenario, any free (non-accelerated) body, moving in the empty ordinary space under no external force is a proper Lorentz frame, in which stationary clocks show proper time and, with respect to which, the velocity of light is isotropic. In the General Theory of Relativity, Einstein introduced the principle of equivalence, extending locally the view of the STR to free motions within gravitational fields. He assumes that locally non-accelerated (free-falling) bodies (zero external force) too are *locally* proper references. Accordingly, a free-falling elevator and or orbiting bodies are proper Lorentz frames in which stationary clocks show proper time and the velocity of light is isotropic.

Clocks stationary within gravitational fields are well-known to run slow exactly as predicted by GR. However, actually it is well-known that the gravitational slowing by the solar field is absent on the GPS clocks, moving with earth round the sun [13] [14] [15]. This absence and the well-known absence of light anisotropy with respect to earth both demonstrate that the orbital motion of earth cancels locally the effects of the solar field. From the present HQS dynamics view, these observations can make a sense only if the orbiting earth is stationary with respect to the local HQS, which entails the conclusion that the HQS necessarily is moving round the sun consistently with the earth's orbital motion [16] [17] [18]. Current theories explain the absence of the solar gravitational slowing of the GPS clocks in terms of the principle of equivalence. However, according to this interpretation of the principle of equivalence, the orbital motion of the GPS clocks with the GPS satellites round earth, in exactly the same conditions, too should cancel the gravitational slowing by the earth's field on them. Nevertheless, the gravitational clock slowing by the earth's field is well observed.

Section 8.B5 solves this problem.

Within gravitational fields, all of Einstein's local free-falling inertial references are mutually non inertial. How can they all be proper references? According to the present work, velocity with respect to the local HQS and not relative velocity is the cause of all the so-called relativistic effects. Therefore, *only references, stationary with respect to the local HQS are proper Lorentz frames* and *only clocks stationary in such proper references can display proper time and moreover only with respect to such proper references is the velocity of light isotropic.* Bodies anyhow moving with respect to the local HQS are *not proper Lorentz frames*. The velocity of light with respect to these non-proper references *cannot be isotropic* and clocks, stationary in such non-proper references *do not show proper time*. The next Section solves this stalemate.

4. The Ingenious Outside-Inside Centrifuge Mechanism of Gravity That Einstein Has Missed

If the HQS gives inertial mass to the elementary particles, it necessarily is responsible too for the gravitational fields, because it is mass that generates the gravitational fields. It is well-known that clocks stationary within a gravitational field show exactly the gravitational slowing predicted by GR. However, recently the GPS clocks, moving with earth round the sun, have shown that the gravitational slowing by the solar field is absent on them. Visibly, the orbital motion of earth cancels the effects of the solar gravitational field, which runs into conflict with Equation (3).

Current theories explain the absence of the solar gravitational slowing on the GPS clocks by the solar field in terms of the principle of equivalence. Accordingly, in the Lorentz frame of earth, earth is stationary, which is alleged to cancel locally the effects of the solar gravitational field. However, the GPS clocks too are moving with the GPS satellites round earth in exactly the same conditions, which too should cancel the effect of the earth's field. However, the observations show different. The gravitational slowing by the earth's field (1.67×10^{-10} sec/sec) is well present on them. It hence is clear that the *absence of the gravitational slowing of the GPS clocks by the solar field*, the *absence of light anisotropy with respect to the moving earth* together with the *non-absence of the gravitational slowing by the earth's field on the GPS clocks, these last moving along orbits making* 55 *degrees with the equator*, demonstrate that *only orbital motions along direct circular equatorial orbits cancel locally all the effects of the gravitational fields.*

In the language of the present work, *the Higgs Quantum Space* (*HQS*) *materializes the local Lorentz frames* (*LFs*), *turning them into local proper LFs, intrinsically stationary with respect to the local HQS.* Only LFs, stationary with respect to the local HQS are proper LFs. On moving, the HQS carries the local proper LFs with it. If the motion of the HQS and hence of the local proper LFs through our laboratories, is spatially uniform, it gives rise only to light anisotropy. However, if its motion is non-uniform, besides light anisotropy, it refracts

the matter waves and light, creating inertial dynamics for the matter particles *moving with respect to the local HQS* and curving the path of light. According to Einstien's principle of equivalence, this inertial dynamics is gravitational dynamics.

The coming **Sections 6, 7 and 8** show that motion of the HQS, round the sun, according to a Keplerian velocity field, consistent with the planetary motions, accurately creates the observed gravitational dynamics and all the observed effects of the gravitational fields on light and on clocks. Please see also References Refs. [16] [17] [18]. In terms of usual spherical coordinates the Keplerian velocity field of the HQS, created by a spherically symmetric source, has the very simple form:

$$\boldsymbol{V}(r) = (GM/r)^{1/2}\,\boldsymbol{e}_{\phi} \tag{5}$$

This is a velocity field only along the ϕ spherical coordinate round the Z axis ($\theta = 0$), in which the magnitude of the velocity of the HQS is spherically symmetric, G is the gravitational constant, M is the mass of the gravitational source (sun), r is the radial spherical coordinate and $\boldsymbol{e}_{\phi}$ is a unit vector along the azimuthal spherical coordinate ϕ.

The present work associates the central idea of GR, according to which *the gravitational pull is an inertial pull* and the central idea of the Higgs theory, according to which the HQS gives mass *and governs the inertial motion of matter-energy* and replaces Einstein's spacetime curvature by a Keplerian velocity field of the HQS. This Keplerian velocity field is the quintessence of the gravitational fields, in which however the gravitational dynamics is not described in terms of geodesic motions, however in terms of inertial motions (wave propagation) in the Keplerian velocity of the HQS. In this scenario, the gravitational acceleration is a centrifugal acceleration and the gravitational pull is a centrifugal pull, which is a fictitious force. Within this velocity field, the observed gravitational dynamics, the gravitational pull, the absence of the solar gravitational slowing of the GPS clocks by the solar field as well as the absence of the light anisotropy with respect to earth are all genuine and natural outcomes of this Keplerian velocity field of the HQS. These observations are all *authentic signatures of the true physical mechanism of gravity in action*.

Motion of this HQS according to a Keplerian velocity field naturally and perfectly implements the ingenious outside-inside and inside-outside spherical centrifuge scenario, observed within the gravitational fields. No other imaginable physical mechanism is able to implement this outside-inside centrifuge mechanism. This ingenious centrifuge mechanism is the true hush-hush of the gravitational physics that GR has missed. It also naturally and accurately accounts for all the effects of the gravitational fields on light and on clocks, as will be shown in the coming **Sections 6, 7 and 8**.

5. Einstein's Theory of Relativity in the Scenario of the HQS Dynamics

It is important to note that, in the scenario of the HQS, the velocity of light c, in

the empty space, is fixed and isotropic with respect to the local HQS and not with respect to the reference of every possible observer, as postulated in the theory of relativity. In the scenario of the HQS, the velocity of light in free space (vacuum) is the characteristic velocity at which the HQS propagates the local phase perturbations of the Higgs order parameter. The HQS is ruled by quantum physics. Therefore, the local phase perturbations of the Higgs order parameter and the consequent steady state velocity fields of the HQS (excitations), caused by the elementary particle fields (vector bosons, quarks and leptons), which cause increase of the energy of the HQS, are ruled by quantum physics. The particle fields are confined by the Higgs mechanism down to 10^{-19} m and quantized according to well defined rules, which lowers the energy of the HQS.

The electromagnetic (EM) field does not couple to the HQS and is not confined by the HQS. Therefore, photons have no rest mass and propagate in empty space at the characteristic propagation velocity c, however *with respect to the local HQS* and not with respect to any observer. The electric field however is not disconnected from the HQS, because the particles, porting the electric charges, couple to the HQS via the hypercharges. Moreover, due to the conservation of electric charge, the number of positive and negative charges necessarily is the same. Therefore, the electric field largely confines itself, so that, from a large scale point of view, only the effects of the gravitational fields are relevant.

Any local reference, stationary with respect to the local HQS, is a local proper Lorentz frame (LF), with respect to which the velocity of light c is fixed and isotropic. However, references moving with respect to the local HQS are non-proper LFs and therefore the (one-way) velocity of light and of neutrinos is anisotropic with respect to them. Within the gravitational fields, the HQS itself is moving according to the Keplerian velocity field Equation (5). In this motion, the HQS carries the local proper LFs with it. Therefore, within the gravitational fields, the local velocity vector of the HQS $\boldsymbol{V}=\left(GM/r\right)^{1/2}\boldsymbol{e}_{\phi}$ adds up to the fixed velocity vector $\boldsymbol{c}$ of light and the effective velocity of light c' is given by $\boldsymbol{c}'=\boldsymbol{c}+\boldsymbol{V}$. However, as shown in **Section 4**, earth is stationary with respect to the local HQS in the solar and the galactic velocity fields and this is why the velocity of light is isotropic with respect to earth and the GPS clocks display proper time.

Clocks are devices that count time in terms of a time standard, which can be a classical or quantum oscillator. The time standard of atomic clocks is the period T of electromagnetic (EM) oscillations in an EM cavity, tuned to the well-defined frequency of the hyperfine transition of Cs atoms. Such clocks measure the time evolution with an incredible precision of a tenth of a nanosecond (~10^{10} sec) or even better. Their time standard is of course affected by velocity with respect to the local HQS (not by relative velocity). Within gravitational fields, the HQS is moving round the gravitational sources according to the Keplerian velocity fielded Equation (5). Therefore, clocks, stationary in the ordinary space within a gravitational field, are implicitly moving at a velocity $-\left(GM/r\right)^{1/2}\boldsymbol{e}_{\phi}$ with respect to the local HQS. This implicit velocity and not the local escape velocity, is

the cause of the gravitational clock slowing. From the present view, *the gravitational clock slowing and the slowing of speeding clocks in free space are due both to the same velocity with respect to the local HQS*. This clock slowing however is different for transverse or longitudinal oscillation of the time standard.

From the view of GR, the coefficient of the last term, in Equation (2), is the square of the effective velocity c' along the time axis (time evolution), where $\boldsymbol{c}$ and $2GM/r$ are intrinsically orthogonal. The effective velocity is given by the formula of Pythagoras $c' = \left(c^2\left(1-2U/c^2\right)\right)^{1/2} = \left(c^2 - 2GM/r\right)^{1/2}$, where $2GM/r$ is the square of the local escape velocity. To first order, the gravitational slowing is $t_0\left(GM/r\right)/c^2$, which is well observed on clocks stationary in the earth's gravitational field. Einstein never has considered the possibility of longitudinal oscillations of the time standard or light round-trips, because, in his view, any ordinary velocity is intrinsically orthogonal to the time axis.

From the viewpoint of the present work, the gravitational time dilation of clocks, stationary within a gravitational field in the ordinary space, is due to the implicit velocity ($\boldsymbol{v}_{impl}\left(r\right) = -\left(GM/r\right)^{1/2}\boldsymbol{e}_{\phi}$). In this scenario, the period T *for longitudinal EM oscillations of the clock's time standard* is lengthened, given by ($T_l = T_0\left(1-\left(GM/r\right)/c^2\right)^{-1}$) and to first order the gravitational slowing of the clock is $t_0\left(GM/r\right)/c^2$. However, for transverse oscillations, the gravitational slowing is reduced to one half this value. Moreover, depending on the direction of observation, the dipole EM radiation, emitted by speeding atoms, can be selective for longitudinal or transverse EM oscillations. Dipole photons emitted along the motion of the atoms are selective for transverse EM oscillations.

Considering *only transverse oscillations of the time standard*, the effective time evolution (velocity along the time axis), in free empty space, is obtained by the formula of Pythagoras $c' = \left(c^2 - v^2\right)^{1/2}$, where c is the fixed velocity of light with respect to the local HQS in zero gravitational field and v is the ordinary velocity of the clock with respect to stationary HQS. However, within a gravitational field, the HQS is itself moving according to the Keplerian velocity field Equation (5) along $+\phi$. In this case the local effective time evolution (velocity along the time axis), given by a clock, *stationary in the ordinary space within the gravitational field* too can be calculated by the formula of Pythagoras $c' = \left(c^2 - GM/r\right)^{1/2}$, where c is the intrinsic time evolution (velocity along the time axis) of the clock's time standard (Cs atoms) *in zero field* and where GM/r is the square of the implicit velocity along $-\phi$. For longitudinal oscillations of the clock's time standard, the period is ($T = T_0\left(1-\left(GM/r\right)/c^2\right)^{-1}$) and the rate of the clock is $t_l = t_0\left(1-\left(GM/r\right)/c^2\right)^{-1}$. To first order, this gives a gravitational clock slowing of $\approx t_0\left(GM/r\right)/c^2$, the same as given by GR.

Now, the first term of the right hand side in Equation (2) describes stretching of the radial distances, due to the spacetime curvature in the gravitational field, given by $\mathrm{d}r^2 = \mathrm{d}r_0^2/\left(1-2U/c^2\right)$. According to GR, from the view of an external observer, this stretching causes an apparent reduction of the velocity of light,

propagating toward the gravitational center. However, from the view of the present HQS dynamics, the velocity of a light beam, propagating toward the gravitational center, *decreases really and not apparently*. It decreases because it necessarily needs to develop an implicit orthogonal velocity component $(GM/r)^{1/2}$ along $-\phi$. The time interval, necessary for light to propagate a distance dr along the radial coordinate, is $\mathrm{d}t = \mathrm{d}r/c = \mathrm{d}r_0 \Big/ \left(c^2 - GM/r\right)^{1/2}$, where $\left(c^2 - GM/r\right)^{1/2}$ is again the effective velocity c' of light, however along the radial coordinate, obtained by the formula of Pythagoras. However this c' is only the radial velocity component of light. The other component is $(GM/r)^{1/2}$ along $-\phi$. Visibly, GR scales the radial distances in units of the effective radial velocity of light.

6. The Gravitational Dynamics in the Solar System and on Earth

The Keplerian velocity field of the HQS (Equation (5)), creating the solar gravitational field is closely consistent with the planetary orbital motions and achieves 436 km/sec on the solar surface. This Keplerian velocity field carries with it the planets and the local proper LFs along *direct nearly circular equatorial orbits* without the need of a central force field. This makes the gravitational dynamics, observed within the solar system, totally obvious. The planetary orbits lie all within the equatorial plane of the solar Keplerian velocity field. So also are practically all planetary satellite orbits. Along such orbits these bodies are all very closely stationary with respect to the local moving HQS (local proper LFs). This motion along direct, circular equatorial orbits is in fact their local resting condition that minimizes their kinetic energy with respect to the local HQS and makes their gravitational (Keplerian velocity) fields very closely spherically symmetric. Excepting only for the very small tides, this cancels locally all the effects of the solar gravitational field on matter, on light and on clocks, exactly as assumed by the current theories with base in the principle of equivalence.

The velocity of light is closely isotropic with respect to earth, *not because of the intrinsic isotropy of light, however because earth is stationary with respect to the local moving HQS* (*local LFs*), the medium propagating light. Also clocks, moving with earth round the sun, display very closely proper time, because they too are very closely stationary with respect to the local HQS in the solar Keplerian velocity field. In fact, the small ellipticity of the planetary orbits evidences that their velocity with respect to the local HQS is only of a few hundreds of meters per second. In the case of earth, the effect of this small velocity on light and on clocks is far too small to be detected even by the current most sensitive instruments. However, the refraction rate of this small velocity by the non-uniform velocity in the solar Keplerian velocity field along a whole year is sufficient to make the orbits of the planets a little bit elliptic and to cause the perihelion precession. Please see details in the next **Section 8**.

The velocity of the HQS in the Keplerian velocity field (Equation (5)) round

earth, in the sense of the Moon's orbital motion (from West to East) and creating the earth's gravitational field, achieves 7.91 km/sec on surface. However, as earth rotates only very slowly (465 m/sec at the equator) toward the East, the earth-based laboratories are moving with respect to the local HQS *toward the West* at an implicit velocity, ranging from 7.445 km/sec at the equator up to 1.91 km/sec in the Polar Regions. Refraction of this implicit velocity creates the gravitational acceleration and the centrifugal pull toward the earth's center on matter, observed on the earth-surface. It also creates the very small light anisotropy of nearly 8 km/sec, barely detected by only a few of the most sensitive Michelson light anisotropy experiments [19]. Please see details in **Section 8.2**. It also gives rise to the very small gravitational slowing of the atomic clocks and the spectral red-shifts, observed on earth. However, although very small, these effects of the earth's field still are much more relevant than the effects by the solar field on earth. The effects of the solar field are extremely small because the orbiting earth is almost stationary with respect to the local HQS in the solar field. These effects simply seem to be absent.

The Keplerian velocity field of the HQS is intermediary between rigid body rotation and potential flow with zero curl. The form of the velocity field of quantum fluids is determined by the limit of non-viscous flow. Due to the order parameter, the differential flow of quantum fluids can be in viscid up to a certain limit of the velocity gradient, even if the curl of the velocity field is non-zero from the classical physics point of view. This property is well-known from the exponential fall of the screening current density (screening velocity fields) in superconductivity. In the HQS this limit determines the $(1/r)^{1/2}$ dependence of the Keplerian velocity field. The curl of the Keplerian velocity field Equation (5) has a form very similar to the magnetic field of a magnetic dipole.

In the Keplerian velocity field, the ϕ and r velocity components of a particle with respect to the local HQS are refracted in opposite senses. This characterizes a *hyperbolic* and not a trigonometric rotation. The differential equation, describing the effects of these refraction rates in the case of a spherically symmetric gravitational source, will be constructed and solved in the coming paragraphs.

In the Keplerian velocity field, the local velocity distribution of the HQS through the $[r,\theta]$ plane seen by a particle with a velocity along the ϕ direction (v_ϕ) and its de Broglie wave fronts in the $[r,\theta]$ plane, corresponds to rotation of the local HQS and of the local inertial reference (IR) round an *overhead axis*. The refraction rate corresponds to an instantaneous angular velocity $\mathbf{W}_\phi(r)$, to be determined, (please see Equation (6)). This rotation axis lies well above the position of the particle. However, the wave-fronts in the $[\theta,\phi]$ plane of the radial velocity component $v_r(t)$ do not see this rotation rate round the overhead axis. They see the opposite rotation of the HQS round the gravitational center $\mathbf{W}_r(r)$. The θ velocity component is not refracted at all, because the velocity field Equation (5) has no component along θ. Besides these refraction rates, there is need of considering the wavelength stretching/compression, due to

the deformations of the HQS in the Keplerian velocity field along certain directions. This affects the velocity of the particles according to de Broglie's equation $p = h/\lambda$. However the r and the ϕ velocity components are not affected by these wavelength deformations. Hence, describing the effects of the gravitational field, in terms of these velocity components and *their effective rotation rates*, the effects of wavelength stretching/compression are automatically taken into account.

In order to obtain quantitative values for the refraction rates of the r and ϕ velocity components of the effective velocity (with respect to the local HQS), the orbital velocity v_{orb} of a particle with a very small mass m in the gravitational field of a very large mass M, along an elliptic orbit ($\epsilon = 0.5$) was computed and plotted very precisely in Figure 1. The values of v_{orb} together with the Keplerian

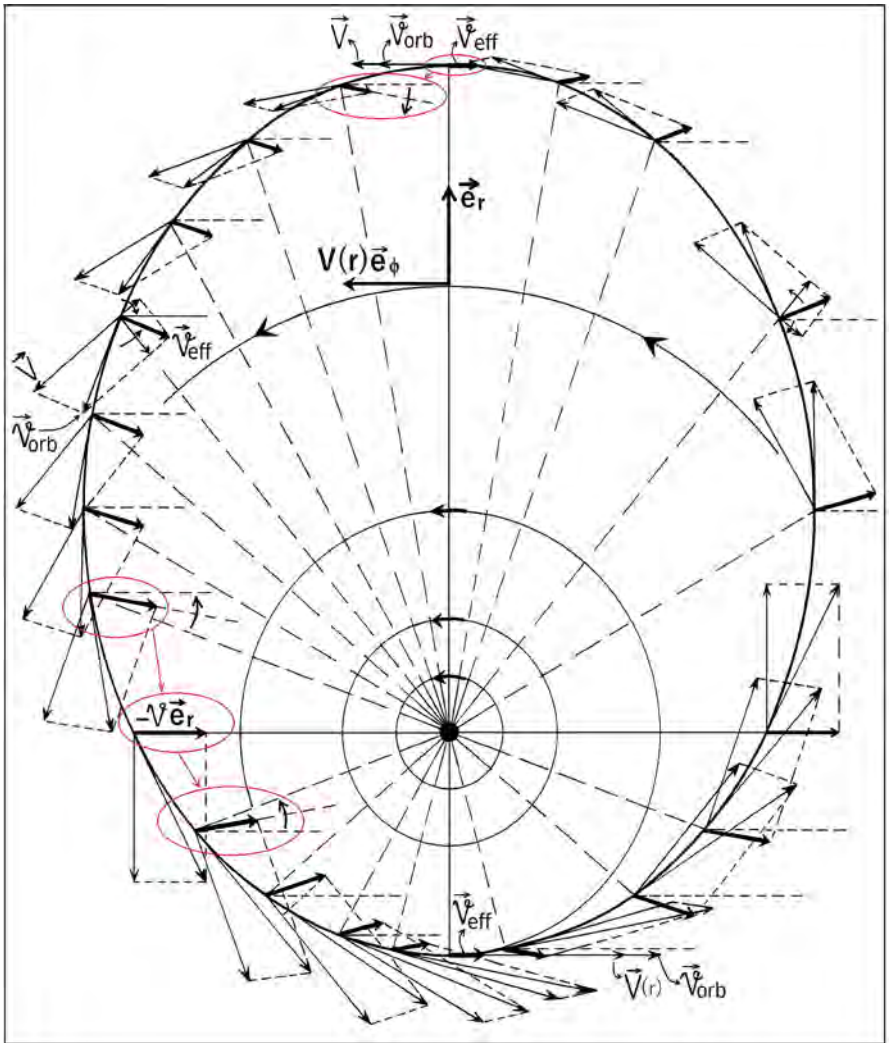

Figure 1. The figure is a very precise graphical representation. The velocity diagrams are shown at a large number of positions along the elliptic orbit, where v_{eff} is represented by the bulky arrows, pointing nearly toward the right. At the top, the rotation rate of the effective (implicit) $-\phi$ velocity component can be read. The rotation rate of the $-r$ velocity component can be read at the left. Please see the encircled diagrams.

velocity $V(r)$, given by Equation (5) and the effective velocity v_{eff}, determined by the equation $v_{eff} = \boldsymbol{V}(r) + \boldsymbol{v}_{orb}$ are plotted at a large number of points along the orbit. Please see carefully especially the encircled velocity diagrams. The obtained refraction rates of the $-r$, $-\phi$ and the $\pm\theta$ velocity components are:

$$\boldsymbol{W}_r(r) = -\frac{1}{2}\left[GM/r^3\right]^{1/2}\boldsymbol{e}_\theta \tag{6a}$$

$$\boldsymbol{W}_\phi(r) = +\left[GM/r^3\right]^{1/2}\boldsymbol{e}_\theta \tag{6b}$$

$$\boldsymbol{W}_\theta(r) = 0 \tag{6c}$$

Please note the opposite sighns in the rotation rates of the r and the ϕ velocity components.

The implicit velocity along $-\phi$ of the small particle of mass m stationary in the gravitational field, of a very much larger mass M is given by:

$$\boldsymbol{V}_{impl} = -(GM/r)^{1/2}\boldsymbol{e}_\phi \tag{7}$$

The refraction rate of this implicit velocity, according to Equation (6b), generates an instantaneous ordinary vertical downward acceleration given by:

$$\boldsymbol{g}(r) = W_\phi(r)\boldsymbol{e}_\theta \times V_{impl}(r)(-\boldsymbol{e}_\phi) = -GM/r^2\,\boldsymbol{e}_r \tag{8}$$

Equation (8) has exactly the form of a formal expression for centrifugal accelerations in a rotating reference and $\boldsymbol{g}(r)$ has clearly the nature of a centrifugal acceleration. It is a spherically symmetric field of *centrifugal accelerations* (by fictitious forces) toward the gravitational center.

A body hold fixed with respect to the ordinary space coordinates within the Keplerian velocity field Equation (5), in fact will be stationary with respect to a non-inertial reference that is *implicitly rotating* oppositely to the local (true) inertial reference, this last truly rotating in the ordinary space according to Equation (6b). Bodies, stationary within the non-inertial earth-based laboratories, necessarily are implicitly moving along circular paths within the local true rotating IR. This however they can do only under a *real upward centripetal force*. This implicit motion along a circular path is not free motion and also does not correspond to geodesic motion in the curved spacetime of GR. While according to GR a free-falling elevator is locally a proper inertial reference, according to the HQS dynamics it is moving along ϕ at a velocity $-(GM/r)^{1/2}$ with respect to the local HQS and hence cannot be a proper reference and also not a proper Lorentz frame. Clocks in such free-falling references are predicted to run slow and the velocity of light is predicted to be anisotropic.

Equation (8) is sufficiently precise only for free-fall along short distances. For large distances of free-fall of a small mass m in the field of a very large mass M, the following elementary linear differential equation must be solved:

$$\frac{\mathrm{d}\boldsymbol{v}(r(t))}{\mathrm{d}t} = \boldsymbol{A}\boldsymbol{v}_0 \tag{9}$$

where $\boldsymbol{\nu}$, is the column matrix of the (ordinary) r and the (implicit) ϕ velocity components of the effective velocity with respect to the local HQS:

$$\boldsymbol{\nu}(t)=\begin{pmatrix}\nu_r(t)\\ \nu_\phi(t)\end{pmatrix} \tag{10}$$

In Equation (9), $\boldsymbol{A}$ is the hyperbolic rotation matrix, defined in terms of the rotation rates, given in Equation (6):

$$\boldsymbol{A}=\begin{pmatrix}0 & W_\phi\\ -W_r & 0\end{pmatrix}=\begin{pmatrix}0 & W\\ \frac{1}{u}W & 0\end{pmatrix} \tag{11}$$

where $W=GM/r^3$ and $u=2M/(M+m)$, the value of which varies from 1, for $m=M$, up to 2 for $m\ll M$.

Dividing both sides of Equation (9) by $\boldsymbol{\nu}_0$, multiplying them by dt and integrating the left hand side from $\boldsymbol{\nu}_0$ to $\boldsymbol{\nu}$, develops into:

$$\log\frac{\boldsymbol{\nu}(t)}{\boldsymbol{\nu}_0}=\int_0^t A\left(r\left(t'\right)\right)\mathrm{d}t' \tag{12}$$

where Adt is an infinitesimal rotation round parallel axes. Equation (12) can be re-written in the exponential form as:

$$\boldsymbol{\nu}(t)=\exp\left[\int_0^t A\left(r\left(t'\right)\right)\mathrm{d}t'\right]\boldsymbol{\nu}_0 \tag{13}$$

Expanding the exponential in series and adding up the terms of the series from $n=0$ to $n=\infty$ results in:

$$\begin{aligned}\boldsymbol{\nu}(t)&=\sum_{n=0}^{\infty}\frac{1}{n!}\begin{pmatrix}0 & \Theta(t)\\ \frac{\Theta(t)}{u} & 0\end{pmatrix}^n\begin{pmatrix}\nu_r(0)\\ \nu_\phi(0)\end{pmatrix}\\ &=\begin{pmatrix}\cosh\left(\frac{\Theta(t)}{\sqrt{u}}\right) & \sqrt{u}\sinh\left(\frac{\Theta(t)}{\sqrt{u}}\right)\\ \frac{1}{\sqrt{u}}\sinh\left(\frac{\Theta(t)}{\sqrt{u}}\right) & \cosh\left(\frac{\Theta(t)}{\sqrt{u}}\right)\end{pmatrix}\times\begin{pmatrix}\nu_r(0)\\ \nu_\phi(0)\end{pmatrix}\end{aligned} \tag{14}$$

The value of $\Theta(t)$ can be computed by integration:

$$\begin{aligned}\Theta(t)&=\int_0^t W\left[r\left(t'\right)\right]\mathrm{d}t'\\ &=\int_{r_0^{\mathrm{CM}}}^{r^{\mathrm{CM}}}\left[\frac{GM}{\left(r^{\mathrm{CM}}+R^{\mathrm{CM}}\right)^3}\right]^{1/2}\frac{\mathrm{d}r^{\mathrm{CM}}}{\dot{r}^{\mathrm{CM}}}\\ &=-\sqrt{u}\cosh^{-1}\left[\frac{r_0^{\mathrm{CM}}}{r^{\mathrm{CM}}(t)}\right]^{1/2}\end{aligned} \tag{15}$$

Inversion of the final term of Equation (15) results in expressions for the hyperbolic cosines and sines:

$$\cosh\left(\frac{\Theta(t)}{\sqrt{u}}\right)=\sqrt{\frac{r_0^{\mathrm{CM}}}{r^{\mathrm{CM}}}}=\sqrt{\frac{r_0}{r}} \tag{16a}$$

$$\sinh\left(\frac{\Theta(t)}{\sqrt{u}}\right)=\sqrt{\frac{r_0^{CM}-r^{CM}}{r^{CM}}}=\sqrt{\frac{r_0-r}{r}} \tag{16b}$$

where the last equality is obvious. Using this result and noting that $\nu\, CM_\phi=\nu_\phi$, Equation (14) becomes:

$$\begin{pmatrix}\nu_r(t)\\ \nu_\phi(t)\end{pmatrix}=\begin{pmatrix}\sqrt{r_0/r}\sqrt{u(r_0-r)/r}\\ \sqrt{(r_0-r)/ur}\sqrt{r_0/r}\end{pmatrix}\times\begin{pmatrix}\nu_r(0)\\ \nu_\phi(0)\end{pmatrix} \tag{17}$$

The particular solution of Equation (9), for free fall of m in the field of M ($m\ll M$), on from r_0 and initial rest, where $\nu_r(t=0)=0$ and $\boldsymbol{\nu}_\phi(0)=\boldsymbol{V}_{impl}(r_0)=-(GM/r_0)^{1/2}\boldsymbol{e}_\phi$, the final solution of Equation (9) is:

$$\nu_r(t)\approx-\left[2\left(\frac{GM}{r(t)}-\frac{GM}{r_0}\right)\right]^{1/2}\boldsymbol{e}_r \tag{18a}$$

$$\nu_\phi(t)=-V_{impl}(r_0)\left[\frac{r_0}{r}\right]^{1/2}=-\left[\frac{GM}{r(t)}\right]^{1/2}\boldsymbol{e}_\phi \tag{18b}$$

Equation (18a) is just the well known expression for the observed vertical free-fall velocity on from rest at r_0, directly showing that the kinetic energy is equal to the difference between the final and the initial potential energies. Equation (18b) is just the implicit (imaginary) velocity as a function of the radial position r. This shows that the refraction rate of the radial velocity component just compensates for the increase of the velocity field as a function of the decrease of the radial coordinate. This assures that free-fall of the particle, on from rest, goes along a vertical (radial) path and hence assures conservation of the angular momentum about the gravitational center. Please observe that, for free-fall on from infinity ($r_0=\infty$), the vertical velocity $\nu_r(r(t))$ is exactly $\sqrt{2}$ times larger than the ϕ velocity, which arises directly from Equation (18) and accomplishes the Virial theorem.

7. Symmetry of the HQS Dynamics Gravitation with Orbital Motions

Consider free-fall experiments at the equatorial region of a rotating planet of radius R like earth rotating at an angular velocity ω in a direct or retrograde sense round the same axis as the Keplerian velocity field Equation (5). The effective velocity $\boldsymbol{\nu}_{eff}$ of such a particle, initially stationary near to the surface of a planet, will be given by:

$$\begin{aligned}\boldsymbol{\nu}_{eff}(\theta)&=\boldsymbol{V}_{impl}(R)+\boldsymbol{\nu}_{rot}(\theta)\\ &=-\left[(GM/R)^{1/2}\mp\omega R\sin\theta\right]\boldsymbol{e}_\phi\end{aligned} \tag{19}$$

where $\boldsymbol{\nu}_{rot}(\theta)=\omega R\sin(\theta)$ is the ordinary velocity, due to the planet's rotation that depends on the latitude via $\sin\theta$. The upper and lower signs are respectively for direct and or retrograde rotation of the planet.

However, rotation of the planet in the same sense as the Keplerian velocity

field of the HQS, gives rise to a trigonometric rotation rate of the effective velocity $\boldsymbol{v}_{eff}$ of the particle, due to the planet's rotation that adds up to the refraction rate, given by Equation (6b) and subtracts for retrograde rotation of the planet. The effective rotation rate of the *effective velocity vector* is:

$$\boldsymbol{\omega}_{eff}(\theta)=\frac{1}{R}\left[V_{impl}\pm(v_{rot})\right]\boldsymbol{e}_{\theta}=\left[\left(GM/R^{3}\right)^{1/2}\pm\omega\sin\theta\right]\boldsymbol{e}_{\theta} \quad (20)$$

where the same convention for the upper and the lower signs as in Equation (19) is used.

Considering the effective velocity (Equation (19) and the effective rotation rate (Equation (20), the effective gravitational acceleration on the planet's surface is:

$$\boldsymbol{g}_{eff}(\theta)=\boldsymbol{\omega}_{eff}\times\boldsymbol{v}_{eff}=-\left[GM/R^{2}-\omega^{2}R\sin^{2}\theta\right]\boldsymbol{e}_{r} \quad (21)$$

The first term in the right hand side of Equation (21) describes the gravitational acceleration toward the gravitational center of the planet in the static situation (see Equation (8)), while the second term is an outward centrifugal term. Most importantly, Equation (21) shows that the effective gravitational acceleration $\boldsymbol{g}_{eff}(\theta)$ in the rotating planet's Keplerian velocity field *is perfectly symmetric for direct or retrograde rotation and thus also for direct or retrograde orbital motion.*

For a body in a strictly circular polar orbit with orbital radius $r>R$, $\boldsymbol{v}_{eff}$ has velocity components along $-\phi$ as well as along $\pm\theta$. The velocity along $-\phi$ is:

$$\boldsymbol{v}_{\phi}=\boldsymbol{V}_{imp}(r)=-\left[GM/r\right]^{1/2}\boldsymbol{e}_{\phi} \quad (22)$$

Along *theta* the velocity is:

$$\boldsymbol{v}_{\theta}=\pm\left[GM/r\right]^{1/2}\boldsymbol{e}_{\theta} \quad (23)$$

While $\boldsymbol{v}_{\phi}$ generates the gravitational acceleration $\boldsymbol{g}(r)=-GM/r^{2}\boldsymbol{e}_{r}$, see Equation (8), the θ velocity component is not affected directly by the HQS-dynamics, because the velocity field Equation (5) has no velocity component along *theta*. However, the rotation rate of the ϕ velocity component plays the role of a centripetal force accelerating the body toward the gravitational center, bending the θ velocity toward the earth's surface. This in particular literally implements the idea of Newtonian gravitation. The effective gravitational acceleration for circular polar orbits is:

$$\boldsymbol{g}_{eff}(r)=-\left[GM/r^{2}-v_{\theta}^{2}/r\right]\boldsymbol{e}_{r} \quad (24)$$

where again the first term in the right hand side is the acceleration toward the gravitational center (please see Equation (8)), while the second term is the corresponding usual upward centrifugal effect.

Together the results, expressed by Equations (21) and (24), show that the effects of the HQS dynamics and the effects of the ordinary motion within the gravitational field are completely independent. They are orthogonal. While the

Keplerian velocity field of the HQS (Equation (5) simulates a central field of fictitious Newtonian gravitational forces, the ordinary orbital motions generate the centrifugal effects, exactly as conceived in Newtonian gravity. This shows that treating the motions, within a spherically symmetric gravitational field, as motions in a hypothetical inertial reference, extending over the whole region, under a hypothetical central field of *fictitious gravitational forces* although not corresponding to reality, gives closely the observed gravitational dynamics. This explains why the Newtonian gravitational theory, although based in the fictitious gravitational forces, works so well.

8. The Effects of the Keplerian Velocity Field of the HQS on Light and on Clocks

8.1. Effects in the Solar System

8.1.1. The Excess Time Delay of Radar Signals in Round-Trips within the Solar System

According to GR, massive astronomical bodies curve spacetime in their neighborhood, as given for weak fields by Equation (3) in the Introduction. This spacetime curvature bends light signals and lengthens the go-return round-trip path of electromagnetic (EM) signals passing by massive bodies, thereby giving rise to an excess time delay (Shapiro Effect). According to the present work the excess time delay is not caused by increase of the geometrical distances. It is due to the effective velocity of the signals in the Keplerian velocity field of the sun. In the case of round-trips between earth and Venus, the solar velocity field is favorable during the prograde travel, increasing the effective signal velocity and reducing the travel time. It however is unfavorable during the retrograde travels, decreasing the effective signal velocity and increasing the return travel time. The problem is totally analogous to that of light round-trips between two mirrors within a laboratory, moving with respect to the local HQS. However, in the solar Keplerian velocity field, the calculation is a little bit more complicated, because the velocity of the signal depends on position.

In the present work, the excess time delay was numerically calculated along straight line paths, separately for travels from earth to Venus and back from Venus to earth in terms of the effective velocity $v_{eff} = \boldsymbol{c}_{\mathrm{HQS}} + \boldsymbol{V}$, where $\boldsymbol{c}_{\mathrm{HQS}}$ is the fixed velocity of light with respect to the local moving HQS. This calculation was repeated for a series of paths, having minimum distances from the center of the sun R = 2, 4, 8, 25, 50 and 100 million km respectively. The calculations were made for these round-trips before and after superior conjunction. The excess time delays were calculated dividing the straight line paths into about 420 segments, shorter segments near to the sun, separately for transverse and longitudinal components of the solar Keplerian velocity field along the signal paths and finally integrated over the full path. More than 99% of the excess time-loss in the retrograde journeys or time-gain in the prograde journeys comes from the longitudinal component of the solar velocity field along the path. The different Earth-Venus

distances, due to the orbital positions as well as the slightly different signal path, due to the motion of earth during each signal round-trip, was taken into account. The obtained results are given in Table 1 and plotted in Figure 2.

Table 1. The first column in Table 1 gives the values of the nominal impact parameters R, the second and third columns give respectively the gain of time (negative) and the loss of time (positive), due to the solar Keplerian velocity field of the HQS in milliseconds (ms) before and after superior conjunction. The forth column gives the effective excess time-delays for full go-return round-trips in microseconds (μs).

R (10^6 km units)	go:Δt(ms)	return:Δt(ms)	Δt_{eff}(μs)
100	−51.987	51.999	12
50	−76.697	76.725	28
25	−70.007	70.056	49
8	−48.585	48.679	94
4	−36.699	36.833	134
2	−27.165	27.351	186
−2	27.351	−27.165	186
−4	36.833	−36.699	134
−8	48.679	− 48.585	94
−25	70.056	−70.007	49
−50	76.725	−76.697	28
−100	51.999	−51.987	12

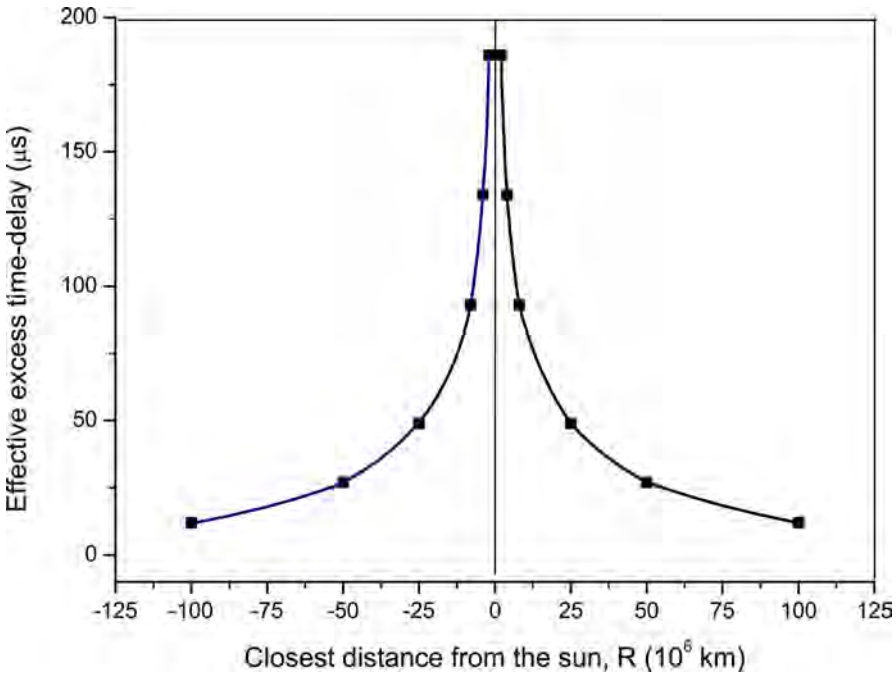

Figure 2. The calculated effective excess time delay, given in microseconds (μs), (fourth column in Table 1) for complete go-return round trips. The calculated data curves practically coincide with those, obtained by Shapiro ref. [20].

The fact that the Keplerian velocity field of the HQS round the sun correctly produces the effective excess time delay (Shapiro effect) fully corroborates the present HQS-dynamics gravitational mechanism.

8.1.2. The Gravitational Light Lensing Effect

Consider two light beams, coming from two distant stars and propagating toward the sun along two parallel paths as shown in Figure 3. First, in the region where the velocity of light c has almost only a radial component, the wave vectors of the two beams will be refracted according to Equation (6a) by a total angle $+\alpha$, thereby the light beams gaining a small velocity component $V(r) = -(GM/r)^{1/2}$ along $-\phi$. This component cancels the drag by the solar velocity field. This however reduces the radial velocity component c_r to $c_r = \left(c_{\mathrm{HQS}}^2 - V^2\right)^{1/2}$. Near to the sun, where the solar velocity field achieves 436 km/sec and is mostly parallel (left in Figure 3) and anti-parallel (at the right) to the beams, refraction by Equation (6b) is dominant and the wave vectors are refracted oppositely by a total angle -2α. Finally, after having passed by the sun and going away in the opposite side, the wave vectors again are refracted according to Equation (6a) by nearly an angle $+\alpha$. However, near to the sun, the solar velocity field is favorable to the prograde ray (left) so that it spends less time near to the sun and hence is refracted by a smaller angle $-(2\alpha - \delta)$. To the retrograde ray however (right) the solar velocity field is unfavorable and hence it spends a longer time near to the sun and refracts by a larger angle $-(2\alpha + \delta)$. This differentiated refractions by δ, due to Equation (6b) causes a (symmetric) convergence of the rays that is responsible for the gravitational light lensing effect.

The value of δ can be calculated simply by multiplying the refraction rate Equation (6b) times the excess (or shortage) of time delays Δt, listed in Table 1.

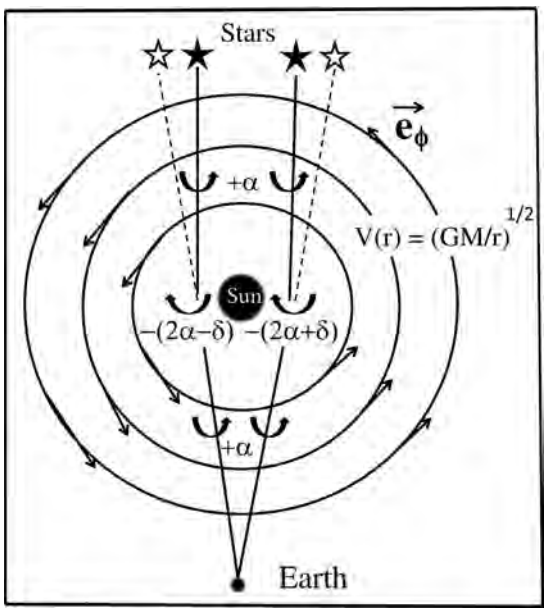

Figure 3. Gravitational light-lensing effect, by a heavy mass (Sun).

On the solar surface $R = 6.9565 \times 10^8$ m and the refraction rate, given by Equation (6b), is $W_\phi \sim 0.0359$ deg/sec. Interpolating the value of Δt in Table 1 for light passing by the surface of the sun, we find the excess time delay at the retrograde side or the shortage of time at the prograde side of closely $\Delta t = \pm 13.5$ ms. The product $W_\phi \times \Delta t$ gives $\delta = 1.745$ arcsec, which is very closely the observed deflection angle, causing the convergence of light passing close by the solar surface.

8.1.3. The Non-Synchronous Arrival of the Pulsar Signals to Equidistant Earth-Based Antennas along the Earth's Orbital Motion

Imaging astronomical objects with the help of interferometric methods can improve the images by orders of magnitude. To this end, it is necessary that the signals from the different receivers be synchronous, which is achieved with the help of the GPS clocks. However, on testing the, so synchronized clocks, by the arrival of the millisecond pulsar signals, there was a surprise. While the arrival of the pulsar signals to the antenna arrays along directions transverse to the earth's orbital motion was synchronous, along the orbital motion of earth the arrival was out of synchrony, up to 4.2 μsec refs. [13] [14].

The aberration of star light is an old and well known feature in astronomical observations from earth. Usually the aberration angle is explained in terms of the orbital velocity of earth $\sin\beta = V/c$. However, according to the present work, this aberration contains an additional feature that arises from the refraction rate Equation (6a) of light propagating from distant objects toward the sun. This refraction rate creates a velocity component of the light signal toward $-\phi$ and thereby reduces the radial velocity component to $c_r = \left(c_{\mathrm{HQS}}^2 - V^2\right)^{1/2}$. Correspondingly it slants the wave fronts by and angle β, so that the wave fronts reach first the leading part of earth and only 4.2 μsec later the rear part.

8.1.4. The Perihelion Precession

An analogous differentiated refraction rate of the propagation velocity $\boldsymbol{v}$ of an orbiting body as in the preceding **Section 8.A3** must be responsible for the perihelion precession of elliptical orbits. At the perihelion $\boldsymbol{v}_{eff}$ is parallel to the velocity field (prograde) and to the orbital velocity, which displaces it more rapidly (than the HQS), so that it has not time enough to recover the tangential direction. It recovers it only somewhat beyond the ideal perihelion point. In this way the perihelion advances a little bit in the prograde sense in each orbital round-trip.

8.1.5. Absence of Effects of the Solar Gravitational Field on the GPS Clocks

In the view of the present HQS-dynamics gravitational mechanism, the slowing of clock rates is caused by velocity with respect to the local HQS and not by relative velocity. Hence, clocks, stationary with respect to the local moving HQS, do not run slow. They show proper time as confirmed by the GPS clocks. The effective velocity of the GPS clocks, moving with earth round the sun, is zero with respect to the local moving HQS because earth is commoving with the local HQS

in the Keplerian velocity field, creating the solar gravitational field. The effective velocity is given by:

$$\boldsymbol{v}_{eff} = \boldsymbol{V}(r) - \boldsymbol{v}_{orb} \cong (GM/r)^{1/2}\boldsymbol{e}_{\phi} - (GM/r)^{1/2}\boldsymbol{e}_{\phi} \approx 0 \tag{25}$$

All clocks orbiting in circular equatorial orbits round an astronomical body, which normally is moving itself in a direct circular equatorial orbit round a larger body (star or galaxy), are stationary with respect to the local HQS (local LFs). Such clocks all are naturally synchronous with respect to each other and all show closely the same proper time throughout the universe.

8.2. Effects of the Earth's Field

8.2.1. The One-Way Light Velocity between Artificial Satellites

In order to measure the one-way velocity of light, it is necessary to have well synchronized clocks at each end of the one-way travel distance. Actually the atomic clocks in orbit can be synchronized by Einstein's method down to 0.1 ns (time for light to propagate 3 cm). This synchronization is especially favorable for clocks along polar orbits. The most precise measurement of the one-way velocity of light was achieved with the help of atomic clocks in the robotic twin satellites of the GRACE project, moving both in the same polar orbit at 500 km of altitude and separated by ~200 km. In order to measure microgravity effects, these clocks need to be synchronized always to better than 0.16 ns. Continuous exchange of EM signals between these satellites, in both senses, has revealed a clear anisotropy of the signal velocity of nearly 8 km/sec, *backward to the motion of the satellites* the same velocity as the orbital velocity of the satellites. [15] This observation evidences that a spatial medium (HQS) propagating the EM signals (light) exists and that it has no relevant velocity along polar orbits. The immediate consequence of this observation is the need of finding out a new interpretation for all the light anisotropy experiments performed in the past century. The next **Section 8.B2** implements this.

8.2.2. The Michelson Light Anisotropy Experiments

The large majority of the Michelson experiments, searched for light anisotropy due to the orbital and cosmic motion of earth. They all found closely null results. This confirms that the orbiting earth is very closely stationary with respect to the local HQS as also evidenced by the absence of the gravitational slowing of the GPS clocks by the solar field. These null results also show that the solar system is stationary in the velocity field of the HQS, generating the gravitational dynamics of the Milky-Way galaxy and that our galaxy is stationary with respect to the HQS, despite the accelerated expansion of the universe.

From the view of the HQS dynamics, the only motion, that causes relevant anisotropy of the light velocity with respect to the earth-based laboratories, is the local velocity field of the HQS round earth itself in the sense of the Moon's orbital motion and creating the earth's gravitational field. On the earth's surface this velocity reaches 7.91 km/sec. This predicts light anisotropy on earth of

somewhat less than 8 km/sec, a second order effect of only 10^{-10}, *constant the whole day and the whole year* and therefore extremely difficult to be detected. Several light anisotropy experiments using laser cavities obtained null results. The small laser cavities are intrinsically unable to detect such low anisotropies, due to their quantized modes. Only a few of the Michelson light anisotropy experiments with the highest sensitivity and *rotating within the earth-based laboratories* have detected such small anisotropies, constant the whole day and the whole year. **Figure 4** displays Miller's results. [19]

82.3. Gravitational Time Dilation and Gravitational Spectral Red Shifts

The gravitational slowing of atomic clocks *stationary in the earth's gravitational field* and the gravitational spectral red-shifts of atoms are now well confirmed experimentally refs. [3] [21] [22]. To first order, these effects are proportional to $(GM/r)/c^2$. On the earth-surface their effect is extremely small, in the order of 10^{-10} and, excepting by Massbauer resonance scattering, are very difficult to be detected.

8.2.4. Gravitational Slowing Of Clocks in Direct Circular Equatorial Orbits Round Earth

According to the present work, slowing of the clock rates is caused by velocity with respect to the local HQS (LFs) and not by relative velocity. The gravitational slowing of the GPS clocks by the solar field, predicted by GR, is absent. These clocks display proper time, because they are stationary with respect to the local moving HQS in the Keplerian velocity field, creating the solar gravitational field. Analogously, clocks, moving in direct circular equatorial orbits round earth, too are stationary with respect to the local HQS in the Keplerian velocity field, creating the earth's gravitational field and too must display proper time. The orbital velocity of the geosynchronous satellites in direct circular equatorial orbits round earth, with an orbital radius of 42,224 km move at nearly 3.1 km/sec. Clocks in these satellites are stationary with respect to the local HQS and hence show proper time. Unhappily, to present date such an experiment is not known.

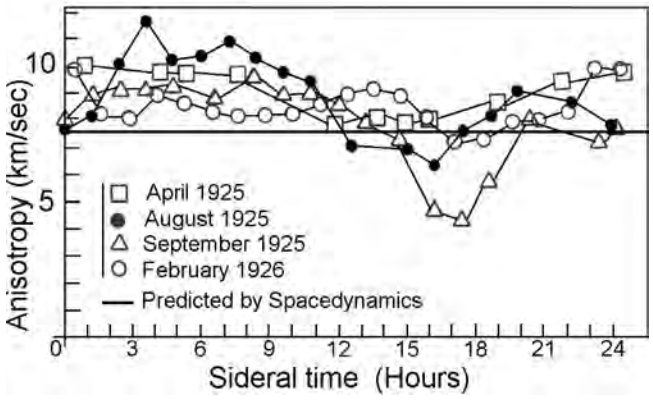

Figure 4. The Nearly West-East light anisotropy, with respect to the earth-based laboratories, obtained 1925 and 1926 by D. Miller that is nearly constant the whole day and the whole year.

8.2.5. Effects of the Velocity Field of the HQS on Clocks Moving in *Non-Equatorial* Circular Orbits Round Earth

In the view of the present work, clocks in direct circular equatorial orbits show proper time. However, clocks in circular polar orbits round earth are slowed two times more than a clocks stationary at the same altitude and clocks in retrograde circular equatorial orbits are slowed four time more than a clock stationary at the same altitude. In particular the GPS satellites move at 2.02×10^4 km of altitude, along non-equatorial circular orbits *inclined* 55 *degrees with respect to the earth's equator* and hence have a considerable velocity with respect to the local HQS in the Keplerian velocity field, creating the earth's gravitational field. The GPS clocks have velocity components, given by $v_0(1-\cos\alpha)$ along $-\phi$ and $v_0\sin\alpha$ along $\pm\theta$, where $v_0 = 3.87$ km/sec and α is the angle of the orbital velocity v_0 with respect to the equator or parallels. The effective velocity at the equator is $v_0\left[2(1-\cos\alpha)\right]^{1/2} = 3.574$ and the estimated average velocity of the GPS satellites with respect to the local HQS over the entire orbit is $\sim 0.8\times3.574 = 2.86$ km/sec. Analogously the Westward velocity of the earth-based station at Colorado highs with respect to the local HQS is about 7.4 km/sec. In addition, the velocity of the Cs atoms of 0.255 km/sec within the atomic clocks as well as a small transverse Doppler shift, due to the implicit velocity of the earth-based stations with respect to the local HQS must be considered. Altogether these effects achieve closely the observed 4.5×10^{-10} sec/sec. ref. [3].

8.2.6. Drag of Neutrinos and Light toward the East by the Earth's Keplerian Velocity Field

From the HQS-dynamics view, the velocity of light in the vacuum has a fixed value ($c = 299792458$ m/sec) *with respect to the local HQS* and not with respect to all the possible inertial references. The velocity of neutrinos is almost equal to the light velocity. Light and neutrinos are dragged, within gravitational fields, by the respective Keplerian velocity fields of the HQS. In the earth's Keplerian velocity field Equation (5), the velocity of the HQS moves from West to East and achieves $V = 7.91$ km/sec on surface. This velocity adds up to the velocity of light and of the neutrinos, giving an effective velocity, given by $c' = \boldsymbol{c}+\boldsymbol{V}$, turning their velocity with respect to earth-based laboratories anisotropic. This is a fundamental prediction of the HQS dynamics gravitational mechanism.

In the neutrino experiment from CERN-Geneva-CH to OPERA-Gran Sasso-IT, the neutrinos speeded under-ground along a straight path of 730 km, making 58 degrees with the Meridians. In this case, the component of the earth's velocity field of the HQS adds 6.716 km/sec to the presumed light velocity in vacuum. This is almost exactly the excess velocity found by the neutrinos team from CERN and gives an effective velocity of $c' = 299799174$ m/sec. Therefore, the neutrinos are predicted to reach the OPERA Lab ~55 ns earlier than presumed for light by the current theories. *This however, does not break the light postulate*. Light, along the same path (in vacuum) too would reach ~55 ns too early to the OPERA Lab.

In 2011 neutrinos from CERN were announced to reach too early to the OPERA Lab by very nearly 60 ns. This however was interpreted as a faster than light velocity, without any reasonable justification [23]. Later the data were withdrawn because of conflict with the light postulate [24]. From the view of the present work, this too early arrival must be correct and does not break the light postulate.

Actually this affair is in standby, waiting for a final verdict. New experiments are in course, also in the USA, in which neutrinos will be shut from the Fermilab (Chicago) to Stanford (South Dakota), distant 1300 km *toward the West*. These neutrinos thus will speed in the opposite sense of the earth's Keplerian velocity field of the HQS that creates the earth's gravitational field. In this case the neutrinos are predicted to reach Stanford *more than* 115 *ns too late*. However, light along the same path (in vacuum) too is predicted to reach too late by the same 115 ns.

If the predicted one-way anisotropy of the neutrinos is confirmed, this experiment, besides the many others, described above in the previous Sections, will turn the HQS dynamics an incontestable reality and constitute it into a top scientific achievement, rivaling in relevance with the discovery of the heliocentric system.

8.2.7. The Astronomical Motions Closely Track the Motion of the HQS throughout the Universe

The planetary orbits lie all closely within the equatorial plane of the solar Keplerian velocity field of the HQS and the orbit of the solar system lies closely within the equatorial plane of the galactic velocity field of the HQS. This orbital configuration minimizes the velocity of the astronomical bodies with respect to the local HQS. Wavelength stretching during the concomitant expansion of the HQS and of the universe reduces the kinetic energy of particles and the energy of radiation with respect to the local HQS, which is well demonstrated by the cosmic microwave background radiation. Moreover, the averaging down of random velocity, during gravitational agglomeration of matter into large matter bodies too reduces the velocity, momentum and kinetic energy of the particles with respect to the local HQS, converting it in heat. Visibly not only the planets of the solar system, not only the solar system in the Milky-Way galaxy, however astronomical bodies in general throughout the universe are very closely stationary with respect to the local HQS in the respective gravitational fields. This predicts the universality of the laws of physics.

8.2.8. Gravitational Waves

The occurrence of gravitational waves was predicted by Einstein's GR. HQS dynamics predicts that binary systems naturally emit gravitational waves. However, the amplitude and frequency of usual binary stars are very low. Binary merges of neutron stars and black-holes however generate amplitudes and frequencies that are observable. In the black-holes the velocity of the HQS in the velocity fields $(GM/r)^{1/2}$, creating the respective gravitational fields, achieves the velocity of

light. In 2016, one century after Einstein's prediction, the occurrence of gravitational waves, generated by the merge of a black-hole binary, finally confirmed Einstein's prediction [25].

9. Final Comments and Conclusions.

The HQS is a macroscopic quantum state of bosons, ruled by the principles of quantum physics. It plays a fundamental role in the microscopic quantum world giving mass and ruling the motion of the elementary particles. It plays a fundamental role in the macroscopic world of gravity too, where a Keplerian velocity field of the HQS Equation (5) implements the outside-inside spherical centrifuge mechanism of gravity that creates the centrifugal effects pulling matter toward the gravitational centers. This ingenious centrifuge mechanism governs the gravitational dynamics on earth, in the solar system and throughout the universe. It too predicts the non-Keplerian galactic gravitational dynamics, without the need of dark matter [26]. The HQS dynamics opens the way to the unification of all the force fields. In the scenario of the HQS dynamics, the astronomical bodies, throughout the universe, are all very closely stationary with the local HQS in the velocity fields creating the respective gravitational fields, which predicts the universality of the laws of physics. The macro physics of the HQS too governs the global dynamics, the accelerated expansion of the universe [12]. Without the presence of the HQS, the matter universe simply would not exist. The HQS literally creates and governs our universe.

Conflicts of Interest

The author declares no conflicts of interest regarding the publication of this paper.

References

[1] Laue, M.V. (1955) *Annalen der Physik*, **38**.

[2] Lorentz, H.A., Einstein, A., *et al.* (1923) The Principle of Relativity. Dover Publications, New York.

[3] Ashby, N. (1996) Mercury, 23-27.

[4] Bailey, H., Borer, K., Combley, F., Drumm, H. and Krienen, F. (1977) *Nature*, **268**, 301-305. https://doi.org/10.1038/268301a0

[5] Anderson, P.W. (1963) *Physical Review Journals Archive*, **130**, 439. https://doi.org/10.1103/PhysRev.130.439

[6] Meissner, W. and Ochsenfeld, R. (1933) *Naturwissenschaften*, **21**, 787-788. https://doi.org/10.1007/BF01504252

[7] Ginzburg, V.L. and Landau, L.D. (1950) *Journal of Experimental and Theoretical Physics* (*JETP*), **20**, 1064.

[8] Higgs, P.W. (1964) *Physical Review Letters*, **13**, 508. https://doi.org/10.1103/PhysRevLett.13.508

[9] Englert, F. and Brout, R. (1964) *Physical Review Letters*, **13**, 321. https://doi.org/10.1103/PhysRevLett.13.321

[10] Carrol, S.M. (2000) arXiv:astro-ph/0004075v

[11] Sola, J. (2013) arXiv:1306.1527v3 [gr-qc]

[12] Schaf, J. (2017) *Int. J. of Adv. Res. in Phys. Sc.*, **4**, 1.

[13] Hatch, R.R. (2004) *GPS Solutions*, **8**, 67-73. https://doi.org/10.1007/s10291-004-0092-8

[14] Hatch, R.R. (2004) *Foundations of Physics*, **34**, 1725-1739. https://doi.org/10.1007/s10701-004-1313-2

[15] Hatch, R.R. (2007) *Physics Essays*, **20**, 83-100. https://doi.org/10.4006/1.3073811

[16] Schaf, J. (2018) *Journal of Modern Physics*, **9**, 1111-1143. https://doi.org/10.4236/jmp.2018.95068

[17] Schaf, J. (2018) *Journal of Modern Physics*, **9**, 395-418. https://doi.org/10.4236/jmp.2018.93028

[18] Schaf, J. (2018) *Journal of Modern Physics*, **9**, 2125-2134. https://doi.org/10.4236/jmp.2018.912133

[19] Miller, D.C. (1933) *Review of Modern Physics*, **5**, 203. https://doi.org/10.1103/RevModPhys.5.203

[20] Shapiro, I.I., *et al.* (1971) *Physical Review Letters*, **26**, 1132. https://doi.org/10.1103/PhysRevLett.26.1132

[21] Pound, R.V. and Snider, J.L. (1965) *Physical Review B*, **140**, B788. https://doi.org/10.1103/PhysRev.140.B788

[22] Brault, J.W. (1963) *Bulletin of the American Physical Society*, **8**, 28.

[23] Adam, T., *et al.* (2011) arXiv:1109.4897v2 [hep-ex].

[24] Adam, T., *et al.* (2012) arXiv:1109.4897v4 [hep-ex].

[25] Abbott, B.P., *et al.* (2016) *Physical Review Letters*, **116**, Article ID: 061102. https://doi.org/10.1103/PhysRevLett.116.061102

[26] Schaf, J. (2018) *Journal of Modern Physics*, **9**, 1883-1905. https://doi.org/10.4236/jmp.2018.910119

Scientific Research Publishing

Journal of Modern Physics, 2019, 10, 256-280
http://www.scirp.org/journal/jmp
ISSN Online: 2153-120X
ISSN Print: 2153-1196

The Meaning of Motions and Their Effects in Einstein's Empty Space and in the Scenario of the Higgs Quantum Fluid Space

Jacob Schaf

Physics Institute UFRGS, Porto Alegre-RS, Brazil
Email: schaf@if.ufrgs.br

How to cite this paper: Schaf, J. (2019) The Meaning of Motions and Their Effects in Einstein's Empty Space and in the Scenario of the Higgs Quantum Fluid Space. *Journal of Modern Physics*, **10**, 256-280.
https://doi.org/10.4236/jmp.2019.103018

Received: January 27, 2019
Accepted: March 4, 2019
Published: March 7, 2019

Abstract

Motion is a ground-laying concept in physics. Its meaning however depends fundamentally on the assumptions about the nature of empty space. In Einstein's theory of relativity (TR), no absolute references can be defined and only relative motions are relevant. This however makes it impossible to understand why the motion of matter obeys the principle of inertia and why there exist laws of motion. The Higgs theory introduces radical changes in the current view about the nature of empty space. It introduces the idea that space is filled up by a real and very powerful quantum fluid medium, giving mass to the elementary particles by the Higgs mechanism. This Higgs Quantum Space (HQS) is locally an absolute reference for rest and for motions. It not only recovers an intrinsic meaning for motions, however literally governs the inertial motion of matter-energy. In this new scenario, the velocity of light is fixed with respect to the local HQS and velocity of matter with respect to the local HQS and not relative velocities are responsible for all the effects of motion. The Higgs mechanism is too responsible for the gravitational dynamics; because it is mass that creates the gravitational fields. Actually several clear experimental observations demonstrate that the HQS is moving round the sun consistently with the planetary motions. The present work therefore replaces Einstein's spacetime curvature by a Keplerian velocity field of the HQS. This velocity field creates the ingenious outside-inside centrifuge mechanism of gravity. It also causes all the observed effects of the gravitational fields on light and on clocks.

Keywords

Applied Physics in Gravitation, Gravitational Fields, Gravitational Effects, Gravitation in the Solar System, Higgs Quantum Space in Gravitation

1. Introduction

The first query about the meaning of motions came about from the fact that local mechanical experiments cannot detect uniform rectilinear motion of the laboratory reference, which is known as Galilean invariance of the laws of mechanics. In Einstein's view, the null results of the light anisotropy experiments demonstrate that local electromagnetic experiments cannot reveal the motions of the earth-based laboratories, too. In the Special Theory of Relativity (STR), Einstein generalized this conclusion, postulating that the laws of physics are all invariant with changes of the reference, which he named Principle of Relativity. In order to implement this assumption, he postulated the intrinsic constancy and isotropy of the velocity of light with respect to every possible inertial reference, which, in his view, is confirmed by the null results of the light anisotropy experiments. With base in these facts, Einstein rejected the Aether theories and concluded that empty space contains nothing that can represent a reference for rest and for motions and or be a medium of propagation for light. Motions have no intrinsic meaning. Only relative motions are relevant in physics and only they cause physical effects. In this way, the STR has reduced motions to simple changes in the spatial configuration of reference points as a function of time.

In the absence of a natural reference for rest and for motions, each observer can simply consider him to be hypothetically stationary and define his own proper reference frame, in which stationary clocks show proper time and meter sticks have proper lengths. In Einstein's view, a hypothetical stationary observer can compare the rate of his clocks and the length of his meter sticks with the rate of moving clocks and the length moving meter sticks. He textually writes [1] [2] that, if the velocity of light is isotropic in the reference of the hypothetically stationary observer, it cannot anymore be isotropic, *from the view of this stationary observer*, in a relatively moving reference. Otherwise, the principle of the constancy of light velocity would be broken. However, anisotropic velocity of light, in the moving reference, is well-known to inexorably lead to an increase of the light go-return round-trip time between two mirrors. In order to make it possible at all that measurements of the velocity of light in the moving reference, by the method of light go-return round-trips and clock, to give the same value as in the hypothetically proper reference, Einstein introduced the idea that, *from the view of the stationary observer*, clocks in the moving reference run slow in exactly the same proportion as the light go-return round-trip times. Moreover, in order for the moving observer to find light to be isotropic in his reference, Einstein added, apparently motivated by the null results of the Michelson light anisotropy experiments, that distances, in the moving reference, are shortened along the direction of motion exactly in a proportion to make the light round-trips to appear isotropic. From this generic thought experiment, Einstein concluded that relatively moving clocks run slow, moving meter sticks are shortened and postulated that the observed velocity of light is a universal constant c that is intrinsically isotropic in any possible inertial reference. He also

concluded and postulated that the laws of physics, discovered in one inertial reference, are good in any other inertial reference, which is the Principle of Relativity.

If the observer in a proper reference defines a rectangular Cartesian coordinate frame (x, y, z), and a time axis t, the changes in the spacetime coordinates, for relative velocity v along the x axis are described by the famous Lorentz transformations:

$$x' = \frac{x - v_r t}{\sqrt{1 - v_r^2/c^2}} \tag{1a}$$

$$y' = y \tag{1b}$$

$$z' = z \tag{1c}$$

$$t' = \frac{t - v_r x/c^2}{\sqrt{1 - v_r^2/c^2}} \tag{1d}$$

where c is the velocity of light.

Within the scenario of the STR these Lorentz transformations reproduce well the observations *on earth*. They in particular, predict that a light pulse, emitted from the origins of a stationary and a moving reference frame, at the exact instant their origins coincide, propagates in both references as spherical wave fronts. Observations *on earth* apparently confirm well the predictions of the STR. However, if they reproduce the experimental observations in other situations *never has been tested*.

The STR has lead to many fundamental and very important discoveries that actually play part in the human life. However, the characteristic reciprocal symmetry between relatively moving observers leads to many unsolvable paradoxes, for which there are no experimental data to confront. From all the problems with the STR, the most serious shortcoming is the fact that it cannot give a satisfying explanation for the origin of the observed inertial behavior of the matter bodies. In the idle empty space of the STR, it is impossible to understand why matter bodies obey the principle of inertia and why they follow laws of motion. Einstein tried to justify the inertial mass in terms of *coupling of local matter to distant matter in the universe*, which however entails an arcane *instantaneous action from the infinite*. A scientifically sound explanation for the origin of the inertial behavior and the inertial mass of matter became known only 60 years later with the Higgs theory. This theory makes radical changes in Einstein's view about the nature of empty space assuming that space is filled up by a real quantum fluid medium.

Actually the atomic clocks in orbit can be synchronized by Einstein's method to within 0.1 ns, time for light to propagate 3 centimeters, which is precision enough to measure the one-way velocity of light. Several experimental observations, achieved with the help of such tightly synchronized atomic clocks in orbit, [3] reveal clear anisotropies of the velocity of electromagnetic signals (light) between the satellites. These observations constitute a conclusive verdict against

the postulate of the intrinsic isotropy of light. The coming **Section 3** gives details. Please see also Refs. [4] [5].

In the General Theory of Relativity (GR) [2] [6] Einstein has introduced the Principle of Equivalence, the equivalence of gravitational and inertial effects. With base in this principle, he extended the ideas of the STR to the physics within gravitational fields. By an ingenious thought experiment he discovered that gravitational fields cause time dilation (slowing of clocks). He imagined an atom in its ground state that after absorbing a photon of energy $E = mc^2$, where m is the relativistic mass of the photon, is lifted in the gravitational field by a working force to an altitude h. Due to the increased mass of the excited atom, the working force must work harder than for the same atom in its ground state. Thereby the excited atom gains an excess energy of mgh. At the higher altitude, the excited atom may relax emitting a photon with the correspondingly increased energy. This increased energy is the excitation energy of this atom at the higher altitude h. By this simple thought experiment, Einstein has demonstrated that a gravitational field lowers the atomic frequencies and slows the rate of clocks. For stationary clocks in sufficiently weak gravitational fields, Einstein obtained a gravitational time dilation, given by $t = t_0\left(1-2U/c^2\right)^{1/2}$, where $2U = 2GM/r$ is the square of the local escape velocity from the gravitational field, in which G is the gravitational constant and M is the mass of the gravitational source. Actually, the atomic clocks, *stationary* in the earth's field, corroborate very precisely the time dilation predicted by GR.

In order to explain the gravitational dynamics, Einstein has introduced the idea that the mass of large astronomical bodies significantly curve the geometry of spacetime in their neighborhood, causing a mix of space and time components. This curvature is expressed by his famous field equations for the metric tensor $g_{\mu\nu}$:

$$G_{\mu\nu} \equiv R_{\mu\nu} - \frac{1}{2} g_{\mu\nu} R = 8\pi G T_{\mu\nu}, \tag{2}$$

In this Equation $R_{\mu\nu}$ is the Ricci curvature tensor, R is the scalar curvature, $g_{\mu\nu}$ is the metric tensor of the space-time geometry, G is the gravitational constant and $T_{\mu\nu}$ is the mass-energy tensor. In this curved spacetime the path of force-free bodies (in orbit or in free-fall) follows geodesic lines. For weak gravitational fields the curved spacetime is approximately characterized by the invariant length of the line element ds, the square of which, in terms of spherical coordinates (r,θ,ϕ), is given by:

$$\mathrm{d}s^2 \approx \left[1-\frac{2U}{c^2}\right]^{-1} \mathrm{d}r_0^2 + r^2 \mathrm{d}w^2 - c^2\left[1-\frac{2U}{c^2}\right]\mathrm{d}t_0^2 \tag{3}$$

where w is the angular term. In this equation the coefficients $\left(1-\frac{2U}{c^2}\right)^{-1}$ and $-c^2\left(1-2U/c^2\right)$ are respectively the diagonal g_{11} and g_{44} components of the Schwarzschild metric tensor. [7] The last term of this equation expresses the gravitational time dilation as viewed by a stationary external observer, where

dt_0 is an infinitesimal time interval in the absence of a gravitational field. In the first term dr_0 is an infinitesimal interval of radial distances in the absence of a gravitational field. According to GR, due to spacetime curvature, the direction of the time axis is different outside and inside a gravitational field. This has the consequence that, from the view of an external observer, the rate of the time evolution of any physical process (clocks) within the field is lowered. The time axis has a space like component, which lets the time like component shorter than cdt_0. Moreover, due to the stretching of the radial distances, in the first term, the velocity of a light pulse, propagating, toward the gravitational center, will appear, from the view of an external observer, to apparently be decreasing. The velocity of light along r has a time like component.

In Einstein's view, *the effects of the gravitational acceleration*, in a free-falling elevator, are locally canceled. This is often alleged, with base in the principle of equivalence, to recover the situation of a proper reference in which *all the effects of the gravitational field* are locally canceled. [8] Free-fall certainly cancels locally the gravitational pull and the light bending. However, to present day, no experimental test proves that free-fall cancels the gravitational time dilation in a free-falling reference.

It is well known that, within a gravitational field, any free-falling reference, fulfilling locally the conditions of an inertial reference at a given point of space, is accelerated and non-inertial with respect to free-falling inertial references at all different points of space. References falling along the same radial coordinate recede from each-other at an accelerated rate and references falling along different radial coordinates approximate each-other at an accelerated rate. Therefore, if elevators fall freely from all different possible altitudes, their velocities, at a given spatial point r_0, have all the possible different velocities from zero up to the local escape velocity $(2GM/r)^{1/2}$. How can all these elevators with all so different velocities, at the same point of space, be proper references? The model of the free-falling references has another even much more serious trouble. It cannot give rise to the gravitational pull. The problem is that the velocity of the free-falling inertial references from the infinite has a constant value $(2GM/r)^{1/2}$ and a fixed direction *at any fixed point of space* r_0. A constant velocity with a fixed direction cannot give rise to an inertial pull. Within the context of the TR, obviously none of the free-falling references has an absolute character and none is preferential. *From the view of a stationary body at any given fixed point* r_0, *the acceleration* of the free-falling inertial references is locally zero ($dv/dt|r_0 = 0$). *The velocity is a function of r however not of time*. Therefore, anybody, brought to rest at any given point r_0 and then released, will remain stationary in an unstable equilibrium. Any perturbation however will initiate a runaway departure *upward or downward*.

The next **Section 2** introduces the scenario of the Higgs quantum fluid spatial medium, responsible for the mechanical properties of matter. **Section 3** shows that a Keplerian velocity field of this Higgs quantum space round the astronomical bodies creates an ingenious outside-inside centrifuge mechanism that gene-

rates the observed gravitational dynamics and gives rise to all the observed effects of the gravitational fields on light and on clocks. **Section 4** implements this centrifuge mechanism in the gravitational dynamics.

2. The Meaning of Motions in the Scenario of the Higgs Quantum Fluid Space

The Higgs theory [9] [10] introduces drastic changes in Einstein's view about the nature of empty space. In order to explain the origin of the inertial behavior of the elementary particles, the Higgs theory introduces the idea that space is filled up by a real quantum fluid spatial medium, giving mass and mechanical properties to the elementary particles by the Higgs mechanism. This Higgs Quantum Space (HQS) is much more than simply a reference for rest and for motions. It literally governs the motions of matter-energy. The Higgs mechanism is the perfect HQS analog of the Meissner effect in superconductivity that gives mass to the photons within superconductors [11]. Motion of the elementary particles in the HQS is propagation of confined wave mechanisms that has a well-defined intrinsic meaning. Motion of these wave mechanisms in the HQS involves a lot of physics that gives to the motions an absolutely different meaning than the dynamics of points in the empty space of the STR, in which there is nothing to which the elementary particles can couple and acquire inertial properties.

In the language of the Field Theories, the Higgs quantum fluid spatial medium arises from the breakdown of the electroweak symmetry immediately after the big-bang, caused by the scalar Higgs field, into the weak force doublet and the electromagnetic (EM) field. Subsequently, while the EM field has preserved its $U(1)$ symmetry, the weak-force doublet has spontaneously broken its $U(1)$ symmetry and, by a second order phase transition, has condensed into a macroscopic quantum fluid state, liberating an enormous amount of energy. The condensate has four components, two charged components with spin one, one chargeless component with spin one and one chargeless with spin zero. The three first components are responsible for the mass of the vector bosons $\left(W^+, W^-, Z\right)$ by the Higgs mechanism. The forth component, to be referred to by Higgs condensate or Higgs Quantum Space (HQS), remains free and is responsible for the mass of the quarks and leptons by an indirect Yukawa like mechanism. The purpose of the present work is not discussing details of the paraphernalia of the Higgs theory, however to implement its very important impact in the scenario of the universe. Note that without mass there is no linear momentum, no angular momentum and no matter universe.

Likewise usual quantum condensates, the Higgs condensate can be described by the usual macroscopic Ginsburg-Landau [12] like order parameter: $\Phi = \phi(r)\mathrm{e}^{i\theta}$ where $\phi(r)$ is an amplitude and $\mathrm{e}^{i\theta}$ is a phase factor. In the condensate the phase θ assumes a well-defined value θ_0 between zero and 2π. This order parameter is a macroscopic wave-function that describes collectively all the bosons of the condensate. It is important to note that, in quantum fluids, no clas-

sical motions can be considered. In the quantum fluids, the motions (flows) are governed by phase gradients of the order parameter, resulting in velocity fields of the condensate (probability currents). This is not so different from Fermions currents in the atomic orbitals.

The order parameter very strongly suppresses disordered and turbulent motions in the condensate. Moreover, even if the *curl* of the velocity field $\boldsymbol{V}(\boldsymbol{r})$ of the quantum fluid is non-zero ($curl\boldsymbol{V}(\boldsymbol{r}) \neq 0$), the flow can be inviscid and totally frictionless (laminar) up to a characteristic limit that depends on each quantum fluid. For instance, in superconductivity, the velocity in the velocity field (screening currents) of the superconducting condensate, confining and quantizing the local magnetic field by the Meissner effect, [13] falls exponentially with the radial distance from the quantized magnetic fluxons. The screening velocity field has a non-zero *curl* and despite this it is perfectly inviscid, laminar and frictionless. In the case of the HQS the zero viscosity holds up to a limit, given by the $(1/r)^{1/2}$ dependence, where r is the distance from the source.

In terms of the Real and Imaginary components of the order parameter, the characteristic form of the potential well, created in the spontaneous breakdown of the $U(1)$ symmetry of boson systems (superfluids, superconductors and also of the Higgs quantum fluid) has the form:

$$U(\rho) = -n\left(\Phi^{*}\Phi\right) + m\left(\Phi^{*}\Phi\right)^{2} \tag{4}$$

Figure 1 visualizes the characteristic form of the potential well of condensed bosons. In Equation (4), the value of the negative coefficient (-n) of the bonding term is considerably larger than the positive coefficient (+m) of the anti-bonding term. Therefore, the minimum of the effective potential energy occurs at a finite value $\Phi^{*}\Phi = n/2m$, which is known as a non-zero vacuum expectation value. Many properties of the different quantum condensates are closely analogous. They differ only by the properties of their constituent particles (bosons) and consequently the different fields that couple to them. The Higgs quantum fluid space is referred to as Higgs Quantum Space (HQS), because it forms the space in which the matter universe budges.

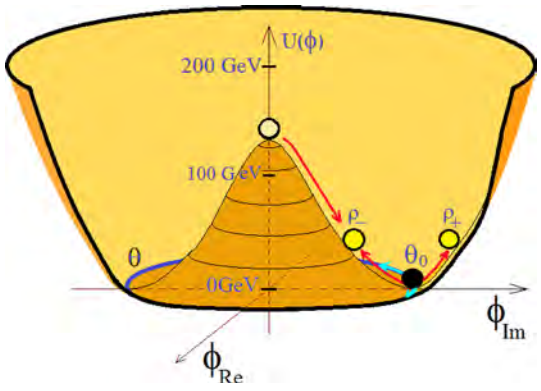

Figure 1. Characteristic potential well of Bose-Einstein Condensates: A red arrow indicates the transition toward the lower energy phase coherent state with the well-defined phase θ_0.

While the conventional quantum fluids (superfluids and superconducting condensates) are stabilized by a low energy gap of only about 1 meV (one millielectronvolt) and condense only at very low temperatures, the transition temperature of the Higgs begins shortly after the big-bang at about 10^{15} K and the condensate is stabilized by a huge energy gap, that, according to the Glashow-Weinberg-Salam electroweak model, achieves 200 GeV. [14] [15] The HQS is an extremely phase rigid and stable quantum fluid. However, likewise the usual quantum fluids, it is at the same time perfectly conservative. Only high energies, in the order of MeVs, can excite local Goldstone modes. However, once excited, these perturbations automatically become indefinitely persistent.

In the conventional and well-known quantum fluids, any local phase gradient causes motion of the condensate along the phase gradient at a velocity proportional to the magnitude of the phase gradient. For instance, an electromotive force difference, applied to the extremities of a superconducting wire, creates an increasing phase gradient along the conductor and an increasing super-current. However, once excited, the current automatically becomes permanently persistent. It can be stopped only by an opposite electromotive force.

Some people insist to call the Higgs quantum fluid spatial medium as quantum aether. In reality this Higgs Quantum Space (HQS) has nothing in common with the Maxwellian aether. The Maxwellian aether is an extremely tenuous hypothetical classical fluid, filling up the empty space. It is at the same time extremely frail and extremely rigid. In GR empty space (vacuum) is described in terms of the stress-energy tensor of a perfect (classical) fluid. A perfect fluid is a system of uncorrelated, well localized and distinguishable ideal particles. The physics of a perfect fluid is a many-body problem. In the Standard Elementary Particle Model, the empty space (vacuum) is described in terms of a nearly infinite number of oscillators. The zero-point energy (vacuum state) of these oscillators leads to the scandalous vacuum energy density that is 120 decimal orders of magnitude larger than shown by observations [14] [15].

The HQS, far from a perfect (classical) fluid, is a macroscopic quantum state of very strongly correlated bosons with spontaneously broken $U(1)$ symmetry and condensed into a highly phase coherent and extremely rigid macroscopic quantum ground state. This condensate is an integrated system, a one body problem, ruled by an extremely powerful Ginsburg-Landau [12] like order parameter. Therefore, the HQS very strongly suppresses the quantum fluctuations and the zero-point energies of the various force fields, turning their contribution to the vacuum energy density irrelevant. The HQS may be conceived as one unique oscillator the size of the universe where the frequency of the Higgs modes tends to zero (takes cosmological eras) and the wave-length tends to the infinite. In this scenario, the universe must be conceived as an adiabatic system, in which the *total energy* (the condensation energy of the Higgs condensate) is conserved. Actually this energy is composed of the residual condensation energy that still has not been converted into other forms of energy and the energy, due to the ordinary matter. Ordinary matter holds back the advance to the minimum

energy in the Higgs potential well Equation (4), analogously as a strong magnetic field holds back the superconducting condensate from its advance to the minimum of energy. In the ground state, the amplitude of the Higgs order parameter is intrinsically very closely constant and the density $\rho = \Phi^* \Phi = \phi^2$ of the condensate is intrinsically highly uniform throughout the volume of the universe, which may solve the horizon and flatness problems of cosmology.

The HQS (Higgs quantum fluid, filling up the whole of space) confines and quantizes the elementary particle fields, giving them inertial mass by a direct or indirect Higgs mechanism. This mechanism is the perfect HQS analog of the Meissner effect in superconductivity. The EM field that couples to the EM vacuum fluctuations does not couple to the HQS and is not confined by the HQS. It remains long-range and the photons have no rest mass in free space. If the HQS gives inertial mass to the elementary particles, it necessarily governs the inertial motion of matter-energy and is *the local ultimate*, *locally absolute and local preferential reference for rest and for motions*. The HQS *materializes the local Lorentz frames* (*LFs*) *into local proper LFs*, *intrinsically stationary with respect to the local HQS*. In this scenario, an observer cannot anymore arbitrarily define his proper reference. The local proper references are intrinsically defined by nature, by the local HQS itself. An observer will be in a proper reference only if he is stationary with respect to the local HQS. This will be seen to be very closely the situation of the planets in the solar system and also is the case of the solar system in the Milky-Way galaxy and in the case of galaxies in general throughout the universe. *This is the true reason of the isotropy of light with respect to earth and of the universality of the laws of physics* [4] [5] [16].

The physical mechanism creating the inertial mass of a field that couples to a quantum condensate is intimately related with the field confining mechanism. In superconductors of type II, the solenoidal vector potential of the magnetic field that couples to the charged superconducting condensate, induces solenoidal phase gradients in the order parameter and, consequently, solenoidal quantized screening currents, the Lorentz forces of which thrust and compress the magnetic field into quantized flux quanta. The inertial behavior of these field quanta (Photons) is due to the fact that their acceleration, within the condensate, needs to create asymmetries in the phase gradients of the order parameter, generating additional screening currents that too are perfectly persistent. This persistence is the origin of their inertial behavior. Quantum fluids have the characteristic property by which any motion and any dynamics, excited in them, is perfectly persistent, giving rise to the inertial behavior. A superconductor also can develop macroscopic screening currents in the border of a superconducting piece. The Lorentz forces, generated by these screening currents, expel the magnetic field (magnetic fluxons) out from the superconductor, because this lowers the effective energy of the superconducting condensate. It also is observed that quickly cooling down a bulky superconductor (from outside), its temperature lowers non-homogeneously and the sample becomes superconducting in the border layer before its interior. In this process the magnetic field is swept inward

and compressed, letting place behind for additional magnetic flux to penetrate from outside. This is the well-known and intriguing high field paramagnetic Meissner effect of superconductors [17]. The magnetic flux compression in this situation is quite similar to the gravitational compression of the matter fields into astronomical bodies that are bubbles of weakened Higgs order parameter. The different topologies in the Meissner effect and in the Higgs mechanism arise from the different ranking of the confined fields.

Internal circulation of quantum fluids can in no way be conceived as classical motions. In quantum physics even the motion of individual particles must be conceived in terms of the propagation of modulated wave-packets. The motion of such wave-packets or wave-functions has locally a wave character; however it too has classical aspects in the measure the wave-packet is localized in a finite region of space, which is the particle character. This is the wave-particle duality. Note that even a superconductor, if it is localized within a finite region of space, has classical aspects. For instance, a cold superconducting piece can move like a classical body. However, the volume of the HQS visibly has no limiting border, which eliminates totally the possibility of observing classical aspects in it. In quantum fluids the wave functions of the bosons are fully entangled. They have lost their individuality and are indistinguishable. The phases of the wave-functions of individual bosons are coherent with those of all the other bosons of the condensate. They are extended and have non-zero amplitude throughout the volume of the condensate. *Within the quantum fluid* there is nothing like a succession of positions of its parts as a function of time. Likewise the motion of electrons in atomic orbitals, the circulation in quantum fluids (probability currents) are created and governed by phase gradients of the order parameter and internally exhibit no classical aspects. Although perfectly real, the flow of quantum fluids is almost totally imperceptible. Only very specific fields, coupling to the quantum fluid are affected by this motion. If the circulation within the quantum fluid is along a closed loop, (analogously as in the atomic orbitals), the phase factor necessarily satisfies quantization rules. This is well known in superfluids and in superconductors and gives rise to the quasi-particles: Rotons, Maxons and Vortices.

If the Higgs mechanism creates the inertial mass of matter, it necessarily is responsible too for the gravitational dynamics, because it is mass that creates the gravitational fields. Without mass there are no gravitational fields and no gravitational dynamics. Likewise the usual quantum fluids move along phase gradients of the respective order parameter, the Higgs quantum fluid medium, too can itself move, in the ordinary space, along phase gradients according to a well-defined velocity field. If this velocity field has a velocity gradient, it creates inertial dynamics on matter-energy, which according Einstein's principle of equivalence is gravitational dynamics. Actually, several experimental observations (please see the next **Section 3**), indicate that the HQS is moving round the sun according to a velocity field consistent with the orbital motion of earth. In such a velocity field earth is stationary with respect to the local HQS and is very

closely a proper reference (proper Lorentz frame) in which clocks show proper time and light is isotropic.

The Higgs Quantum Space (HQS) is much more than simply a local ultimate (locally absolute) reference for rest and for motions. It literally governs the inertial motion of matter-energy (wave-packets). In the scenario of the HQS, the velocity of light has a fixed value c and is isotropic with respect to the local HQS and not with respect to every possible observer. This velocity c is the maximum velocity at which the order parameter of the Higgs condensate (HQS) transmits the phase perturbations. The HQS provides a *locally absolute meaning* to the motions. On the other hand, the velocity of light is anisotropic in any reference (LF) moving with respect to the local HQS. Moreover, all effects of motion on particles, on light and on clocks are due exclusively and uniquely to velocity with respect to the local HQS and not to relative velocity. The local HQS constitutes a *local absolute reference* for rest and for motions and the velocity with respect to the local HQS is absolute velocity, however only locally.

In the TR, the elementary particles are seen as existences in themselves, innately having mass, charge, spin etc. They are intrinsically associated with fields. According to this theory, their motion has no intrinsic meaning and only relative velocity is relevant to physics. In the Higgs theory the elementary particles are seen as confined field (wave) objects, as local perturbations in the Higgs order parameter. Their motion with respect to the local HQS has yes locally an intrinsic meaning. The HQS offers no mechanical resistance to the motion of these particles because; 1) it is a perfectly conservative quantum fluid and 2) these particles propagate in it as localized wave mechanisms and hence cannot collide with the local HQS. Likewise usual water and sound waves, these wave mechanisms, from the perspective of an observer moving with respect to the local HQS, are affected by Doppler shifts. However, likewise usual quantum fluids the HQS too can itself move according to a certain velocity field and distort it causing wavelength stretching-contraction and refractions. Actually various experimental observations demonstrate that the HQS is moving round the sun and round earth according to macroscopic Keplerian velocity fields, giving rise to the ingenious outside-inside centrifuge mechanism of gravity that is responsible for the observed gravitational dynamics.

3. The Effects of Motion with Respect to the Local HQS in Free-Space and within Gravitational Fields

In conventional physics, motion is change of position in the ordinary space as a function of time. In order to describe motions, it is necessary to define first a reference frame with space and time coordinates. A system of orthogonal Cartesian axes (x, y, z), scaled by units of length and a clock scaled by units of time t is the most usual definition. The position and motion of a point can be made by specifying the coordinates along the x, y and z axes as a function of time t, or in terms of the spherical coordinates (r, θ, ϕ) as a function of time t. If this refer-

ence frame represents the absolute rest, velocities with respect to it are absolute velocities. In his Theory of Relativity (TR) Einstein rejected the possibility of an absolute reference and hence, from the view of the TR, absolute motions are a meaningless concept. Einstein insisted that only relative motions and relative velocities are relevant in physics. In this scenario, every observer can arbitrarily define his own proper reference and consider all the other references as moving references. However, all the proper references, defined by all the different observers are equivalent and none of them is preferable. This leads to the problematic reciprocal symmetry between inertial observers. Consider two observers A and B in motion with respect to each other. In the view of each observer, his clock shows proper time and his meter sticks have proper lengths. However, in the view of observer A, the clock of B runs slow and in the view of observer B, the clock of A runs slow. This is the famous twin paradox to which there is no possible solution. Many other unsolvable paradoxes can be found in the literature.

In the scenario of the HQS, the definition of references is radically different from that in the TR. In the scenario of the HQS, which is the *local ultimate* (*locally absolute*) *reference* for rest and for motion of matter-energy, Einstein's inertial observer cannot anymore arbitrarily define his own proper reference. He only can consider him to be in a proper reference if he is stationary with respect to the local HQS. The Local HQS is the local proper (absolute) reference for rest and for motion. However, the HQS can itself move and, if this motion is non-homogeneous, the reference changes from point to point. Therefore, a universal absolute and proper reference is not possible. Only local absolute references can be defined, in which a stationary clock shows proper time and light is isotropic. Any local reference, moving with respect to the local HQS is not a proper reference. In this scenario, the references of two observers, at different points of space, can both be proper references. This however is possible only if both are stationary with respect to the local HQS. It will be seen that the planets of the solar system are all very closely stationary with respect to the local HQS and so implement very closely this situation.

Clocks count time with the help of a time standard that may be a classical or a quantum oscillator. Such oscillators are essentially wave-packets propagating in go-return round-trips within a potential well. In the case of the atomic clocks, the time standard is an electromagnetic (EM) cavity in which the oscillations of the EM field are tuned to the very stable frequency of the hyperfine transition of Cs atoms. These clocks can measure time within a precision better than 0.1 ns. However, such time standards are affected by velocity of the clocks with respect to the local HQS. The oscillation period of the time standard is ruled by the effective velocity of the wave-packets (Photons) in the go-return propagation within the cavity and within the atomic shells of the Cs atoms. Such effects are well-known from the Ives-Stilwell like experiments [18]. It however is important to note that in these experiments the Hydrogen atoms speeded at several thou-

sand km/sec. The experimental observations, to be discussed here, after the coming Equation (6) below, show that the earth-based laboratories do not achieve 8 km/sec), which certainly cannot introduce a detectable effect in the Ives-Stilwell experiments. The period T of the round-trip times of the time standards, moving at a velocity v *with respect to the local HQS*, is given by the well known equation:

$$T(v) = T_0\left(1 - v^2/c^2\right)^{-n} \tag{5}$$

where T_0 is the period of a Cs atom stationary with respect to the local HQS (the proper reference). The exponent is $n = 1/2$ for oscillations transverse to $\boldsymbol{v}$ and $n = 1$ for longitudinal oscillations. Hence, the clock rate depends on the value of the velocity v of the clock with respect to the local HQS and also on the direction of the oscillations of the time standard with respect to the velocity vector of the clock. Interestingly, the rate of clocks decreases in exactly the same proportion as the light go-return round-trip time between two mirrors. This is not a mere coincidence. In fact, the go-return light round-trips between two mirrors and the go-return of the electromagnetic field in the potential well of the time standard (oscillator) are affected in exactly the same proportion by motion with respect to the local HQS [18]. Therefore, measurements of the velocity of light, by the method of light go-return round-trips and clock, necessarily are independent from the velocity of the laboratory with respect to the local HQS. However, this invariance clearly is an experimental artifact and in no way proves that the *one-way velocity of light* really is an invariant.

Actually, several clear-cut experimental observations are in conflict with the relativistic conception. Clocks stationary within gravitational fields (on earth) show exactly the gravitational slowing predicted by GR (please see last term in Equation (3)). The GPS clocks, moving with earth round the sun, could easily detect the gravitational slowing by the solar field. They however show no any effect [19] [20]. Clearly the orbital velocity of earth cancels the gravitational slowing by the solar field, demonstrating that earth effectively is a proper reference (stationary with respect to the local HQS). Current theories explain this absence in terms of Einstein's principle of equivalence. However, these same GPS clocks too are moving along circular orbits round earth and, according to this interpretation of the principle of equivalence, this orbital motion too should cancel the gravitational slowing be the earth's field. However, the gravitational slowing by the earth's field is well observed. References [4] [16] explain exactly why.

In the past century a large number of light anisotropy experiments, performed on earth, searching for light anisotropy, due to the orbital and cosmic motion of earth, gave null results. From the perspective of the present HQS, these observations consistently confirm that earth is stationary with respect to the local HQS and is a proper reference (a proper Lorentz frame). The absence of the gravitational slowing of the GPS clocks by the solar field and the absence of light anisotropy with respect to the moving earth, in reality are the signature of the true

physical mechanism of gravity, as will be shown hereafter. Einstein could have concluded from the observed null results of the light anisotropy experiments that earth is stationary with respect to the spatial medium propagating light. Rapidly he would have discovered the ingenious outside-inside centrifuge mechanism of gravity [4] [16]. He nevertheless had reasons to think otherwise.

Actually the atomic clocks in orbit can be synchronized by Einstein's method to within a precision of 0.1 ns or better, time for light to travel 3 centimeters. For clocks moving in polar orbits, this synchronization method is especially favorable, because the go-return travel time between the earth-based station and the satellites is isotropic along the whole orbit (please see Equation (6) below). With the help of these tightly synchronized atomic clocks, the one-way velocity of electromagnetic signals (light) has precisely been measured. Such measurements are very helpful to define the characteristic form of the velocity field of the HQS. The most precise measurements of the one-way velocity of EM signals (light) was achieved with the help of the atomic clocks in the robotic twin satellites of the GRACE project, moving at nearly 8 km/sec along a same polar orbit, at 500 km of altitude and separated by about 200 km. In the measurements of microgravity effects, EM signals are continuously exchanged forward and backward between these satellites. Moreover, their clocks need to be synchronized to better than 0.16 ns. In these experiments, the one-way velocity of the EM signals was measured in both senses. The results have shown a clear anisotropy of about 8 km/sec, backward to the orbital motion of the satellites. This value is exactly the orbital velocity of the satellites and corresponds to about 17 ns of excess or shortage of time of flight [3]. This observation unambiguously breaks the intrinsic isotropy of light and has the consequence that the null light anisotropy results, found in the past century, need a new interpretation. In fact the observed null results of the light anisotropy experiments are not due to the intrinsic isotropy of light, however to the fact that the moving earth is stationary with respect to the local HQS.

The above experimental observations all together demonstrate that earth is stationary with respect to the local HQS in the solar field and that the velocity of the HQS round earth (and round the sun) *has no North-South component*. However, earth obviously cannot be considered to be in a privileged kinematical condition in detriment to all the other planets. All the planets must equally be nearly stationary with respect to the local HQS. This is not difficult to accomplish as the planets move all along direct circular orbits that lie all closely within the plane of the solar system. The above described experimental observations can make a sense only if the HQS is circulating round the sun according to a Keplerian velocity field, consistent with the planetary orbital motions and round earth consistently with the orbital motion of the Moon. In spherical coordinates, the form of the velocity field $V(r,\theta,\phi)$ is:

$$\boldsymbol{V}(r) = (GM/r)^{1/2}\,\boldsymbol{e}_{\phi} \tag{6}$$

In this Equation, G is the gravitational constant, M is the mass of the gravita-

tional source (sun), r is the radial spherical coordinate and $\boldsymbol{e}_{\phi}$ is a unit vector along the azimuthal spherical coordinate $+\phi$. This is a very simple velocity field round the Z axis. It has a non-null component only along the $+\phi$ spherical coordinate. In this velocity field *the magnitude* of the velocity is spherically symmetric. This Keplerian velocity field is responsible for the ingenious outside-inside centrifuge mechanism of gravity that is the quintessence of the gravitational fields. **Section 4** will show that it accurately creates the observed gravitational dynamics, the orbital motions, the gravitational acceleration, the gravitational pull etc. Refs. [4] [5] [16] also show that it accurately produces all the observed effects of the gravitational fields on light and on clocks. It causes the observed gravitational slowing of the atomic clocks, stationary in a gravitational field, exactly as predicted by the GR. It predicts the absence of the gravitational slowing of the GPS clocks by the solar field. [4] It predicts the absence of light anisotropy with respect to earth. It precisely predicts the observed Shapiro effect [21] not as a result of the increased geometrical distances, due to the spacetime curvature, however as a result of the effective velocity of the radar signals ($c' = c \pm GM/r$) in the the go and return travels in the solar Keplerian velocity field of the HQS. [4] [16] It also predicts all the other observed effects of the solar and the earth's gravitational fields on light and on clocks. **Sections 4** gives more details.

In the solar Keplerian velocity field Equation (6) that achieves 436 km/sec on the solar surface and about 30 km/sec at the earth's orbit, earth is moving round the sun along a direct nearly circular equatorial orbit at a velocity very closely equal to that of the local HQS. The absence of the gravitational slowing of the GPS clocks by the solar field and the absence of light anisotropy, with respect to earth, show that earth effectively is very nearly stationary with respect to the local moving HQS. It is locally very closely a true proper and preferential reference, a local proper Lorentz frame. The velocity of light is isotropic with respect to earth, not because of the intrinsic isotropy of light, however because the velocity of light is fixed with respect to the local HQS and earth is stationary with respect to this locally moving HQS.

Earth has its own Keplerian velocity field of the HQS in the sense of the Moon's orbital motion (toward the East). The earth's velocity field achieves 7.91 km/sec on surface. However, earth rotates only very slowly. Therefore, the earth-based laboratories have a velocity with respect to the local HQS of nearly $V = 8$ km/sec, *toward the West* and are nearly, however not exactly proper references. The effect of this velocity on light and on clocks is extremely small and constant the whole day and the whole year, in the order of $V^2/c^2 = 10^{-10}$ and very difficult to detect by light anisotropy. Light anisotropy of about 8 km/sec has been detected by only some of the most sensitive genuine Michelson experiments [22]. Please see **Figure 2**.

The effects of this small velocity however are well detected by the gravitational slowing of atomic clocks on earth. [8] It also has been detected by Mössbauer effect in the atomic spectral red-shifts [23]. The HQS gravitational mechanism

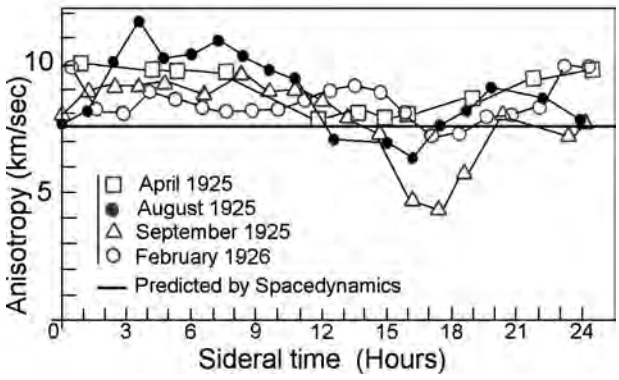

Figure 2. The Nearly West-East anisotropy of light, with respect to the earth-based laboratories, constant the whole day and the whole year, by D. Miller.

too gives a simple explanation to the gravitational slowing of the GPS clocks by the earth field, that are moving round earth along non-equatorial orbits, making 55 deg with the earth's equator [4]. It also predicts dragging of the Neutrinos along their path from CERN to Gran-Sasso IT *Southeast*, making 58 deg with the Meridians. The West-East velocity of the HQS in the earth's Keplerian velocity field boosts up the velocity of Neutrinos *as well as of light* by 6.7 km/sec, causing them both to arrive 55 ns *too early* to Gran-Sasso. However, this too early arrival of the Neutrinos *in no way proves that Neutrinos exceed the light velocity*. In the mega-experiment, to be implemented in coming years, Neutrinos will be shot *toward the West* from Fermilab (IL) to Stanford (SD). In this case, the Neutrinos are predicted to reach Stanford *too late by about* 115 *ns*. Please see details in Ref. [24].

The theory of relativity (TR) has lead to a number of very important discoveries, like time dilation and the increase of mass with velocity. It provided the relation between mass and energy and has lead to the discovery of the gravitational time dilation etc. Actually, many experimental observations, realized in the earth-based laboratories, with particles speeding at very high velocities (comparable to the velocity of light), apparently corroborate the predictions of the TR. However, from the present HQS dynamics view, earth is very closely stationary with respect to the local HQS in the Keplerian velocity field of the HQS, creating the solar field. Moreover, the solar system is stationary in the Milky-Way galaxy etc. Earth is very closely a true and not a hypothetical proper reference. However, because of the bold assumption of the TR that the earth-based laboratories can be assumed by the laboratory observers to be hypothetically stationary references, the predictions of the TR, *for experiments on earth*, coincide very closely with the predictions in the scenario of the HQS dynamics. This coincidence however is true only in this specific and very particular circumstance. In other circumstances this coincidence is predicted to fail. In reality these experimental observations in no way corroborate the TR. They in fact simply show the effects of the high velocity with respect to the local HQS, in which the earth-based laboratories are nearly stationary. Earth is very closely a true proper reference. Saying

that these observations corroborate the TR is like assuming that the atmospheric pressure is a universal constant throughout the universe and claiming that precise measurements (of the atmospheric pressure) in the hold of a ship, navigating round earth, confirm this naif assumption.

In free space, the HQS is the local ultimate (local absolute) reference for rest and for motions of matter-energy. However, within gravitational fields, the HQS moves according to a Keplerian velocity field, given by (Equation (6) and can only locally be a proper (absolute) reference. Moreover, such local proper references are themselves moving and rotating round an over-head axis with the local HQS in the Keplerian velocity field. Therefore, within gravitational fields, it is impossible to define a *universal proper reference* in the sense of the conventional view. Only local proper references can be defined, which themselves are moving with the local HQS. In this scenario, the planets in the solar system that are moving with the local HQS along different orbits within the plane of the solar system, are each one locally very closely stationary with respect to the local moving HQS and are each one locally nearly a proper reference. Their slightly elliptic orbits give account that they have small velocities, with respect to the local HQS, only of hundreds of m/sec. Each planet is locally very closely (however not exactly) a proper reference, with respect to which the velocity of light is very nearly isotropic and clocks, moving with them, show very closely proper time.

The velocity of the planets can be measured from earth, using the spectral frequency shifts. In reality the planets are locally very closely stationary with respect to the local HQS and locally emit the radiation with proper frequency. These frequencies however are shifted by the time rate of stretching compression of the wavelengths by the velocity field of the HQS along the path of light, simulating Doppler shifts. It can be shown that the values of these frequency shifts are identical to the Doppler shifts, caused by their conventional relative velocities. The frequency of light, coming from the stars in the distant galaxies is shifted by the local wavelength stretching-compression within the velocity field of the local HQS, generating the respective galactic gravitational dynamics as well as by the cosmic expansion of the HQS, causing the recession between the galaxies. The isotropy of light, with respect to earth, is the most far-reaching evidence that earth is very nearly stationary with respect to the local HQS and is closely a proper reference. Visibly, the astronomical bodies throughout the universe are all very nearly stationary with respect to the local HQS in the respective gravitational fields and are nearly proper references. This entails the universality of the laws of physics without the need of the Principle of Relativity.

4. Origin of the Gravitational Dynamics in the Keplerian Velocity Field of the HQS

The present work associates the central idea of the Higgs theory, according to

which the HQS governs the inertial motion of matter, with the central idea of GR, according to which the gravitational dynamics is inertial dynamics and replaces Einstein's spacetime curvature by a Keplerian velocity field Equation (6) of the HQS. In this Keplerian velocity field, the horizontal velocity of the HQS along the $+\phi$ increases with decreasing radial coordinates r in the neighborhood of any point of space. This creates a rotation of the local HQS and thus of the local inertial references *round an over-head axis*. The idea that the local rotating HQS represents locally a rotating inertial reference may seem stupid. In fact however it is not stupid at all, because it is the HQS, ruling the inertial motion of matter-energy and is the local ultimate (proper) reference for rest and for motions that is itself locally so rotating. Hence, a body, stationary in the ordinary space within a gravitational field (within the Keplerian velocity field), *is implicitly moving oppositely along a circular path*, within de locally proper inertial reference, round the same over-head axis and necessarily under an *upward centripetal force*. In this scenario, *the gravitational pull essentially is a centrifugal pull toward the gravitational center*. This gives rise to the *ingenious outside-inside centrifuge mechanism of gravity* that Einstein has missed. It is a completely new and physically genuine gravitational mechanism that continuously pulls us against the ground. This ingenious outside-inside centrifuge mechanism resolves one of the most recurrent conundrums of fundamental physics. It fully and transparently elucidates the origin of the gravitational pull and of the gravitational dynamics. This Keplerian velocity field of the HQS is consistent with the planetary orbital motions and is the quintessence of the gravitational fields. It accurately creates the observed gravitational dynamics without the need of a central force field and also correctly generates all the effects of the gravitational fields on light and on clocks. A detailed description of all these effects is here impossible because it would take too many pages. The interested reader is advised to Refs. [4] [5] [16] were a detailed description is given. Here only some basic steps will be outlined.

The vorticity of the HQS in the Keplerian velocity field Equation (6) is intermediary between rigid-body rotation and the irrotational potential flow. Due to the increasing horizontal velocity of the local HQS with decreasing r in this velocity field, the wave fronts of the matter waves of the particles, stationary in the ordinary space and thus moving with respect to the local HQS along $-\phi$ (wave fronts in the $[r,\theta]$ plane) are refracted at a locally well-defined time rate. Moreover, due to the characteristic Keplerian velocity field, the ϕ and the r velocity components are refracted in opposite senses. While the ϕ component is refracted, due to the increasing (horizontal) velocity of the HQS along $+\phi$ for decreasing radial coordinate, giving rise to the rotation of the local inertial reference round the over-head axis, the r velocity component (wave-fronts in the (θ,ϕ) plane is refracted oppositely, due to the variation of the local velocity of the HQS round the gravitational center with decreasing r. The rotation of the r component is a residual effect, reminiscent from the rigid-body rotation round

the gravitational center. The θ velocity component is not refracted at all, because the velocity of the HQS in the Keplerian velocity field Equation (6) has no component along the θ coordinate and becuse the velocity along ϕ is constant with θ (for fixed r). The opposite refraction rates of the r and the ϕ velocity components constitutes not a trigonometric however a hyperbolic rotation. Figure 3 displays velocity diagrams along an elliptic orbit round the gravitational source with eccentricity $\epsilon = 0.5$. The diagrams show the precisely calculated orbital velocities v_{orb} of the orbiting particle, the velocity of the local HQS and the effective velocity v_{eff} of the particle with respect to the local HQS at a large number of positions along the orbit.

In this figure, the effective rotation rates of the ϕ velocity component (top) and of the r velocity component (left) can precisely be read. The effective rotation rates $\boldsymbol{W}$ of the r, ϕ and θ velocity components are given by the equations:

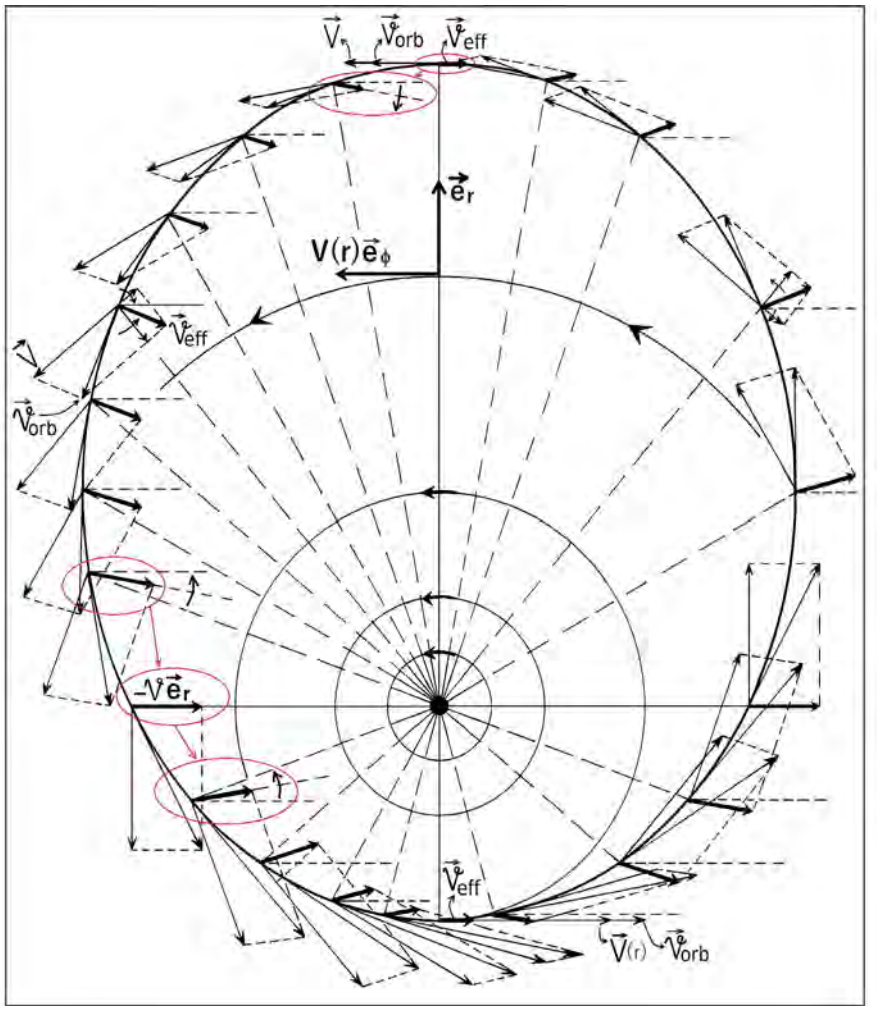

Figure 3. The figure is a very precise graphical representation, showing the velocity diagrams at a large number of positions along the orbit, where $\boldsymbol{v}_{eff}$ (bulky arrows,) was obtained using the vector relation: $\boldsymbol{v}_{eff} + \boldsymbol{V}(r) = \boldsymbol{v}_{orb}$.

$$\boldsymbol{W}_r(r) = -\frac{1}{2}\left[GM/r^3\right]^{1/2}\boldsymbol{e}_\theta \tag{7a}$$

$$\boldsymbol{W}_\phi(r) = +\left[GM/r^3\right]^{1/2}\boldsymbol{e}_\theta \tag{7b}$$

$$\boldsymbol{W}_\theta(r) = 0 \tag{7c}$$

These rotation rates depend only on the radial coordinate *r*, because the velocity gradient of the velocity field Equation (6) has only a radial component. These effective rotation rates include the effects of the wavelength stretching-compression. Note that these opposite rotation rates that are different for *r* and ϕ components characterize a non-symmetric hyperbolic rotation. This is the characteristic that naturally accomplishes the Virial theorem.

A particle of mass *m*, stationary in the ordinary space, within the Keplerian velocity field, created by a mass *M*, has an implicit velocity (wave fronts in the $[r,\theta]$ plane) pointing along $-\phi$:

$$\boldsymbol{V}_{impl} = -\left(GM/r\right)^{1/2}\boldsymbol{e}_\phi \tag{8}$$

This velocity is implicit because it cannot be described in the ordinary space. It is the negative of Equation (6). The refraction rate of this implicit velocity, according to Equation (7b), generates an instantaneous ordinary vertical downward acceleration given by:

$$\boldsymbol{g}(r) = W_\phi(r)\boldsymbol{e}_\theta \times V_{impl}(r)\left(-\boldsymbol{e}_\phi\right) = -GM/r^2\,\boldsymbol{e}_r \tag{9}$$

This expression is exactly the usual expression for centrifugal accelerations in a rotating reference. It describes a central field of centrifugal accelerations toward the gravitational center from the equator to the Poles. However, within the Keplerian velocity field Equation (6), the local *non-inertial rotating reference*, in which the particle is stationary, does not rotate in the ordinary space. Its rotation is implicit and opposite to the ordinary rotation of the local proper inertial reference. These opposite rotations cancel in the ordinary space.

The planets in the solar system are all moving very closely along circular orbits that lie all closely within the equatorial plane of the solar Keplerian velocity field (Equation (6)). This minimizes their velocity and kinetic energy with respect to the local HQS. The velocity of the planets with respect to the local moving HQS is very low, only of a few hundreds of m/sec. The planets thus are very closely proper Lorentz frames, in which *all the effects of the solar field are locally very nearly canceled*. Therefore, clocks, moving with the planets, show proper time, the velocity of light is isotropic with respect to them and the gravitational pull of the solar field on them is locally zero. All this is valid too for the Moon, which too is moving along a closely direct circular equatorial orbit round earth in approximately the equatorial plane of the earth's Keplerian velocity field. The gravitational tides are residual effects, due to the mutual distortions in the respective Keplerian velocity fields of the HQS.

The expression Equation (9) is precise enough only as long as the vertical velocity is very low. In order to get a precise description for free fall along large

radial distances, it is necessary to solve the elementary linear differential equation:

$$\frac{\mathrm{d}\boldsymbol{\nu}\left(r\left(t\right)\right)}{\mathrm{d}t}=\boldsymbol{A}\boldsymbol{\nu}_0 \tag{10}$$

where $\boldsymbol{\nu}_0$ and $\boldsymbol{\nu}$ are respectively the initial and the final column velocity matrices of the (ordinary) r and the (implicit) ϕ velocity components of the effective velocity with respect to the local HQS:

$$\boldsymbol{\nu}\left(t\right)=\begin{pmatrix}\nu_r\left(t\right)\\ \nu_\phi\left(t\right)\end{pmatrix} \tag{11}$$

and $\boldsymbol{A}$ is the hyperbolic rotation matrix (a rank 2 tensor) defined in terms of the rotation rates, given in Equation (7) as:

$$\boldsymbol{A}=\begin{pmatrix}0 & W_\phi\\ -W_r & 0\end{pmatrix}=\begin{pmatrix}0 & W\\ \frac{1}{u}W & 0\end{pmatrix} \tag{12}$$

where $W=GM/r^3$ and the coefficient $u=2M/\left(M+m\right)$ accounts for the asymmetric distribution of kinetic energies between the interacting masses m and M, that is approximately 2 for $m\ll M$ and is 1 for $m=M$. This matrix effectuates hyperbolic rotations round parallel axes of the velocity components in Equation (11).

Dividing both sides of Equation (10) by $\boldsymbol{\nu}_0$, multiplying them by $\mathrm{d}t$ and integrating the left hand side from $\boldsymbol{\nu}_0$ to $\boldsymbol{\nu}$, develops into:

$$\log\frac{\boldsymbol{\nu}\left(t\right)}{\boldsymbol{\nu}_0}=\int_0^t A\left(r\left(t'\right)\right)\mathrm{d}t' \tag{13}$$

where $A\mathrm{d}t$ is an infinitesimal rotation round parallel axes. These successive infinitesimal rotations commute. Equation (13) can be re-written in the exponential form as:

$$\boldsymbol{\nu}\left(t\right)=\exp\left[\int_0^t A\left(r\left(t'\right)\right)\mathrm{d}t'\right]\boldsymbol{\nu}_0 \tag{14}$$

Expanding the exponential in series and adding up the terms of the series from $n=0$ to $n=\infty$ results in:

$$\begin{aligned}\boldsymbol{\nu}\left(t\right)&=\sum_{n=0}^{\infty}\frac{1}{n!}\begin{pmatrix}0 & \Theta\left(t\right)\\ \frac{\Theta\left(t\right)}{u} & 0\end{pmatrix}^n\begin{pmatrix}\nu_r\left(0\right)\\ \nu_\phi\left(0\right)\end{pmatrix}\\ &=\begin{pmatrix}\cosh\left(\frac{\Theta\left(t\right)}{\sqrt{u}}\right) & \sqrt{u}\sinh\left(\frac{\Theta\left(t\right)}{\sqrt{u}}\right)\\ \frac{1}{\sqrt{u}}\sinh\left(\frac{\Theta\left(t\right)}{\sqrt{u}}\right) & \cosh\left(\frac{\Theta\left(t\right)}{\sqrt{u}}\right)\end{pmatrix}\times\begin{pmatrix}\nu_r\left(0\right)\\ \nu_\phi\left(0\right)\end{pmatrix}\end{aligned} \tag{15}$$

which is the general solution of Equation (10).

The value of $\Theta\left(t\right)$ can be computed by integration, making use of the change of variable $\mathrm{d}t\Rightarrow\mathrm{d}r$ method. Inverting the obtained result, gives:

$$\cosh\left(\frac{\Theta(t)}{\sqrt{u}}\right)=\sqrt{\frac{r_0^{CM}}{r^{CM}}}=\sqrt{\frac{r_0}{r}} \tag{16a}$$

$$\sinh\left(\frac{\Theta(t)}{\sqrt{u}}\right)=\sqrt{\frac{r_0^{CM}-r^{CM}}{r^{CM}}}=\sqrt{\frac{r_0-r}{r}} \tag{16b}$$

where r_0 is the initial radial coordinate. Using this result in Equation (15) the general solution takes the form:

$$\begin{pmatrix} v_r(t) \\ v_\phi(t) \end{pmatrix}=\begin{pmatrix} \sqrt{r_0/r} & \sqrt{u(r_0-r)/r} \\ \sqrt{(r_0-r)/ur} & \sqrt{r_0/r} \end{pmatrix}\times\begin{pmatrix} v_r(0) \\ v_\phi(0) \end{pmatrix} \tag{17}$$

and the particular solution of Equation (10) for free fall of m in the field of M ($m \ll M$), on from initial rest at r_0, where $v_r(t=0)=0$ and $\boldsymbol{v}_\phi(0)=\boldsymbol{V}_{impl}(r_0)=-(GM/r_0)^{1/2}\boldsymbol{e}_\phi$ is:

$$v_r(t)\approx-\left[2\left(\frac{GM}{r(t)}-\frac{GM}{r_0}\right)\right]^{1/2}\boldsymbol{e}_r \tag{18a}$$

$$v_\phi(t)=-V_{impl}(r_0)\left[\frac{r_0}{r}\right]^{1/2}=-\left[\frac{GM}{r(t)}\right]^{1/2}\boldsymbol{e}_\phi \tag{18b}$$

Equation (18a) is just the well known expression for the observed vertical free-fall velocity on from rest at r_0. It directly shows that the kinetic energy $1/2\,mv_r^2$ is equal to the difference between the final and the initial potential energies. Equation (18b) is just the implicit (imaginary) velocity as a function of the radial position *r*. It shows that the refraction rate of the radial velocity component just compensates for the increase of the velocity field as a function of the decrease of the radial coordinate. This assures that free-fall of the particle, on from rest, goes along a vertical (radial) path and hence assures conservation of the angular momentum about the gravitational center. Please observe that, for free-fall on from infinity ($r_0=\infty$), the vertical velocity $v_r(r(t))$ is exactly $\sqrt{2}$ times larger than the ϕ velocity, which arises directly from Equation (18) and accomplishes the Virial theorem.

The full steps of the solution of Equation (10) are given in Ref. [4]. This Reference too shows that the gravitational mechanism, created by the Keplerian velocity field of the HQS (Equation (6)) is perfectly symmetric with orbital motions. In fact, the Keplerian velocity field simulates the effects of a central field of gravitational accelerations, while the orbital motions simulate the outward centrifugal effects, exactly as conceived in Newtonian gravity. It also is shown that the Keplerian velocity field correctly predicts all the actually known experimental observations. It in particular causes very precisely the observed gravitational light lensing effect, due to the differentiated refraction times by Equation (7b) for prograde and retrograde light path. **Section 5.5** of Ref. 4 and **Section 8. A2** of Ref. 16 show the details. However, some other effects too are predicted, for which actually there are no experimental data to confront withy.

5. Concluding Comments and Considerations.

According to the STR, the velocity of light *has the same value in any inertial reference* and in a reference moving at a relative velocity v with respect to the hypothetically stationary reference, the time axis has a different direction. It has a space like component $\boldsymbol{v}$, so that, from the view of the stationary observer, its component along the time axis in his own reference is shorter and the rate of time evolution of all physical processes in the moving reference seems reduced to $t = t_0\left(1-v^2/c^2\right)^{-1/2}$. In their turn, the space-like distances, in the moving reference, have a time-like component and seem to be shorter. However, an observer in the moving reference can say the same about the times and distances in the hypothetically stationary reference, which is the problematic reciprocal symmetry problem of the STR. In the present scenario of the HQS, the velocity of light has a fixed value *c with respect to the local HQS*. In a reference, moving at a velocity *V*, *with respect to the local HQS*, the velocity of light is anisotropic and the time evolution of all the physical processes is lowered because of the effective velocities $\left(c^2 \pm V^2\right)^{1/2}$. The time evolution is given by $T = T_0\left(1-V^2/c^2\right)^{-n}$ where $n = 1/2$ for transverse oscillations and $n = 1$ for longitudinal oscillations. The spatial distances are not altered and the reciprocal symmetry does not exist.

According to GR, from the view of an external observer, the rate of the time evolution t' of the physical processes (clocks), in a laboratory stationary within a gravitational field, is lower as indeed observed, given by $t' = t_0'\left(1-2GM/rc^2\right)^{-1/2}$, where $2GM/r$ is the local escape velocity. GR explains this in terms of space-time curvature, in which the time axes have different directions inside and outside the field. Within the field, it has a component along *r*. The problem with GR is that it cannot explain why the gravitational slowing by the solar field is absent on the GPS clocks, moving with earth round the sun. It cannot, because the orbital velocity of earth cannot cancel the space-like velocity component along *r*. It in fact *adds a new component*. In the scenario of the present HQS dynamics gravitation, a body (clock), stationary in the ordinary space within a gravitational field, has an implicit velocity $V(r) = -\left(GM/r\right)^{1/2}\boldsymbol{e}_\phi$ with respect to the local HQS, due to the Keplerian velocity field of the HQS along $+\phi$, creating the gravitational field. This implicit velocity of the body is a *true velocity with respect to the local moving HQS*. For longitudinal oscillations of the clock's time standard, the clock rate is $T(r) = T_0(r)\left(1-GM/rc^2\right)^{-1}$, which causes exactly the same clock slowing as predicted by GR. In the language of GR, the time axis of this stationary clock *has a space-like component along* $-\phi$ (not along *r*). In this situation, the orbital velocity of earth along $+\phi$ naturally cancels the implicit velocity (and the space like component of the time axis) and thereby cancels the gravitational slowing of GPS clocks, due to the solar field. However, *only orbital motions along direct circular equatorial orbits can cancel this implicit velocity*. Any different orbital velocities do not cancel the gravitational slowing, as demonstrated by the GPS clocks in the non-equatorial orbits round earth. The orbit-

al motion of earth gives in addition a natural explanation to the absence of light anisotropy with respect to earth; because the orbiting earth is stationary with respect to the local moving HQS.

Also, according to GR, from the view of an external observer, the velocity of a light pulse, propagating, toward the gravitational center, will seem to gradually reduce its velocity. GR explains this reduction in terms of a time like (implicit) component of the radial distances (stretching of the radial distances), due to spacetime curvature, which the external observer cannot see. From the view of the HQS dynamics gravitation the radial velocity component of light c' really decreases, given by $c' = \left(c^2 - GM/r\right)^{1/2}$. It decreases because the light pulse necessarily develops a lateral velocity component $\left(GM/r\right)^{1/2}$ along $-\phi$, which is due to the refraction rate (Equation (7a)) of the light velocity component along *r*. This component too is not seen by the external observer.

From the view of the present HQS dynamics, the absence of the gravitational slowing of the GPS clocks and the absence of light anisotropy with respect to earth are both due to the fact that earth is very closely stationary with respect to the local HQS in the Keplerian velocity field creating the solar gravitational field. Moreover, all the experimental observations with particles, having very high velocities within the earth-based laboratories that *apparently* corroborate the predictions of the TR, do not corroborate them at all. These observations simply are the effects of the very high velocities with respect to the local very slowly moving HQS. All these observations are the obvious signature of the ingenious outside-inside centrifuge mechanism of gravity, created by the solar Keplerian velocity field of the HQS.

The concern of the present work has not been simply constructing mathematical models that can simulate the observations, however to get understanding for these observations in terms of *real and genuine physical mechanisms*. This has largely been achieved. The HQS, retrieves *locally an absolute* (*however non-universal*) *reference* for rest and for motions, recovering locally an intrinsic meaning for motions. In the present view, the local HQS plays a fundamental role in the microscopic world of quantum physics as well as in the macroscopic world of gravitation, opening a way toward the unification of the fundamental forces.

Conflicts of Interest

The author declares no conflicts of interest regarding the publication of this paper.

References

[1] Einstein, A. (1905) *Annalen der Physik*, **17**, 891-921. https://doi.org/10.1002/andp.19053221004

[2] Lorentz, H.A., Einstein, A., Minkowski, H. and Weyl, H. (1923) The Principle of Relativity. Dover Publications, New York.

[3] Hatch, R.R. (2007) *Physics Essays*, **20**, 83-100. https://doi.org/10.4006/1.3073811

[4] Schaf, J. (2018) *Journal of Modern Physics*, **9**, 1111. https://doi.org/10.4236/jmp.2018.95068

[5] Schaf, J. (2018) *Journal of Modern Physics*, **9**, 395. https://doi.org/10.4236/jmp.2018.93028

[6] Laue, M.V. (1955) *Annalen der Physik*, **38**.

[7] Schwarzschild, K. (1916) Sitz. Preuss. Akad. d. Wiss., Part 1, 424.

[8] Ashby, N. (1996) Mercury, 23-27.

[9] Higgs, P.W. (1964) *Physical Review Letters*, **13**, 508. https://doi.org/10.1103/PhysRevLett.13.508

[10] Englert, F. and Brout, R. (1964) *Physical Review Letters*, **13**, 321. https://doi.org/10.1103/PhysRevLett.13.321

[11] Anderson, P.W. (1963) *Physical Review Journals Archive*, **130**, 439. https://doi.org/10.1103/PhysRev.130.439

[12] Ginzburg, V.L. and Landau, L.D. (1950) *Journal of Experimental and Theoretical Physics* (*JETP*), **20**, 1064.

[13] Meissner, W. and Ochsenfeld, R. (1933) *Naturwissenschaften*, **21**, 787-788. https://doi.org/10.1007/BF01504252

[14] Carrol, S.M. (2000) The Cosmological Constant. arXiv:astro-ph/0004075

[15] Sola, J. (2013) Cosmological Constant and Vacuum Energy: Old and New Ideas. arXiv:1306.1527v3 [gr-qc]

[16] Schaf, J. (2019) *JMP*, **10**, 225-255. https://doi.org/10.4236/jmp.2019.103018

[17] Dias, F.T., *et al.* (2010) *Physica C*: *Superconductivity and Its Applications*, **470**, S111-S112. https://doi.org/10.1016/j.physc.2010.01.018

[18] Ives, H.E. and Stilwell, G.R. (1938) *Journal of the Optical Society of America*, **28**, 215-226. https://doi.org/10.1364/JOSA.28.000215

[19] Hatch, R.R. (2004) *GPS Solutions*, **8**, 67-73. https://doi.org/10.1007/s10291-004-0092-8

[20] Hatch, R.R. (2004) *Foundations of Physics*, **34**, 1725-1739. https://doi.org/10.1007/s10701-004-1313-2

[21] Shapiro, I.I., *et al.* (1971) *Physical Review Letters*, **26**, 1132. https://doi.org/10.1103/PhysRevLett.26.1132

[22] Miller, D.C. (1933) *Review of Modern Physics*, **5**, 203. https://doi.org/10.1103/RevModPhys.5.203

[23] Pound, R.V. and Snider, J.L. (1965) *Physical Review Journals Archive*, **140**, B788. https://doi.org/10.1103/PhysRev.140.B788

[24] Schaf, J. (2018) *Journal of Modern Physics*, **9**, 2125. https://doi.org/10.4236/jmp.2018.912133

Journal of Modern Physics, 2019, 10, 281-293
http://www.scirp.org/journal/jmp
ISSN Online: 2153-120X
ISSN Print: 2153-1196

New Cosmology: The Global Dynamics of the Higgs Quantum Space and the Accelerated Expansion of the Universe

Jacob Schaf

Universidade Federal do Rio Grande do Sul (UFRGS), Instituto de Fsica, Porto Alegre-RS, Brazil
Email: schaf@if.ufrgs.br

How to cite this paper: Schaf, J. (2019) New Cosmology: The Global Dynamics of the Higgs Quantum Space and the Accelerated Expansion of the Universe. *Journal of Modern Physics*, **10**, 281-293.
https://doi.org/10.4236/jmp.2019.103019

Received: November 7, 2018
Accepted: March 4, 2019
Published: March 7, 2019

Abstract

This work investigates the nature of the empty space and of the energy accelerating expansion of the universe, within the context of the Higgs theory. It is consensus among the cosmologists that dark energy, accelerating the expansion of the universe, is energy of the empty space (vacuum) itself. According to the Higgs theory, empty space (vacuum) is filled up by a real quantum fluid medium, closely analogous to the superconducting condensate, giving mass to the elementary particles by the Higgs mechanism. This spatial medium is the holder of the vacuum energy. Current theories describe the empty space (vacuum) in terms of the stress-energy tensor of a perfect fluid and estimate the vacuum energy density in terms of zero-point energies of the various force fields. They come to the scandalous conclusion that the vacuum energy density is 120 decimal orders of magnitude larger than shown by the observations. In the context of the Higgs theory, empty space, far from a perfect fluid, is a very strongly correlated boson condensate, a *perfect quantum fluid* ruled by the principles of quantum physics and governed by a powerful order parameter. This order parameter is stabilized by a huge energy gap that, according to the Glashow-Weinberg-Salam electroweak model, achieves more than 200 GeV. This huge energy gap very strongly suppresses the quantum fluctuations and the zero-point energies. This lets clear that estimating the vacuum energy density in terms of the zero-point energies cannot be correct. The expanding universe does not create more and more vacuum energy and does not expand against a negative pressure. The universe is an adiabatic system that conserves the total mass-energy and expansion only reduces the vacuum energy density. Calculations within this context show that the vacuum energy density converges closely to the observed value.

Keywords

Dark Energy, Vacuum Energy, Cosmological Constant, Higgs Theory, Expanding

Universe

1. Introduction

When Friedman [1] discovered that the solution of Einstein's field equations [2] [3] of General Relativity (GR) in a Robertson-Walker universe, [4] [5] leads to an expanding universe, Einstein immediately has included a cosmological term to get solutions for a static universe, because, in his view, only a static universe could be reasonable. The field equations, including the cosmological term took the form:

$$R_{\mu\nu} - \frac{1}{2} g_{\mu\nu} R + \Lambda g_{\mu\nu} = 8\pi G T_{\mu\nu}, \tag{1}$$

This is an equation for the four components of the metric tensor of a curved spacetime, in which, $R_{\mu\nu}$ is the Ricci curvature tensor, R is the scalar curvature, $g_{\mu\nu}$ is the metric tensor of the space-time geometry, G is the gravitational constant, $T_{\mu\nu}$ is the stress-energy tensor of the matter universe and Λ is the well known cosmological constant with dimension of $(\text{length})^{-2}$. However, when Hubble discovered that the universe effectively is expanding, Einstein considered the inclusion of the cosmological term as his biggest blunder.

In the Friedmann-Lemaître-Robertson-Walker universe, the effect of the local gravitational sources can be seen as local perturbations. Such a universe usually is modeled in terms of the four-dimensional energy-momentum tensor of a homogeneous and isotropic perfect fluid (uncorrelated particles), with a spatially constant vacuum energy density ρ_v and an isotropic negative pressure p:

$$T_{\mu\nu} = (\rho_v + p) U_\mu U_\nu + p g_{\mu\nu} \tag{2}$$

where U_μ (U_ν) is the local four-velocity of the perfect fluid and $g_{\mu,\nu}$ is the metric tensor.

In the absence of ordinary matter-energy (empty and static universe), $T_{\mu\nu}$ in Equation (2) reduces to T_{00}, which is interpreted as the energy density of the vacuum ρ_v. From the perspective of the elementary particle physics, the cosmological constant is proportional to the energy density of the vacuum and, importantly, the local density of this vacuum energy remains constant during the expansion of the universe [6] [7]. Therefore, expansion creates additional vacuum energy, which leads to the odd negative pressure of the perfect fluid. The vacuum of elementary particle physics usually includes the zero-point energies, associated with the various force fields. Altogether, these contributions lead to the theoretical vacuum energy density ρ_v^{th}, given by:

$$\rho_v^{th} = 10^{110} \,\text{erg}/\text{cm}^3. \tag{3}$$

However, the experimental observations, with the help of I_a supernovae, [8] [9] as well as with the help of cosmic microwave background radiation, [10] showed that the universe is not only expanding. The expansion rate is accelerat-

ing. The big question then is: What causes the accelerating expansion of the universe? These experimental observations also have provided approximate values for the actual vacuum energy density ρ_v^{obs} given by:

$$\rho_v^{obs} \sim 10^{-10}\,\mathrm{erg}/\mathrm{cm}^3 \tag{4}$$

The gap between the theoretical estimation in Equation (3) and the experimental observations in Equation (4) amounts to the scandalous 120 decimal orders of magnitude [6] [7] and decreases not much, even with the most favorable estimates. This enormous difference has revived Einstein's dilemma about the cosmological constant. It lets clear that something very fundamental is wrong with the assumption of particle physics about the nature of empty space (vacuum). The Robertson-Walker universe cannot be described in terms of a perfect fluid and the vacuum energy is not the zero-point energy of the ground states of the various force fields. This makes the discussion about the vacuum energy density and the cosmological constant more actual than ever.

The accelerating expansion of the universe is actually a well established observational fact. The consensus among the cosmologists is that dark energy is not ordinary mass-energy, however is energy of empty space (vacuum) itself. It also is consensus that the energy of the vacuum distributes it very homogeneously throughout the universe. The goal of the present work is showing that all these features arise naturally and appropriately within the context of the global Higgs Quantum Space (HQS) dynamics.

It is totally clear that within the current view about the nature of empty space, a solution of the vacuum energy density problem is well out of reach. Only radical changes can open the way to a solution. The present work challenges this impasse within the new scenario of the Higgs theory [11] [12]. Recent experimental observations in the LHC in Geneva CH give support to the Higgs theory. According to this theory, empty space (vacuum) is not empty at all. It is filled up by a quantum fluid medium, a quantum condensate or Higgs condensate (HC) that is analogous to the superconducting condensate (SCC). However, while the condensation of the SCC occurs only at very low temperatures and is stabilized by an energy gap of only 1 meV, the HC is believed to have initiated condensation at 10^{15} K and is stabilized by a huge energy gap that, according to the Glashow-Weinberg-Salam electroweak model, achieves more than 200 GeV.

The current theories describe empty space in terms of a perfect fluid and the zero-point energy of a huge (almost infinite) number of uncorrelated oscillators. However, quantum condensates and in particular the HC, far from a perfect fluid of uncorrelated particles, are strongly correlated and highly phase coherent macroscopic quantum states of bosons with broken $U(1)$ symmetry and ruled by a very strong order parameter (collective wave-function). While in perfect fluids the particles respond individually to a perturbing field, in quantum condensates, the response always is collective involving all the particles of the condensate, through their order parameter. This turns the quantum condensate able to develop a screening velocity field, confining the perturbing field by effects like

the well-known Meissner effect in superconductors. This is believed to take place too in the HQS and is known as Higgs mechanism. Quantum condensates are like an army company, in which any attack always is an attack against all the members and has the coordinated response of the entire company.

The huge energy gap of the HC or Higgs Quantum Space (HQS) turns its order parameter extremely stable and rigid. It behaves like one unique entity (one unique oscillator) the size of the universe. Due to this huge energy gap, the order parameter of the HQS very strongly suppresses local quantum fluctuations and the zero-point energies. Therefore, the usual estimates of the vacuum energy density, in terms of quantum fluctuations and the zero-point energies of a perfect fluid, cannot be correct. On the other hand, local steady state excitations (local Goldstone modes) of the HQS require high energies, in the order of MeVs. However, the HQS at the same time is perfectly conservative. Therefore, excitations once created, automatically become indefinitely persistent.

The vacuum fluctuations causing the Casimir effect and the Lamb shift in Quantum Electrodynamics are often claimed to corroborate the correctness of the methods of particle physics to estimate the vacuum energy density. However, both these effects are of electromagnetic (EM) nature. The EM field has its $U(1)$ symmetry preserved and is long-range. It is not a quantum fluid. Moreover, the contribution of the zero-point fluctuations of the EM field to the vacuum energy density is very low. Contrarily, the Higgs Quantum Space (HQS) is an integrated entity, ruled by a very strong and rigid order parameter, which means wave lengths of the Higgs modes tending to the infinite and to zero frequency.

The next **Section 2** outlines with more details the nature and physical properties of the HQS filling up the empty space. As the properties of the HQS are closely analogous to the well-known properties of the superfluids and the superconducting condensates, the well known properties of these quantum fluids can be used as paradigm. Many of these properties are generic to all quantum condensates. The coming **Sections 3 and 4** will discuss the origin of the accelerating expansion of the universe from the perspective of the theoretical and experimental knowledge respectively, showing that within the scenario of the HQS, the vacuum energy density naturally approaches the observed value.

2. The Nature of the Empty Space

According to the Higgs theory, immediately after the big-bang, when the temperature fell through 10^{15} K a scalar field, present throughout space, has caused the breakdown of the electroweak symmetry into the weak force doublet $SU(2)$ and the electromagnetic (EM) field. While the EM field remained with its $U(1)$ symmetry unbroken, the weak force doublet has spontaneously broken its $U(1)$ symmetry and given rise to the Higgs condensate (HC). The HC is stabilized by a huge energy gap, which, according to the Glashow-Weinberg-Salam electroweak model, achieves more than 200 GeV

[6] [7]. The condensation energy of the HC plays the role of the vacuum energy and of the cosmological constant in Equation (1). It will be seen to be ultimately responsible for the accelerated expansion of the universe. The present work will not discuss details of the Higgs theory; however will rather implement its important practical consequences and the role of the HQS in the life of the universe.

Bose-Einstein (BE) phase correlation between the wave functions of the bosons enforces phase coherence and breakdown of the $U(1)$ symmetry, because this lowers the energy of the boson system. In this phase transition all the bosons condense into the same quantum ground state, in which they all assume the same phase, thereby forming a highly coherent quantum fluid state. Their wave-functions entangle, turning the bosons indistinguishable. This condensation is a second order phase transition that involves no latent heat. The condensation energy is released gradually down to absolute zero temperature. The Higgs condensate is a quantum fluid medium, ruled by the principles of quantum physics and with properties closely analogous to the superconducting condensate. It fills up the whole of space and is the quintessence of the empty space (vacuum). Likewise the conventional quantum condensates, the HQS too is intrinsically highly homogeneous throughout the universe.

Analogously as the superconducting condensate (SCC), the Higgs condensate too can be described by a Ginsburg-Landau like [13] complex order parameter $\Phi(r,\theta)=\phi(r)\mathrm{e}^{i\theta}$, a collective wavefunction in which $\phi(r)$ is the amplitude and $\mathrm{e}^{i\theta}$ is the phase factor. $\Phi(r,\theta_0)=\phi(r)\mathrm{e}^{i\theta_0}$ is the resting condition, the ground state of the condensate and $\rho=\Phi^*\Phi$ is the local condensate density that intrinsically is constant throughout the volume of the condensate.

BE phase correlation between the boson wefunctins gives rise to a *negative* potential energy (bonding) term, the value of which increases linearly with the condensate density ρ. Another positive potential energy (anti-bonding) term arises from repulsive core interaction between the bosons that increase with the squared density ρ^2 and prevents collapse of the system. The effective potential is:

$$V(\rho)=-n\rho+m\rho^2 \tag{5}$$

where however the negative coefficient (-*n*) of the bonding term is considerably larger than the positive coefficient (*m*) of the anti-bonding term. Because of the negative coeficient (-*n*), the minimum of the effective potential occurs not for $\rho=0$, however for a finite value $\rho=n/2m$. This is known as a non-zero vacuum-expectation-value that is homogeneous throughout the volume of the condensate. In terms of the components of Φ the Higgs potential energy well has the form of a Mexican sombrero. **Figure 1** depicts the form of this potential well in terms of the Real and Imaginary components of the order parameter. This form of the potential is characteristic of all quantum condensates.

The deepness of the potential well depends on the strength of the phase correlation between the bosons as well as on the phase coherence length. While in the conventional quantum fluids (superfluids and SCC) the coherence length is

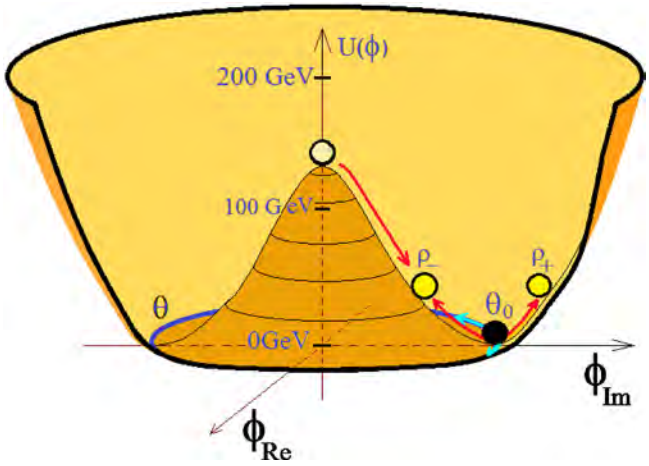

Figure 1. Characteristic potential well created during Bose-Einstein Condensation. The figure depicts locally the form of the Mexican sombrero potential in terms of the Real and the Imaginary components of the order parameter, where the given energy scale is for the Higgs condensate. A red arrow indicates the transition toward the lower energy phase coherent state with the well-defined phase θ_0. The figure also indicates the low volumetric density (ρ_-) and the high volumetric density (ρ_+) situations. While ρ_- drives accelerating contraction, ρ_+ drives accelerating expansion of the condensate. This is related with the Higgs mode. The global Goldstone mode is indicated along the blue bottom circle.

rather short (tens of Angströms) and the deepness of the potential well is of only 1 meV, in the Higgs condensate it achieves hundreds of GeV and its phase coherence may be very long-range. The fact that the phase of the condensate (θ_0) can take any value between 0 and 2π, without changing the energy, proves that the spontaneous breakdown of the $U(1)$ symmetry preserves the gauge symmetry of the Lagrangian.

The Higgs theory introduces profound changes in Einstein's view about the nature of empty space (vacuum). Being responsible for the inertial mass, the HQS is not only a local ultimate reference for rest and for motions of matter-energy, however literally governs these motions. The HQS, giving mass to the elementary particles, too is responsible for the gravitational dynamics; because it is mass that creates the gravitatonal fields. The Higgs theory provides by the first time a scientifically sound explanation for the origin of inertial mass of the elementary particles. The origin of the inertial mass is intimately related with the persistence of all excitations in the HQS. The Higgs theory pictures to us a universe in which the HQS plays a fundamental role both in the microscopic world of quantum physics as well as in the macroscopic world of gravitation. The HQS thus links together the physics of the quantum world and the physics of gravitation, which opens the way for their unification [14].

The nature of the HQS is profoundly different from that a perfect fluid. In a perfect fluid the particles are all independent, well localized and have their $U(1)$ symmetry preserved. In such a perfect fluid the particles are uncorrelated and respond individually to any perturbing field. This turns this perfect fluid

unable to develop collective and cooperative effects and is why these perfect fluids cannot confine, quantize an interacting field, nor can it develop a mechanism creating inertial mass for it. Contrarily, quantum fluids are formed by strongly correlated bosons with spontaneously broken $U(1)$ symmetry and condensed into a unique long-range phase coherent macroscopic quantum state. Such a quantum fluid is an integrated system, ruled by a complex order parameter. The HQS is governed by an extremely strong and powerful order parameter, which means that Higgs modes have extremely long wavelength tending to infinity. Only high energies can excite local (Goldstone like) modes with shorter wavelengths. They however automatically become persistent and are not virtual particles, because the HQS strongly suppresses quantum fluctuations and is perfectly conservative. The amplitude of the Higgs order parameter is highly uniform throughout the volume of the universe. This can solve the horizon and the flatness problems.

3. Nature of the Energy Accelerating the Expansion of the Universe

On spontaneously breaking down the $U(1)$ symmetry, the spin zero Higgs particles create a deep potential energy well of the form depicted in **Figure 1**. They condense into a negative energy state liberating the corresponding energy difference. In this process the total energy is conserved. Nothing is created from nothing. As Stephen Hawking liked to say, in order to create a mountain, it is enough to excavate a big hole. If the universe is an adiabatic system the energy liberated during the condensation remains within the universe in various forms. Such a behavior is well-known from the condensation of the usual ^{4}He into a superfluid, in which the condensation energy can in part be converted into quasi particles (Rotons, Maxons and vortices). In the condensation of superfluids and superconducting condensates a considerable amount of heat energy is liberated, which normally is removed by efficient cryogenics. Insufficient removal or dissipation of the condensation energy necessarily slows down or even stops the condensation rate.

The Higgs condensate (HC) fills up the space of the whole universe. To now, nothing indicates that an external world exists that can remove and absorb the very huge amount of condensation energy. Therefore, the only possible way to the universe reducing its energy density and temperature is by adiabatic expansion, converting its energy into kinetic energy of expansion and into confined mass-energy particles. The condensation of the Higgs condensate necessarily is an adiabatic process, analogous to the condensation of clouds, during the ascension and adiabatic expansion of warm and humid air. In the Higgs boson condensation however no external pressure opposes the expansion. Therefore, the expansion rate is free and accelerated. In this adiabatic process, the total energy must be conserved. The only way to lower the *energy density* and the temperature of the HC and of the universe is by volumetric expansion. Along this

process, a large part of the condensation energy is converted into mass-energy and kinetic energy of the expanding universe. This expansion stretches the wavelengths of the particles and of radiation as a function of time, thereby reducing the momentum and kinetic energy of the particles, according to the de-Broglie equation $\left(p = h/\lambda\right)$ with respect to the local HQS. This is why actually all matter in the universe is very closely stationary with respect to the local moving HQS and the temperature is close to zero. It also lowers the frequency and the energy of the radiation from distant sources (Hubble red-shift) and has shifted the frequency of the primordial Hydrogen radiation to the microwave frequency.

The presence of the ordinary fermion matter (concentrated mainly in stars and galaxies) represents a source of persistent phase perturbation and phase disorder of the Higgs order parameter. This holds back the advance toward the fully broken $U(1)$ symmetry and to the minimum of energy in the HC in the potential well **Figure 1**. The actual low temperature of the universe, of about 2.7 K, indicates that the universe lies deeply, near to the bottom of the Higgs potential well.

From the perspective of the present work, the total energy E of the universe may be calculated by the equation:

$$\begin{aligned} E &= \int_{V(t)} \rho_v(t)\,\mathrm{d}V = \rho_v(t)\int_{V(t)} \mathrm{d}V \\ &= \rho_v(t)V(t) = E_0 = \text{Constant} \end{aligned} \tag{6}$$

In this Equation, $V(t)$ is the total volume of the universe as a function of time, $\rho_v(t)$ is the time dependent vacuum energy density that is highly uniform (constant) over the volume of the universe and $E_0 = 200\ \text{GeV} \times V_0$ is the total initial energy of the universe with respect to the bottom of the potential well at the epoch of the electroweak break-down, which must be conserved.

The energy of the HC within the Higgs potential well depends on the volumetric density $\rho = \Phi^*\Phi = |\phi|^2$. If $\rho > n/2m$ or $\rho < n/2m$, the energy of the HC is not minimum. Please see **Figure 1**. If $\rho > n/2m$ and the number of Higgs particles is fixed, the universe can lower its energy by accelerated expansion. The Higgs condensate (HC) and with it the matter-energy universe lie deeply within the Higgs potential energy well **Figure 1**, however not at the minimum of energy. The matter fields, perturbing the order parameter and causing phase disorder of the Higgs order parameter, hold back the advance toward the minimum of energy. The situation is analogous to that of a superconductor below the transition temperature, however under a strong applied magnetic field. The phase perturbations of the magnetic field on the superconducting order parameter too hold back the advance of the SCC toward its minimum of energy. It can even destroy superconductivity for sufficiently high fields. Observations show that actually the expansion rate of the universe is accelerating. This indicates that $\rho > n/2m$. However, if $\rho < n/2m$, the HC can lower its energy by accelerated contraction. Apparently the universe can cycle between periods of free expansion and of free contraction.

Due to the very strong suppression of the fluctuations and of the zero-point energies of the various force fields by the HQS, all these contributions to the vacuum energy density are negligibly low. The only relevant vacuum energy is the condensation energy liberated during breakdown of the $U(1)$ symmetry. However, to parameterize the vacuum energy density as a function of the volume of the universe is difficult, because the size of the universe at the epoch of the electroweak symmetry and the $U(1)$ symmetry breakdowns is not well known. Moreover, this condensation energy was liberated only gradually as the temperature fell. The temperature of the universe is a better parameter. The electroweak symmetry break-down is believed to have initiated closely after the big-bang, when the temperature fell through temperatures between 10^{15} K and 10^{12} K. On from the recombination epoch and formation of the Hydrogen atoms, the temperature gradually fell down to the actual 2.7 K, known from the cosmic-microwave-background radiation. However, the average temperature of the universe certainly is a little bit higher, because of the hot stars and galaxies. Maybe 3 K is a good guess.

$$\rho_v = 200\ \text{GeV} \times \frac{3}{10^{12}} = 0.6\ \text{eV} \sim 2\times 10^{-10}\ \text{ergs}/\text{cm}^3 \tag{7}$$

This result is equivalent to about 10^{-29} g/cm^3 (about 6 Hydrogen atoms per cubic meter). However, although this mass-energy density is very low, it is constant over the entire space of the universe. Integrating it, gives a value about 14 times that of the visible mass-energy in the universe. This last however is confined in the astronomical bodies. On the other hand, the well known relation between the vacuum energy density ρ_v and the cosmological constant Λ is:

$$\Lambda = \frac{8\pi G\rho_v}{c^2} \sim 10^{-52}\ \text{m}^{-2} \tag{8}$$

where G is the gravitational constant and c is the velocity of light in the vacuum.

The present calculation of the vacuum energy density, while giving values close to the observations, also helps to understand the intriguing coincidence problem of cosmology. Why are actually the values of the vacuum energy and of the visible ordinary matter-energy so closely similar? The actual small residual vacuum energy density consists of two parts: The condensation energy that still has not decayed because the temperature of the universe is not absolute zero (bare cosmological constant). According to the present work, the phase perturbation of the Higgs order parameter by the ordinary (visible) matter-energy in the universe is responsible for the major part of the residual vacuum energy density. This explains why actually the total vacuum energy and the total visible matter energy are so closely similar. On the other hand, the only relationship of the HQS, with ordinary matter-energy, is giving mass to the elementary particles and ruling their inertial motion. In this scenario, the only way of the HQS-dynamics (vacuum energy) to affect the motion of ordinary matter-energy is by inertial dynamics effects, which after Einstein's principle of equivalence are gravitational effects.

4. Experimental Evidence That the Accelerating Expansion of the Universe Keeps to the Accelerating Expansion of the HQS Itself

Clocks, stationary within gravitational fields, are well known to show exactly the gravitational slowing predicted by GR. However, the GPS clocks moving with earth round the sun show no sign of the gravitational slowing by the solar field [15] [16] predicted by the GR. This observation, together with the null results of the Michelson light anisotropy experiments, demonstrates that the HQS, ruling the motion of matter-energy, is circulating round the sun according to a Keplerian velocity field, consistently with the planetary motions. It certainly is also moving round every other astronomical body consistently with the local main astronomical motions and generating the respective gravitational fields. The HQS materializes the local Lorentz Frames (LFs) turning them into local proper LFs. This Keplerian velocity field of the HQS is the quintessence of the gravitational fields and is shown in Refs. [14] [17] to accurately create the observed gravitational dynamics on earth, in the solar system and also to create the observed non-Keplerian rotation of the galaxies *without the need of dark matter*. It moreover produces correctly all the observed effects of the gravitational fields on light and on clocks. In the Keplerian velocity field of the sun, earth and all the other planets of the solar system are closely stationary with respect to the local moving HQS and thus with respect to the local proper LFs. The planets simply are carried round the sun by the solar Keplerian velocity field of the HQS. The solar system too is stationary with respect to the local HQS in the galactic velocity field and carried around the center of the Milky-Way gralaxy. The observed absence of the gravitational slowing of the GPS clocks by the solar field and the isotropy of light with respect to earth are both obvious signatures of the physical mechanism of gravity in action in the solar field.

The Keplerian velocity field of the HQS round the sun and the velocity field round the galactic center properly explain the isotropy of light with respect to earth. It however cannot explain why the recession between the galaxies too causes no light anisotropy. The fact that the velocity of light is isotropic with respect to earth, despite its orbital motion round the sun and despite the orbital motion of the solar system in the Milky-Way galaxy and *also despite the relative motion and recession between the galaxies*, demonstrates that the accelerated recession between the galaxies too lets earth stationary with respect to the local moving HQS. Despite the accelerated expansion of the universe, our Milky-Way galaxy remains stationary with respect to the local HQS. It certainly would not be reasonable to assume that our galaxy is in a privileged kinematic circumstance with respect to the HQS in detriment to all the other galaxies in the universe. All the galaxies must equally be closely stationary with respect to the local moving HQS. These facts entail the conclusion that the HQS, governing the inertial motion of matter and propagating light, besides moving round earth, round the sun and round the center of the Milky-Way galaxy, according to ve-

locity fields, consistent with the local main astronomical motions also is expanding consistently with the recession between the galaxies.

Within this scenario, the Hubble spectral red-shifts of light from distant galaxies are not usual Doppler shifts and the red-shift of the cosmic microwave background radiation are due to the time-rate of stretching of the wavelength, due to the expansion of the HQS, their medium of propagation and the ultimate reference for rest and for motions. It is easy to show that this stretching of the wavelength, as a function of time, causes exactly the same red-shift as the usual Doppler shift, due to conventional recession. The expansion of the HQS, stretching the wavelength of the particles and of light, reduces the kinetic energy of the particles with respect to the local HQS and the energy of the radiation. Moreover, the velocity of oppositely moving matter bodies is averaged down and converted into heat during the gravitational agglomeration into the large astronomical bodies. These observations naturally explain why the velocity of all the large astronomical bodies with respect to the local HQS is actually so small (only hundreds of meters per second) throughout the universe.

In summary, the HQS, ruling the inertial motion of matter and the propagation of light, is circulating round earth, round the sun and round the galactic center, consistently with the local main astronomical motions. These velocity fields are the quintessence of the gravitational fields. In the local HQS-dynamics round the sun and round the galactic center, earth is very closely stationary with respect to the local moving HQS, so that the orbital motion of earth and the motion of the solar system within the galaxy cause no relevant light anisotropy with respect to earth. The observed absence of the gravitational slowing of the GPS clocks by the solar field perfectly corroborates this conclusion. The null light anisotropy results however demonstrate in addition that the accelerating expansion of the universe too lets earth, the solar system and the Milky-Way galaxy and all the other galaxies stationary with respect to the local HQS. This concomitant expansion of the HQS and of the matter universe ultimately explains the observed isotropy of light with respect to earth and shows that the accelerated expansion of the visible universe keeps to the accelerating expansion of the HQS itself. The fact that all the astronomical bodies throughout the universe are very closely stationary with respect to the local HQS predicts the universality of the laws of physics.

Dark energy is not ordinary mass-energy, but is energy of the HQS itself, energy of the vacuum. The total vacuum energy is closely similar to the total visible matter-energy, because it is the visible matter-energy that holds back the HC from its minimum of energy. Also, due to the fact that the HQS is a quantum fluid, ruled by an order parameter, this energy necessarily distributes it very homogeneously throughout the universe. Moreover, the HQS, ruling the inertial motion of matter-energy, interacts with ordinary matter-energy only by inertial effects, causing inertial dynamics, which, according to Einstein's Equivalence Principle, are gravitational effects. This shows that the HQS-dynamics naturally

meets all the characteristic properties of dark energy that are consensual among the cosmologists. It however entails a fundamental additional feature: The accelerating expansion of the universe perfectly keeps to the accelerated expansion of the HQS itself.

5. Conclusion

The Higgs Quantum Space (HQS) is a very strongly correlated quantum fluid medium, ruled by an order parameter and stabilized by a huge energy gap. This order parameter very strongly suppresses the local quantum fluctuations and the zero-point energies of the weak and strong nuclear fields, turning their contribution to the vacuum energy density irrelevant. Therefore, the estimate of the vacuum energy density, in terms of the zero-point energies leads to a completely wrong value. On the other hand, the universe is an adiabatic system. The only possible way of it reducing its energy density and temperature is by expansion, converting its energy partly into kinetic energy of expansion and partly into confined mass-energy. The fact that the actual residual energy is mostly due to the phase disorder, created by the presence of the ordinary mass-energy, explains the actual similarity of the total vacuum energy and of the totally visible matter-energy. Finally, the zero light anisotropy on earth demonstrates that, in the accelerated expansion of the universe, the visible matter universe keeps to the accelerated expansion of the HQS itself.

Conflicts of Interest

The author declares no conflicts of interest regarding the publication of this paper.

References

[1] Friedmann, A. (1924) *Zeitschrift für Physik*, **21**, 326-332. https://doi.org/10.1007/BF01328280

[2] Einstein, A. (1916) *Annalen der Physik*, **49**, 769-822.

[3] Lorentz, H.A., Einstein, A., Minkowski, H. and Weyl, H. (1923) The Principle of Relativity. Dover Publications, New York.

[4] Robertson, H.P. (1936) *Astrophysical Journal*, **83**, 257. https://doi.org/10.1086/143726

[5] Walker, A.G. (1937) *Proceedings of the London Mathematical Society*, **42**, 90-127. https://doi.org/10.1112/plms/s2-42.1.90

[6] Carrol, S.M. (2000) Determination of Dark Energy and Dark Matter from the Values of Redshift for the Present Time, Planck and Trans-Planck Epochs of the Big-Bang Model. arXiv:astro-ph/0004075v

[7] Sola, J. (2013) Cosmological Constant and Vacuum Energy: Old and New Ideas. arXiv:1306.1527v3 [gr-qc]

[8] Riess, A., *et al.* (1998) *The Astronomical Journal*, **116**, 1009. https://doi.org/10.1086/300499

[9] Perlmutter, S., *et al.* (1999) *The Astronomical Journal*, **517**, 565. https://doi.org/10.1086/307221

[10] Lobo, F.S.N. (2006) *Classical and Quantum Gravity*, **23**, 1525. https://doi.org/10.1088/0264-9381/23/5/006

[11] Higgs, P.W. (1964) *Physical Review Letters*, **13**, 508. https://doi.org/10.1103/PhysRevLett.13.508

[12] Englert, F. and Brout, R. (1964) *Physical Review Letters*, **13**, 321. https://doi.org/10.1103/PhysRevLett.13.321

[13] Ginzburg, L. and Landau, L.D. (1950) *Journal of Experimental and Theoretical Physics* (*JETP*), **20**, 1064.

[14] Schaf, J. (2018) *Journal of Modern Physics*, **9**, 395. https://doi.org/10.4236/jmp.2018.93028

[15] Hatch, R.R. (2004) *GPS Solutions*, **8**, 67-73. https://doi.org/10.1007/s10291-004-0092-8

[16] Hatch, R.R. (2004) *Foundations of Physics*, **34**, 1725-1739. https://doi.org/10.1007/s10701-004-1313-2

[17] Schaf, J. (2018) *Journal of Modern Physics*, **9**, 1111. https://doi.org/10.4236/jmp.2018.95068

Journal of Modern Physics, 2019, 10, 294-301
http://www.scirp.org/journal/jmp
ISSN Online: 2153-120X
ISSN Print: 2153-1196

P-V Criticality of a Modified BTZ Black Hole in 2 + 1 Dimensional Intrinsic Time Quantum Gravity

A. S. Kubeka

Department of Mathematical Sciences, University of South Africa, Science Campus, Florida, South Africa
Email: kubekas@unisa.ac.za

How to cite this paper: Kubeka, A.S. (2019) P-V Criticality of a Modified BTZ Black Hole in 2 + 1 Dimensional Intrinsic Time Quantum Gravity. *Journal of Modern Physics*, **10**, 294-301.
https://doi.org/10.4236/jmp.2019.103020

Received: December 14, 2018
Accepted: March 8, 2019
Published: March 11, 2019

Abstract

Intrinsic time quantum geometrodynamics is a formulation of quantum gravity naturally adapted to 3 + 1 dimensions. In this paper we construct its analogous 2 + 1 formulation, taking note of the mathematical structures which are preserved. We apply the resulting construction to convert the BTZ black hole metric to ITQG framework. We then modify the BTZ black hole in order to investigate the existence of the P-V criticality in ITQG theory.

Keywords

Intrinsic Time Quantum Geometrodynamics, Modified BTZ Black Hole, 2 + 1 Quantum Gravity, Black Hole P-V Criticality, Van der Waals Fluid, Liquid-Gas Phase Transition

1. Introduction

P-V criticality of a modified BTZ black hole was recently studied by Kubeka and Sadeghi in [1]. They introduced some anstaz that gives a modified BTZ black hole and then showed that this modified BTZ black hole is satisfied by the equation of state of Liquid-gas phase transition. Also Sadeghi [2] studied the P-V criticality of Logarithmic corrected Dyonic charged AdS black hole by considering a charged AdS black hole which is in fact a holographic dual of a van der Waals fluid. They showed that the holographic picture is still valid. The logarithmic corrections arise due to the fluctuations in thermal properties which are important when the black hole is small and these fluctuations are interpreted as quantum effects.

The theory of quantum Gravity that encompasses the notion of intrinsic time

(Intrinsic Time Quantum Geometrodynamics, ITQG) was recently formulated by Ita *et al.* [3]. The foundational work for the theory was laid down in [4]-[10]. In [11], Ita *et al.* solved the long outstanding Wheeler-DeWitte equation in Quantum Geometrodynamics and derived cosmological exact solutions that are characterized by the Schrodinger wave functionals that in turn have two physical degrees of freedom in accordance with the Yamade problem in quantum gravity. The theory seems to resolve all the outstanding problems in quantum gravity that have been highlighted by other prominent theories of quantum gravity like Loop Quantum Gravity (LQG) in one single stroke and in clean manner Ita *et al.* [12]. The success and validity of this theory will be tested by future research.

In this paper we study the transform of the modified BTZ black hole into the ITQG formalism and then establish the existence of the P-V criticality as done in the literature. The paper is structured as follow: In Sec. 2, we reformulate the ITQG formalism in 2-dimension, and in Sec. 3, we reformulate the BTZ black hole within the context of ITQG. In Sec. 4, we study and establish the existence of the P-V criticality of a modified BTZ black in ITQG theory, and then lastly in Sec. 5 conclude the paper.

2. Quantum Gravity in 2 + 1 Dimension

In [3] a formulation of intrinsic time quantum geometrodynamics (ITQG) is presented, which is applicable to 3 + 1 dimensional spacetime. We would like to study an analogous 2 + 1 formulation corresponding to two spatial and one temporal dimension. There are a few similarities and differences which will be noted in this paper. Let us start off by taking, as the basic variables, a unimodular spatial two-metric $\bar{q}_{ij}$ with $\det \bar{q}_{ij} = 1$ and a mixed-index, traceless, momentric variable $\bar{\pi}^i_j$ with $\delta^j_i \bar{\pi}^i_j = 0$. For index conventions in this paper, lower case Latin symbols $i, j, \cdots$ will denote spatial indices in two-space, taking values 1 and 2. Upon these variables let us confer the following commutation relations

$$\begin{aligned} &\left[\bar{q}_{ij}(x), \bar{q}_{kl}(y)\right] = 0; \left[\bar{q}_{ij}(x), \bar{\pi}^k_l(y)\right] = i\hbar \bar{E}^k_{l(ij)} \delta(x-y); \\ &\left[\bar{\pi}^i_j(x), \bar{\pi}^k_l(y)\right] = \frac{i\hbar}{2}\left(\delta^i_l \bar{\pi}^k_j - \delta^k_j \bar{\pi}^i_l\right)\delta(x-y), \end{aligned} \tag{1}$$

where $\delta(x-y)$ denotes the two dimensional delta function, and $\bar{E}^k_{l(ij)} = \frac{1}{2}\left(\delta^k_i \bar{q}_{lj} + \delta^k_j \bar{q}_{li} - \delta^k_l \bar{q}_{ij}\right)$ is a traceless projector, with $\delta^l_k \bar{E}^k_{l(ij)} = \bar{q}^{ij} \bar{E}^k_{l(ij)} = 0$, and $\bar{E}^k_{l(kj)} = \frac{3}{2}\bar{q}_{lj}$. Let us define generators $T_a(x) = \frac{1}{\hbar\delta(0)}(\sigma_a)^j_i \bar{\pi}^i_j(x)$, where $(\sigma_a)^i_j$ for $a = 1,2,3$ denote the Pauli spin matrices. Then contracting the middle relation of (1) with $(\sigma_a)^l_k$ we get the following relation

$$\left[\bar{q}_{ij}(x), T_a(y)\right] = i(\sigma_a)^l{}_{(i}\bar{q}_{lj)} \frac{\delta(x-y)}{\delta(0)}, \tag{2}$$

namely that the two-metric $\bar{q}_{ij}$ transforms in the spin-two irreducible representation of $SU(2)$. Contraction of the last relation of (1) with $(\sigma_a)_i^j (\sigma_b)_k^l$ yields the relation

$$\left[T_a(x), T_b(y)\right] = \frac{i}{2}\epsilon_{abc}T_c \frac{\delta(x-y)}{\delta(0)}, \tag{3}$$

which is the $SU(2)$ Lie algebra with structure constants ϵ_{abc}. Hence the momentric variables in the 2 + 1 formulation of ITQG transform, as a triplet of $SU(2)$ generators, in the adjoint representation of $SU(2)$.

Having conferred upon the fundamental variables a $SU(2)$ Lie-algebraic interpretation, it is next of interest to determine the $SU(2)$ invariants and their physical interpretation. From the Fierz identity for $SU(2)$

$$(\sigma_a)^i_j (\sigma_a)^k_l = \frac{1}{2}\left(\delta^i_l\delta^k_j - \frac{1}{2}\delta^i_j\delta^k_l\right), \tag{4}$$

We have, upon carrying out a contraction with $\bar{\pi}_i^j\bar{\pi}_k^l$, the following relation

$$\left(\hbar\delta(0)\right)^2 T_a T_a = \frac{1}{2}\bar{\pi}_i^j\bar{\pi}_j^i \equiv \Delta, \tag{5}$$

namely that the quadratic Casimir invariant for $SU(2)$ is proportional to the traceless modes of the Wheeler-DeWitt kinetic operator, forming the Hamiltonian for the free theory.

The dynamics of the evolution of the basic variables of the theory with respect to T and the gauge invariant part of the intrinsic time $\ln q^{1/3}$ are encoded in the Physical Hamiltonian which we define as $H_{Phys} = \frac{1}{\beta}\int_\Sigma \mathrm{d}^3x\sqrt{\Delta}$, and a unitary evolution operator

$$U(T, T_0) = T\exp\left[\frac{i}{\hbar}\int_{T_0}^T H_{Phys}(T')\delta T'\right]. \tag{6}$$

This acts on a basis of states forming a separate $SU(2)$ multiplet at each spatial point $\prod_x |m,l\rangle_x$, satisfying the $SU(2)$ angular momentum relations

$$T_3(x)\prod_y |m,l\rangle_y = m\prod_y |m,l\rangle_y;\ \sqrt{\Delta}\prod_y |m,l\rangle_y = \hbar\delta(0)\sqrt{l(l+1)}\prod_y |m,l\rangle_y. \tag{7}$$

One can construct from this a basis of $SU(2)$ spin-network states, with the $SU(2)$ singlets being diffeomorphism invariant. In this analogy to Loop Quantum Gravity, these states must be deemed to be in a momentum space representation.

3. The BTZ Black Hole in Intrinsic Quantum Gravity

Let us consider the metric for a BTZ black hole

$$\mathrm{d}s^2 = g_{00}\mathrm{d}t^2 + g_{rr}\mathrm{d}r^2 + g_{\varphi\varphi}\left(\mathrm{d}\varphi + N^\varphi \mathrm{d}t\right)^2, \tag{8}$$

where we have defined

$$g_{00} = -N^2 = -\left(-M + \frac{r^2}{l^2} + \frac{j^2}{4r^2}\right);\ g_{rr} = \frac{1}{N^2};\ g_{\varphi\varphi} = r^2;\ N^\varphi = -\frac{j}{2r^2};\ N^r = 0. \tag{9}$$

We will now put the metric (8) into the language of ITQG **by calculating the fundamental basic variables of the theory**. From the determinant of the spatial two-metric $q = q_{rr}q_{\varphi\varphi} = \dfrac{r^2}{-M + \dfrac{r^2}{l^2} + \dfrac{j^2}{4r^2}}$, we can construct the unimodular spatial two-metric

$$\bar{q}_{ij} = q_{ij}q^{-1/2} = \begin{pmatrix} \dfrac{1}{r}\left(-M + \dfrac{r^2}{l^2} + \dfrac{j^2}{4r^2}\right)^{-1/2} & 0 \\ 0 & r\left(-M + \dfrac{r^2}{l^2} + \dfrac{j^2}{4r^2}\right)^{1/2} \end{pmatrix} \tag{10}$$

with $\det \bar{q}_{ij} = 1$. Next, we will construct the momentric variables $\bar{\pi}^i_j$. The extrinsic curvature is given by $K_{ij} = \dfrac{1}{2N}\left(-\dot{q}_{ij} + \nabla_i N_j + \nabla_j N_i\right)$. We will need the lowered index form of the shift vector

$$N_r = q_{rr}N^r + q_{r\varphi}N^\varphi = 0; \quad N_\varphi = q_{\varphi r}N^r + q_{\varphi\varphi}N^\varphi = r^2\left(-\frac{1}{2r^2}\right) = -\frac{j}{2}. \tag{11}$$

Since the three-metric is time independent, then $\dot{g}_{\mu\nu} = 0$ and only the covariant derivatives of the shift vector components will contribute

$$K_{rr} = \frac{1}{N}\nabla_r N_r = 0, \quad K_{\varphi\varphi} = \frac{1}{N}\nabla_\varphi N_\varphi = 0. \tag{12}$$

For the covariant derivatives we have

$$\nabla_r N_\varphi = \partial_r N_\varphi - \Gamma^r_{r\varphi}N_r - \Gamma^\varphi_{\varphi r}N_\varphi = \partial_r\left(j/2\right) - 0 - \frac{\partial_r q_{\varphi\varphi}}{2q_{\varphi\varphi}}N_\varphi = \frac{\partial_r r^2}{2r^2}\frac{j}{2} = \frac{j}{2r}$$

$$\nabla_\varphi N_r = \partial_\varphi N_r - \Gamma^r_{\varphi r}N_r - \Gamma^\varphi_{\varphi r}N_\varphi = 0 - 0 + \frac{j}{2r}; \tag{13}$$

Using $N = \sqrt{-M + \dfrac{r^2}{l^2} + \dfrac{j^2}{4r^2}}$ and substituting (13) and (12), we have $K_{r\varphi} = \dfrac{j}{2Nr}$ with the following representation

$$K_{ij} = \frac{j}{2r}\left(-M + \frac{r^2}{l^2} + \frac{j^2}{4r^2}\right)^{-1/2}\begin{pmatrix} 0 & 1 \\ 1 & 0 \end{pmatrix}. \tag{14}$$

The contravariant form is given by

$$K^{ij} = q^{im}K_{mn}q^{mj} = \frac{j}{2r}\left(-M + \frac{r^2}{l^2} + \frac{j^2}{4r^2}\right)^{-1/2}\begin{pmatrix} 0 & 1 \\ 1 & 0 \end{pmatrix}, \tag{15}$$

which after the matrix multiplication yields the same components as K_{ij}. To get the momentric variables we must first compute the traceless form of K^{ij}, which is already traceless. In the ADM metric theory, we denote spatial 3-metric and its barred conjugate momentum on a spatial slice Σ of four dimensional space-time of topology $M = \Sigma \times R$ by $q_{i,j}$ and $\tilde{\pi}^{ij}$ respectively. The ADM conjugate

momentum is given by $\tilde{\pi}^{ij} = \frac{1}{2}\sqrt{q}\left(K^{ij} - q^{ij}K\right) = \frac{1}{2}\sqrt{q}K^{ij}$. These leads to the barred momentum

$$\bar{\pi}^{ij} = q^{1/2}\left(\tilde{\pi}^{ij} - \frac{1}{2}q^{ij}\tilde{\pi}\right) = \frac{q}{2}K^{ij}, \tag{16}$$

with matrix representation

$$\tilde{\pi}_i^j = \bar{q}_{im}\bar{\pi}^{mj}$$

$$= \frac{jr}{4}\left(-M + \frac{r^2}{l^2} + \frac{j^2}{4r^2}\right)^{-3/2}\begin{pmatrix} 0 & \frac{1}{r}\left(-M + \frac{r^2}{l^2} + \frac{j^2}{4r^2}\right)^{-1/2} \\ r\left(-M + \frac{r^2}{l^2} + \frac{j^2}{4r^2}\right)^{1/2} & 0 \end{pmatrix} \tag{17}$$

4. P-V Criticality in Modified BTZ Black Hole in Intrinsic Quantum Gravity

To modify the BTZ black hole metric, we have from (10), $\bar{q}_{ij} = \frac{1}{g(r)}$ where

$$g(r) = r\left(-M + \frac{r^2}{l^2} + \frac{j^2}{4r^2}\right)^{1/2} + h(r,p) \tag{18}$$

and $h(r,p)$ is function that must be determined. After differentiation and further simplification we get

$$\begin{aligned} g'(r) = -M^{1/2} + \left(\frac{M^{-1/2}r^2}{2} - M^{1/2}r^2\right)\frac{1}{l^2} + \left(\frac{M^{-1/2}}{2} + M^{1/2}\right)\frac{j^2}{4r^2} \\ -\frac{M^{-1/2}}{2}\left(\frac{r^2}{l^2}\right)^2 + \frac{M^{-1/2}}{2}\left(\frac{j^2}{4r^2}\right)^2 + h'(r,p) \end{aligned} \tag{19}$$

But the position of the black hole event horizon is determined by the larger root of $g(r_+) = 0$, and by using the Euclidean trick we have the black hole temperature given by

$$\begin{aligned} T &= \frac{1}{\beta} = \frac{g'(r_+)}{4\pi} \\ &= -\frac{M^{1/2}}{4\pi} + \frac{1}{4\pi}\left(\frac{M^{-1/2}r^2}{2} - M^{1/2}r^2\right)\frac{8\pi}{3}P + \frac{1}{4\pi}\left(\frac{M^{-1/2}}{2} + M^{1/2}\right)\frac{j^2}{4r^2} \\ &\quad -\frac{1}{4\pi}\frac{M^{-1/2}r^4}{2}\left(\frac{8\pi}{2}\right)^2 P^2 + \frac{M^{-1/2}}{2}\frac{1}{4\pi}\left(\frac{j^2}{4r^2}\right)^2 + h'(r,p) \end{aligned} \tag{20}$$

where in the case of the asymptotically BTZ black hole the pressure P is

$$\begin{aligned} P &= \frac{-1}{8\pi}\Lambda = \frac{3}{8\pi}\frac{1}{l^2}, \\ \Rightarrow \frac{8\pi}{3}P &= \frac{1}{l^2}. \end{aligned} \tag{21}$$

From the Wan der Waals relation

$$T=\left(P-\frac{a}{v^2}\right)(v+b)=Pv-Pb+\frac{a}{v}-\frac{ab}{v^2}, \tag{22}$$

with

$$v=2r, \tag{23}$$

we have

$$T=2Pr_+-Pb+\frac{a}{2r_+}-\frac{ab}{4r_+^2}. \tag{24}$$

Now in order to find $h(r,P)$ we use the anstaz

$$h(r,P)=A(r)+PB(r,P), \tag{25}$$

with

$$h'(r,P)=A'(r)+PB'(r,P). \tag{26}$$

So from (20), (24) and (26) we have

$$\begin{aligned}&\frac{-M^{1/2}}{4\pi}+\left(\frac{M^{-1/2}r_+^2}{2}-M^{1/2}r_+^2\right)\frac{2}{3}P+\left(\frac{M^{-1/2}}{2}+M^{1/2}\right)\frac{j^2}{4r_+^2}\frac{1}{4\pi}\\&-\frac{M^{-1/2}}{2}\frac{r_+^4}{4\pi}\left(\frac{8\pi}{3}\right)^2P^2+\frac{M^{-1/2}}{2}\left(\frac{j^2}{4r_+^2}\right)^2\frac{1}{4\pi}+\frac{A'(r)}{4\pi}+\frac{P'B(r)}{4\pi}\\&-2Pr_++Pb-\frac{a}{2r_+}+\frac{ab}{4r_+^2}=0.\end{aligned} \tag{27}$$

From which we have the following two independent equations

$$\left(\frac{M^{-1/2}r_+^2}{2}-M^{1/2}r_+^2\right)\frac{2P}{3}-\frac{M^{-1/2}}{2}r_+^4\left(\frac{8\pi}{3}\right)^2\frac{P^2}{4\pi}+\frac{PB'(r)}{4\pi}-2Pr_++Pb=0,$$

$$-\frac{M^{1/2}}{4\pi}+\frac{1}{4\pi}\left(\frac{M^{-1/2}}{2}+M^{1/2}\right)\frac{j^2}{4r_+^2}+\frac{M^{-1/2}}{2}\frac{1}{4\pi}\left(\frac{j^2}{4r_+^2}\right)^2+\frac{A'(r)}{4\pi}-\frac{a}{2r_+}+\frac{ab}{4r_+^2}=0, \tag{28}$$

for which we are able to solve for $A(r)$ and $B(r)$ as follows

$$\begin{aligned}A(r)&=4\pi\frac{a}{2}\ln(r_+)+\pi ab\frac{1}{r_+}+M^{1/2}r_++\left(\frac{M^{-1/2}}{2}+M^{1/2}\right)\frac{j^2}{4r_+}-\frac{M^{-1/2}}{6}\left(\frac{j^2}{4}\right)^2\frac{1}{r_+^3},\\B(r)&=4\pi r_+^2-4\pi br_++M^{-1/2}\frac{r_+^5}{10}\left(\frac{8\pi}{3}\right)^2P-\left(\frac{M^{-1/2}r_+^3}{6}-\frac{M^{1/2}r_+^3}{3}\right)\frac{8\pi}{3}.\end{aligned} \tag{29}$$

But putting the above results for $A(r)$ and $B(r)$ into (25) and then put the resulting explicit expression for $h(r,P)$ into (18), and using (22) we get the modified expression for $g(r)$ given by

$$\begin{aligned}g(r)=r&\left(-M+\frac{r^2}{l^2}+\frac{j^2}{4r^2}\right)^{1/2}+2\pi a\ln(r)+\frac{\pi ab}{r}+M^{1/2}r\\&+\left(\frac{M^{-1/2}}{2}+M^{1/2}\right)\frac{j^2}{4r}-\frac{M^{-1/2}}{6r^3}\left(\frac{j^2}{4}\right)^2+\frac{3r^2}{2l^2}-\frac{3br}{2l^2}\\&+\frac{M^{-1/2}r^5}{10l^4}-\left(\frac{M^{-1/2}r^3}{6}-\frac{M^{1/2}}{3}r^3\right)\frac{1}{l^2}\end{aligned} \tag{30}$$

which gives us the modified BTZ black hole from which

$$\begin{aligned} T &= \frac{1}{4\pi} g'(r)\Big|_{r=r+} \\ &= \frac{M^{-1/2} r^2 P}{3} - \frac{2M^{1/2} r^2 P}{3} + \frac{a}{2r} - \frac{ab}{4r^2} + 2Pr - bP - \left(\frac{M^{-1/2} r^2}{2} - M^{1/2} r^2 \right) \frac{2P}{3} \end{aligned} \tag{31}$$

thus solving for the pressure P and further simplifications we get

$$P = \frac{1}{\left[-b + 2r\right]} \left[T - \frac{a}{2r} + \frac{ab}{4r^2} \right]. \tag{32}$$

From the above, we observe that Equation (32) was also derived in [1] in another different formalism of quantum gravity. Thus we have shown that Equation (32) must be universal for the modified BTZ black hole irrespective of the formalism used. Thus continuing further we are then able to find the BTZ black hole critical points T_c, P_c, and V_c as

$$V_c = 3b,$$

$$P_c = \frac{a}{27b^2}$$

and

$$T_c = \frac{8a}{27b} \tag{33}$$

using the conditions

$$\frac{\partial P}{\partial V} = 0 \quad \text{and} \quad \frac{\partial^2 P}{\partial V^2} = 0. \tag{34}$$

Then finally from (33) we are able to find an interesting relation which is exactly the same as for the Van der Waals fluid called the thermodynamic critical compressibility factor and it is universal number predicted for the modified BTZ black hole [1].

$$\frac{P_c V_c}{T_c} = \frac{3}{8}, \tag{35}$$

Therefore from above results, we conclude that the modified BTZ black hole also exhibit the thermodynamic P-V criticality behavior in ITQG framework.

5. Conclusion

It is a well known fact that usual BTZ black does not have the critical behavior in P_c, T_c, V_c. But in order for the black hole to have these behaviors, it needs to be modified and we do the transformation by using a suitable anstaz as function $h(r, p)$. In our case, we modified the BTZ black hole within the frame work of ITQG formalism and we showed that indeed the modified BTZ black hole exhibits the P-V criticality and thus the results are the same as that of the Van der Waals fluid.

Acknowledgements

ASK would like to thank Prof. Eyo Eyo Ita III for the advices and discussions regarding the problem and my employer the University of South Africa for providing me with the conducive environment and facilities to conduct the research of this paper.

Data Availability

No data was used to support this study.

Conflicts of Interest

The author declares that there are no conflicts of interest regarding the publication of this paper.

References

[1] Sadeghi, J. and Kubeka, A.S. (2016) *International Journal of Theoretical Physics*, **55**, 2455-2459. https://doi.org/10.1007/s10773-015-2882-x

[2] Sadeghi, J., Pourhassan, B. and Rostami, M. (2016) *Physical Review D*, **94**, 064006. https://doi.org/10.1103/PhysRevD.94.064006

[3] Ita, E.E., Soo, C. and Yu, H.-L. (2015) *Prog. Theor. Exp. Phys.*, 083E01.

[4] DeWitt, B.S. (1967) *Physical Review Journals Archive*, **160**, 1113. https://doi.org/10.1103/PhysRev.160.1113

[5] Dirac, P.A.M. (1958) *Proceedings of the Royal Society of London A*, **246**, 333.

[6] Klauder, J.R. (2006) *International Journal of Geometric Methods in Modern Physics*, **3**, 81-94. https://doi.org/10.1142/S0219887806001028

[7] Lin, C.Y. and Soo, C. (2009) *Physics Letters B*, **671**, 493-495. https://doi.org/10.1016/j.physletb.2008.12.051

[8] Murchadha, N.O., Soo, C. and Yu, H.-L. (2013) *Class. Quantum Grav*, **30**, 095016. https://doi.org/10.1088/0264-9381/30/9/095016

[9] Soo, C. and Yu, H.-L. (2014) *Prog. Theor. Phys*, **2014**, 013E01.

[10] Wheeler, J.A. (1968) Superpsace and the Nature of Quantum Geometrodynamics, in Battelle Rencontres, 1967. In: DeWitt, C.M. and Wheeler, J.A., Eds., *Lectures in Mathematics and Physics*, W. A. Benjamin, New York.

[11] Ita, E.E. and Soo, C. (2015) *Annals of Physics*, **359**, 80-96. https://doi.org/10.1016/j.aop.2015.04.016

[12] Ita, E.E. and Kubeka, A.S. (2016) *Universe*, **2**, 18. https://doi.org/10.3390/universe2030018

Journal of Modern Physics, 2019, 10, 302-309
http://www.scirp.org/journal/jmp
ISSN Online: 2153-120X
ISSN Print: 2153-1196

Peak of Electron Density in F2-Layer Parameters Variability at Quiet Days on Solar Minimum

Emmanuel Nanéma[1,2*], Moustapha Konaté[2], Frédéric Ouattara[2]

[1]Centre National de la Recherche Scientifique et Technologique (CNRST), Institut de Recherche en Sciences Appliquées et Technologies (IRSAT), Ouagadougou, Burkina Faso
[2]Université Norbert ZONGO, Laboratoire de Recherche en Météorologie de l'Espace (LAREME), Koudougou, Burkina Faso
Email: *nanema_emmanuel@yahoo.fr

How to cite this paper: Nanéma, E., Konaté, M. and Ouattara, F. (2019) Peak of Electron Density in F2-Layer Parameters Variability at Quiet Days on Solar Minimum. *Journal of Modern Physics*, **10**, 302-309.
https://doi.org/10.4236/jmp.2019.103021

Received: February 1, 2019
Accepted: March 8, 2019
Published: March 11, 2019

Abstract

This study deals with Peak of electron density in F2-layer sensibility scale during quiet time on solar minimum. Peaks of electron density in F2-layer (NmF2) values at the quietest days are compared to those carried out from the two nearest days (previous and following of quietest day). The study uses International Reference Ionosphere (IRI) for ionosphere modeling. The located station is Ouagadougou, in West Africa. Solar minimum of phase 22 is considered in this study. Using three core principles of ionosphere modeling under IRI running conditions, the study enables to carry out Peak of electron density in F2-layer values during the quietest days of the characteristic months for the four different seasons. These parameters are compared to those of the previous and the following of the quietest days (the day before and following each quietest selected day) at the same hour. The knowledge of NmF2 values at the quietest days and at the two nearest days enables to calculate the relative error that can be made on this parameter. This calculation highlights insignificant relative errors. This means that NmF2 values at the two nearest days of each quietest day on solar minimum can be used for simulating the quietest days' behavior. NmF2 values obtained by running IRI model have good correlation with those carried out by Thermosphere-Ionosphere-Electrodynamics-General Circulation Model (TIEGCM).

Keywords

Ionosphere, Peak of Electron Density in F2-Layer, Solar Cycle, Quiet Day, International Reference Ionosphere Model

1. Introduction

Ionosphere layer is an important site for radio waves reflection because of its

composition in particles. This layer moves like a plasma and so, is electrically neutral. Solar radiations hit the particles in this layer and causes ionization. Ionization of particles in ionosphere layer due to solar radiations creates electrons and ions in the layer. Ionosphere composition in particles enables to determine the critical frequency of radio waves frequency of transmitters. Critical frequency of radio waves is closely linked to the density of electron in the F2-layer. Many works about ionosphere parameters determining have been done during these last years [1]-[10]. The main purpose of these different studies is to carry out ionosphere parameters for telecommunication, navigation, electrical disturbance predictions. Several models have been developed for ionosphere investigation. In previous studies, we used International Reference Ionosphere model, Thermosphere-Ionosphere-Electrodynamics General Circulation Model, and data [11]-[17] to carry out ionosphere parameters. The present study is focused on the calculation of relative error on Peak of electron density in F2-layer values at the limits of the quietest days for different seasons during solar minimum, compared to those of the quietest days. In this work, we calculate the relative error value on NmF2. The study is based on quiet time variation of solar cycle 22 at Ouagadougou station and uses International Reference Ionosphere (IRI) model for ionosphere investigation. 2012-version of IRI is used to run the model.

2. Methodology—Fundamentals

In this study, the minimum year (1985) of solar cycle 22 is considered for Peak of electron density in F2-layer behavior. Ionosphere modeling using IRI study is focused on the following three core principles: 1) The characteristic months are March, June, September and December for spring, summer, autumn and winter respectively. 2) The five quietest days of each characteristic month are used. 3) Solar minimum is characterized by sunspot number Rz < 20 and Aa ≤ 20 nT. During quiet time conditions, the five quietest days characterize the whole month in each season. We consider the two nearest days (previous and following) of each quietest day in the characteristic month as the boundaries. Ouagadougou is located in West Africa. The following input parameters are used for running IRI model during solar minimum at the station: Year = 1985, Longitude = 358.5˚E, Latitude = 12.5˚N, Height = 500, Stepsize = 1. With above input parameters, NmF2 time values are obtained on "List Model data". These values are exported in an Excel file for plotting.

Table 1 highlights the five quietest days selected in each season on solar minimum.

3. Results and Discussion

Figures 1-4 present NmF2 time variation carried out by running IRI model under

Table 1. Retain days during solar minimum (1985) of cycle 22.

March	June	September	December
9, 13, 21, 22, 25	3, 14, 16, 18, 19	2, 3, 4, 5, 29	8, 9, 21, 23, 29

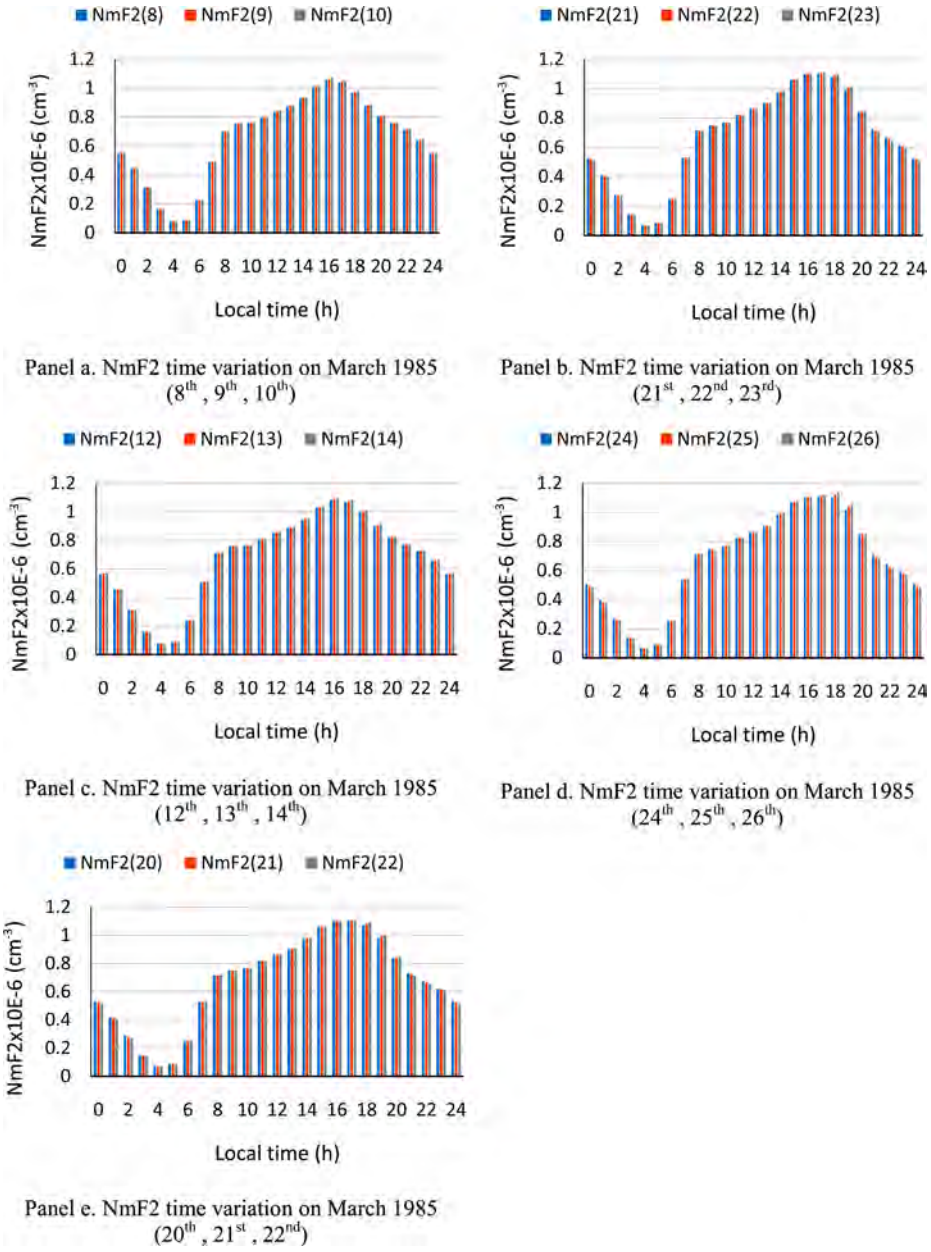

Figure 1. NmF2 time variation on March 1985.

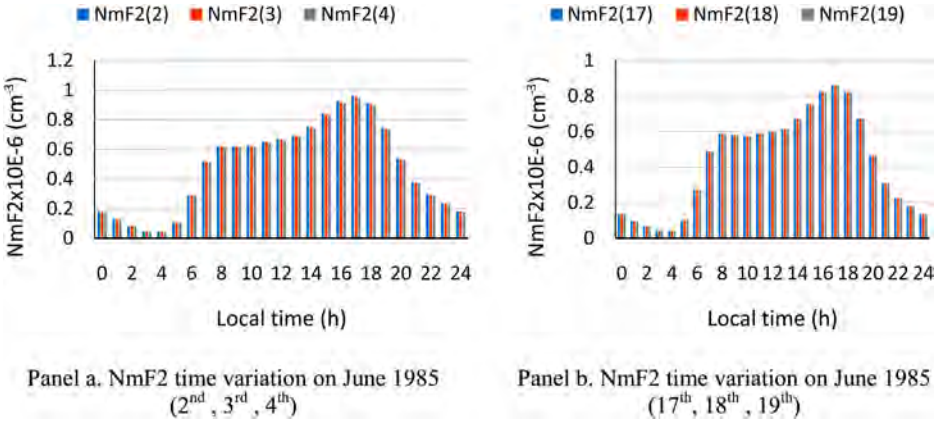

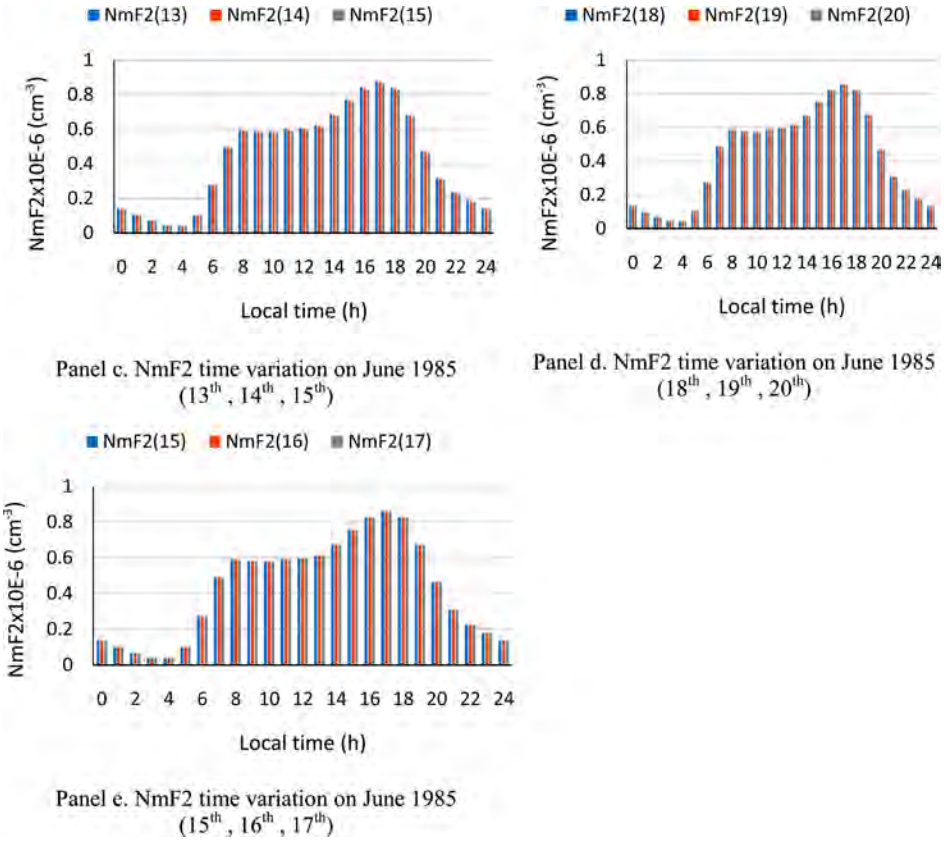

Panel c. NmF2 time variation on June 1985 (13^{th}, 14^{th}, 15^{th})

Panel d. NmF2 time variation on June 1985 (18^{th}, 19^{th}, 20^{th})

Panel e. NmF2 time variation on June 1985 (15^{th}, 16^{th}, 17^{th})

Figure 2. NmF2 time variation on June 1985.

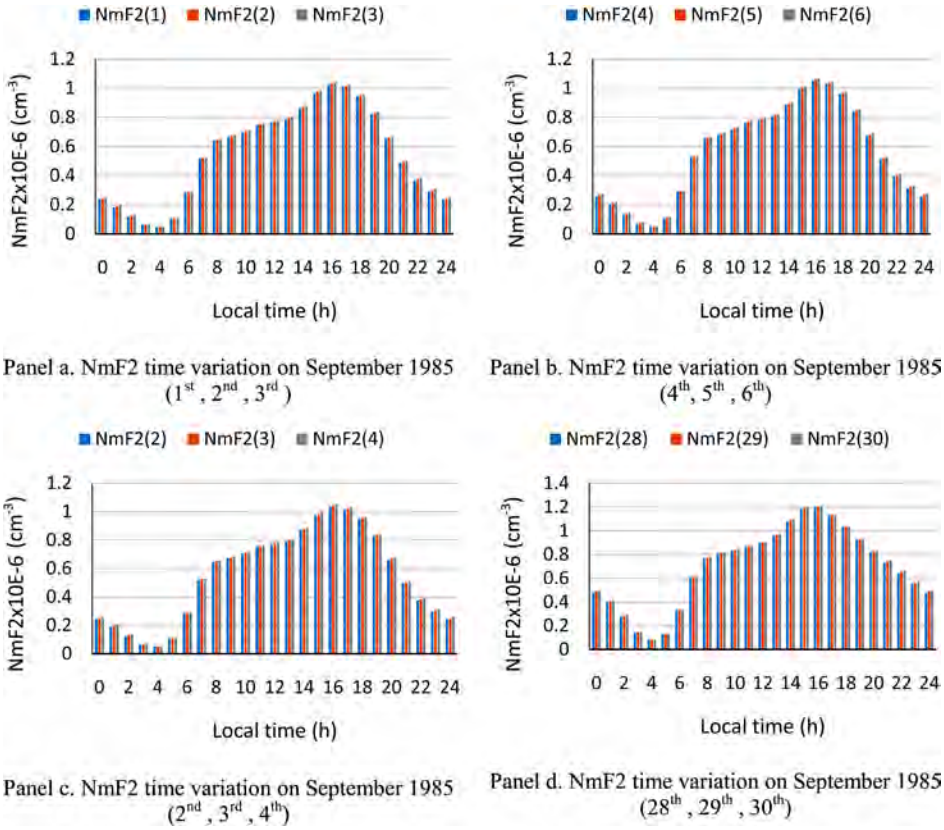

Panel a. NmF2 time variation on September 1985 (1^{st}, 2^{nd}, 3^{rd})

Panel b. NmF2 time variation on September 1985 (4^{th}, 5^{th}, 6^{th})

Panel c. NmF2 time variation on September 1985 (2^{nd}, 3^{rd}, 4^{th})

Panel d. NmF2 time variation on September 1985 (28^{th}, 29^{th}, 30^{th})

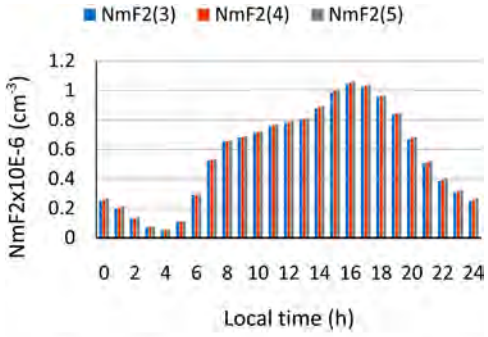

Panel e. NmF2 time variation on September 1985 (3^{rd}, 4^{th}, 5^{th})

Figure 3. NmF2 time variation on September 1985.

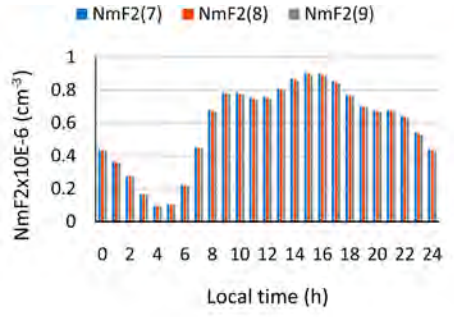

Panel a. NmF2 time variation on December 1985 (7^{th}, 8^{th}, 9^{th})

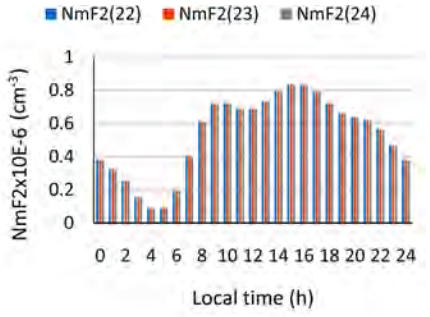

Panel b. NmF2 time variation on December 1985 (22^{nd}, 23^{rd}, 24^{th})

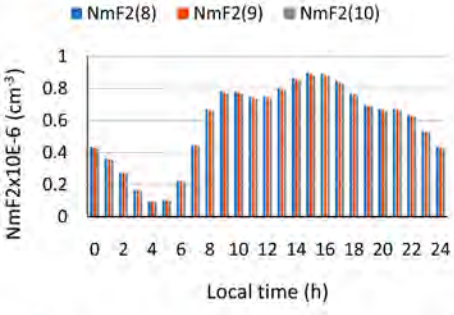

Panel c. NmF2 time variation on December 1985 (8^{th}, 9^{th}, 10^{th})

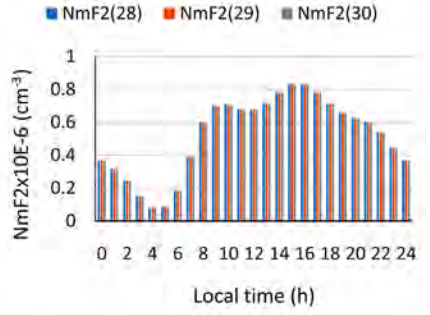

Panel d. NmF2 time variation on December 1985 (28^{th}, 29^{th}, 30^{th})

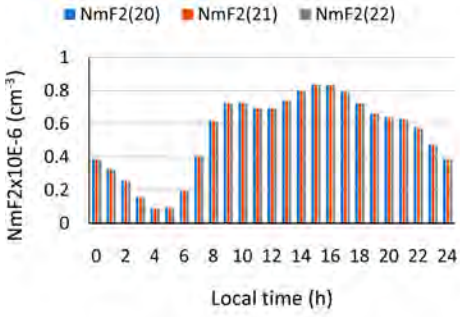

Panel e. NmF2 time variation on December 1985 (20^{th}, 21^{st}, 22^{nd})

Figure 4. NmF2 time variation on December 1985.

its 2012-version for the retain days previously found in Table 1. On each figure, we present NmF2 time profiles on five different panels. Each panel highlights NmF2 time variations for three days that are the quietest day, the previous and the following day.

Relative error on Peak of electron density parameter in F2-layer is calculated by the following Equation (1):

$$\frac{\Delta \mathrm{NmF2_i}}{\mathrm{NmF2_i}} = \frac{\left|\mathrm{NmF2_i}\left(\mathrm{D}\right) - \mathrm{NmF2_i}\left(\mathrm{D}\pm 1\right)\right|}{\mathrm{NmF2_i}\left(\mathrm{D}\right)} \tag{1}$$

In Equation (1), $\mathrm{NmF2_i(D)}$ is the Peak of electron density value at i hour for D-day. D-day is the quietest day. $\left(\mathrm{D}\pm 1\right)$ are respectively the previous (D − 1) and the following (D + 1) day of the quietest day. $\mathrm{i}\in[0,24]$. The step for i values variation is 1.

Calculating the relative error on Peak of electron density in F2-layer for Figures 1-4 corresponding to March (spring), June (summer), September (autumn) and December (winter) gives the following ranges:

On March 1985:

$$\frac{\Delta \mathrm{NmF2_i}}{\mathrm{NmF2_i}} \in \left[0\%, 4\%\right] \tag{2}$$

On June 1985:

$$\frac{\Delta \mathrm{NmF2_i}}{\mathrm{NmF2_i}} \in \left[0\%, 2\%\right] \tag{3}$$

On September 1985:

$$\frac{\Delta \mathrm{NmF2_i}}{\mathrm{NmF2_i}} \in \left[0\%, 4\%\right] \tag{4}$$

On December 1985:

$$\frac{\Delta \mathrm{NmF2_i}}{\mathrm{NmF2_i}} \in \left[0\%, 1\%\right] \tag{5}$$

The range of $\frac{\Delta \mathrm{NmF2_i}}{\mathrm{NmF2_i}}$ variation given by (2), (3), (4) and (5) is inferior to 4%. Peak of electron density in F2-layer values vary slightly from the quietest day to its two nearest selected days. This means that $\mathrm{NmF2_{D\text{-}1}} \sim \mathrm{NmF2_D} \sim \mathrm{NmF2_{D+1}}$ at the same time Calculated relative error at each hour between the quietest day and its two nearest days is inferior to 4% for NmF2. However, NmF2 value is a multiple of 10^5 $\mathrm{cm^{-3}}$. In each panel, a variation of 4% is insensible on NmF2 value. This enables to conclude that a 4% variation on NmF2 does not influence measurably Peak of electron density in F2-layer. So, using NmF2 value at the nearest days of quietest day doesn't introduce a sensitive error on this parameter.

4. Conclusion

In this study, Peak of electron density in F2-layer parameter is carried out by the

use of IRI model. The study highlights insignificant relative errors on NmF2 carried out from the quietest days on solar minimum of phase 22 at Ouagadougou station. This means that using NmF2 values at the nearest days of each quietest day instead of those of the quietest day doesn't introduce significant error. The contribution of this study is the possibility to neglect the relative error on Peak of electron density in F2-layer parameter due by considering the value of this parameter at the limits of each quietest day on solar minimum at low latitudes. This means that we can use either NmF2 carried from the quietest day or those from the nearest days to characterize the quietest day behavior. For a next study, this method will be applied to NmF2 variability on solar maximum.

Conflicts of Interest

The authors declare no conflicts of interest regarding the publication of this paper.

References

[1] Pedatella, N.M., Forbes, J.M., Maute, A., Richmond, A.D., Fang, T.-W., Larson, K.M. and Millward, G. (2011) *Journal of Geophysical Research*, **116**, A12309. https://doi.org/10.1029/2011JA016600

[2] Roble, R.G., Ridley, E.C., Richmond, A.D. and Dickinson, R.E. (1988) *Geophysics Research Letter*, **15**, 1325-1328. https://doi.org/10.1029/GL015i012p01325

[3] Wang, W., Wiltberger, M., Burns, A.G., Solomon, S.C., Killeen, T.L., Maruyama, N. and Lyon, J.G. (2004) *Journal of Atmospheric and Solar-Terrestrial Physics*, **66**, 1425-1441. https://doi.org/10.1016/j.jastp.2004.04.008

[4] Richmond, A.D., Ridley, E.C. and Roble, R.G. (1992) *Geophysics Research Letter*, **19**, 601-604. https://doi.org/10.1029/92GL00401

[5] Burns, A.G., Wang, W., Killen, T.L. and Solomon, S.C. (2004) *Journal of Atmospheric and Solar-Terrestrial Physics*, **66**, 1457-1468. https://doi.org/10.1016/j.jastp.2004.04.009

[6] Weimer, D.R. (2005) *Journal of Geophysical Research*, **110**, A05306. https://doi.org/10.1029/2004JA010884

[7] Jin, S. and Park, J.U. (2007) *Earth Planet Space*, **59**, 287-292. https://doi.org/10.1186/BF03353106

[8] Bittencourt, J.A. and Chryssafidis, M. (1994) *Journal of Atmospheric and Solar-Terrestrial Physics*, **56**, 995-1009. https://doi.org/10.1016/0021-9169(94)90159-7

[9] Ouattara, F. and Rolland, F. (2011) *Scientific Research and Essays*, **6**, 3609-3622. https://doi.org/10.5897/SRE10.1050

[10] Qian, L., Burns, A.G., Chamberlin, P.C. and Solomon, S.C. (2010) *Journal of Geophysical Research*, **115**, A09311. https://doi.org/10.1029/2009JA015225

[11] Ouattara, F. and Nanéma, E. (2014) *Physical Science International Journal*, **4**, 892-902. https://doi.org/10.9734/PSIJ/2014/9748

[12] Ouattara, F. (2013) *Archives of Physics Research*, **4**, 12-18.

[13] Ouattara, F. and Nanéma E. (2013) *Archives of Applied Science Research*, **5**, 55-61.

[14] Nanéma, E., Ouédraogo, I., Zoundi, C. and Ouattara, F. (2018) *International Journal of Geosciences*, **9**, 572-578. https://doi.org/10.4236/ijg.2018.99033

[15] Nanéma, E., Gnabahou, D.A., Zoundi, C. and Ouattara, F. (2018) *International*

Journal of Astronomy and Astrophysics, **8**, 163-170.
https://doi.org/10.4236/ijaa.2018.820311

[16] Nour, A.M., Frédéric, O., Louis, Z.J., Frédéric, G.A.M., Emmanuel, N. and François, Z. (2015) *International Journal of Geosciences*, **6**, 201-208.
https://doi.org/10.4236/ijg.2015.63014

[17] Nanéma, E., Zerbo, J.L., Konaté, M. and Ouattara, F. (2018) *Journal of Scientific and Engineering Research*, **5**, 62-68.

Journal of Modern Physics, 2019, 10, 310-343
http://www.scirp.org/journal/jmp
ISSN Online: 2153-120X
ISSN Print: 2153-1196

The Equation of the Universe (According to the Theory of Relation)

Russell Bagdoo

Saint-Bruno, Quebec, Canada
Email: rbagdoo@gmail.com, rbagdoo@yahoo.ca, mberbag@videotron.ca

How to cite this paper: Bagdoo, R. (2019) The Equation of the Universe (According to the Theory of Relation). *Journal of Modern Physics*, **10**, 310-343.
https://doi.org/10.4236/jmp.2019.103022

Received: December 25, 2018
Accepted: March 11, 2019
Published: March 14, 2019

Abstract

A new equation is found in which the concept of matter-space-time is mathematically connected; gravitation and electromagnetism are also bound by space-time. A mechanism is described showing how velocity, time, distance, matter, and energy are correlated. We are led to ascertain that gravity and electricity are two distinct manifestations of a single underlying process: electro-gravitation. The force of gravitation arises of electromagnetism—inherently much stronger—divided by the cosmological space-time. The radius of space-time belongs to the family of electromagnetic waves: the wavelength is the radius (10^{26} m) of the universe and the period (10^{17} s) is its cosmological age. For the first time, the cosmological time, considered as a real physical object, is integrated into a "cosmological equation" which makes coherent what we know regarding the time (its origin, its flow …), the matter, and space. It sets up a mathematical model allowing us to interpret dark energy (or cosmological constant) as being both "negative" and "tired" energy. After an introduction with a brief history of unifications and the presentation of two roughly equal ratios arising out from Dirac's large-number hypotheses which relate to the ratio of electric force to gravitational force and the ratio of the age of the universe to the atomic time unit associated with atomic processes, we present in §2 this new equation of quantum cosmology which operates the reconciliation between the macrocosm and the microcosm. In §3 and §4, we discuss the irreversible cosmological time resulting from the equation, as well as the role of the mass (heavy) relative to the gravitational constant G. In §5 we discuss the links that the equation establishes between gravitation (structure of condensation) and electromagnetism (structure of expansion), between relativity and quantum theory. We apply the formula to Planck's time. We speak of the new essential variable M_{vp}^2, and briefly of a new principle, the principle of compensation. In §6 we discuss the negative energy solutions banned by physics, and we deplore that half of the universe escapes us. We present the electro-gravitation in §7, from the equation which repre-

sents a super hydrogen atom. In § 8 we show that the global mass (gravitational) is variable: it increases during the expansion while the mass of the elementary particles decreases. In §9 we approach the spontaneous symmetry breaking; when it occurs, the arrows of the equation are momentarily reversed: such a mechanism would apply to the Allais effect, also mentioned in §6.4. §10 and §11 deal with the energy linked by the equation to matter through expansive space-time. The equation transforms electromagnetic kinetic energy into a gravitational mass, considered as a potential energy. Entropy increases according to the arrow of time towards the future. In §12 we discuss of the prevailing theory of inflation. We note the similarity between the proclaimed acceleration of current expansion and inflation. Physicists have interpreted the positive cosmological constant in terms of vacuum energy which would be 10^{120} times higher than the dark energy density deduced from the astronomical measurements. However, the high theoretical value of the vacuum energy (and the cosmological constant) has no observable pending in the cosmos. In §13 we suggest that these several orders of magnitude difference problem are solved by the theory of relation, which indicates a deceleration of the expansion. Finally, in § 14, we close by speaking of a model of cyclic universe and about the object of this paper, a dynamic equation that allows to build a quantum cosmology.

Keywords

Theory of Relation, Quantum Cosmology Equation, Irreversible Cosmological Time, π, New Variable, Negative Energy

1. Introduction

1.1. History of Unifications

Historically [1], Newton's discovery of the law of gravitation can be appreciated as the first "unification", combining the laws of heaven and earth. The next great leap took place in the mid 1860's with Maxwell's theory of electromagnetism uniting electricity and magnetism. In 1905, Einstein created the special theory of relativity connecting space and time and associating the concepts of matter and energy. In 1915, he proposed general relativity, which explained gravitation as the marriage of space-time and matter-energy. In the 1960's, the works of S. Weinberg, A. Salam and S. Glashow led to the unification of the electromagnetic interaction and the weak nuclear interaction. The next step, namely the unification of the electroweak and strong interactions, drove to the electronuclear theory (GUT) whose predictions were the object of no conclusive result. As for the ultimate synthesis—the unification of gravitation and GUT—it has defied all attempts.

1.2. Dirac's Conjecture

More than seventy years ago, Paul Dirac suggested that more than a coincidence was at work between the age of the universe in atomic time units and the ratio of

the electric force between an electron and a proton to the gravitational force between the two $\left[ke^2/\left(GM_pM_{e^-}\right)=10^{40}\right]$ [2] [3]. The most fundamental unit of time would be one associated with atomic processes, because it would depend only on basic natural constants, such as the electric charge (e), the mass of the electron (M_{e^-}), or the speed of light (c). This time unit, which appears throughout physics as the basic time scale for atomic and nuclear processes, is roughly the time required for light to travel the electron radius: $10^{-15}\,\mathrm{m}/10^{8}\,\mathrm{s}=10^{-23}\,\mathrm{s}$. Thus the evaluated age of the universe (10^{17} s) in atomic time units is $10^{17}\,\mathrm{s}/10^{-23}\,\mathrm{s}=10^{40}$. Dirac postulated that the near equality of these two numbers was a manifestation of some as yet the unknown deeper law of nature that required them to be nearly equal for all time. The problem is that the age of the universe is increasing. If the quantity between the two 10^{40} is to be maintained, then one of the other numbers must change with time. For many physicists, the gravitational constant (G) seems the only plausible candidate which can vary in spite of general relativity, which states that G is a physical constant whose numerical value is fixed.

Our reflections and insights on this issue have made us discover the theory of Relation (let us understand well: the word "relation" means connection, link, and it is not excluded that it means "unification") whose mode of action decrypts the order of the cosmos. It proposes a model of quantum cosmology through an equation that builds a relationship between electromagnetism, Newtonian gravitation, special relativity, quantum physics and general relativity.

2. Equation of the Theory of Relation

2.1. The Equation

Let us compare the electrostatic and the gravitational forces between two protons in the same nucleus, with a distance of 0.2 nanometers [4]. We will use the MKS system which has the advantage of incorporating the constants of the permittivity of free space and of permeability of free space. The value of the Coulomb constant k is $1/4\pi\varepsilon_o=8.9875\times10^{9}\ \mathrm{N\cdot m^2/coul^2}$. The value of the constant ε_o, called permittivity of free space, is $8.8542\times10^{-12}\ \mathrm{coul^2/N\cdot m^2}$. According to Coulomb's law, the electrostatic repulsive force is $F_e=q^2/\left(4\pi\varepsilon_oR^2\right)=5.775\times10^{9}$ N; $e^2/\left[4\pi\left(8.8541878\times10^{-12}\right)\left(0.2\times10^{-9}\right)^2\right]$. The attractive Newtonian force is $GM_{op}^2/R^2=4.666\times10^{-45}\,\mathrm{N}$. The ratio is $F_e/F_g=ke^2/GM_p^2=1.23\times10^{36}$.

Let us pursue Dirac's suggestion on the time, and replace the ratio by a universal time factor with the constants G and c: $F_e/F_g=t_oc/G$; $F_e=F_gt_oc/G$. And suppose we relativize the masses of the protons, in accordance with special relativity, as if they were moved with a speed of 200,000 km/s, we would obtain

$$\begin{aligned} &ke^2\Big/\left[R_o\left(1-v^2/c^2\right)^{\frac{1}{2}}\right]^2 \\ &=G\left[M_{op}\Big/\left(1-v^2/c^2\right)^{\frac{1}{2}}\right]^2\Big/\left[R_o\left(1-v^2/c^2\right)^{\frac{1}{2}}\right]^2\left[t_oc/G\right], \end{aligned} \tag{1}$$

thus we would have

$$ke^2 = M_{VP}^2 t_o c. \tag{2}$$

[M_{op} is rest-mass; $M_{op}\left(1/\left(1-v^2/c^2\right)^{1/2}\right)$ gives M_{vp}, *i.e.*, rest-mass + kinetic energy (T); $v = 200,000$ km/s $= 2/3c$].

Note that in this model, the speed of the relativized protons is identified with the estimated speed of the recession of galaxies and that it determines all other variables. We found reasonable to adopt the speed $2/3c$. Since this is dependent on astronomical observations which are constantly evolving, the speed will be adjusted accordingly.

Particles come in pairs, each with a counterpart antiparticle

$$\pm ke^2 = \pm\left[M_{op}/\left(1-v^2/c^2\right)^{1/2}\right]^2 t_o c \tag{3}$$

$$2.3\times10^{-28}\ \text{kg}\cdot\text{m}^3\cdot\text{s}^{-2} = \left[\left(1.672\times10^{-27}\ \text{kg}\right)/\left(1-4/9\right)^{\frac{1}{2}}\right]^2\left(1.528\times10^{17}\ \text{s}\right)\left(3\times10^8\right)$$

$$2.3\times10^{-28}\ \text{kg}\cdot\text{m}^3\cdot\text{s}^{-2} = \left(2.2439\times10^{-27}\ \text{kg}\right)^2\left(1.528\times10^{17}\ \text{s}\right)\left(3\times10^8\right).$$

We ascertain that the link between the charge squared and the relativized proton's mass squared confers a universal time of 1.5283×10^{17} s multiplied by c. That time gives 4.84 billion years $\left[\left(1.5283\times10^{17}\right)/\left(365.24\times24\times60\times60\right)\right]$.

2.2. Linear Time and Transverse Time

This time for a speed of 200,000 km/s gives a time well below the 13 to 15 billion light-years expected. Relativized protons should be with a much lower rate to obtain these ages. Therefore, the radius $t_o c$ of about 15 billion light-years could be confused with both an electromagnetic wave and a gravitational wave. The two are transverse. However, since we assimilate the speed of the relativized protons to the velocity of recession of galaxies and that the latter is not evaluated less than $2/3c$, we exclude this possibility.

The other alternative is to consider that the cosmological time of Equation (2) is a mathematical "linear time" that evolves as a "longitudinal" ray of light. A point particle on a cosmological space-time ray will go straight ahead, such as a Euclidean space-time line, from one point to another. It will cross the radial radius $t_o c$ (=A-Z), in 4.84 billion light-years. This radius can then become confused with a longitudinal gravitational wave or a longitudinal electromagnetic wave. Although we do not know these waves, they cannot be forbidden in theory. We believed for a long time that sound waves were exclusively longitudinal while they are also transverse.

Linear time, that is to say, the time required for a particle to travel a distance A-Z in a straight line as would make a longitudinal wave, matches with 15.21 billion years in circular time, or linear time multiplied by π. The circular time expresses the required time for a particle can travel the same length in rotating around the line, as would a transverse wave [5].

One can imagine that a wave rolled up around the radial line A-Z would travel it in the 5.21 billion years, which is linear time multiplied by π. It fits a transverse electromagnetic wave

$$ke^2 = M_{VP}^2(\pi)t_o c. \quad (4)$$

Of this expression, one must keep in mind that π is used for winding the particle spirally around the radial length $t_o c$. It could be a transverse electromagnetic wave but it could also be a transverse gravitational wave. Mathematically, the equation should be

$$(\pi)ke^2 = M_{VP}^2(\pi)t_o c. \quad (5)$$

From a physical point of view, we prefer however the Equation (4), because it allows highlighting, for the same distance, the transverse character (and thus electromagnetic) with respect to the linear character. It can be said that the second of the longitudinal wave is worth the second of the transverse wave divided by π. It means that a particle will browse transversely a distance A-Z while in the same time another particle will cover a radial distance A-Z × π. We estimate that it is adequate and corresponds roughly to the observations. The photon is the boson of the transverse electromagnetic wave of space-time.

It has been shown that space-time is electromagnetic (vacuum minimum energy, etc.). So, using the basic unit of time, the second, considered electromagnetic, the universe was estimated at about 15 billion light-years. Our equation, calculated for a relativistic velocity of 2/3c for the protons, gives 15 billion light-years using π. We estimate that it is adequate and consistent with the observations. The photon is the boson of the transverse electromagnetic wave of space-time.

If this transverse electromagnetic wave was unfolded into a longitudinal electromagnetic wave, the distance A-Z would be multiplied by π, what would give 47 billion longitudinal light-years. We would have, always at the speed of light, distances at least three times the length of the distances presently estimated. The seconds of this longitudinal electromagnetic wave would have a time three times shorter than the seconds of the transverse wave.

The particles that may be associated with longitudinal electromagnetic waves and longitudinal gravitational waves could be the neutrino and the graviton. The longitudinal electromagnetic wave already exists. The gravitational wave, which has always been considered to be transverse, would have been captured in 2015. This does not exclude the existence of a longitudinal gravitational wave [6].

2.3. Formula of the Expansion

We know that nucleons are forming 99.97% of the known matter. Neutron and proton are two states of the nucleon. Suppose that the protons of our equation are galaxies which move away at 2/3*c*, then we get a "cosmological equation" that determines the age and distance of the universe in relation to the speed of recession of galaxies. The more the speed of recession of distant galaxies de-

creases (velocity $\sim c^2/c^2$ at the beginning toward lower speeds: v^2/c^2), the more they move away from the Earth and the more the age of the universe increases. Velocity, distance, and age are correlated for the first time in an equation. The flight of the galaxies at $2/3c$ corresponds to 15 billion years. Both numbers are roughly consistent with the real estimates of science.

The Equation (4), in the form

$$\pm(\pi)ke^2 = \pm M_{VP}^2(\pi)t_o c \tag{6}$$

is the equation of the expansion. It establishes a clear mathematical link between electromagnetism and gravitation. The term "$(\pi)t_o c$" corresponds to the radius of the universe. To the right-hand side, matter (M_{VP}^2), space and time ($t_o c$) are mathematically related into one whole.

It can be seen in the Equation (1) that the expression $G\left[M_{op}/\left(1-v^2/c^2\right)^{1/2}\right]^2 \Big/ \left[R_o\left(1-v^2/c^2\right)^{1/2}\right]^2$ links Newtonian gravitational force and relativity. We get a relativized Newtonian gravitation, which means, firstly, that gravity is a reality everywhere and, secondly, that special relativity is not only a mathematical utility, not just a Galilean reference frame without gravity. Both are linear theories applied to a tri dimensional Euclidean geometry with linear-plan space-time. These are applied to a linear two-dimensional Euclidean space-time with flat linear theories. In addition, electromagnetism is also a linear theory.

In Newton's theory of gravitation, the force GMm/r^2 transmits instantaneously an energy or a signal. Newton was unhappy with the instantaneous or "action at a distance" phenomenon associated with gravity. Poincaré (1904), Minkowski (1908), and de Sitter (1911) agreed that gravity must propagate with the speed of light. For according to special relativity nothing moves faster than light, not even gravity. None of the several gravity theories—even from Einstein, that was consistent with special relativity in that the speed of the propagation of gravity was the speed of light—was satisfactory. In the proposed equation, the combination of the Lorentz transformation and $t_o c$ ensures that the velocity of light or gravity does not go faster than the velocity of the universal constant c [7].

According to the theory of Relation, gravity is not a separate force, but an aspect of electromagnetism. Both forces are joined by the four-dimensional space-time. In fact, the gravity results from the dissolved energy of the expanding electromagnetism which does not stop creating the space-time. Deep down, electric and gravitational forces are part of a common superforce: electro-gravitation. Like magnetism and electricity are two sides of electromagnetism [8]. In subatomic particle physics, electro-gravitation takes the aspect of the electrostatic force, and the gravitation force, 10^{36} weaker, plays no direct role there. When the pair of particles with both positive electric charges which repel and move away at nearly the speed of light, creating the "space-time" between them, electromagnetism decreases with distance and takes the name gravity. On the large scale, electro-gravity becomes gravity. We are led to think of the gravi-

tational forces as being electromagnetic forces with attractive charges acting in space-time instead of in the subatomic world. The driving force of expansion, caused by the initial explosion, would result from the repulsive charges of the electromagnetic forces operating in the universe [9].

2.4. Other Relativistic Expressions

Here are other relativistic expressions that express the mass variation of a moving proton as a function of velocity and cosmological time. They do not take account here of π as if $t_o c$ was longitudinal and not transverse. The same applies to the rest of the paper.

(M_{op} is the rest mass; $M_{op}\left(1/\left(1-v^2/c^2\right)^{1/2}\right)$, or ΔM_p is the kinetic energy T; M_{vp} is the relativized mass with kinetic energy; $v = 2/3c$)

$$ke^2 = M_{op} + \left\{M_{op}\left[\left(1/\left(1-v^2/c^2\right)^{1/2}\right)-1\right]\right\}^2 t_o c \tag{7}$$

$$2.3\times10^{-28} = \left[\left(1.6725\times10^{-27}\right)+\left(5.71\times10^{-28}\right)\right]^2\left(1.52\times10^{17}\,\mathrm{s}\right)\left(3\times10^8\right),$$

or

$$ke^2 = \left(M_{op}\times\Delta M_p\right)^2 t_o c \tag{8}$$

$$2.3069\times10^{-28} = \left[\left(1.6725\times10^{-27}\right)(1.3416)\right]^2\left(1.5283\times10^{17}\,\mathrm{s}\right)\left(3\times10^8\right).$$

Relativistic expression for kinetic energy of a moving proton (quantum mass)

$$T = M_{vp}c^2 - M_{op}c^2 = M_{op}c^2\left[\left(1/\left(1-v^2/c^2\right)^{1/2}\right)-1\right]. \tag{9}$$

Potential energy for the electrostatic field of point charges united to potential energy for the gravitational field

$$\begin{aligned} &-ke^2/\left[R_o\left(1-v^2/c^2\right)^{1/2}\right]^2 \\ &= -\left\{G\left[M_{op}/\left(1-v^2/c^2\right)^{1/2}\right]^2 t_o c\right\}/\left\{\left[R_o\left(1-v^2/c^2\right)^{1/2}\right]G\right\}. \end{aligned} \tag{10}$$

Formula of the total energy of the proton in function of e, c, and t_o

$$ke^2 = M_{VP}^2 t_o c;\ M_{vp} = \left(ke^2/t_o c\right)^{1/2};\ M_{op} = \left(1-v^2/c^2\right)^{1/2}\left(ke^2/t_o c\right)^{1/2}$$

$$E = M_{op}c^2 + T = M_{vp}c^2 = \left(ke^2c^3/t_o\right)^{1/2} \tag{11}$$

$$E = M_{op}c^2 = \left[\left(1-v^2/c^2\right)\left(ke^2/t_o c\right)c^4\right]^{1/2} = \left(1-v^2/c^2\right)\left(ke^2c^3/t_o\right)^{1/2}. \tag{12}$$

This is for the fermion. New formula of energy for the boson (m_o) is

$$E = m_o c^2 = M_{vp}^2 hc/ke^2 \tag{13}$$

$$ke^2 = M_{VP}^2 t_o c;\ ke^2 = M_{VP}^2 h/m_o c;\ ke^2 = M_{VP}^2 hc/m_o c^2.$$

This means that electricity is a manifestation of energy like energy and matter are equivalent. Proton (and neutron) and electron are grains of electricity. The masses of proton and electron have EM origin: $M_{vp} = \left(ke^2/t_o c\right)^{1/2}$, and the mat-

ter is composed of grains of electricity. Matter atom is done of a multitude of elementary particles that are electricity, so properties of matter must be explained by properties of electricity.

On the basis of $ke^2 = M_{VP}^2 t_o c = M_{VP}^2 2GM^o/c^2 = M_{vp}^2 2GM^o c^2/c^4$, the new formula of the energy of the ordinary matter of the universe will be

$$E = M^o c^2 = ke^2 c^4 / \left(M_{VP}^2 2G\right). \quad (14)$$

3. Cosmological Time

The Equation (2) $\left[ke^2 = M_{VP}^2 t_o c\right]$ is written with a real and cosmological time (neither relative nor absolute) that governs the infinitely small and the infinitely large. It allows considering time as a real entity which contains in itself the difference between the past and the future. It can open a new chapter of the physics because so far, the more the physical theories have been developed, the more the notion of time has become evanescent. First with the introduction of relativity in 1905 which made it lose its absolute character; the notions of present or of duration turning dependent on the observer; an overt indifference where time becomes intimately linked to space for which this distinction has no meaning. Then with quantum mechanics, two decades later, who dived in the "fuzzy" the idea of time. The laws of microphysics show no preferred flow direction. At such an extent that for physicists if a broken glass is never spontaneously repaired, it is not because we cannot go back in time, but simply because the configuration "repaired" is less probable than "broken" [10].

Nevertheless, in the cosmological theories of Einstein, de Sitter and Lemaître, new ideas related to the character of universal space had been introduced, but no corresponding progress was achieved regarding the idea of time, except to the extent that the phenomenon of expansion tended to suggest a finite past, rather than an infinite past. Just as Einstein did make the progress that is known by analyzing concepts like that of simultaneity, similarly the next progress of physical theory will be obtained by taking again the analysis of time to the point where he left it.

The cosmological time found in the equation would be the age of the universe. The reference is the beginning of space-time from the Planck time. It would recover a character not absolute as before the relativistic revolution, but universal that would integrate the difference between the past and the future with the acquirements of this revolution that unites time and space. The energy associated with the immateriality and the mass associated with ordinary matter could be stored in two opposite and complementary structures. This "new" time and this new energy and mass ratio would redefine general relativity, making it global and compatible with the quantum rules [9].

If we admit that the universe is a kind of expanding super-atom that gives the age of the universe, then we have an arrow to the future which is the same of at least three arrows of time that distinguish the past from the future: thermodynamics (disorder increases) cosmological (universe expansion rather than contraction), psychological (we remember the past, not the future) [11]. The flat

space-time, *i.e.*, zero curvature, makes the universe seem as being very close to the special case, intermediate between open and closed universe. The closed universes collapse eventually, and may then undergo further cycles of expansion and collapse, like a bouncing balloon. A universe closed by gravity is the equivalent of a black hole. We assume that the universe is at the highest of his jump and is about to plunge forward, which means that the cosmological time continues by orienting towards the big crunch, while the thermodynamic time passes from cold to hot.

In any event, the colossal amount of kinetic energy contained in the original proton varies with time. In fact, energy relieved by two energetic protons which move away from each other engenders the radius of the universe. The term "$t_o c$" corresponds to the radius of the universe and represents the cosmological time linked to the universal thermodynamics. We say that this cosmo-thermodynamics time, that shapes the radius of the universe, stems from two charges in the form of relativized protons which run away from each other creating so the space-time of this universe. One could say that the pairs of protons go away simultaneously from the center in all directions and two opposite directions constitute geometrically the diameter. This simultaneity suggests another time behind the thermodynamic time that we could call "duration". The velocity v of the Lorentz transformation indicates both the speed of the proton which decreases with expansion and its remaining mass (rest + kinetic energy). The released energy is propagated with velocity *c*, as an electromagnetic wave, which suggests that the frequency decreases with time [12].

4. The "Flow" of Time and the Universal Constant *G*

Lancelot L. Whyte in a short essay, *Archimedes or the Future of Physics* (1927) [13], pointed out that in each of the two major physical theories of the twentieth century, the fundamental role was played by a particular natural constant: In relativity by *c*, the velocity of light in vacuum, and in quantum theory by h, the Planck constant. He suggested that the next progress would be associated with a new fundamental constant that would concern the flow of time. The idea that time can be an active factor of causality means from the mathematical point of view that t must appear in the expression of the law. Such a law would express the fact of the historical and irreversible duration, or the "flow". The irreversible flow of time (cosmological time), linked to the irreversible phenomenon of expansion and our consciousness of the one-way flow of time, becomes a *necessary* element of any theory of the structure of nature. Thus, while the first principle of thermodynamics, that of conservation of energy, concerns time only as a simple "duration," the second principle implies the idea of flow. This notion of flow is fundamental and we consider that the expansion of the universe is its supreme manifestation.

Based upon the fundamental unit of time and on the fundamental physical constants, this cosmological time confirms the intuition of Paul Dirac, namely

that the dimensionless number 10^{40} is not a constant but a variable of time in relation to the age of our universe. He thought that this number was determined by particle physics and also by the gravitational influence of the entire universe. In 1937 and in1938, he proposed that G varies like the inverse age of the universe, so as the universe expanded from the big bang, the gravitational constant, or force, became weaker and weaker as time passed until today when we experience the present very weak force of gravity. But he was unable to apply it to Einstein's gravity theory [14].

For our part, we postulate that the gravitational mass of the universe varies *proportionally* to the age of the universe [7] [15]. If we assert that the electric forces and the gravitational force which are exerted between two particles of identical mass are disproportionate, the gravitational interaction is reduced to almost nothing. We have previously (section 2.1) replaced the numerical difference 10^{36} (for protons) by the factor ($t_o c/G$). Although Dirac has concluded that it is G which varies with time, we note that G is excluded from the equation, just like for special relativity: $\left[ke^2/r_v^2 = \left(GM_{vp}^2/r_v^2\right)/\left(t_o c/G\right) = ke^2 = M_{VP}^2 t_o c\right]$. It is the mass M_{vp} which varies rather than the constant G. In fact, even if G retains its status of an invariable constant of nature, as for general relativity, it turns out to vary through his substitute, the mass, which is amended from time. This confirms the intuition of Dirac and entails a modification of the gravity leading to a new kind of cosmology in which it is as much the mass of the particles as the mass of the whole universe which changes with time.

Ultimately, the theory of Relation considers that the mass of elementary particles changes with time (we do not speak here of the naked mass which remains invariant), that G is a fixed constant of the nature and that the space-time of the theory of Relation ($t_o c$) is almost the same as that of special relativity (tc): a four-dimensional Euclidean space-time continuum [11], except that he contains an electromagnetic aspect.

5. Link between Quantum Mechanics and General Relativity

5.1. Theory of Relation

According to the theory of Relation [16], the classical gravitation is almost zero at the Planck time because its energy is entirely in the potential state, the inverse of the kinetic energy of the electromagnetic interaction. Thus in equation

$$ke^2 = M_{VP}^2 t_o c = 2GM^o/c^2, \tag{15}$$

the kinetic energy of the squared mass of the relativized proton (M_{vp}^2) decreases in an inversely proportional way to the time and to the mass of the ordinary matter (M^o). The time generated by the expansion is inversely proportional to the quantum mass which decreases and proportional to the ordinary mass which grows, while we keep G of general relativity as a fixed constant of nature. Although $t_o c$ looks like the Euclidian four-dimensional space-time continuum of special relativity [11], it is dissociated by its irreversibility and its electromag-

netic aspect.

If we write $ke^2 = M_{VP}^2 t_o c = M_{VP}^2 h/m_o c$, the cosmological time which extends from 10^{-43} s to 10^{17} s, associated with h and c, reveals the quantum structure of space-time itself, which means a limit to the divisibility of space and above all to the divisibility of time.

One can imagine big implications if we write

$$ke^2 = M_{VP}^2 t_o c = M_{VP}^2 h/m_o c = M_{VP}^2 2GM^o/c^2. \quad (16)$$

5.2. Structure of Expansion and Quantum Theory

In this proposed model of quantum cosmology, there are two associated structures (expansion and condensation) of the world and a time scale incorporated into two different theories, quantum mechanics and relativity, each of which is of fundamental importance. In

$$\pm ke^2 = \pm\left[M_{op}/\left(1-v^2/c^2\right)^{1/2}\right]^2 h/m_o c = \pm\left[M_{op}/\left(1-2^2/3^2\right)^{1/2}\right]^2 h/m_o c \quad (17)$$

or

$$\pm ke^2 = \pm M_{VP}^2 h/p, \quad (18)$$

we associate electromagnetism, Newtonian gravitation, special relativity and quantum physics. The formula $t_o c = h/m_o c$ expresses the electro-gravitational field bound to M_{VP}^2.

Protons (M_{VP}^2) represent the stable particles of matter of the expanding universe. They move in every given direction at a speed less than c. So at any epoch posterior to the Planck era, the system fills the *inside* of a Euclidian sphere of radius $t_o c$. The nearest particles from the center, which emerge from the Planckian era, seem to move away with a speed v very close to c. At the beginning, their rest mass is covered with a huge kinetic energy. The speed of the expansion decreases and the kinetic energy of protons are subject to a transformation into a sort of frozen energy, in bodies with mass. We suppose arbitrarily that the speed of the particles of the current universe is $2/3c$ [17]. The proton—likened to a galaxy because it consists of protons—will be livened up at the most in a uniform motion at a constant speed when he will have exhausted almost all its kinetic energy and will be close to its rest mass (1.6725×10^{-27} kg). It is a "zero" speed motion and this could mean that the expansion will be replaced by a contraction into a new region that did not exist before and that the universe will go towards a new *space-time bounce* [18].

By uniting $E = m_o c^2$ of the relativity with $E = h\nu$ of the quantum theory, we obtain $t_o c = h/m_o c$. This field produces energy packets which are bosons. The particle mediator m_o represents as much the quanta-photon as the quanta-graviton. The latter (we are talking about the graviton from the big bang) carries the gravity and is similar to the photon of electromagnetism. Both are moving at the speed of the light, have energy but no rest mass. Their paths can be represented by straight lines in Euclidean space. If we talk of an electromag-

netic field for the photon, we speak of an electro-gravitational field for the graviton. The electro-gravitational wave "$t_o c$" could belong to the family of electromagnetic waves. A de Broglie wave is associated with their motion and is affiliated with the speed of the proton.

5.3. Structure of Condensation and General Relativity

The term GM^o/c^2 represents the structure of condensation, and general relativity in a more global than local aspect. Einstein saw a possibility to obtain a geometrical interpretation of gravitational forces analogous to centrifugal forces. Centrifugal forces and gravitational forces are proportional to the mass of the body which they are applied [19]. The equivalence between inertial, gravitational and centrifugal forces is $F = ma = GMm/r^2 = mv^2/r$. Radius is GM^o/v^2. With velocity c, $r = GM^o/c^2$. This expression of the radius of general relativity is, in fact, the Schwarzschild radius. In Equation (4), we said that $t_o c$ was the radius of the universe. So $R = t_o c = GM^o/c^2$. For reason of symmetry, we will take $2\pi GM^o/c^2$ as the relevant universal radius. Assuming a relativistic cosmic speed of $2/3c$, the mass of the present universe will be

$$\pm ke^2 = \pm\left[M_{op}/\left(1-v^2/c^2\right)^{1/2}\right]^2 2\pi GM^o/c^2 \tag{19}$$

$$\pm 2.3069\times10^{-28}\,\mathrm{kg}\cdot\mathrm{m}^3\cdot\mathrm{s}^{-2} = \pm\left(2.2439\times10^{-27}\,\mathrm{kg}\right)^2 2\pi GM^o/c^2.$$

We then obtain $M^o = 9.82\times10^{51}\,\mathrm{kg}$. Because the mass is related to $t_o c$ and that t_o is a "linear time", the mass is $9.82\times10^{51}\ \mathrm{kg}\times\pi = 3.08\times10^{52}\ \mathrm{kg}$. This is approximately the estimated mass of the universe, which tends to confirm the version of Mach's principle incorporated into Einstein's theory [20].

According to this, the structure of space-time depends on the average distribution of all matter in the universe. And inertia of an object depends on the structure of space-time. Einstein's equations produce the adequate Machian influences in a closed universe in which there is enough matter to gravitationally bend space on itself.

The expression $2\pi GM^o/c^2$ means that the radius of the universe must be compressed so that the escape velocity is equal to the speed of light [21].

5.4. Planck Time

At Planck time ($\hbar/c = 3.5177\times10^{-43}\,\mathrm{s}$), if we apply

$$\pm ke^2 = \pm M_{VP}^2 t_o c = \pm M_{VP}^2 h/m_o c = \pm M_{VP}^2\, 2GM^o/c^2, \tag{20}$$

the mass of the "baryon-proton" M_{vp} will be $1.479\times10^3\,\mathrm{kg}$ ($2.3069\times10^{-28} = M_{VP}^2\, 3.51\times10^{-43} c$).

The wavelength $\lambda = t_o c = R = h/2\pi = \hbar = 1.05458\times10^{-34}\,\mathrm{m}$. We use $\hbar$ with the Planck time and the Planck length: this is consistent with $t_o c$, which is linear, not circular.

With the de Broglie wave that travels at the speed of light as that of the particle m_o, the boson m_o gives $2.09\times10^{-8}\,\mathrm{kg}$ ($ke^2 = M_{VP}^2 h/m_o c$). We employ

$h/m_o c$ because quantum mechanics describes a particle, not a radius.

With $ke^2 = M_{VP}^2 2\pi GM^o/c^2$, general relativity determines the mass of the universe at Planck time, $M^o = 2.26\times10^{-8}\,\text{kg}$. We utilize $2\pi GM^o/c^2$ (not GM^o/c^2), considering that the term describes a mass with a circumference, not a radius.

Instead of having $M_{\text{Planck}} = \left(hc/2\pi G\right)^{1/2} = 2.1768\times10^{-8}\,\text{kg}$, which seems to be one of two similar masses, we have $M^o m_o = hc/2\pi G$, which are two different masses: $m_o = 2.09\times10^{-8}\,\text{kg}$ of quantum theory and $M^o = 2.26\times10^{-8}\,\text{kg}$ of general relativity. The Planck mass 2.1768×10^{-8} kg is actually the average of these two distinct masses $\left(M^o m_o\right)^{1/2}$. Their numerical value corresponds to Planck mass and that makes think of the famously hidden variables.

5.5. New Variable: M_{vp}^2

The new parameter M_{VP}^2, or $\left[M_{op}/\left(1-v^2/c^2\right)^{1/2}\right]^2$, is an essential element. Its value changes throughout the expansion. It can be suspected of being the non-zero mean value in the vacuum of the Higgs field. It would be the scalar field of the Higgs ocean at the origin of the inertia of matter which measures the force that must be applied to an object to provide it a given acceleration. One can also conjecture that it is a hidden variable in the sense that Einstein understood it: the mass of the particle associated with the wave that would commit a serious infringement of Heisenberg's principle of uncertainty [22] [23]. It would then be possible to predict with precision any future state of the universe; the associated wave would say more than the probabilities of the particle found in different places. It could also be a mathematical tool to grasp what was really under Planck's values; at microsecond 10^{-43}, the universe is thought to have had a size close to zero and to have been infinitely hot [11] [24]; it is the birth of the universe, but it is not the zero point of the singularity.

The Lorentz transformation of this variable [12] inscribes the equation in a relativistic cosmology (although our mathematical model is central and global whereas general relativity is above all peripheral and local). The velocity v of this transformation, starting from the speed of light and moving towards 0 (it would be about $2/3c$ today), constitutes a variable velocity of light. Thus the limit of a signal it was thought up till now to be that first measured with the light waves was much greater at the beginning of the history of the universe. The exchanges of heat could, therefore, be made much faster, which would have led the cosmos to have the same temperature everywhere. This would explain the remarkable precision with which the spectrum of fossil radiation appears to us today as that of a quasi-perfect black body. And that's what we are observing today. The measurements made by the COBE, WMAP and Planck satellites show that the cosmic background radiation is rather homogeneous and isotropic from the point of view of its temperature on the sky, which implies that it is the same for the density of matter. And if one attempts to understand these observations in the classical models of the expansion of the universe discovered by Friedmann,

Lemaître, Robertson, and Walker in relativistic cosmology, one cannot succeed.

5.6. Principle of Compensation

The important point is that by virtue of the principle of Compensation of the theory, m_o and M^o are related. When m_o decreases (as well as M_{VP}^2 on whom m_o depends), M^o, which represents the global mass of the universe, increases. M_{vp}^2 and m_o form the kinetic energy of the universe which decreases, whereas M^o constitutes the potential energy that grows as heavy weight.

5.7. A time Scale Associated with the Clocks of Two Opposing Spacelike Theories

The cosmological time t_o does not stop growing at the speed of rays of light and it is interpreted as the "age" of the system. The term $t_o c$ is at the same time the radius of the expansion and the wave of the expansion. Its metric yields the clock of the universe. It indicates that contrasting energies of particles follow the same course of time (order of 10^{60} between 10^{-43} s and 10^{17} s, between 10^{-35} m and 10^{25} m). The different speeds v of M_{VP}^2 correspond to various values of t_o.

One can find a mathematical relation binding the times that the quantum clock and the clock of general relativity assign respectively to a series of events. This relationship can be used to compare, or convert, the epochs in one scale in epochs in the other. Unlike those who think that these two clocks have no common point, that anyway we need "mass" to build a clock by pointing out that m_o has no mass, we believe we can build a clock universal without necessarily needing a rest mass [17].

You can take the content of the energy of m_o, by converting into a no rest mass or a virtual mass [18]. In this respect, we got $t_o c = h/m_o c$; $m_o = 4.824\times10^{-68}$ kg $= 2.7\times10^{-32}$ eV. The moving mass ($m_o c$) pilots an associated wave, also at the speed of light ($t_o c = 4.58\times10^{25}$ m) with a period of 1.5283×10^{17} s. Or ($\pi t_o c = \pi 4.58\times10^{25}$ m) with a period of $\pi 1.5283\times10^{17}$ s. The specific frequency will be $v = m_o c^2/h$. Even if their frequencies will be below zero, and that the time between two beats of the current clock in the vacuum is as long as the age of the universe, it does not prevent building a cosmic clock that will be as significant than a clock within the ordinary matter according to the relation $t_o c = GM^o/c^2$.

These two clocks are interconnected due to the principle of Compensation. Thus, the particles which weigh 10^{-68} kg are the photon or the graviton of the empty space-time grafted to the mass of the current universe (~10^{52} kg). At the Planck epoch, the ordinary mass of relativity and the quantum mass of the photon (or graviton) had substantially the same value, about 10^{-8} kg.

6. Negative Energy

6.1. Ocean of Negative Energy of the Theory of Relation

In the theory of Relation, there are more than two interconnected clocks (4) that

allow us to speak of the universe as a sort of universal metronome. Always by virtue of the principle of Compensation, there is a transformation of so-called "negative" energy into "positive" energy. The flat space-time ocean of special relativity merges here with Higgs ocean, also assimilated with Dirac ocean, themselves amalgamated with "ether" ocean (minimal energy of the vacuum). Even if each ocean retains its specficity, misunderstood, it is part of a vast ocean, the matrix of atom and vacuum. According to our equation, there would be a transformation of a space-time more and more flat into space-time more and more locally curved. (Einstein gave his power to the idea of local curvature of space by postulating that the geometry of the universe was curved by the masses it contained and that this geometry determined the movement of material objects within it).

It is presumed that at the beginning, as much matter as antimatter were created. Why has matter triumphed? Almost all of the specialists believe that a dissymmetry would have tipped in favor of matter. We do not believe that a surplus generated by the asymmetrical reaction of the particles, during a great annihilation, would have made a tiny difference favoring a bit of matter that would have structured itself to become our world [25]. We also adopt the hypothesis of an originally symmetrical universe, but we differ on the mechanism that would have favored matter. According to us, from the initial spark, there would have been a universe shared in equal parts between positive and negative matter, but part of positive matter would have taken the direction of the nascent universe, while the negative counterpart would return to the sea of negative energy. And this progressively throughout the expansion, even today, though feebly. This transformation of negative energy into positive energy is a long quiet river and not a titanic flash of light of a fraction of a second. The universal dynamic is that energy is transformed into matter, under the impulse of a decelerating expansion that began with a speed close to that of light. The universal dynamic is that energy is transformed into matter under the impulse of an expansion which decelerates with time and which began with a speed very close to that of light. Particles and antiparticles from negative energy (Dirac sea, Higgs ocean) materialize. A separation mechanism allows antiparticles of negative energy to go in the opposite direction to the ocean to form the lands (matter), thus becoming particles of positive energy, while the positive energy antiparticles plunge into the ocean of negative energy. In conclusion, the sea of negative energy ebbs and the islands of positive matter rise. One could imagine lands that emerge while the ocean level drops.

But if it does not look that way and physicists seem to want to impose a violation of the CP symmetry which would leave an excess of matter, it is precisely because they have suppressed the negative energy.

6.2. Invalidation of Negative Energy

We are thus at the heart of a problem which goes back to the conflict of ether in

the nineteenth century. Einstein stopped this war in 1905, declaring that the "luminiferous aether," the supposed carrier of light, to be unobserved, hence nonexistent. Around 1930, Dirac pointed out that the energy-momentum-mass relation

$$E^2 = c^2 p^2 + m^2 c^4, \tag{21}$$

associated with special relativity, has two roots. It calls for both positive and *negative* energy:

$$\pm E = \left(c^2 p^2 + m^2 c^4\right)^{1/2}. \tag{22}$$

He asked himself what to do with the negative energy solutions

$$E = -\left(c^2 p^2 + m^2 c^4\right)^{1/2}. \tag{23}$$

Since all negative-energy states have lower energy than any positive-energy state, Dirac wondered why there were any filled positive states, since according to Hamilton's law all entities tend to seek the lowest-energy state. He suggested that all of the negative energy states must be filled, like the filled electron shells in the Pauli exclusion scheme. Then, unless a "vacancy" occurred, positive energy particles would "float" on the surface of the negative-energy "sea" and stay positive.

Dirac's "sea" of filled negative energy states, while it satisfied the equation, did not satisfy the physics community. Heisenberg, Pauli, Jordan and others excluded those solutions that have a negative E to get over the difficulty in the classical theory. They refused the requirement of a sea of negative-energy states, insisting that theory should be based on observables alone.

6.3. Principle of Causality Preserved with the Commutation of Spacelike Particle and Antiparticle

It has been decreed that only positive energy is real. This certainty has been mathematically padlocked with the positive energy theorem. Rules have been established not to violate the principles of Relativity (not to exceed the speed of light) as well as the principle of causality (not to allow travel in time that would authorize backward causation on a cause that has already produced its effects), and which are compatible with quantum theory (by adding "constraints" to its formalism which guarantee that the creation of a particle necessarily precedes its annihilation). Thus, causality is expressed by means of rules of commutativity of fields operators. We speak of particles and antiparticles which must have the same mass and opposite electric charges. A creation operator $\Phi^*(x)$ of a particle at the space-time point x and the annihilation operator of this same particle $\Phi(y)$ at the space-time point y must commute to a separation of x and y of the spacelike and not commute for a timelike separation. These rules prevent a particle from propagating on a spacelike line (which would mean that the particle would propagate faster than light) and, for propagation on a timelike line, that the creation of the particle preceded its annihilation. These rules can be

satisfied only if the decomposition in plane waves of the field operators has negative frequency modes. And what do we do with these modes which, in quantum physics, correspond to negative energies, *i.e.*, the particles that go back in time? They are reinterpreted as positive energy antiparticles that follow the normal course of time [26]. The final argument is always that negative energy is impossible, with no imaginable physical meaning.

6.4. Validation of Negative Energy

We believe that this is how Physics has missed half of reality. Although it seems that we live in a universe of matter without constituted antimatter, there is no reason to eliminate solutions with negative energy in quantum mechanics [27]. Furthermore, negative mass is natural in the general theory of relativity and one can exclude it only by an *ad hoc* assumption extraneous to the Einstein's theory.

We specify that the relation electrostatic charge-gravitational relativized mass, which is associated with a cosmological and thermodynamics time, has two roots

$$\left[ke^2\right]^2 = \left[M_{VP}^2 t_o c\right]^2. \tag{24}$$

It calls for both positive and *negative* universe:

$$\pm ke^2 = \left[M_{VP}^4 \left(t_o c\right)^2\right]^{1/2}. \tag{25}$$

We are convinced that the recognition of the negative energy solution can find mathematical rules in the quantum theory of fields that allow the concept of antiparticle, and that of antimatter in general, to be compatible with relativity and causality [26]. Like the solution of positive energy where the principle of causality is preserved with the commutation of "spacelike" particles and antiparticles. The original theory of Dirac would be valid. His model, according to which space is not at all empty but occupied by an infinite sea of invisible particles of negative energy, constitutes a necessary physical theory. Positive energy matter lies above this bottomless sea of negative energy states. This is in consonance with the theory of Relation, which encompasses the atom and the vacuum, and in line with its "principle of Compensation"—similar to Pauli's exclusion principle—which would greatly prohibit transitions to the sea, but would favor the transition of negative energy antiparticles from the sea towards the positive energy emerged lands.

6.5. Allais Effect and Negative Energy

The idea of negative mass must be taken seriously because of the desperate theoretical situation into which physics has been thrust by the anomalous behavior of discovered phenomena which cannot be explained by Newtonian gravitation and general relativity. The Allais eclipse effect is one of those. In the 1950s, Maurice Allais, interested in the influence of gravitational and magnetic fields on the movement of the paraconical pendulum, detected an exceptional deviation of the pendulum movement during the solar eclipses of 30 June 1954

and 2 October 1959. Allais, Saxl, and Jeverdan carefully observed the behavior of three types of pendulums during solar eclipses. The pendulums exhibited significant abnormal behavior at the beginning of the phenomenon, indicating that the Moon strongly interfered with the gravitational connection between Earth and Sun at that moment. This physical anomaly, dubbed Allais effect, linked to perturbations of motion of pendulums or instruments of gravitational measurement, was also observed with varying degrees of success by others during solar eclipses [28].

The pendulums detected disturbances that sometimes indicate a drop in gravity sometimes an increase. Either a kind of antigravity, as if the involved celestial bodies lost positive energy-mass (mass M^o decreases) or a kind of over-gravity as if they were impregnated with an increased gravity (the mass M^o increases) [5] [29] [30]. To explain the antigravity phase, one can say that the body which is eclipsing breaks symmetry and adopts a code of behavior that belongs to a negative mass. In principle, positive mass attracts negative as well as positive mass, while negative mass repels both types of mass [31]. If masses of negative energy existed, they would behave as unexpected way as the Moon during a solar eclipse.

During the eclipse, the Moon interferes strongly with the Earth-Sun gravitational connection. In an unstable equilibrium on the point of conjunction between the curvature of the Earth which makes it its satellite and the curvature of the Sun which would make it its satellite, the Moon would then act as a negative mass. It would repel the Earth and the Sun which attract it: an anti-gravity disturbance detected by the pendulum on Earth. This conclusion could be erected as a principle that we will call the "macroscopic exclusion conjecture": The bodies which improvise themselves as a satellite around the central celestial body can only provoke repulsion, comparable to the principle of exclusion concerning the atom.

7. The "New" Gravitational Force: Electro-Gravitation

The equation

$$ke^2 = M_{vp} m_{ve-} 1836.1 \; t_o c \tag{26}$$

represents the super-hydrogen atom of the universe. The proton is contained in the nucleus, while the electron rotates around the nucleus at very high velocity in a circular orbit [19] [23]. M_{vp} is 1836.1 times more massive than m_{ve-}. The number 1836.1 indicates that the fundamental level of the hydrogen atom is in precarious equilibrium above a well of negative energy states. Dirac proposed that the principle of exclusion of Pauli forbid to an electron any transitions below the fundamental state because states were occupied by an infinite sea of invisible particles of negative energy. The empty space ($1836.1 \; t_o c$) is not empty. Dirac asserted that if the Pauli principle forbade transitions to the sea, nothing prevented an upward transition of the electrons from the sea to a positive energy level. This implies that particles and antiparticles can be created from an infinite

and invisible reservoir of negative energy. There may be annihilation (the energy of their mass is conserved and transformed into photon), but it may also be that the negative energy particle returns to the sea, while its antiparticle would go in the opposite direction, so becoming a positive energy particle. There would be a continuous creation effect of positive energy. The matter would thus be incessantly created throughout the expansion [32],

$$\left\{\left[M_{op}\Big/\left(1-v^2/c^2\right)^{1/2}\right]\left[M_{op}\Big/\left(1-v^2/c^2\right)^{1/2}\right]^2 1836.1\ \ G\right\}\Big/\left[R_o\left(1-v^2/c^2\right)^{1/2}\right]^2 \tag{27}$$
$$= ke^2G/R_v^2\ \ t_oc = m_{ve-}v^2r_{e-}G\Big/\left(R_v^2\ \ t_oc\right).$$

The gravitational force exerted by the proton on the electron of a hydrogen atom has the same magnitude as the electrostatic force of the super-hydrogen atom, in which the attraction between the positive charge of the proton and the negative charge of the electron keeps the electron in orbit around the nucleus at a distance of the order of the radius of the universe.

The two equations, $ke^2 = m_{e-}v^2r_{e-}$ and $ke^2 = \hbar^2\Big/\left(m_{e-}r_{e-}\right)$, are for a hydrogen atom, with an electron that moves around a proton at an average distance of 5.29177×10^{-11}m and at a speed of $c/137.036$. We write

$ke^2 = M_{vp}m_{ve-}1836.1\ \ t_oc = m_{e-}v^2r_{e-} = \hbar^2\Big/\left(m_{e-}r_{e-}\right)$.

Classical gravitational charge is $m_{e-} = M_{vp}m_{ve-}1836.1\ \ t_oc\Big/\left(v^2r_{e-}\right)$.

Relativistic gravitational charge is $m_{ve-} = ke^2\Big/\left(M_{vp}1836.1\ \ t_oc\right)$.

By substituting, $m_{ve-} = m_{e-}v^2r_{e-}\Big/\left(M_{vp}1836.1\ \ t_oc\right)$, and then using $m_{e-} = \hbar^2\Big/\left(ke^2r_{e-}\right)$, we obtain $m_{ve-} = \hbar^2v^2\Big/\left(ke^2M_{vp}1836.1\ \ t_oc\right)$.

Here we have a new aspect of gravitation. In electro-gravitation, the gravitational mass is also called gravitational charge and proves to be the same thing as the inertial mass, within the principle of equivalence of general relativity [19]. Consequently, the gravitational masses have signs, as for electric charges: attraction between opposite charges and repulsion between same charges. Thus, gravitational force is not exclusively an attraction. Gravitation would be the electromagnetic force diluted by space-time. Two repellent protons in a helium nucleus, separated by a fermi [33]

$$\begin{aligned}\text{Em force} &= ke^2\Big/\left[R_o\left(1-v^2/c^2\right)^{1/2}\right]^2\\ &= \left\{G\left[M_{op}\Big/\left(1-v^2/c^2\right)^{1/2}\right]^2 t_oc\right\}\Big/\left\{\left[R_o\left(1-v^2/c^2\right)^{1/2}\right]^2 G\right\}\end{aligned} \tag{28}$$

$$\text{Grav. force} = G\left[M_{op}\Big/\left(1-v^2/c^2\right)^{1/2}\right]^2 = ke^2G/t_oc. \tag{29}$$

If we replace in the macrocosm the proton by a star and the electron by a body which orbits in a circle around, we obtain the Newtonian formula of the universal gravitation in relation to electromagnetism. Theoretical heresy? Einstein tried in vain to unify gravitation and electromagnetism because the electromagnetic forces are proportional to the charge and not to the mass. By assuming that

gravitation is a manifestation of electromagnetism, maybe it will be easier to bridge the gap with general relativity, which gives a geometrical interpretation of force mathematically consistent with gravitation.

8. Variable Global Mass during the Great Expansion

8.1. Cyclical Universe

The theory of Relation advocates the concept of a cyclic universe at variance with the "increase of entropy forever", while it does not dispute that the present stars are melting away into radiation [34]. After a sufficient time, the total entropy would reach a maximum and the universe would be "heat death" [35], Electro-gravitation should then pull the entire universe back towards a final "big crunch," which is the mirror image of the initial big bang in reversed time [36]. But it is actually a forward descent that happens, like a balloon that makes leaps. In this way, the macroscopic laws would not be a reversal of the invariable time but a reversal of the thermodynamic time which would go from the cold to the warm. The story of the universe would then consist of a long journey from a big repulsive "singularity" to a big attractive "singularity". A closed universe that would have undergone a series of alternating cycles of compression and expansion.

8.2. Variable Mass of the Universe. As the Expansion Expands, The Overall Mass of the Universe Increases While the Mass of the Elementary Particles Decreases

The ordinary mass of the universe increases with expansion. M^o of GM^o/c^2 increases on a cosmological timescale oriented towards the future. On the other hand, the mass of the elementary particles decreases [37]. We have seen in 5.1 that the classical gravitation is almost null at the time of Planck because its energy is entirely at potential state, in opposition to the kinetic energy of the electromagnetic interaction. And in 5.5, that when M_{VP}^2 and m_o, which form the kinetic energy of the universe, decrease, then M^o, which constitutes the potential energy, grows as a gravitational mass.

With $ke^2 = M_{VP}^2 t_o c = M_{VP}^2 2\pi GM^o/c^2$, general relativity determines the mass of the universe at Planck time; $M^o = 2.26\times10^{-8}\text{kg}$. With $ke^2 = M_{VP}^2 t_o c = M_{VP}^2 h/m_o c$, the de Broglie wave which travels at speed of light, like its particle m_o, determines the boson "intrinsic" mass (or the non-rest mass corresponding to kinetic energy or energy of motion): $m_o = 2.09\times10^{-8}\text{kg}$. The mass of Planck $2.1768\times10^{-8}\text{kg}$ is, in fact, the average of these two distinct masses $\left(M^o m_o\right)^{1/2}$; the former grows with the expansion to become the mass of the current universe, while the latter diminishes to become the boson of the present space-time. It is quite clear that during the expansion the mass of the elementary particles decreases in an order of magnitude ~10^{60} and that the global mass of the universe increases by the same order of magnitude.

At Planck's time ($\hbar/c = 3.5177\times10^{-43}\text{s}$), the mass of the "baryon-proton"

M_{vp} is $\sim 1.479\times10^{3}\,\mathrm{kg}$. M_{VP}^{2} shapes a boson worth $\sim 2.17\times10^{6}\,\mathrm{kg}$. The inverse of this number gives $\sim 4.608\times10^{-7}\,\mathrm{kg}$, which is near the mass ($M^{o}=2.26\times10^{-8}\,\mathrm{kg}$) of the universe at Planck time. The assessed mass of this boson for the current universe is worth $\left(2.2439\times10^{-27}\,\mathrm{kg}\right)^{2}=5.035\times10^{-54}\,\mathrm{kg}$. The inverse of this number gives $\sim 1.986\times10^{53}\,\mathrm{kg}$, which is close to the overall mass of the current universe $\left(\sim 3.08\times10^{52}\,\mathrm{kg}\right)$. Some will see a coincidence in these numbers, where we see a connection, *i.e.*, a coincidence that is not a coincidence.

Let us stress that the mass of the proton (or electron) is a universal constant which remains invariant whatever the epoch. What changes with expansion is not the naked mass, it is the electromagnetic energy that forms a solid mantle; this mantle gets rid of his threads throughout the time to wrap and increase the gravitational mass. In Equations (7) and (8), $\left\{M_{op}\left[\left(1\Big/\left(1-v^{2}/c^{2}\right)^{1/2}\right)-1\right]\right\}$ and ΔM_{p} represent the kinetic energy which envelopes the rest mass of the elementary particle.

8.3. As the Expansion Progresses, the Atomic Dimensions Raise at the Rate of the Mass of the Elementary Particles Which Diminishes

On a cosmological time scale from the beginning towards the current age, the masses of all the elementary particles would have decreased while the atomic dimensions would have enhanced. The mass of an atom decreases with time, but its electric charge remains the same. As a result, electrons should orbit farther and farther from the atomic nucleus. The electrons would reach lower energy levels, which would require a lower energy input to dislodge them; conversely, a smaller amount of energy would be released when an electron falls into an internal orbit. The radiation emitted by a current atom would be less energetic and would have a wavelength longer than that of an atom of the past.

A body traveling a spatial length in the empty space would undergo this effect coming from that electromagnetic space itself whose wavelength increases with distance. And paradoxically, according to the principle of Compensation of the theory of Relation, this same body would undergo the effect of the global increase of the universe. This is what would explain the Pioneer anomaly. The difference between the observed trajectory and the expected trajectory of a number of not piloted space probes traveling outside the solar system or on its margins, especially the Pioneer 10 and 11 probes, would be caused by the space-time which undergoes inertia (decrease of vacuum energy) for the benefit of an increase in classic gravitation. This has allowed measuring a tiny but constant deceleration of the order of $\left(8.74\pm1.33\right)\times10^{-10}\,\mathrm{m\cdot s^{-2}}$, as a blue-shift for probes [9].

8.4. Cosmic Past

Within a great contraction, the galaxies approach each other by accelerating. Inside the galaxies takes place the phenomenon of the shrinkage of the atomic di-

mensions while the masses of the elementary particles increase. The electrons should orbit more and more near the atomic nucleus and attain higher energy levels, which would require a higher energy input to expel them. More energy would be released when an electron falls into an internal orbit; the radiation emitted by such an atom would be more energetic and would have a wavelength shorter than that of a current atom.

With the equation

$$ke^2 \leftarrow M_{VP}^2 t_o c \quad \text{or} \quad ke^2 \leftarrow M_{VP}^2 \lambda, \tag{30}$$

we can have a mathematical look back into the cosmic past. If the universe was contracting, the velocities of the protons-galaxies (M_{VP}^2) would be reversed, so that the wavelength of the space-time wave ($t_o c$) would decrease and mass of the protons-galaxies would increase. Particle and wave are equivalent and interchangeable, as are mass and energy [20] [38]. The gravitational energy is then transformed into an electromagnetic energy.

This suggests that in distant galaxies, presumed old, the atoms that emitted light would have been smaller than the atoms of the present galaxies. The wavelength of this light would be shorter and this light would be less red than that produced by the same atoms in a terrestrial laboratory. The cosmological redshift could be explained in terms of shrinkage of atoms and of the ensuing weaker reddening of light [37].

In 1998, two independent teams of astrophysicists, relying on the observation of distant type 1a supernovae, announced that the expansion of the universe did not slow down as previously thought, but was accelerating. We have already expressed our disagreement with this interpretation [9] [39]. Firstly because the determination of spatial distances in the universe is extremely imprecise. In fact, it is inconsistent to establish a link between the analysis of supernovae observations that belong to galaxies animated by movements governed by unknown equations (galaxies sometimes attracted to a galactic center, others towards the outside) and an acceleration of the expansion of space that cosmologists are unable to describe. Secondly because it could quite possibly be a case involving the assumption of temporal distances. Seeing *far* into space still means seeing *early*, according to the theory of Relation, these supernovae turned out to be less luminous and more distant than what could be deduced from their redshift because they accelerate towards the origin.

9. Spontaneous Breaking of Symmetry and Variation of Masses

In the equation

$$ke^2 \rightarrow M_{VP}^2 t_o c \rightarrow M_{VP}^2 h/m_o c \rightarrow M_{VP}^2 2\pi G M^o/c^2, \tag{31}$$

the arrow indicates the direction towards the future of the great cosmic expansion. The global mass M^o grows while the mass M_{VP}^2 and m_o of the particles lessen.

This relation between the standard model of cosmology (that of the big bang)

and that of particle physics gives close exchanges between these two models, what establishes a maximum fundamental state of matter counterbalanced by a fundamental state of minimum energy for space-time. The boson M_{VP}^2 can be amalgamated to a scalar boson of zero mass of a scalar field forming part of a global symmetry of the space-time continuum. The bosons would be like marbles in the channel (the bottom) of a Mexican hat. It is the true vacuum, that of the fundamental state of minimum global energy in which the field of matter does not nullify: the marbles can roll into the trench without energy spending [40].

But this symmetry at the level of the equation can sometimes be broken at the level of the solutions. Under the effect of uncontrollable fluctuations (thermal, quantum, etc.), the dynamics of a system with some symmetry temporarily reaches a state that does not have this symmetry. One can invoke this spontaneous symmetry breaking mechanism as well at the microscopic level—such as the Higgs mechanism in electro-weak unification—than at the macroscopic level, like the Allais anomaly.

When the broken symmetry is a local symmetry, the arrows in the equation are momentarily inverted

$$ke^2 \leftarrow M_{VP}^2 t_o c \leftarrow M_{VP}^2 h/m_o c \leftarrow M_{VP}^2 2\pi G M^o/c^2, \tag{32}$$

which implies a drop in energy in the form of matter (gravitational) in favor of energy in the form of radiation. The particles of M^o become null while the boson M_{VP}^2 and m_o behave like marbles in the channel which are going to settle down at the top of the hat in unstable equilibrium. They are in a state of false vacuum with a higher local energy, which causes the emergence of the masses of the intermediate bosons of the electroweak unification. M^o takes back its mass when the marbles run in the continuum of stable minimum state of energy.

A similar mechanism would apply to the Allais effect, discussed in section 6.4. The eclipse acts as an intermittent cosmological constraint that triggers a phase transition mechanism. The pendulum detects disturbances that sometimes indicate a drop in gravity sometimes a rise. Either a kind of antigravity, as if the marbles were hoisted at the top of the hat (mass M^o decreases) in unstable equilibrium; Or a kind of over-gravity, as if they were descending to a lower level by piercing the channel, with lower energy and more gravity (mass M^o increases) [5] [29] [30].

10. Energy, Matter and Expansion

The cosmological time of this space-time is coming from the kinetic energy of protons. It is an indicator of the energy propagated at the speed of light. The element "$t_o c$" refers to a radius from the center point of a sphere created by the initial great boom (in this case, the Planck length of the Planck sphere, but it may shrink going towards the absolute zero.) Probably due to an earlier big crush, the universe began in a "cosmic fireball" and the proton was nothing else

than a gigantic kinetic energy. This garnered energy is electromagnetic and by parting from the barrier *c*, the inertia of the particle began to fall vertiginously. When the speed went down to 99.999% of the speed of light, its mass was not more than the rest mass multiplied by 500. The decreased speed of a thousandth entailed a division by two of the kinetic energy, and the expansion of the latter served more and more to decrease the speed. The proton, as a grain of quantum matter, is quickly emptied of most of its kinetic energy, and its rate of expansion for the present universe would be rendered to 2/3*c* or 200,000 km/s. Its relativized mass is $2.2439\times10^{-27}\,\text{kg}$. The deceleration decreased inertia and moves closer to its rest mass.

The equation theoretically binds energy to matter *via* the expansionist space-time at the speed of light. It transforms electromagnetic kinetic energy into gravitational mass, by considering the latter as a potential energy. Such a transformation, inconceivable in the modern physics, tidies up in two well-separated categories, the mass connected to the material world and the energy associated with the immateriality. According to the equation, the same quantity of energy which decreases since the era of Planck, on one side, and the same quantity of matter which increases by the other one. Such a dichotomy is made in the context of two structures: the structure of the expansion for the kinetic energy which decreases with cosmological time, and the structure of condensation which increases over the same cosmological time to become the present universe [16].

Thus in Equation (4) $\left[\pm ke^2=\pm M_{VP}^2(\pi)t_oc\right]$, M_{VP}^2 decreases and t_oc increases. In the equation written in the form (3) $\left[\pm ke^2=\pm\left[M_{op}\Big/\left(1-v^2/c^2\right)^{1/2}\right]^2(\pi)t_oc\right]$, the increase of quantum mass obtained by the relativization, or the Lorentz transformation, going from v^2 to c^2, is nothing else than the huge kinetic energy of the universe when it began in a "cosmic fireball."

The energy expanded creating space-time, and cooled. We can see this freezing in the formula in two ways because there are two speeds. First, the decrease of the speed of "M_{VP}^2" cause a gradual drop in the temperature and a slowing down of the rate of expansion falls, and a concomitant increase in the gravity. These fermions, *a priori* in a state of radiation, were at their maximum speed until around 300,000 years. The decoupling of matter from radiation took place when the velocity passed under c. Second, the velocity *c* of the electromagnetic wavelength of space-time: When the universe became the one of today, *T* and density of radiation were reduced; "t_oc" transports some less energetic bosons, each second contains less energy-event, and the universe as a whole does not significantly change at every second.

Our model is able to give regions of the observable universe the time to exchange heat since the big bang. Thermal equilibrium would have had time to settle and temperatures to become uniform. This allows us to refute the inflation

phase at the beginning (with a factor of expansion and contraction of space of at least e^{55}), the proposed solution to solve the problem of causally separated regions.

According to the equation, the kinetic energy can be converted into time. Conversely, time can become kinetic energy. With relativity, mass and energy have been found to be interchangeable; now mass, energy and time can be considered as different manifestations of the same physical quantity. In this regard, time is a container of energy and has a mass. The electro-gravitational wave carries energy.

This radial movement is an electromagnetic wave. We can say that the radius of space-time belongs to the family of electromagnetic waves; the wavelength is the radius (~10^{26} m) of the universe and the period (~10^{17} s) is its age. Like in Maxwell's electromagnetic theory of light, the wave of space-time is a wave of oscillating electric and magnetic fields propagating in space [41]. We can call it an electro-gravitational wave or electromagnetic wave of space-time. It carries energy and momentum. In fact, it is the stationary electromagnetic wave, or the "background" radiation at $2.7K^{o}$, or the energy of the empty space. The ratio between space-time wavelength and cosmic gamma rays wavelength is $\left(10^{26}\,\mathrm{m}/10^{-14}\,\mathrm{m}\right)\approx 10^{40}$.

11. Electromagnetic Energy, Space-Time and Entropy

The idea embodied in the equation "$ke^2 = M_{VP}^2 t_o c$" is that the energy-mass is transformed in space-time. Space-time becomes a part of physics based on the conservation of energy, rather than an arena in which that physics takes place. The way in which the transformations work in the equation reveals that electricity, energy-matter, space-time, are inextricably linked, and should be regarded as forming our universe in a four-dimensional continuum. It implies that the principle of conservation of electricity is as important that the principle of conservation of energy [42]. The charges keep always their contents during the transformation energy-matter-space-time.

The first law of thermodynamics, the conservation of energy, is *quantitative* and considers the time as a simple "duration", while the second principle is *qualitative* and involves the flow idea. The passage of time is irreversible as much as the expansion is irreversible and suggests a finished past [17]. The second law of thermodynamics says that entropy never decreases for an isolated system. The universe as a whole has the character of an isolated system, and the law of entropy which grows in the time provides the arrow toward the future.

The growth of entropy characterizes the degradation of energy. The processes transformers of one form of energy into another are also irreversible (we are always going from "hot" to "cold"). Entropy can be written in the thermodynamic form $S = Q/T^{o}$ (Q: quantity of heat given to a system; T^{o}: absolute temperature) [38] [43] [44]. If a quantity of heat does not change, and T^{o} decreases, S increases, meaning that the preservation of the quality of the energy quantities is

not preserved.

We can make the equivalence with our equation:

$$ke^2/dM_p^2 \to dt_o c$$

$$Q/dT^o \to dS. \tag{33}$$

The term ke^2 contains the quantity of heat, the total energy of the isolated system; M_{VP}^2 is rest mass + T, and $t_o c$ contains entropy of the empty space-time. The latter is not a vacuum but actually a plenum of particles and antiparticles being created and annihilated [32].

With time, the total entropy of the isolated system goes up moving toward a state of maximum probability. The variation of entropy is positive because the system receives heat. If we take the relation $Q = Mc^o T^o$ (Q: quantity of heat. M: mass. c^o : specific heat. T^o : temperature), $S = Q/T^o = Mc^o T^o/T^o = Mc^o = t_o c$. We may say that space-time $t_o c$ possess a mass with a specific heat Mc^o.

However, the energy cannot come down indefinitely. It will reach the last level of the availability and will have no more transformation capacity [34] [43]. The universe would then undergo a re-contraction in accordance with the closed model of Friedmann-Lemaitre in which space is finite and of positive curvature, and in which the expansion is decelerating.

12. Inflationary Aberration

12.1. Accelerated Expansion

The observation says that the expansion of the universe is almost offset by the gravity exerted by all matter. The universe dilates at a singular speed close to the critical line that separates the big freeze universe of the big crunch universe. We are very close to a point of balance between expansion and gravity. If all the energy released by the big bang was lower of a tiny fraction, the matter would return back and would collapse into a giant black hole. If it were slightly stronger, the matter would disperse so quickly that galaxies could not even form.

Although the world seems near its critical point, making it impossible to determine with certainty what will be its evolution, the provisional consensus is that the universe will end in big freeze, because it was found that the expansion was going by accelerating. It is postulated that there is some unknown energy that annoys gravity and causes the accelerated expansion of the universe. Einstein called the "cosmological constant" that element which could counteract the contraction caused by gravity. Rejected, then restored it is now called "dark energy". One might think officially, since 1998, that dark energy exerts a negative pressure which has the effect of causing the acceleration of the universe. But it turns out that the interpretation as much as the facts are inconclusive.

12.2. 1a Supernovae

We have questioned (section 8.4) the interpretation of observational data in mid-1990 of type 1a supernovae (SNe 1a). By measuring with unequalled preci-

sion the remains of fourteen supernovae at distances varying between 7 and 10 billion light-years, astronomers discovered that the light coming from them was 50% dimmer than it should have been according to the estimates of their distances. They interpreted the dimness as evidence that the supernovae were 10 to 15% farther away than they should have been if the expansion of the universe was slowing down. [7] The calculations obtained by the Hubble space telescope, then by telescopes located in Hawaii, Australia and Chile, were published in 1998 [45]. They too easily ruled out the criticisms which underline the decrease of the radiant energy by absorption (interstellar dust absorbs light that becomes bland), or something of the evolutionary process of the supernovae that has been misunderstood [39]. It has been suggested that the "inflection point" where the rate of expansion has ceased to decline and begin to rise under the effect of dark energy would have occurred some 5 to 8 billion years ago. Others believe that the expansion has started to speed up over 1.5 billion years ago. The acceleration of the universe has been confirmed as were the Ptolemy epicycles in the past.

12.3. Cosmological Blunder

We believe that the basic rules of cosmology were truncated to the point of creating a cosmological anachronism. Previous to the estimation of recessions exceeding c, the radial flight of the galaxies was interpreted as a process translating a *general expansion of space*. It has often been proposed as an example of the expansion of the space that of a rubber balloon on the surface of which are stuck confetti which represent the galaxies.

If the balloon is inflated, its surface is stretched and the confetti is moving away from each other with an apparent speed which is increased in so far as the radius of the balloon is growing. In space-time, "length" may refer to temporal length as well as spatial length. So we can receive the radiations emitted in the distant past by a system that reached speeds close to c, to which the expansion of space-time gives an apparent flight velocity greater than c. This way of thinking seems long gone because it involves the center the universe [7] [43]. However, our equation claims this center of the universe. In the expression M_{VP}^2, or $\left[M_{op}\Big/\left(1-v^2/c^2\right)^{1/2}\right]^2$, of our equation, the speed v is almost c, if not c, at the beginning, then decreases as the space-time is created. There is not an alternative. The expansion continues, the clusters of galaxies into which "matter" is distributed, are becoming more widely separated, but the rate of expansion also continues to decline from c towards 0.

In astronomy, telescopes are machines to go back in time. To see far into space, we must see far in time. Further we see, weaker we see. The more a galaxy is distant, the more it moves quickly toward the big bang, primordial explosion which gave rise to the expanding universe [7]. Conversely, it decelerates as it gets closer to us [46]. But since 1998, the film of the history of the universe upside down until his first picture seems an anachronism. See far, which means see "sooner", became "later" with the telescopes. The cosmologists concluded that

the more supernovae appear pale, the more galaxies recede from each other and accelerate towards tomorrow, towards the big freeze.

With this different astronomical vision, fundamentally spatial, whose velocity v starts from 0 to increase towards c, the flight of galaxies is today construed as a process of acceleration of isolated systems relative to other isolated systems. For theorists, it is as if, undeniably, the galaxies were moving away from each other with speeds which are all the greater in that the distance between them is itself larger. There are galaxies which recede from us at a speed close to ninety-five percent of that of light. Based on the Doppler effect of emission-line quasars, some redshifts are so important that in applying the Hubble formula, they display some radial velocities such as our galaxy and the quasars seem to be moving apart from each other at speeds *exceeding the speed of light.* No matter if, in the first place, a source of radiation that would exceed the speed of propagation of light, would *necessarily be invisible* since, in second place, the farce of the epicycles of inflation, that continues to accelerate the universe, will necessarily render it hyperbolic [43].

12.4. Relativity with Inflationary Sauce

With relativity, the center is everywhere in the universe, which means that there is no real center. Strong with this *a priori* which excludes the irreversible time (and sometimes time itself), the reasoning of the modern astronomers led to this: the observer that I am and that I perceive as being at rest on Earth is part of a galaxy is, from that point of view, also in movement with a speed of expansion where there comes a time when it will be higher than the speed of light [18]. No matter the objection in principle of special relativity.

Since there is no center of the universe, one would think that the explanation according to which the radial escape of galaxies is the consequence of the initial explosion could not be retained. To explain the big bang, on the contrary, one will become Copernican again, and one will make general relativity to assert that space expands faster than light, because space represents neither matter nor energy. Which is senseless, because to explain the flatness of the present universe, Alan Guth suggested that the universe had ended up in a "false vacuum" at the time of the era of G.U.T. (10^{-35} s), and this excited state would look like an empty space, but filled with energy. In general relativity, the energy and pressure are sources of gravitation, and a negative pressure causes a gravitational repulsion. This repulsive effect would have provoked a period of exponentially accelerated expansion. The universe would have swollen to the size of the present universe. Around 10^{-32} s, the false vacuum would de-excite towards the true vacuum, the flatness, and all the energy of the false vacuum would have been released in the form of particles and heat. The universe would have restarted with a dark energy that would have made the flat space [32].

Apart depreciate relativity by making it appear that the false vacuum energy did not contain energy whereas the high expansion rate of the latter exceeded

the speed of light, the theory of inflation brings an insoluble problem for the multiple theories of inflation: a dark energy that would contain the infinite kinetic energy, essential to the evolution of the *hyperbolic universe*, and that would have a density of 10^{122} times greater than that found in the empty space [45].

12.5. Cosmological Constant: 10^{122} or 10^{0}

The experimental indications of a positive value for the cosmological constant also come from independent measurements of primordial density fluctuations observed in the Cosmic Microwave Background (CMB). The raw data from the experiences of scientific teams WMAP, COBE, Boomerang, and Maxima which have performed measurements on the fluctuations of CMB radiation favor the model of inflation. Inflation is a model produced from the high-energy physics, according to which the universe would have recorded, in the first fractions of a second of its evolution, a wildly high expansion rate, so that space would have become flat [45]. The teams concluded that the total density parameter (Ω_{tot}) was $\Omega = 1$ for a Euclidean universe. Both methods (supernovae and CMB) suggest that Ω_m (m: matter) is close to 0.3 and that it is needed to get to a flat universe, to add a contribution $\Omega_\lambda = 0.7$, coming from a cosmological constant with a positive value. The cosmological constant plays the role of an energy density. Its value can be expressed in the same units as the density of matter, for example in grams per cubic centimeter. The Ω_λ factor is convenient for assess the contribution of the cosmological constant to the total density of the universe.

However, in the present situation, even though everyone seems to agree on the existence of a cosmological constant, its value deducted from astronomy is absolutely not compatible with that calculated by theoretical physicists. Several models are possible to calculate the value of λ within the framework of the theories of unification, but the predicted value in most cases is 10^{122} times superior to the limits prescribed by astronomical observation. Dark energy should be very dense, which is the opposite of the density of the vacuum.

12.6. Astrophysical Calculations Just for Laughs

The dominant cosmology, starting from the cosmic microwave background radiation, considers that the big bang occurred about 13.8 billion years ago. That is an obvious dilemma since astronomers observe stars older than the universe [46]. In 1995, they had already observed them with the Hubble Space Telescope. Estimates from observations dating back to 2000 placed the star HD 140283, which lies a mere 190 light-years from Earth in the constellation of Libra, as old as 16 billion years. In 2013, it seems this star, nicknamed *Methuselah*, was 14.46 billion years old. Astronomers (Howard Bond, of Pennsylvania State University and the Space Telescope Science Institute in Baltimore) were puzzled because it seems the star was still older than the universe itself. Of course, they add a margin of 800 million years, meaning that the star might actually be 13.7 billion years old, barely

younger than the universe as it is currently understood. If that pattern continues, we can expect to observe some clusters of "galaxies older than the universe" to complete the picture of the problem of "stars older than the universe" [47].

12.7. Inflation Lobby

There is no question to minimize the importance of data collected by the experiments since never observational cosmology has reached such precision. But the bundle of more or less plausible assumptions to extract the cosmological parameters from observational data, error bars to calculate a range of angular spectra of CMB fluctuations which are then compared to the observed spectrum, the adjustment "at best" of various parameters that can be deduced, have left the door open to biased analyses and interpretations that should have been taken with much more caution.

For some silent scientist, the fine analysis of the angular fluctuation spectrum rather suggests that the maximum likelihood is 1.2 Ω. The experimental balance would tip in favor of a spherical space, finite volume, although in a large radius of curvature, and ever expanding thanks to the cosmological constant. However, the lobby of inflation, strengthened by the fact that $\Omega = 1$ is consistent with the data of four scientific teams, focused its efforts towards the scenario of a spectrum of fluctuations caused by inflation. The goal is to find the worst adjustments between various cosmological parameters which would give $\Omega < 1$. The model of inflation has played in cosmology for over half a century the role of an original concept which became an orthodox thought. Disguised under the noble term of paradigm, it would have exercised a real intellectual terrorism to any opposite thought [45].

13. Energy, Velocity and Cosmological Constant

According to the theory of Relation [9] that we stand for, based on the dynamic equation of quantum cosmology, and consistent with the big bang and the scenario of the decelerated expansion, the kinetic energy of the beginning (amalgamated with negative energy and dark energy) creates not only space-time but also ordinary matter, and therefore the macroscopic gravity. Given the brute force of the big bang, the energy released at the time of creation of the universe was immeasurable. Given the brute force of the big bang, the energy released at the time of creation of the universe was immeasurable. From the first minutes, the expansion quickly converted most of this energy into ordinary matter. The energy of the primordial proton was at first moved at speed of light which has the value c. With speeds approaching that of light, we get a Planck time (10^{-43} s) and a relativized proton has a mass of 10^{3} kg, which is a fundamentally new value in physics. Then the speed decreased gradually as the energy spread and turned into matter as we know it.

Since galaxies are moving away at a constant speed estimated 200,000 km/s, the cosmological time is about 15 billion light-years and the relativized proton

weighs 2.2439×10^{-27} kg, according to results given by the formula above. It appears that $2/3c$ is the speed where there is no longer a deceleration (from c to $2/3c$) observable. It would be close to the critical point where there seems to be an extraordinary coincidence between gravity and expansion. A speed of 100,000 km/s would give about 26 billion light-years. The proton would then have exhausted its kinetic energy, reached its rest mass and the universe would seem moved by a movement at zero speed.

Certainly, a general dilation of the space-time would be unverifiable because we undergo it ourselves. Unless the solution is included in the cosmological constant (density measurement), the kinetic energy of the proton, which poured his energy into creating the space-time of our universe, is assimilated to a negative cosmological constant and a dark energy. It comes into play in larger scales and affects the expansion of the universe. It decreased by nearly 100%, from 10^{122} to around 10^{0} at the present time. Because of the decreasing rate of speed, the universe expands more slowly. The kinetic energy acts as a positive pressure gas that binds the galaxies and slows the expansion. It exercises a tension which retains and brings things together, at the same time it spreads in the manner of a stretched elastic. It causes the deceleration of the universe [16] [18].

Our equation is the first to include the irreversible time. During this time, energy constitutes a variable field, very high in the phases of the primordial universe, in agreement with the calculations of physicists, but which falls very low during cosmic evolution, in accordance with the value now measured by astronomers. Dark energy (or cosmological constant) would be a "tired" energy. Bear in mind to not confuse the tired dark light with the tired white light, which stipulates that the light could have been energetically degraded and thus redshifted, during his trip through space intergalactic. However, although the light undergoes the redshifts under the influence of the Doppler effect due to the recession velocity of distant galaxies, there is no evidence that today allows to permanently eliminate the theory of tired light [37]. The theory of Relation, which combines the degraded dark light of the structure of the expansion with the shifted white light of the condensation structure, is part of the big bang theory.

We get a model of the universe that has the "temporal" behavior of closed models (in expansion-contraction), and which has the "spatial" behavior of spatially finite models. It can be likened to the oscillatory universe of Einstein-Tolman (1931), the Euclidean model of Einstein-de Sitter (1932), or the closed Friedmann-model (1922) [45] [48].

14. Conclusions

The equation $\left[ke^2 = M_{VP}^2(\pi)t_o c\right]$ of the theory of Relation gives the impression of being the mathematical confirmation of the standard big bang theory, in which all the energy-matter began in an instant of time in a colossal explosion. The universe first spread to its maximum rate, then it was gradually slowed down by gravitational attraction, which now gives a sphere with a radius that is

nearly 15 billion light-years. Deceleration can be represented by an electromagnetic space-time wave, assimilated to a negative cosmological constant, which acts at the cosmos scale as an engine of expansion (the lost energy is transformed into a gravitational matter that tends to regroup). Electricity, energy-matter and space-time are linked in a four-dimensional continuum.

We envisage cosmological history from the perspective of a cyclical universe. We saw in a previous article [9] that everything happens as if there are two universes in one. It is like if, in spite of the matter and radiation created at the big bang, there is enough excess of kinetic energy left for the pre-universe, which is slowly and automatically converted into our universe gravitation energy. Because of the inversion of the arrow of cosmological time, based on the laws of thermodynamics, the energy of the world that has contracted is negative compared to the positive energy of our expanding world. The expansion would have been preceded by a period of contraction and it would not have occurred at the same time for all the matter. In the shrinking world much of the matter contracted faster than the other, giving the big crush which is for us the big bang. Isolated pieces of matter from the contracted pre-universe would have been delayed in their appearance and development. There would have been mini bangs following the main big bang [12], a kind of violent explosive effect of strong negative pressure within a localized region where an important creative mechanism took place.

The formula introduces cosmological time into the heart of a physics that has never made the essential distinction between past and future. A cosmological, thermodynamic "space-time", from the past to the future, joins electromagnetism, Newtonian gravitation, special relativity, general relativity and quantum physics. It is important to consider this space-time as precisely the dynamic variable that allows us to consider the entire universe as the physical system where quantum nonseparability can describe as being in union two (of) uncoupled objects that have already interacted with each other, gravitationally or by exchanging radiation. In this respect, the equation finally permits a quantum cosmology.

There is still much to be said about this equation, which distinguishes three types of mass: fermionic, bosonic and that of the ordinary matter of the universe. We can find the state of the fermions in relation to the exact changing mass of the bosons, for any state of the mass-energy in the "irreversible" time. The equation is therefore in line with Yukawa's theory [20] [49] which postulates that there is an infinity of particles corresponding to an infinity of possible states of matter, and with the idea of a supersymmetry that interchanges fermions with bosons, and vice versa. In this way, this equation at once quantum and relativistic is God's equation [35].

Conflicts of Interest

The author declares no conflicts of interest regarding the publication of this paper.

References

[1] Kaku, M. and Trainer, J. (1987) Beyond Einstein, Bantam New Age, New York, 10, 20, 21, 30, 31, 35.

[2] Will, C.M. (1986) Was Einstein Right? Basic Books, Inc., New York, 153, 166-167.

[3] Eddington, A. (1995) Space, Time & Gravitation. Cambridge University Press, Cambridge, 1920, 178, 179.

[4] Bramand, P., Faye, P. and Thomassier, G. (1980) Physique, Terminale C, E., Eurin-Hachette, Paris, 52-55.

[5] Bagdoo, R. (2015) Recycled Relativity. https://vixra.org/abs/1506.0125

[6] Bagdoo, R. (2016) Neutrino's Temporal Oscillations, 7, 11, 15. http://vixra.org/abs/1605.0005 https://www.academia.edu/25111027

[7] Moffat, J.W. (2009) Reinventing Gravity. Thomas Allens Publishers, Toronto, 121, 122, 162, 206-208.

[8] Davies, P.C.W. and Brown, J. (1988) Superstrings. Cambridge University Press, Cambridge, 5-26-27-47.

[9] Bagdoo, R. (2008) The Pioneer Effect: A New Theory with a New Principle. http://vixra.org/abs/0812.0005 https://www.academia.edu/5535864

[10] Prigogine, I. and Stengers, I. (1992) Entre le temps et l'éternité, Champs, Flammarion, 129-133.

[11] Hawking, S.W. (1988) A Brief History of Time. Bantam Books, New York, 117, 134, 145-152. https://doi.org/10.1063/1.2811637

[12] Bagdoo, R. (2009) Arcade 2 Extragalactic Emission and Dark Matter as Seen by the Theory of Relation. http://vixra.org/abs/1302.0003 https://www.academia.edu/5538299

[13] Whyte, L.L. (1927) Archimede or the Future of Physics. Kegan Paul, Trench, Trubner and Co., Ltd., London.

[14] Cohen-Tannoudji, G. (1991) Les constantes universelles, Hachette, 112.

[15] Gamow, G. (1962) La gravitation, Payot, Paris, 136-137.

[16] Bagdoo, R. (2013) The Energy in Virtue of the Principle of Compensation. http://vixra.org/abs/1301.0180 https://www.academia.edu/5539802

[17] Whitrow, G.J. (1955) La structure de l'Univers, Gallimard. 161-169.

[18] Smolin, L. (2006) The Trouble with Physics. Houghton Mifflin, 15, 21, 22, 106, 251.

[19] Orear, J. (1967) Fundamental Physics. John Wiley and Sons, New York, 87, 100, 156, 284-287.

[20] Gribbin, J. (1991) À la poursuite du Big Bang. Champs, Flammarion, 133-134, 248, 326-328.

[21] Greenstein, G. (1983) Le Destin des étoiles. Seuil, Paris, 166.

[22] De Closet, F. (2004) Ne dites pas à Dieu ce qu'il doit faire. Édition du Seuil, 342.

[23] Atkins, K.R. (1970) Physics. John Wiley and Sons, New York, 8, 90.

[24] Ferguson, K. (1992) Stephen Hawking. Bantam Books, New York, 141-142.

[25] Trefil, J.S. (1983) The Moment of Creation. Macmillan Publishing Company, 171-175.

[26] Klein, É. (2009) Les tactiques de Chronos. Champs Sciences, 105-106.

[27] Duquesne, M. (1974) Matière et antimatière. Presses Universitaires de France, 62.

[28] Hotson, D.L. (2002) Dirac's Equation and the Sea of Negative Energy, Part 1, Infinite Energy. Issue 43.

[29] Bagdoo, R. (2009) Link between Allais Effect and General Relativity's Residual Arc during Solar Eclipse. http://vixra.org/abs/1302.0089 https://www.academia.edu/5537473

[30] Bagdoo, R. (2013) Lunar Eclipses and Allais Effect. http://vixra.org/abs/1311.0156, https://www.academia.edu/5539813

[31] Will, C. (1989) The Renaissance of General Relativity. The New Physics, 31, 32.

[32] Davies, P. (1989) Les forces de la nature. Armand Colin, 78, 170.

[33] Stevenson, R. and Moore, R.B. (1967) Theory of Physics. W. B. Saunders Company, Philadelphia & London, 126, 174.

[34] Jeans, J. (1937) The Mysterious Universe. University Press, Cambridge, 132-133.

[35] Adair, R.K. (1987) The Great Design. Oxford University Press, New York, 147, 209.

[36] Herbert, N. (1989) Faster than Light. Plume-Penguin Books, New York, 48-113.

[37] Silk, J. (1997) Le Big Bang. Éditions Odile Jacob, 471, 480, 568.

[38] Wilczek, F. and Devine, B. (1987) Longing for the Harmonies. W. Norton and C., New York, 43, 49, 311, 320, 363, 368.

[39] Bagdoo, R. (2011) Cosmological Inconstant, Supernovæ 1a and Decelerating Expansion. http://vixra.org/abs/1304.0169 https://www.academia.edu/5539777

[40] Cohen-Tannoudji, G. and Spiro, M. (2013) Le boson et le chapeau mexicain. Gallimard, Folio Essais, 268-275.

[41] Pagels, H.R. (1982) The Cosmic Code. Bantam New Age, New York, 5, 9, 237-243.

[42] Rousseau, P. (1950) La Conquête de la Science. Arthème Fayard, Paris, 202, 203.

[43] Cuny, H. (1971) L'aventure cosmique. Les éditeurs français réunis, 162, 166, 168, 173.

[44] Bénézé, G. (1961) Le nombre dans les sciences expérimentales. Presses Universitaires de France, 93-96.

[45] Luminet, J.-P. (2001) L'Univers chiffonné. Folio essais, 86-87, 91, 300-304, 314-316, 321, 373-374, 460.

[46] Thuan, T.X. (1995) Un astrophysicien. Champs Flammarion, 19, 34, 35.

[47] Cosentino, M. (1993) Origine et destin de notre Univers par une nouvelle Cosmologie de l'atome jusqu'aux confins du Cosmos. Bonnefoy-Editeur.

[48] Tolman, R.C. (1987) Relativity, Thermodynamics and Cosmology. Dover Publication, 401-403, 412-415, 439-444, 484-487.

[49] Jolivet, R. (1965) Logique-Cosmologie. Emmanuel Vitte, Lyon, 383.

Journal of Modern Physics, 2019, 10, 344-361
http://www.scirp.org/journal/jmp
ISSN Online: 2153-120X
ISSN Print: 2153-1196

Two Physical Constraints upon the Motions of Celestial Bodies

Xiaobai Ai

Shanghai Institute of Applied Physics, The Chinese Academy of Sciences, Shanghai, China
Email: hsiaobaiai@outlook.com, mraixiaobai@163.com

How to cite this paper: Ai, X.B. (2019) Two Physical Constraints upon the Motions of Celestial Bodies. *Journal of Modern Physics*, **10**, 344-361.
https://doi.org/10.4236/jmp.2019.103023

Received: January 24, 2019
Accepted: March 11, 2019
Published: March 14, 2019

Abstract

There exist two physical constraints upon the motions of celestial systems. **Constraint 1** reveals during collapse or explosion motion of celestial bodies that there would be an unattainability upper limit for their compact intensity (total mass M/scale size R), which arises from the Lorentz invariance of the time-like metric in local four-dimensional continuum in Einstein's theory of special relativity. **Constraint 2** points that the average mass density of nucleon would be an unsurpassed upper limit for bulk normal matter in nature, which arises from Heisenberg's uncertainty principle. A very important effect is that the combination of these two physical constraints would prevent the formation of black holes.

Keywords

General Theory of Relativity, Gravitation Collapsing, Schwarzschild Metric, Schwarzschild Singularity, Centre Singularity, Black Hole, Compact Intensity, Heisenberg's Uncertainty Principle

1. Introduction

Hawking (1942-2018) in his last few years continued to issue negative voices on the black hole theory [1] [2] that he had participated in as a leading scholar. However, the lack of convincing physical arguments is a prominent weakness in his last works, especially in the "smooth inflation exiting" article written by Hawking, S. and Hertog, T. [2]. Many physicists believe that their new idea was not practical: "their research results being in an empty mathematical framework", "ignoring many details of the development of the universe", "only being speculations without any practical basis". Other scholars who did deny the black hole theory have similar deficiencies, for instance, see [3] [4].

It is well known that since 1916 Schwarzschild firstly solved a solution of

Einstein's gravitational field equation for outside a static and spherically symmetric vacuum field with central mass M *i.e.* the Schwarzschild metric:

$$ds^2 = c^2\left(1-\frac{2GM}{Rc^2}\right)dt^2 - \left(1-\frac{2GM}{Rc^2}\right)^{-1} dR^2 - R^2\left(\sin^2\theta d\phi^2 + d\theta^2\right), \quad (1)$$

where r,θ,ϕ are the usual polar coordinates, G being the constant of gravitation, R is the scale of radius, c is the speed of light in vacuum. If there are no physical constraints, there would be two singularities in Equation (1): the singularity of Schwarzschild ($R_S = c^2/2G$) and the singularity of centre ($R = 0$). In the 1920s, some famous physicists, including Einstein and Eddington, did not believe the outcome from Equation (1) and a used famous opinion was that "there should be certain laws in nature to prevent the stars from evolving into such absurd outcomes". But scholars had been looking for the laws over a decade, and didn't still know what they were. Therefore, during an unstoppable gravitational collapse, the formation of singularities would be inevitable physical state.

By the 1930s, there seemed to be a consensus in astronomical community that the singularity of Schwarzschild could be eliminated by re-selecting coordinates. In 1933, Lemaître, G. used a moving metric, the infinite red-shift horizon was eliminated, but the white hole would be created [5]. In 1935, Einstein and Rosen showed that they applied the Einstein-Rosen Bridge (or Schwarzschild wormhole) to replace the singularity of Schwarzschild [6]. During 1960, Kruskal applied the dynamic metric instead of Schwarzschild coordinate, then the space-time would be divided into four regions, and the white hole would appear [7]. On the surface of the collapsing body, they used coordinate transformations to eliminate Schwarzschild singularity. In fact, they just used new puzzles instead of old ones. Almost at the same time, Finkelstein wanted to use the Eddington-Finkelstein coordinates to eliminate the singularity of Schwarzschild, but he gave birth to the white hole monster [8]. Mei, X.C. pointed out that "black holes with singularities" "caused by the mathematical description of curved space-time", but he could not give the physical principles to study gravitational collapse only in the flat space-time [9] [10] [11].

Recently the most sensational event for physical world is that physicists in United States and Europe have announced that: from February 11, 2016 to August, 2017, they have observed GW150914, GW151226, GW170104 and GW170817 four gravitational wave (GW) events. In 2017, the Nobel Prize in Physics was awarded to Weiss, R., Thorne, K. and Barish, B. for their role in the direct detection of GW. It is a firm fact that GW has been detected. Taking GW150914 [12] [13] as an example which has been modeled with the techniques of numerical relativity [14] [15] [16], the GW is strictly credible to be measured, but the resulting analysis confirmation is not yet convincing and still in doubt. Question is mainly from two points: a) The numerical simulation method usually uses preconceived premises to construct the model, then the "computer experiment" is used to adjust repeatedly until the parameters suitable for or matching the observed data would be found. The existence of black holes in nature is the premise

of numerical simulation, if there are no black holes in nature world, what shall we do? It is a pity, the published results of GW150914 lacked key data to confirm black holes, *i.e.* lacked the scales R_1 of M_1 $(29M_\odot)$ and R_2 of M_2 $(36M_\odot)$ from the parameters provided in the analysis paper [12] [13]. The scale of $62M_\odot$ might not be obtained until the final merging stage. In short, it is very important to get M_1/R_1 and M_2/R_2 firstly. b) It is generally believed that the energy of gravitational wave comes from the sum of the conversion of various kinetic energy and the release of gravitational binding energy from collapsing celestial bodies which would have a higher conversion efficiency [17]. Gursky, H. toke a single proton as an example and pointed out that in [18]: "We can get a clue by calculating the potential energy of a single proton on the surface of stars of decreasing size but of $1M_\odot$, thus of increasing density, as given by

$$\phi = \frac{GM_\Theta m_p}{R} = GM_\Theta^{2/3}\rho^{1/3}m_p. \tag{2}$$

Hence, even if a single proton landed on the surface of stars might release all its gravitational binding energy, which would be still less than half of its rest energy. So do other materials.

Consequently, in [12] and [13], a small part of the energy of $3.2M_\odot c^2$ radiates as a gravitational wave, but where is the most part of the matter of $3.2M_\odot$? Or where do the most part of the matter of $3.2M_\odot$ go?

Because gamma-ray bursts were not monitored synchronously in the final merger stage and subsequently no gamma-ray burst were detected [12]. Is there a new pattern of material disappearance to be recognized? Or through some unknown mechanism, $3.2M_\odot$ of matter has been converted into the energy of a short gamma-ray burst and the afterglow which have been missed? Obviously some alternative conclusion may be considered also. A temporary and more reasonable explanation for the gravitational wave event GW150914 should be that a pair of merged objects with $29M_\odot$ and $36M_\odot$ merging into a single collapsed object with $62M_\odot$, and a small part of the energy of $3.2\mathrm{M}_\odot c^2$ has been radiated as a gravitational wave in the following "circular" motions. The above arguments are also applicable to the events of GW 151226, GW 170104 and GW 170817.

Recently, the STAR Collaboration at Brookhaven National Laboratory's Relativistic Heavy Ion Collider (RIHC) measured the polarization of the decay products of Λ hyperons which are emitted from the quark-gluon plasma (QGP) produced by ultra-relativistic collisions between heavy atomic nuclei traveling close to the speed of light and has determined the rotational speed of QGP were about $(9\pm1)\times10^{21}$ times/sec [19]. Scientists at the Thomas Jefferson National Accelerator Institute in the United States found, firstly, that the pressure in the center of the proton is around $10^{35}P_a$ (*i.e.* $10^{36}\,\mathrm{erg/cm^3}$) [20]. Although with larger statistical uncertainties, the high rotation rate of bulk QGP material and high pressure states resemble white dwarfs and neutron stars, hence [19] and [20] not only provide experimental insights into the physics of the strong nuclear

force, but also forces us to ponder: because of $\omega R < c$, where ω being is the rotation rate of QGP in [19], as long as the natural normal matter, such as elementary particles, has a geometric scale R, [19] and [20] would imply that, for the high-density normal material in nature, there would exist some upper limits of physical property such as the material density, the energy density, high pressure and etc. which would not be reached or be unsurpassed. Anyhow, [19] and [20] prompt the author to re-examine the theory of relativity and quantum mechanics and to find that the keys to unlock the mysteries of black hole would hide in our neglected life experience and the careless research style.

In Section 2, the present author argues that at least two criteria might be used to judge whether an observed celestial body being as a "black hole candidate". In Section 3, the careless style of study and some neglected experiences in previous studies are pointed. In Section 4, the first restriction on the motions of celescial systems is derived from the Lorentz invariance of the time-like metric in local four-dimensional continuum in Einstein's theory of special relativity (SR) which prevents the gravitational collapse of compact object reached general relativistic instability stage from Schwarzschild radius. In Section 5, the second restriction on the motions of celescial systems is derived from Heisenberg's uncertainty principle which reveals that the mean density of normal matter in nature has an unsurpassed upper limit. In Section 6, the new physics included in Constraint 1 and Constraint 2 will be discussed. In Section 7, some remarks are given.

2. Available Criterion

If the gravitational collapse to a black hole is unavoidable during the late evolution of a massive celestial body, then observers standing outside and far away from Schwarzschild radius will never be able to observe it, the reason was pointed out by Weinberg G.: "The collapse to the Schwarzschild radius therefore appears to an outside observer to take an infinite time" [21]. As we all know, the collapsing celestial body still has a strong gravitational field and during the collapsing process there will be a variety of external substances that will continue to be pulled into. Hence the community of astronomy and physics are still concerned about whether indirect evidence of the existence of black holes can be obtained from astronomical observations. Therefore, many indirect methods to identify black holes were proposed: such as Hawking's black hole radiation; the gravitational waves generated by the non-spherical symmetric component of gravitational field changing sharply with time or a merger of two celestial bodies; X-ray or X-ray bursts from accretion disks around black holes; radiations or emissions of matter from the accretion disk falling into a black hole, and so on. Unfortunately, these phenomena of expectation are only the criteria for pre-selection, but the credible evidence has not yet been found, because the similar phenomena may also occur in the movement of other celestial bodies. However, if one wants to deny many candidates for black holes, there exists available compact intensity (M/R) criterion.

For an unknown compact celestial body, its total mass M and its scale of radius R (or diameter $2R$) usually are measured firstly. According to Equation (1), if celestial bodies can reach or break through Schwarzschild radius in gravitational collapse, the compact intensity (M/R) should be

$$\frac{M}{R} > \frac{c^2}{2G}\left(\approx 6.75\times 10^{27}\ \mathrm{g/cm}\right). \tag{3}$$

Otherwise, some material or most material of the candidate would be still outside of "Schwarzschild radius" of an expected black hole. Hence, the magnitude of M/R should be an important criterion.

Example 1: The giant elliptical galaxy Messier 87 (M87) at the center of the Virgo cluster of galaxies is a strong radio source, an active galaxy and a very strong source of gamma rays. The Hubble Faint Object Spectrograph (FOS) was used to measure the rotation velocity of the ionized gas disk at the center of M87, the FOS data indicated a central mass of 2.4 billion solar masses, with 30% uncertainty [22]. In the past, M87 was thought as a 50 billion solar masses center span about 300 light-years across. Recently, using the High Energy Stereoscopic System Cherenkov telescopes, scientists measured the variations of the gamma ray flux coming from M87 and found that the flux changed over a matter of days, which might suggest the diameter of M87 being only round 0.1 ly [23]. Even so, the evaluating values of compact intensity is only $M/R \approx 1.0\times 10^{26}\ \mathrm{g/cm}$, in fact, which does not support M87 being a reliable candidate of the black hole.

Example 2, let us Sagittarius A* at the centre of our Milky Way. [24] gave that Sagittarius A* weights 4.3 million times of the Suns, [25] gave that an intrinsic size of the radio-emitting region of the galactic center compact non-thermal radio source of only 1 AU in diameter at 3.5 mm. For $1\ \mathrm{AU} \approx 1.496\times 10^{13}\ \mathrm{cm}$, the evaluating results are: $M/R \approx 1.14\times 10^{27}\ \mathrm{g/cm}$, the mean density $\rho \approx 4.8\ \mathrm{g/cm^3}$. At least, the present measured result of M/R does not support Sagittarius A* being a reliable candidate of a super-massive black hole. May be, a consolation argument says: the radio-emitting region being outside the center of "black hole", the gravitational collapse in Sagittarius A* still continues, its scale R would be further reduced and more accurate measurements should be awaited in the future. However, the negative opinions will be supported by another two astronomical observations.

a) Red-shift

If there is a black hole, the gravitational potential energy near the event horizon varies greatly. It is generally believed that the linear spectrum of iron may be detected in the region closest to the black hole. More scholars estimate that X-ray or gamma radiation should be the dominant radiation near the event horizon. In fact, if radiation would be measured, regardless of the form of radiation, the gravitational red shift value must be considerable. Therefore, the value of gravitational red-shift should be another important criterion.

The compact intensity M/R might be expressed in terms of gravitational red-shift as

$$\frac{M}{R}=\frac{c^2}{2G}\left[1-\frac{1}{(1+z)^2}\right], \tag{4}$$

where z is red-shift which may be evaluate by

$$z=\frac{\lambda-\lambda_0}{\lambda_0}=\frac{\lambda}{\lambda_0}-1, \tag{5}$$

where λ_0 is the characteristic wavelength of the emitter and λ the observed apparent wavelength respectively. If there are no spectral lines of distinguishable wavelengths, the red shift should be calculated by energy also:

$$1+z=\frac{\lambda}{\lambda_0}=\frac{\nu_0}{\nu}\to\frac{\hbar\nu_0}{\hbar\nu}=\frac{E_0}{E}, \tag{6}$$

where E_0 is the energy of the emitting radiation and E the energy of observed radiation respectively. One may see that as long as the measured red-shift z is a limit value, which would only indicate that the scale size of the collapsing bodies is always greater than "Schwarzschild radius".

As an example, let us consider a quasar with a large red-shift value. For $z\geq 0.25$, the red-shift-apparent visual magnitude diagram in [26] displays dispersion, which seems to imply that there is no correlation between apparent visual magnitude and red shift, which is very different from a better linear distance-red-shift relation for z in the range from 0.003 to 0.2 [27]. As a matter of fact, it only implies that: i) the simple linear Hubble's law no longer gives the correct distant radical scale; ii) the dispersion in red shift-apparent magnitude diagram in [26] means that for distant objects with $z\geq 0.25$ there exists several very different physical red shift mechanisms: cosmological red-shift, gravitational red-shift, due to high speed ejecting, the influence of the deceleration parameter q_0 in cosmology, the effect of evolution and some new kind principles of physics. Hence, regardless the details of debate about the nature of the red shifts of the distant objects, the gravitational red-shifts would be always involved. As long as the above arguments are accepted, even with red-shift greater than 0.25, the core of the distant celestial objects cannot be associated with any black hole model. For example, S50014 + 813 with 40 billion solar masses [28] and $z\approx 3.366$ [29] [30], its gravitational red-shift must undoubtedly be less than 3.366. If a misuse of $z\approx 3.366$ as its gravitational red shift to estimate $\frac{M}{R}\approx 6.39\times 10^{27}\ \mathrm{g/cm}$, still $<6.75\times 10^{27}\ \mathrm{g/cm}$.

Generally speaking, As long as the red shift data are available, it would just prove that the scale of the collapsed object is still larger than "Schwarzschild radius $R_S\left(=c^2/2G\right)$".

b) X-ray or Gamma ray

Can we determine the physical properties of the sources from the characteristics of the energy spectra of the measured X-rays or gamma rays? May the measured X-rays or gamma rays radiations be used as signs for black hole candidates or other origins? The mechanisms of gamma-ray emission are diverse, including electron-positron annihilation, the inverse Compton Effect, from the

gamma decay of radioactive nuclei in supernovae, hyper-novae, pulsars, blazars and active galaxies and etc. Of course the energy spectra from compact objects and their surrounding environments are cluttered and difficult to measure, even the highest photon energy reaches the TeV level, but the energy spectra of gamma rays produced from the gravitational collapse would still regularly searchable. For example, proton fall to a star, the more regular energy spectra around 100 keV implies that radiations may come from white dwarfs; 100 MeV radiations from neutron stars, 300 - 400 MeV radiations might produced in more compact object—quark star (or called QGP star) that has been speculated for a long time. In fact, as long as the energy spectra of regular rays can be distinguished from the measured messy spectra, whether it is about 100 MeV or 300 - 400 MeV, which would certainly mean that the scale size of the collapsing celestial object is still greater than Schwarzschild radius.

3. Deficiencies in Previous Studies

As we all know, Minkowski delivered his famous "space-time" speech at the Conference of Scientists held in Cologne on September 21, 1908 [31]. In this speech, Minkowski extended Einstein's theory of special relativity (SR) [32] to space-like ($ds^2 < 0$), light-like ($ds^2 = 0$) as well as time-like ($ds^2 > 0$) three statuses for space-time continuum, where $ds^2 = c^2dt^2 - dx^2 - dy^2 - dz^2$. Later, Einstein accepted Minkowski's contribution and laid the foundation of general theory of relativity (GR) and he pointed out in his book "The Meaning of Relativity" wrote in 1922, that "*As in the special theory of relativity, we have to discriminate between time-like and space-like line elements in the four-dimensional continuum*" [33]. I don't know why the predecessors, including Einstein himself, forgot this statement, which contained the power they were looking for to prevent the gravitational collapsing of catastrophe. When applying GR to study the gravitational problems, is there any guarantee of physical laws to implement Einstein's "distinction"? The answer is yes, because human beings have not only thousands of years of practical experience, but have GR already.

Practical Experience:

1) Since the beginning of human ancestors, we have been pursuing the universality of natural laws and have realized the universality from the practice of thousands of years and astronomical observation in different places on the earth. In the progress of the civilization, we have far more knowledge of astronomy than our ancestors from four channels for astronomical information: electromagnetic radiation, cosmic ray particles, neutrinos (anti-neutrinos) and gravitational waves. In addition to extreme physical states, we have thought that, the production mechanism of those events happened in distant celestial bodies would be contained within the physical laws obtained by various research institutions (local inertial systems) on Earth. In other words, at present, we have applied the knowledge of physics obtained in local inertial systems on Earth to study events occurring on distant celestial bodies. Above historical experience

should not be forgotten, the summary of worth recalling is roughly as follows:

Particle Physics → origin of the universe, dark matter, compact stars, active galactic nuclei, supernova explosions and etc.;

Nuclear Physics → elemental origins, star structure and evolution, neutron star cooling, solar and cosmic neutrinos, cosmic rays and etc.;

Atomic, Molecular → interstellar molecules, astrochemistry, interstellar microwave sources and etc.;

Plasma and Beam Physics → radiation power structures, Supernova remnants, pulsar magnetosphere, star wind, cosmic particle acceleration mechanism and etc.;

Condensed Matter → interstellar dust, Nebula, white dwarf structure, neutron star structure and etc.;

…

and so on and so forth.

The most gratifying thing is that bold use has achieved a great success. This point proves that in any space locality or time period in the universe, no matter the event being a slow process or a violent explosion, which would be considered as an event occurring in a flat local inertial system.

2) As we all know, matter is not only the basic substance of physics, but also includes measurable electromagnetic field, gravitational field and vacuum field of various virtual particles which cannot be measured directly. However, since there is no indisputable evidence to hint that those accompaniments such as electromagnetic field, gravitational field and/or background vacuum field do take part into gravitational collapse, consequently, during the catastrophic gravitational collapsing processes, only those wrecks with non-zero rest mass torn apart by tidal action such as "dust" grains, gas-dust complex, material molecular clusters, nuclei, and individual elementary particles are the leading role. So that the universal speed limit in Einstein's time-like SR must be considered. In other words, we must adhere the Lorentz invariance of Minkowski local time-like metric as one of the axioms needed in studying the collapsing or exploding process.

Un-negligible Theoretical Pillar:

1) Let's think about the progress of physics from the perspective of epistemology.

It took about 300 years to express the universality of knowledge in theory and practice. Because the success of electromagnetic field theory promoted the development of Galileo's principle of relativity (Galileo transformation) into Einstein's principle of relativity (Lorentz transformation), and then to inertia relativistic principle (the principle of equivalence), which led to the birth of GR. In this process, it was found that there were many restrictive functional relationships (relativistic effects) between physical quantities. It was found that algebra and geometry may be used as mathematical tools to express physical laws equivalently. Of course, algebra expressions and the algebraic expressions of geometry concepts have their own characteristics, but just being tools. GR is generally

regarded as a satisfactory modern theory of gravity with tensor potential. In fact, the greatest contribution of GR to whole (!) physics system is to expound and to prove that any locality in the universe would be a flat inertial system, where any laws of physics found on Earth could be applied. This is the theoretical pillar of using the laws of physics found in earth within the mass and distance scales of the universe.

2) SR is not a special branch of physics like nuclear physics, particle physics and etc., but the restrictive relationship between physical quantities revealed by SR would apply to all branches of physics. Einstein and many physicists modified mechanics, optics, electrodynamics, statistical mechanics and quantum mechanics with the constraints of these discoveries, so that the original branches of physics may be applied to low-speed and high-speed motion conditions, as well as physical states under extreme conditions. The establishment of GR seems to expand the concept of inertial system, but it also reduces the concept of inertial system to locality. However, we may rest assured that SR would be used in any processes of any locality in our observable universe. One may see that the rest of this article will prove that the story of black holes should be rewritten, because the scale size of collapsing objects would be always larger than the old concept—Schwarzschild radius.

4. Constraint 1

This section deals with another feature of the axiomatic system. The SR and the GR are axiom systems, which are the systems with formal logic. All the theoretical inferences are included in their premises and are determined uniquely by its premises with consistence, independence as well as completeness. From the arguments mentioned in Sections (2) and (3), one may see that without the limitations of certain physical principles, the use of GR will inevitably lead to the infinite collapse of late celestial bodies in evolution, firstly crossing the Schwarzschild radius and until to the singularity of centre ($R=0$). However, coupled with the Lorentz invariance of Minkowski's time-like metric, some new physical results different from the current black hole theory should be obtained.

Combine Equation (1) and condition $\mathrm{d}s^2 > 0$, one may have an algebraic equations (7) with a "greater sign (>)":

$$c^2\left(1-\frac{2GM}{Rc^2}\right)\mathrm{d}t^2 > \left(1-\frac{2GM}{Rc^2}\right)^{-1}\mathrm{d}R^2 - R^2\left(\sin^2\theta\mathrm{d}\phi^2+\mathrm{d}\theta^2\right). \tag{7}$$

In order to keep the inequality direction of Equation (7), the following positive condition are necessary:

$$1-\frac{2GM}{Rc^2} > 0, \tag{8}$$

or

$$R > \frac{2GM}{c^2}. \tag{9}$$

or

$$M/R < c^2/2G\left(\approx 6.75\times10^{27}\ \mathrm{g/cm}\right). \tag{10}$$

Thus, the first constraint upon the motion of late celestial bodies may be obtained naturally. Obviously, this restriction eliminates the singularity of Schwarzschild:

Constraint 1—During collapse or explosion motion of celestial bodies, a special constant $c^2/2G$ is an unattainability upper limit of the compact intensity M/R, *i.e.* $M/R < c^2/2G\left(\approx 6.75\times10^{27}\ \mathrm{g/cm}\right)$.

As long as to note that comparing with M and R, such as angular momentum J, charge Q and cosmic constant L involved in other metrics are negligible physical quantities, so that, the above **Constraint 1** would apply not only to Schwarzschild metric, but also to other metrics, such as Kerr metric and etc.

According to Equation (10), the following properties of average density may be obtained:

$$\rho_m M^2 < \frac{3c^6}{32\pi G^3} \approx 7.3\times10^{82}\left(\mathrm{g/cm}\right)^3, \tag{11}$$

where ρ_m is mass density. If change ρ_m to energy density ρ_E, E is total energy, then

$$\rho_E E^2 < \frac{3c^{12}}{32\pi G^3} \approx 5.3\times10^{145}\left(\mathrm{erg/cm}\right)^3. \tag{12}$$

One may find that the motion of celestial bodies is governed by Equations (11) and (12). A derivable conclusion beyond expectation is that **Constraint 1** also reveals that during the process of an expansion or an explosion of celestial body system, the continuous creation of matter from vacuum (?) is inevitable. It is really "something comes from nothing"! On the contrary, in the process of collapse, with the increase of mass density and energy density it would lead to the decrease of total mass (energy). Except various radiations (including infrared, optical, radio, X-ray and gamma rays), energetic particles or spurted material (e.g. the jets) ejected from the accreted disks and gravitational waves generated by the release of gravitational binding energy etc., a new losing way of mass unfolds, because the disappearance of 3.2 $M_\odot$ in [12] and [13] is apparently proceeding rapidly through some unknown mechanisms. That is to say, as long as the Equations (11) and (12) are met, the matter should continuously disappear into the vacuum, "something goes back to nothing", which might also be a reasonable physical channel. Maybe a very short gamma-ray burst would originate here. What actually happens? This should be confirmed by the energy spectra of short gamma-ray bursts.

It should be recalled that Weinberg used to have a similar result $\left(MG/R\right) < 4/9$ [*i.e.* $M/R < 0.89c^2/G$] [34]. Although Weinberg's upper limit was slightly different from **Constraint 1**, but careful reading [34], one may find that in order to

obtain $(MG/R) < 4/9$, Weinberg used a non-physical "to have r_{∞}^2 negative" condition (*i.e.* imaginary value of point). As one read the following words: "It is difficult to imagine that a fluid sphere with a large density near the surface than near the center could be stable" [35], one may know that Weinberg still considered the infinite collapse, hence, his mistakes in [34] [35] are obvious.

Some people once believed that the contribution of variables to mathematics was attributed to Descartes, R. In fact, when the sign of inequality entered mathematics, the variables, the motion of variables, the moving direction of variables and the limit of motion were all brought into mathematics. All physical equations expressed by inequalities imply that there must be "unattainable" or "insurmountable" restrictions on a certain physical state. It is noteworthy that conditional Equations (3) and (10) have dynamic characteristics already, and the calculated Schwarzschild radius would be a variable now and only with instantaneous value. However, "**Constraint 1**" and Equation (11) would still not prevent collapse, but only impose one strong restriction on the collapsing of compact bodies. According to Equation (11), even for late evolving celestial bodies, if the collapsing time is long enough, their volume will collapse to a small enough size, and it seems inevitable that they would still collapse to a state with very high mass density, even onto or pass Schwarzschild singularity. In fact, this is impossible, because the new achievement of high energy physics [19] implies that Heisenberg's uncertainty principle will give one more physical constraint.

5. Constraint 2

A quark-gluon plasma (QGP) or quark soup is a state of matter in quantum chromodynamics (QCD) which exists at extremely high temperature and/or density. This state is thought to consist of asymptotically free strong-interacting quarks and gluons, which are ordinarily confined by color confinement inside atomic nuclei or other hadrons. Although they are all complex QCD systems [36], the order of magnitude of their bulk properties may still be estimated by basic natural constants.

According to the theoretical principle, the density of micro QGP in [19] might be estimated from its rotational speed data. Because of the universal speed limit given by time-like SR, the upper limit on the rotational speed of micro QGP would mean that there should be an upper limit on the mass density and energy density of micro QGP. Obviously, the formation mechanism of micro QGP might be different from that of white dwarfs, neutron stars and the presumed quark stars (QGP stars). The former is formed by strong-interaction, the latter by gravitation. Therefore, for micro QGP, there might be a "strong interaction gravitational constant" G_S similar to the gravitational constant G. The author will present a detailed discussion of this topic at a later date.

Let us turn to see [20]. The pressure in the center of the proton was measured around $P = 10^{35} P_a$ (*i.e.* 10^{36} erg/cm^3) [20], its mass density ρ_{pm} may be estimated as

$$\rho_{pm} = \frac{P}{c^2} \approx 10^{15}\ \mathrm{g/cm^3}.$$

Atoms, nuclei and sub-nuclear particles do not have clear boundaries. What is the calculated value of proton radius? Tell the truth, the proton radius remains a puzzle today. However, there are indeed ambiguous physical scales. At present, it is generally accepted that the charge radius of protons is about $(0.84 \sim 0.87)\times 10^{-13}\,\mathrm{cm}$. According to [20], an equivalent radius $\tilde{R}_p$ of protons would be estimated as:

$$\tilde{R}_p \sim \sqrt[3]{3m_p/4\pi\rho_m} \approx 0.736\times 10^{-13}\,\mathrm{cm}$$

which is obviously smaller than its charge radius and much larger than the generally accepted proton Compton wavelength. Therefore, the proton mass density ρ_{pm} calculated from the normal proton's Compton scale size should be larger than the data obtained from the present measured value [20].

The smallest possible scale r of a microscopic object being bound up with molecule, atom or nucleus must be related to the Heisenberg uncertainty principle:

$$\Delta r \cdot \Delta p \geq \hbar,$$

where $p(=mv)$ is its momentum. In history, both Davisson-Germer experiment and Heisenberg uncertainty principle were all published in 1927 [37] [38]. The Davisson-Germer experiment equivalently gave another expression of the uncertainty principle for microscopic objects:

$$d\sin\theta_n = n\lambda > \lambda = h/p$$

where d, for nickel, is line spacing, λ is the wavelength associated with electrons with average momentum p, n is an integer. A first-order maximum of intensity is to be expected at an angle θ_1 ($n = 1$) [37]. Written in the following form commonly used in discussing micro-objects:

$$r \cdot p \geq \hbar.$$

Take notice

$$r \geq \frac{\hbar}{m_i v} > \frac{\hbar}{m_i c},$$

where $\hbar/m_i c$ is the Compton wavelength of the discussing micro-object m_i, its mean density ρ_{im} has the following relation

$$\rho_{im} = \frac{m_i}{\frac{4}{3}\pi r^3} < \frac{m_i}{\frac{4}{3}\pi\left(\frac{\hbar}{m_i c}\right)^3}\left(\sim \frac{3m_i^4 c^3}{4\pi\hbar^3}\right). \tag{13}$$

An estimative figure might be carried out only for current matter—normal elementary particles, for instance, the "absolutely stable" proton (m_p), or slowly decaying neutron (m_n), the calculating results are the same in the order of magnitude:

$$\rho_{im} < \frac{3m_i^4 c^3}{4\pi\hbar^3}\left(\sim 4.3\times 10^{16}\ \mathrm{g/cm^3}\right), \tag{14}$$

where m_i is the mass of proton (m_p) or the mass of neutron m_n. If substituting the mass of Higgs particle into Equation (14), the resulting upper limit would be much larger than Equation (14). Nevertheless, even if there would exist Higgs condensation (?) Which would be in vacuum, unlike the normal substances in our directly observable nature world.

Is there any inkling in nature to support Equation (14)? In recent decades in order to create and study vacuum excitations, vacuum phase transitions as well as a sheer surmise of mini black-hole, the ultra-relativistic heavy ions collision is considered as an effective way. The earlier data have been confirmed that QGP exist at an approximate extremely high temperature of 4 trillion (2×10^{12}) degree Celsius [39], the evaluating mass density of QGP fireball has almost reached $1\text{GeV}/\left(\text{c}^2\cdot\text{fm}^3\right)$, *i.e.* around $1.8\times10^{15}\,\text{g}/\text{fm}^3$, which is less than the mass density of nucleon. Therefore QGP (quark soup) likes a big nucleus, and a nucleon likes a small bowl of quark soup. Consequently, the observational mass density of QGP in [39] agrees with Equation (11). This point would seem that "quark confinement" state and Equation (11) suggest following constraint:

Constraint 2—The average mass density of nucleon may be an unsurpassed upper limit for the normal matter in nature world.

Let Equation (11) / M^2 < Equation (14), it turns that

$$\frac{3c^6}{32\pi G^3 M^2} < \frac{3m_i^4 c^3}{4\pi\hbar^3},$$

it is clear that

$$M > m_i \cdot \left(\frac{\hbar c}{2Gm_i^2}\right)^{3/2} \sim 0.65\times M_\odot. \tag{15}$$

Seemingly, **Constraint 2** or Equation (14) still could not stop the formation of black hole, however, a very important effect of combining two constraints reveals that there would exist an unattainability lower limit of total mass $0.65\times M_\odot$ for a compact object made up of normal matter. If the "strong interaction gravitational constant" G_S might be determined, the limit of mass of micro QGP would be determined also. Will there be any evidence? Aford, M. *et al.* took note "*the observed absence of fast-spinning young stars*" and tried to solve it [40]. Since the rotation speed is related to the mass density, the limit of the rotation speed indicates that there is an upper limit of the mass density. Therefore, it is absolutely impossible for late-type evolving celestial bodies to collapse to the singularity of centre ($R=0$), in other words, the singularity of centre ($R=0$) in Schwarzschild metric has been eliminated.

6. More New Physics

Except for the generation and annihilation of matter and antimatter, we have never seen many substances created or disappeared during a very short time interval. Our common sense approach in the past may negate the possibility of the continuous creation or continuous extinction of vast substance. However, SR

and GR combine with Heisenberg's uncertainty principle reveal some new physics knowledge which we still do not know so far:

1) In the traditional understanding of gravitational collapse, the collapsing body only collapses. Although the system has reached the instability of general relativity, the uncontrolled gravitational collapse would not stop, even if the scale size of the collapsed body approaches Schwarzschild radius, the total mass M would not decrease. **Constraint 1** and Equation (10) give another dynamic model of gravitational collapse, that is, with the decrease of scale size, the total mass M of gravitational collapsed body also decreases, so as to ensure that compact intensity of the collapsed body always conforms to the laws within **Constraint 1** and Equation (10).

2) **Constraint 1** pointed out that this total mass reduction would be possible, but it is not yet clear about the detailed physical mechanisms and processes. At present, this article is just a guess that the new place might be vacuum, but it still does not known how to use astronomical observations to confirm this guess.

3) Around 1970s, Penrose, R. and Hawking, S. proved that under certain conditions (the validity of general relativity, the positive of energy, the universality of matter, and causality), gravitational collapse and physical singularity may be the inevitable fate of massive objects [41]-[47]. However, adding the Lorentz invariance of time-like metric, those concepts such as photon balls, event horizons, capture surfaces, white holes, wormholes, Einstein–Rosen bridges and so on would be all gone with negating the black hole. In addition, from Equation (14) and Equation (15), it may see that the big bang model of the universe still exists, and the expansion of the universe and the creation of matter also exist, and there does not exist the big bang model with the singularity of centre ($R=0$) in nature. Equations (14) and (15) favor Gamow's fireball big bang model [48], which was based on and developed the "*hypothèse de l'atome primitif*" (hypothesis of the primeval atom) proposed by Lemaître in 1931.

4) Take advantage of derivatives $\mathrm{d}M/\mathrm{d}t$, $\mathrm{d}\rho/\mathrm{d}t$, $\mathrm{d}R/\mathrm{d}t$, **Constraint 1** and Equation (11) also manifests some new relations between relative rate of matter creation (or extinction) with the relative variable rates of scale R and mean density ρ:

During the expanding motion ($\mathrm{d}M/\mathrm{d}t>0, \mathrm{d}R/\mathrm{d}t>0, \mathrm{d}\rho/\mathrm{d}t<0$):

$$\frac{2}{M}\frac{\mathrm{d}M}{\mathrm{d}t}<\frac{2}{R}\frac{\mathrm{d}R}{\mathrm{d}t}<-\frac{1}{\rho}\frac{\mathrm{d}\rho}{\mathrm{d}t}, \tag{16}$$

and during the collapsing motion($\mathrm{d}M/\mathrm{d}t<0, \mathrm{d}R/\mathrm{d}t<0, \mathrm{d}\rho/\mathrm{d}t>0$):

$$-\frac{2}{M}\frac{\mathrm{d}M}{\mathrm{d}t}>-\frac{2}{R}\frac{\mathrm{d}R}{\mathrm{d}t}>\frac{1}{\rho}\frac{\mathrm{d}\rho}{\mathrm{d}t}. \tag{17}$$

5) It deserve to be mentioned that thinking of the expansion process of the universe, by means of Hubble's empirical law, link the velocity of recession of a distant celestial body and its distance from us $\mathrm{d}r/\mathrm{d}t=H_0 r$ (where H_0 is the Hubble constant at present), it turns

$$\frac{\mathrm{d}\rho}{\mathrm{d}t}=\frac{\mathrm{d}(M/V)}{\mathrm{d}t}=\frac{\rho}{M}\frac{\mathrm{d}M}{\mathrm{d}t}-3\rho H_0 \tag{18}$$

Combining Equation (16) and Equation (18), One may find that in cosmic expansion, the upper limit of the relative matter creation rate and the lower limit of the relative mass density decreasing rate would be controlled by Hubble constant at present H_0.

$$-\frac{1}{\rho}\frac{\mathrm{d}\rho}{\mathrm{d}t}>2H_0 \quad \text{and} \quad \frac{1}{M}\frac{\mathrm{d}M}{\mathrm{d}t}<H_0. \tag{19}$$

6) From the arguments mentioned above, we can see that the characteristics of the creation of matter in the process of expansion of universe are different from the steady-state cosmological model [49] [50], but the common point is that new substances are constantly created from vacuum. If vacuum is a physical channel for observing the disappearance of matter in the universe, it should also be a physical channel for the creation of matter, which may be one of the physical reasons for the expansion of the universe and producing dark matter.

7. Remarks

Some remarks should give as follows:

1) We study systems that would be large or small systems, or closed systems or open systems, and the impact of the environment on the systems is often very important. It is now recognized that a complete nature world (Universe) contains an observable universe incorporated with an infinite vacuum. With the passage of time, we now know that although vacuum has Lorentz invariance, but it is actually quite complicated. If some matter disappears or creates without a trace as the collapses or expands takes place, how do we describe the laws of conservation in the universe (including conservation of mass-energy, of baryons, of leptons, of electric charge and etc.)?

2) From a universal point of view, the law of conservation of energy should now be expressed as follows: The total energy of the Universe is conserved. If one part of the Universe obtains some form of energy, the other part will inevitably lose the same energy. No violations of this principle were found. In short, the observable universe and vacuum constitute an infinite, circular, and mutually transformed natural world.

3) Exactly as we know that Lorentz invariance is the inevitable outcome of two original postulates of SR. Bietenholz gave an introductory review about the ongoing search over more than 12 years for the evidence of Lorentz invariance violation (LIV) in ultro-high energy cosmic rays [39]. The extreme Lorentz factors with the order of $\gamma=1/\sqrt{1-\beta^2}\sim 10^{11}$, but no LIV has been observed so far. So there's no need to waste any more time on the search for LIV.

4) **Constraint 1**, **Constraint 2** and the combination of them expose the existence of new physics, and put forward a lot of open questions also:

a) In the observable universe, if matter would be created from vacuum, why does vacuum only create matter not antimatter?

b) What is the spatial structural feature of new creating matter? Does it show some analogy with the structure of filaments in the supernova remnant or the reticular behavior in the very large-scale of an evolving universe?

c) May the forming new matter be one of the candidates for dark matter and dark energy?

d) Are we fortunate enough to make some morphological observations before and after the supernova explosion to confirm that if there might also be material creation in an explosion in a local area of the universe?

8. Conclusion

Theory without practice is empty theory, and practice without theoretical guidance is blind practice. Therefore, we must sum up practical experience by theory. On the basis of historical experience, supported by SR and GR, inspired by the latest developments in particle physics and high energy physics, the mystery of the singularity of Schwarzschild and the singularity of centre over the past century would be able to eliminate by adding only two physical restrictions on the Schwarzschild metric. This work fully proves the ancient Chinese motto: "Truth is simple", like the Ockham's Razor quote, which is worth thinking about.

Acknowledgements

This work was supported by the National Science Foundation of China Grant No. U1532260.

Conflicts of Interest

The author declares no conflicts of interest regarding the publication of this paper.

References

[1] Hawking, S. arXiv:1401.5761v1 [hep-th]

[2] Hawking, S. and Hertog, T. arXiv:1707.07702v3[hep-th]

[3] Mersini-Houghton, L. and Peiffer, H. arXiv:1406.1525 or arXiv:409.1837

[4] Vachaspati, T., *et al.* (2007) *Physics Review D*, **76**, 024005. https://doi.org/10.1103/PhysRevD.76.024005

[5] Lemaître, G. (1933) *Annales de la Société scientifique de Bruxelles*, **A53**, 51-85.

[6] Einstein, A. and Rosen, N. (1935) *Physics Review*, **48**, 73. https://doi.org/10.1103/PhysRev.48.73

[7] Kruskal, M. (1960) *Physics Review*, **119**, 1743. https://doi.org/10.1103/PhysRev.119.1743

[8] Finkelstein, D. (1958) *Physics Review*, **110**, 965. https://doi.org/10.1103/PhysRev.110.965

[9] Mei, X.C. (2011) *International Journal of Astronomy and Astrophysics*, **1**, 109. https://doi.org/10.4236/ijaa.2011.13016 https://www.Scirp.org/journal/ijaa

[10] Mei, X.C. (2014) *International Journal of Astronomy and Astrophysics*, **4**, 656. https://www.scirp.org/journal/ijaa

https://doi.org/10.4236/ijaa.2014.44060

[11] Mei, X.C. (2013) *Journal of Modern Physics*, **4**, 974-982. https://doi.org/10.4236/jmp.2013.47131 https://www.scirp.org/journal/jmp

[12] Abbott, P., *et al.* (2016) *Physical Review Letters*, **116**, Article ID: 061102. https://doi.org/10.1103/PhysRevLett.116.061102

[13] Klimenko, S., Vedovato, G., Drago, M., Salemi, F., Tiwari, V., Prodi, G.A., *et al.* (2016) *Physical Review*, **D93**, Article ID: 042004. https://doi.org/10.1103/PhysRevD.93.042004

[14] Pretorius, F. (2005) *Physical Review Letters*, **95**, 121101. https://doi.org/10.1103/PhysRevLett.95.121101

[15] Campanelli, M., Lousto, C.O., Marronetti, P. and Zlochower, Y. (2006) *Physical Review Letters*, **96**, Article ID: 111101. https://doi.org/10.1103/PhysRevLett.96.111101

[16] Baker, J., *et al.* (2006) *Physical Review Letters*, **96**, Article ID: 111102. https://doi.org/10.1103/PhysRevLett.96.111102

[17] Hoyle, F. and Fowler, W. (1963) *Nature*, **197**, 533. https://doi.org/10.1038/197533a0

[18] Avrett, E. (1976) Frontiers of Astrophysics. Harvard University Press, Cambridge, and London, 156.

[19] The STAR Collaboration (2017) *Nature*, **548**, 62. https://doi.org/10.1038/nature23004

[20] Burkert1, V., *et al.* (2018) *Nature*, **557**, 396.

[21] Weinberg, S. (1972) Gravitation and Cosmology: Principles and Applications of the General Theory of Relativity. John Wiley and Sons, New York, 347.

[22] Harms, R., *et al.* (1994) *The Astrophysical Journal Letters*, **435**, L35. https://doi.org/10.1086/187588

[23] Wirsing, B. (2006) Discovery of Gamma Rays from the Edge of a Black Hole. Max Planck Society.

[24] Gaensler, B. (2011) Extreme Cosmos. New South Publishing, Sydney, 174.

[25] Shen, Z.Q., Lo, K.Y. and Liang, M.C. (2005) *Nature*, **438**, 62. https://doi.org/10.1038/nature04205

[26] Burbidge, G. and Burbidge, E. (1969) *Nature*, **224**, 21. https://doi.org/10.1038/224021a0

[27] Peach, J. (1969) *Nature*, **223**, 1141. https://doi.org/10.1038/2231140a0

[28] Gaensler, B. (2011) Extreme Cosmos. New South Publishing, Sydney, 152.

[29] Osmer, P., *et al.* (1994) *The Astrophysical Journal*, **436**, 678. https://doi.org/10.1086/174942

[30] Kaspi, S., *et al.* (2007) *The Astrophysical Journal*, **659**, 997. https://doi.org/10.1086/512094

[31] Minkowski, H. (1952) The Principle of Relativity, a Collection of Original Memories. Dover Publications, New York, 73.

[32] Einstein, A. (1989) The Collected Papers of Albert Einstein. Vol. 2, Princeton University Press, Princeton, Doc 23.

[33] Einstein, A. (1955) The Meaning of Relativity. Princeton University Press, Princeton, 64.

[34] Weinberg, S. (1972) Gravitation and Cosmology: Principles and Applications of the

General Theory of Relativity. John Wiley and Sons, New York, 331.

[35] Weinberg, S. (1972) Gravitation and Cosmology: Principles and Applications of the General Theory of Relativity. John Wiley and Sons, New York, 332.

[36] Schmidt, C. and Sharma, S. (2017) *Journal of Physics G: Nuclear and Particle Physics*, **44**, Article ID: 104002. https://doi.org/10.1088/1361-6471/aa824a

[37] Davisson, C. and Germer, L. (1927) *Nature*, **119**, 558. https://doi.org/10.1038/119558a0

[38] Heisenberg, W. (1927) *Z. Physik*, **43**, 172. https://doi.org/10.1007/BF01397280

[39] Bietenholz, W. (2011) *Physics Report*, **505**, 145. https://doi.org/10.1016/j.physrep.2011.04.002

[40] Aford, M., *et al.* (2012) *Physical Review D*, **85**, Article ID: 044051. https://doi.org/10.1103/PhysRevD.85.044051

[41] Penrose, R. (1965) *Physical Review Letters*, **14**, 57. https://doi.org/10.1103/PhysRevLett.14.57

[42] Hawking, S. (1966) *Proceedings of the Royal Society*, **294A**, 511.

[43] Hawking, S. (1966) *Proceedings of the Royal Society*, **295A**, 490.

[44] Hawking, S. (1967) *Proceedings of the Royal Society*, **300A**, 187.

[45] Hawking, S. (1967) *Proceedings of the Royal Society*, **308A**, 433.

[46] Hawking, S. and Penrose, R. (1970) *Proceedings of the Royal Society*, **A314**, 529. https://doi.org/10.1098/rspa.1970.0021

[47] Penrose, R. (1969) *La Rivista del Nuovo Cimento*, **1**, 252.

[48] Gamow, G. (1946) *Physical Review*, **70**, 572. https://doi.org/10.1103/PhysRev.70.572.2

[49] Hoyle, F. (1948) *Monthly Notices of the Royal Astronomical Society*, **108**, 372. https://doi.org/10.1093/mnras/108.5.372

[50] Hoyle, F. (1949) *Monthly Notices of the Royal Astronomical Society*, **109**, 365. https://doi.org/10.1093/mnras/109.3.365

Journal of Modern Physics, 2019, 10, 362-370
http://www.scirp.org/journal/jmp
ISSN Online: 2153-120X
ISSN Print: 2153-1196

Superimposing Scales and Doppler-Like Effect

Edward Szaraniec

Retired from the Cracow University of Technology, Kraków, Poland
Email: edszar@pk.edu.pl

How to cite this paper: Szaraniec, E. (2019) Superimposing Scales and Doppler-Like Effect. *Journal of Modern Physics*, **10**, 362-370.
https://doi.org/10.4236/jmp.2019.103024

Received: February 12, 2019
Accepted: March 11, 2019
Published: March 14, 2019

Abstract

The observable universe together with the observer, both on sufficiently large scale, succeeds in their self-entaglement and paradoxical inconsistency. For consistency, the observable universe and the observer have to be on different scale (size) provided, the cosmological principle is preserved as an approximation in a limit. The point is the *univers' principle* itself. Our proposal for the disentaglement is *superimposition out of complexity*. The distance contraction, as observed in electrical soundings over horizontally stratified earth (static system), is identified as a counterpart of Doppler shift in dynamical systems. An alternative answer to the question about an effective cause of the Doppler shift sounds the heterogeneities under superimposing scales. The energy propagating in stratified universe exhibits a shift which could be attributed not only to the expansion but alternatively to fluctuations across different scales. When nothing is said or predetermined about kinematics of a system, both causes might share in the effect. It opens different static and kinematic possibilities, which challenge established theories of energy/information transmission and/or sounding at a distance as well as pertinent technology in prospect.

Keywords

Disentaglement, Distance Contraction, Doppler Effect, Rama Effect, Superimposition, Univers' Principle

1. Introduction

The Universe consists in mass and energy, in structures not violating the basic laws of mathematical physics. While the spatial size of universe is still unknown, it is possible to speculate on the observable universe only, then implying existence of an observer. Depending on size of the observable universe and relative scale of the observer, the Universe of particular size is viewed in superimposing scales. Hence scale and size are the open questions.

Paradoxically, the observable Universe, without human observer viewed himself on a sufficiently large scale, is not complying with the cosmological principle requirements. Due to this incosistency, sufficiently large structures cannot exist. Explicitly, the observer has to be of the same scale as the observable universe is, following the cosmological principle. In other words, the observer and the observable universe are self-entangled in the cosmological principle.

To get them disentangled and to avoid ulterior speculations, the World at particular size will be referred to as the observable universe with an observer included, independly on their (universe and/or observer) size and scale. Subsequently, the following principle is postulated.

The *univers' principle* is stated as: "Viewing on a sufficiently large World of particular size, the properties of underlying observable universe at some different scale are the same for all potential observers".

This principle contains an implicit qualification and some testable consequences not discussed in here.

1.1. Scale Model of the Universe

Scale model of the entire Universe is lacking because of the sheer size of it: one cannot reasonably create the model including all the components from atom to supercluster, and simultaneously scales their distances and sizes [1].

The difficulty is overcome by examining the Universe by universes, thus at different realms. We start at Planck size object and zoom out to the observable Universe, throughout the superimposed worlds. In each step of the way, we use the room we are in to physically represent a realm of particular universe. Looking for smart materials that can represent the objects within each realm, all to scale, a common 1-D profile across all the universes could be built up, towards a scale model of the Universe as a whole, like the particle in a box model in quantum mechanics.

The object in a box model of the World is under the rule of second order differential equation: either Schrodinger's, or Laplace's or else Helmholtz's ones. Separation of variables leads to a new (phantom) variable.

As to the Universe as a whole, this is a plural superimposition of underlying universes, in succession. For instance, the cosmos, the layered earth, a rock, an atom ..., all of them are homogeneous on some scale.

To understand more, a dynamic analysis of these systems is needed, this would show how energy flows across both spatial scales and time. Fortunately, this type of analysis is already performed for the geophysical distant soundings over a horizontally stratified earth. The multiscale concepts used in geophysical scattering theory, especially in DC field, have a tread deserving a sweeping statement, however.

1.2. Self-Entanglement, Disentaglement and Complexity

Following the gravity force, the masses are structured so is the energy. The ob-

servable universe together with the observer, both on sufficiently large scale, succeeds in their self-entanglement and paradoxical inconsistency. For consistency, the observable universe and the observer have to be on different scale/size provided the cosmological principle is preserved as an approximation in a limit. The point is the *universal principle* itself.

Consequently, the deduction is: "All constituent at hand (size and scale, homogeneity and heterogeneity, and possibly others) are self-entangled components". Our proposal for the disentaglement is *superimposition out of complexity.*

Complex systems are based on relationships, and their properties of self-organization, interconnections and evolution. They are emergent phenomena in the sense that they are the spontaneous outcome ot the interactions among the many constituent units with unexpected properties and regularities. Hence they are like the designed smart materials that have one or more properties that can be significantly changed in a controlled fashion by external stimuli, such as electric or magnetic fields, or light.

2. On Superimposition through Complexity

DC geoelectric theory goes into details of anisotropy and homogeneity throughout pseudo-, macro- and micro-anisotropy.

Background. Energy propagating throughout a medium undergoes multiple backward and forward reflections at the inhomogeneities. Resulting total travel time is greater when compared to propagation in homogeneous medium. In a sense, instead of inhomogeneities, one may alternatively and equivalently assume homogeneous medium and the space expanding. In electrical soundings over horizontally stratified earth the equivalence of differently layered media is known since early days of the method [2] [3]. The effect of resistivity sounding at the surface of a massive layering is the same as that for a finely layered structure provided that depth scale is stretched at each point by the local value of the so-called pseudoanisotropy coefficient and, in addition, the resistivity is specified as a kind of average resistivity [4] [5]. This effect of equivalence has been confirmed in a multitude of geophysical cases (see also the sub-section 2.2. Superimposing Scales below).

In geoelectric prospecting over horizontal layering it is up to standard to take this effect into account. Its exposition is a firm subject of geoelectrical monographs, and textbooks [6].

Rationale. In geophysical investigation of horizontally stratified earth the inhomogeneous media are studied under different scales. There are at least two scales involved: 1) the scale of inhomogeneities (microscale), 2) less detailed scale (macroscale) related with the size of a region under investigation.

Horizontal stratification implies material property (proper impedance) varying in one particular direction. It is a rough and frequent approximation in many geophysical cases. A possible generalization is the spherical stratification

under cosmological principle or else a box model of stratification considered as a one-dimensional system. In perpendicular directions the proper impedance being constant, this aspect of directional nonuniformity finds its expression in geophysical notion of pseudoanisotropy.

Of particular interest is a class of finely layered media exhibiting a repetitive or cyclic structure (proper impedance evolving between high and low values). Following geophysical theory, such pseudoanisotropic media are reparametrized under cumulative transformation, to get a massive layering. The rationale for use of these transformations is based on the knowledge that for cyclic media the transformed impedance is specified as pseudoimpedance (kind of mean impedance), and the scale is stretched by an overall value of the so-called pseudoanisotropy coefficient.

For a given cyclic pseudoanisotropic medium there exists a homogeneous isotropic medium that behaves, in the limit, exactly as does the given medium under the same excitation. This is to mean that a medium, which is viewed in the microscale as cyclic pseudoanisotropic, appears as a homogeneous medium when viewed in a macroscale. This is accompanied by distance contraction.

Physical basis. Geophysical static theory of cyclic stratified media [5] [7] [8] is generalized or modified in this note in various aspects. In substance, the framework is completed by time domain, and the medium is considered to have a repetitive (cyclic) structure in all directions.

It is worth noting that the formulation developed for horizontally stratified (one dimensional) media is applicable to general situations when proper impedance vary in space (three dimensions). To this end the medium is assumed to be discretized in all directions, and the results, having no side effects and relative to a facultative direction, could be generalized to all the directions.

If medium viewed in a macroscale exhibits the pseudoimpedance and contraction coefficient which are both constant over a region of interest, it is said to be pseudohomogeneous. The rationale for studying such media is a multitude of geophysical observations transportable to 3-D space. The pseudohomogeneity in 3-D approach might be an inherent property of the media of physical interest, provided that the micro- and macro-scales are sufficiently different. This expectation is based on cumulative nature of the transformation involved as well as on isotropy postulated for largest regions.

Governing equation. To conceptualize the problem, the governing equation is taken in the form of scalar wave equation. For a time harmonic field U, we have

$$\rho\nabla\cdot\rho^{-1}\nabla U\left(r,t\right)+k^2U\left(r,t\right)=0 \tag{1}$$

when $U(r, t)$ can be either U_x, U_y, or U_z field component, and $k=\omega^*/v$.

The above is the Helmholtz wave equation for an inhomogeneous, isotropic, and source-free medium. In addition, proper impedance, $\rho(r)$, and wave velocity, $v(r)$, are both functions of position, $r=r\left(x,y,z\right)$.

Following classical theory, in a stock-still system there is no anomalous frequency, that is to say ω^* is the same as wave frequency ω ($\omega^*=\omega$). When Dopp-

ler shift, $\omega^* = \omega H$, is observed, we may define $v^* = v/H$, that is to say $k = \omega/v^*$. In this case v^* takes interpretation in terms of moving source and/or expanding medium. Alternative interpretation of anomalous frequency is just the point of this note.

Reparametrization. We consider stratified medium, locally (in microscale) materialized through proper impedance varying possibly in all directions [5] [8] [9] [10] but we are considering variations in only one direction, that is to say $\rho(r)$. Let a larger region of size W be investigated by an observer located at the origin, where the cumulative parameters are introduced:

$$T(r) = \int_0^w \rho(r)\mathrm{d}r \quad \text{and} \quad S(r) = \int_0^w \rho^{-1}(r)\mathrm{d}r, \quad w \in W. \tag{2}$$

These are used to define pseudoimpedance, and pseudodistance:

$$\rho^* = \sqrt{T/S} \quad \text{and} \quad r^* = \sqrt{T \cdot S} \tag{3}$$

as well as pseudoanisotropy coefficient

$$\Lambda = r^*/r, \quad \Lambda \geq 1. \tag{4}$$

The bound for Λ is known in mathematical geophysics [5]. For further use the contraction coefficient is introduced

$$\theta = \Lambda - 1, \quad \theta \geq 0. \tag{5}$$

These way the medium is reparametrized into pseudoimpedance varying in only one pseudodirection, $\rho^*(r^*)$.

Cyclic, and pseudohomogeneous medium. When proper impedance of a medium is varying between high and low values, in a direction r, such medium is said to be repetitious, or cyclic. The media, cyclic in all directions could be considered but we refer to 1D space as investigated in geophysical theory.

Typical distance between successive local extrema of impedance is of order denoted as Δr. Consider a medium which is cyclic in a microscale (typical distance Δr), and when

$$W/\Delta r \to \infty, \quad \Delta r > 0, \quad W < \infty. \tag{6}$$

For global seeing, in macroscale the space metrized as $\rho^*(r^*)$ is applied. The medium appearing in a macroscale is said to be isotropic and pseudohomogeneous if the resulting both pseudoimpedance and contraction coefficient reveal as directionless and constant over a macrospace. As known in geophysical prospecting, the locally alternating parameter exhibits globally the quasi-homogenity while distance is stretched by pseudoanisotropy coefficient, Λ.

$$\rho(r^*) \approx const., \quad \Lambda(r^*) \approx const. \tag{7}$$

2.1. Doppler-Like Effect

In conformity with scale relationship, Equation (4), the scale for homogeneous medium is stretched by a factor Λ when passing to pseudohomogeneous medium. The effect of contraction is well known in direct current resistivity sounding

over horizontally stratified earth [11] [12], where Λ is termed as pseudoanisotropy coefficient. For horizontally stratified media (proper impedance varying in z-direction only), the governing Equation (1) takes the form

$$\frac{\delta^2 U}{\delta x^2}+\frac{\delta^2 U}{\delta y^2}+\frac{\delta^2 U}{\delta z^{*2}}=0 \tag{8}$$

when asterix refers to alternative as to homogeneity of a medium. The options $\delta z^*=\delta z$ (inhomogeneous medium), or $\delta z^*=\Lambda\delta z$ (pseudohomogeneous medium) yield different depth of a layer. Eventually, but it is not the practice, the horizontal scales are to be contracted, yielding $\delta x^*=\delta x/\Lambda$, and $\delta y^*=\delta y/\Lambda$.

Doppler-likeness of this effect consists in the following. For 3-D pseudohomogeneous medium, we have

$$\delta x^*=\Lambda\delta x,\ \delta y^*=\Lambda\delta y,\ \delta z^*=\Lambda\delta z \tag{9}$$

and substitution $\omega^*=\Lambda\omega$ is possible in the governing Equation (1), then becoming

$$\frac{\delta^2 U}{\partial x^{*2}}+\frac{\delta^2 U}{\delta y^{*2}}+\frac{\delta^2 U}{\delta z^{*2}}+\frac{\omega^{*2}}{v^2}U=0,\ U=U\left(r^*,t\right),\ r^*=r^*\left(x^*,y^*,z^*\right) \tag{10}$$

Now anomalous wave frequency ω^* may take interpretation either in a fine scale of heterogeneities, Equation (1), or in a coarser scale of regional investigation, Equation (11). Thus contraction coefficient, θ, appears as a static counterpart of Doppler shift, as detailed further on.

Relative to the expansion, the governing equation could be read

$$\frac{\delta^2 U}{\partial x^2}+\frac{\delta^2 U}{\delta y^2}+\frac{\delta^2 U}{\delta z^2}+\frac{\omega}{v^{*2}}U=0,\ U=U\left(r,t\right),\ v^*=\Lambda v \tag{11}$$

2.2. Superimposing Scales

In DC geosounding, there is a stock-still layering and so is the varying frequency models. Suppose, with no *à priori* knowledge about homogenity, the measurements taken on earth surface indicates the depth H, or h for homogeneous, or heterogeneos layers, respectively. Thus, further examination (drilling) is performed, in practice. The final assignment is made depending on the ratio H/r. The resulting correction is attributed to different metric properties of homogeceous and heterogeneous layering. The effect is referred to as *superimposition of scales.* This way (by drilling), the homogenity-heterogenity self-entanglement becomes unraveled in the case.

What is a principal difference between superimposition and superposition methods like additive color, or substractive color methods, or else a moiré pattern? Physical manifestation of a superposition is frequently the interference whereas the superimposition consists in medium identification in a communication channel, used to convey information, or energy throughout. This could be the physical transmission media, or a multiplexed medium in a logical connection. Possibly, the Laplacian mirror window [13] should be more comprehensive

in answering the question.

3. Discussion: Expansion or Heterogeneities?

Equivalence, or analogy in mathematical description of physical phenomena in time, frequency, and space is well known [4]. Quite naturally, the Doppler shift can be due not only to movement of the source or expansion of space but also to greater travel time owed to inhomogeneities.

Introducing Equation (5) into (4) yields

$$r^* - r = \theta r \tag{12}$$

which in static systems is quantified by

distance correction = contraction coefficient · simple distance.

When the time is introduced to reach kinematical systems, the shift related to equation (11) is quantified by

emitted frequency – observed frequency = contraction coefficient · observed frequency

with

coeff. = (observed wavelength – emitted wanelength)/emitted wavelength.

Similarly, relative to the expanding universe, the expansion rate related to equation (12) is quantified by

receding velocity of a galaxy = Hubble constant · current distant to the galaxy.

Note that contraction coefficient is dimensionless quantity whereas Hubble constant is dimensioned in t^{-1}.

The energy propagating in inhomogeneous universe exhibits a shift which could be attributed not only to the expansion of space but alternatively to fluctuations in material properties (inhomogeneities). When nothing is known about kinematics of a system's structure, both causes might share in the effect.

An Example

Let us consider an example of 1D space divided between large segments, r_v, with void occupancy individualized with proper impedance ρ_v, and small segments, r_p, with particle occupancy individualized with proper impedance ρ_p. The large and small segments interleave and value of 10^{32} is assumed for the ratio r_v/r_p. In the 1D universe of such sparsely distributed particles, a very high impedance's contrast is to be assigned for contraction coefficient to match high absolute values (up to the Hubble's constant in the expanding universe).

On the other hand, when there is a number of scales, in hierarchical sequence, the effects of subsequent reparemetrizations are multiplied [5]. Let us take into investigation a mega-region of size much larger than macro-region W. Let the same relations are settled between mega- and macro-scales, as it was for macro- and micro-scales. The outcoming pseudoanisotropy coefficient is obtained as a product of coefficients graded by the size of corresponding subregions. Effective Doppler-like shift is increasing with the size of a region under investigation.

4. Conclusions

- The affirmative answer to the introductory question opens different static as well as kinematic possibilities, which challenge established theories of expanding universe and energizing big bang. First step in such prospects was made quite recently [14] putting geophysical theory and Hubble's law in parallel. Stock-still system—a void with sparsely distributed particles—stands up as a scenario for propagation of electromagnetic waves accompanied with Doppler-like effect along with a Hubble-like law.
- The distance contraction, as observed in electrical soundings over horizontally stratified earth (static system), is identified as a counterpart of Doppler shift in dynamical systems. An alternative answer to the question about an effective cause of the Doppler shift sounds the heterogeneities under superimposing scales.
- Otherwise, the theory is indicative for new technologies in energy transmitting materials or information (communication) channels: layering, material profile, vocal tract are to be adequately structured. The application of augmented or/and extended reality to support understanding of the cognitive processes was helpful in establishing a steady progress in the research of electrical impedance tomography (EIT), leading to important developments. "These developments have excited interest in practitioners and researchers from a broad range of disciplines, including mathematicians devoted to uniqueness proofs and inverse problems, physicists dealing with bioimpedance, electronic engineerers involved in developing and extending its applications, and clinicians wishing to take advantage of this powerful new imaging method" [15].
- At sub-atomic level there is the Raman spectroscopy dealing with the scattering of light with no its absorption [16]. The resulting Raman shift [17] provides a fingerprint to identify molecules and has a wide variety of applications in biology and medicine, and others [18]. This microscale effect has to be seen in parallel with the macroscale Doppler Effect.

Conflicts of Interest

The author declares no conflict of interests regarding the publication of this paper.

References

[1] Knisely, L. (2011) Size and Scale of the Unverse. http://wise.ssi.berkeley.edu/documents/ScaleRealmsUniverse.pdf

[2] Schlumberger, C., Schlumberger, M. and Leonardon, E.G. (1934) *Transactions of the AIME*, **110**, 159-182.

[3] Maillet, R. and Doll, H.G. (1932) Théorème relatif aux millieux electriquement anisotropes et ses applications à la prospection electrique *Ergänzung-Hefte für angewandte Geophysik*, III, I, Akademische Verlag, Leipzig, 101-124.

[4] Cohen, L. (1995) Time-Frequency Analysis. Prentice Hall, Englewood Cliffs.

[5] Maillet, R. (1947) *Geophysics*, **12**, 529-556. https://doi.org/10.1190/1.1437342

[6] Koefoed, O. (1979) Geosounding Principles, 1: Resistivity Sounding Measurements. Elsevier, Amsterdam.

[7] Szaraniec, E. (1976) *Geophysical Prospecting*, **24**, 528-548. https://doi.org/10.1111/j.1365-2478.1976.tb00953.x

[8] Szaraniec, E. (1982) *Geophysical Prospecting*, **30**, 127-137. https://doi.org/10.1111/j.1365-2478.1982.tb00418.x

[9] Orellana, E. (1963) *Geophysics*, **28**, 99-110. https://doi.org/10.1190/1.1439158

[10] Szaraniec, E. (1972) *Geophysical Prospecting*, **20**, 212-236. https://doi.org/10.1111/j.1365-2478.1972.tb00630.x

[11] Szaraniec, E. (2001) *Journal of Seismic Exploration*, **9**, 199-210.

[12] Szaraniec, E. (2002) *Journal of Seismic Exploration*, **10**, 341-352.

[13] Trott, M. (2017) How Laplace Would Hide a Goat: The New Science of Magic Window. https://blog.wolfram.com/author/michael-trott/

[14] Szaraniec, E. (2003) Doppler-Like Effect and Doubful Expansion of Universe. arXiv: astro-ph/0310023

[15] Holder, D.S. (Ed.) (2004) Electrical Impedance Tomography: Methods, History and Applications. CRC Press, Boca Raton. https://doi.org/10.1201/9781420034462

[16] Wikipedia, Raman Spectroscopy.

[17] Tivari, G. (2018) CV Raman, Raman Effect on Raman Spectroscopy and Raman Scattering. https://guaravtivari.org

[18] Aiyar, S.A. (2010) Raman Effect: Fingerprinting the Universe. Times of India Blog.

Journal of Modern Physics, 2019, 10, 371-401
http://www.scirp.org/journal/jmp
ISSN Online: 2153-120X
ISSN Print: 2153-1196

Generating Compatibility Conditions and General Relativity

J.-F. Pommaret

CERMICS, Ecole des Ponts Paris Tech, Paris, France
Email: jean-francois.pommaret@wanadoo.fr, pommaret@cermics.enpc.fr

How to cite this paper: Pommaret, J.-F. (2019) Generating Compatibility Conditions and General Relativity. *Journal of Modern Physics*, **10**, 371-401.
https://doi.org/10.4236/jmp.2019.103025

Received: December 14, 2018
Accepted: March 11, 2019
Published: March 14, 2019

Abstract

The search for the *generating compatibility conditions* (CC) of a given operator is a very recent problem met in general relativity in order to study the *Killing* operator for various standard useful metrics. Accordingly, this paper can be considered as a natural continuation of a previous paper recently published in JMP under the title *Minkowski, Schwarschild and Kerr metrics revisited*. In particular, we prove that the intrinsic link existing between the lack of *formal exactness* of an operator sequence on the jet level, the lack of *formal exactness* of its corresponding symbol sequence and the lack of *formal integrability* (FI) of the initial operator is of a purely homological nature as it is based on the *long exact connecting sequence* provided by the so-called *snake lemma* in homological algebra. It is therefore quite difficult to grasp it in general and even more difficult to use it on explicit examples. It does not seem that any one of the results presented in this paper is known as most of the other authors who studied the above problem of computing the total number of generating CC are confusing this number with the *degree of generality* introduced by A. Einstein in his 1930 letters to E. Cartan. One of the motivating examples that we provide is so striking that it is even difficult to imagine that such an example could exist. We hope this paper could be used as a source of testing examples for future applications of computer algebra in general relativity and, more generally, in mathematical physics.

Keywords

Formal Theory of Systems of Partial Differential Equations, Compatibility Conditions, Acyclicity, Formal Integrability, Involutivity, Differential Sequence, Janet Sequence, Spencer Sequence, General Relativity, Killing Systems

1. Introduction

If X is a manifold of dimension n with local coordinates $\left(x^1,\cdots,x^n\right)$, let us in-

troduce the tangent bundle $T=T(X)$ and the cotangent bundle $T^*=T^*(X)$, the q-symmetric tensor bundle S_qT^* and the bundle $\wedge^rT^*$ of r-forms. In General Relativity, there may be different solutions of Einstein equations in vacuum like the Minkowski, the Schwarzschild and the Kerr metrics for example. For fixing the notations and with more details, if $\omega\in S_2T^*$ is a nondegenerate metric, that is $det(\omega)\neq 0$, and if j_q denotes all the derivatives of an object up to order q, we may construct the Christoffel symbols γ through the Levi-Civita isomorphism $(\omega,\gamma)\simeq j_1(\omega)$ and, using the language of jet bundles, (ω,γ) is a section of $J_1(S_2T^*)$ that will be simply written $(\omega,\gamma)\in J_1(S_2T^*)$. Then we can introduce the well-known Riemann tensor $\rho=(\rho^k_{l,ij})\in\wedge^2T^*\otimes T^*\otimes T$ with $\rho_{kl,ij}+\rho_{lk,ij}=0$ after lowering the upper index by means of ω *and* $\delta\rho=0$ where $\delta:\wedge^2T^*\otimes T^*\otimes T\to\wedge^3T^*\otimes T$ is the Spencer δ-map. Introducing the Ricci tensor $\rho_{ij}=\rho^r_{i,rj}=\rho_{ji}$ or the Einstein tensor $\epsilon_{ij}=\rho_{ij}-\frac{1}{2}\omega_{ij}\omega^{rs}\rho_{rs}$, the 10 non-linear Einstein equations are described by $\epsilon_{ij}=0$ or, equivalently, by $\rho_{ij}=0$ when $n=4$.

Now, if $\mathcal{E}$ is a fibered manifold over X with fiber dimension m and local coordinates (x^i,y^k) with $i=1,\cdots,n$ and $k=1,\cdots,m$, we may introduce the tangent bundle $T(\mathcal{E})$ over $\mathcal{E}$ with local coordinates (x,y,u,v) and the *vertical bundle* $V(\mathcal{E})$ with local coordinates $(x,y,u=0,v)=(x,y,v)$ which are both vector bundles over $\mathcal{E}$. We shall denote by the capital letters $\Omega\in S_2T^*,\Gamma\in S_2T^*\otimes T,R\in\wedge^2T^*\otimes T^*\otimes T$, the respective *linearizations* of ω,γ,ρ which are sections of the respective vertical bundles. Introducing the *Lie* derivative $\mathcal{L}$ of geometric objects, it is therefore possible to introduce the corresponding first order *Killing* operator $\mathcal{D}:T\to\Omega\in S_2T^*:\xi\to\mathcal{L}(\xi)\omega$, the first order *Christoffel* operator $\Omega\to\Gamma\in S_2T^*\otimes T$ in such a way that $Christoffel\circ Killing:T\to\Gamma\in S_2T^*\otimes T:\xi\to\mathcal{L}(\xi)\gamma$ and the second order *Riemann* operator $\Omega\to R\in\wedge^2T^*\otimes T^*\otimes T$ in such a way that $Riemann\circ Killing:T\to R\in\wedge^2T^*\otimes T^*\otimes T:\xi\to\mathcal{L}(\xi)\rho$ both with its *contraction* $\Omega\to S_2T^*$ called *Ricci* operator. For example, it is known that $2\omega_{rk}\gamma^k_{ij}=(\partial_i\omega_{rj}+\partial_j\omega_{ir}-\partial_r\omega_{ij})$ that we shall write simply, using formal notations, $2\omega\gamma=(\partial\omega+\partial\omega-\partial\omega)$ and thus $2\omega\Gamma+2\gamma\Omega=(d\Omega+d\Omega-d\Omega)$. We have proved in ([1] [2] [3] [4]) that the so-called gravitational waves equations are nothing else than $ad(Ricci)$ by introducing the *formal adjoint* operator. It is important to notice that the *Einstein* operator $\Omega\to E_{ij}=R_{ij}-\frac{1}{2}\omega_{ij}\omega^{rs}R_{rs}$ is self-adjoint with 6 terms though the *Ricci* operator is *not* with only 4 terms. Recently, many physicists (See [5] [6] [7] [8] [9]) have tried to construct the *compatibility conditions* (CC) of the *Killing* operator for various types of background metrics, in particular the three ones already quoted, namely an operator $\mathcal{D}_1:S_2T^*\to F_1$ such that $\mathcal{D}_1\Omega=0$ generates the CC of $\mathcal{D}\xi=\Omega$. We have proved in the above references the following crucial results:

- These CC may contain a certain number of second and third order CC. It is therefore crucial in actual practice to select the successive generating CC of

order $1,2,3,\cdots$ till we stop because of noetherian arguments ([10]).

- These CC only depend on the Lie algebra structure (dimension of the solution space and commutation relations) of the corresponding Killing operator, which, even though it is finite dimensional with dimension $\leq n(n+1)/2$ that is 10 obtained for the Minkowski metric, may have dimension 4 for the Schwarzschild metric and dimension 2 for the Kerr metric.
- The only two canonical sequences that can be constructed from an operator or a system, namely the Janet and Spencer sequences, are structurally quite different. Indeed, the *Janet bundles* $F_0,\cdots,F_n$ appearing in the Janet sequence are concerned wit geometric objects like ω,γ,ρ, while the *Spencer bundles* $C_0,\cdots,C_n$ are far from being related with geometric objects, the simplest example being $C_0=R_q\subseteq J_q(E)$. In the case of Lie equations considered, the central concept is not the *system* but rather the *group* as it can be seen at once from the construction of the *Vessiot structure equations* ([3] [11] [12] [13]).

The authors who have studied these questions had in mind that the total number of generating CC could be considered as a kind of "*differential transcendence degree*", also called "*degree of generality*" by A. Einstein in his letters to E. Cartan of 1930 on absolute parallelism ([14]), the modern definition being that of the "*differential rank*" ([10] [12] [15] [16]). We must say that Cartan, being unable to explain to Einstein his theory of exterior systems, just copied the work of Janet published in 1920 ([17]) in his letters to Einstein, published later on as the *only* paper he wrote on the PD approach, but without ever quoting Janet who suffered a lot from this behavior and had to turn to mechanics.

Such a result will be obtained in the framework of differential modules as its explanation in the framework of differential systems is much more delicate and technical ([10] [12] [18]).

First of all, with our previous assumptions, $D=K[d]$ is a noetherian domain and we can restrict our study to finitely generated differential modules which are therefore finitely presented (See [14] for more details). Let thus M be defined by a finite free presentation giving rise to the long exact sequence:

$$0\to L\to D^p\xrightarrow{\mathcal{D}}D^m\xrightarrow{p}M\to 0$$

where the differential operator $\mathcal{D}$ is acting on the right by composition with action law $(P,\mathcal{D})\to P\circ\mathcal{D},\forall P\in D$, p is the canonical residual projection and $L=ker(\mathcal{D})\subset D^p$. The image $im(\mathcal{D})\subset D^m$ is called the *differential module of equations* and is thus finitely generated because D is a noetherian differential domain.

DEFINITION 1.1: The *differential rank* $rk_D(M)$ over D of a differential module M is the differential rank over D of the maximum free differential submodule F of M and we have the short exact sequence $0\to F\to M\to T\to 0$ where $T=M/F$ is a torsion module over D. In particular, if $F\simeq D^r$, then $rk_D(M)=r$.

The following useful proposition proves the *additivity property* of the differential rank and is used in the next two corollaries ([3] [10] [12]):

PROPOSITION 1.2: If we have a short exact sequence $0 \to M' \xrightarrow{f} M \xrightarrow{g} M'' \to 0$ of differential modules, then $rk_D(M) = rk_D(M') + rk_D(M'')$.

COROLLARY 1.3: If $\mathcal{D}$ is a linear partial differential operator with coefficients in a differential field K and $ad(\mathcal{D})$ is the *formal adjoint* that can be obtained formally or through an integration by parts, then $rk_D(\mathcal{D}) = rk_D(ad(\mathcal{D}))$.

COROLLARY 1.4: (*Euler-Poincaré characteristic*) For *any* finite free differential resolution of a differential module M, then $rk_D(M)$ is equal to the alternate sum $\chi_D(M)$ of differential ranks of the free differential modules of the resolution.

We obtain therefore $rk_D(L) - p + m - rk_D(M) = 0$ and it follows from noetherian arguments that the differential module $L \subset D^p$ *is finitely generated but not free in general* and we may look for a minimum number of generators which may be differentially dependent in general as we shall see in the next examples. It thus remains to provide examples of such computations showing that these two numbers are not related and must therefore be found totally independently in general, apart from the very exceptional situation met when there is only a single generating CC.

In actual practice, working in the system framework, starting with a system $R_q \subset J_q(E)$ of order q on E and introducing the *canonical projection* $\Phi : J_q(E) \to F_0 = J_q(E)/R_q$, we shall construct for each $r \geq 0$ a family of FI systems $B_r = im(\rho_r(\Phi)) \subseteq J_r(F_0)$ such that $B_{r+1} \subseteq \rho_1(B_r) = J_1(B_r) \cup J_{r+1}(F_0) \subset J_1(J_r(F_0))$ projects onto B_r, that is B_{r+1} is defined by more generating PD equations than the ones defining B_r both with its prolongations, and start to get equality when r is large enough in the projective limit $B_\infty \to \cdots \to B_{r+1} \to B_r \to \cdots \to B_1 \to F_0 \to 0$. *The striking result is that there may be gaps in the procedure*, that is we shall even provide a tricky example where one can have a single generating CC of order 3, then no *new* generating CC of order 4 *and* 5, but *suddenly* a new generating CC of order 6 ending the procedure. We do not believe that such situations were even known to exist.

2. Motivating Examples

We provide below three examples, pointing out that it is quite difficult to exhibit such examples.

EXAMPLE 2.1: With $n = 3, m = dim(E) = 2, dim(F_0) = 5$ and $K = \mathbb{Q}$ while keeping an upper index for any unknown, let us consider the following system $R_1 \subset J_1(E)$ with $dim(R_1) = 3$ because $par_1 = \{\xi^1, \xi^2, \xi_1^2\}$ and corresponding Janet tabular:

$$\begin{cases} \Phi^5 \equiv \xi_3^2 = 0 \\ \Phi^4 \equiv \xi_3^1 = 0 \\ \Phi^3 \equiv \xi_2^2 = 0 \\ \Phi^2 \equiv \xi_2^1 + \xi_1^2 = 0 \\ \Phi^1 \equiv \xi_1^1 = 0 \end{cases} \qquad \begin{array}{|ccc|} \hline 1 & 2 & 3 \\ 1 & 2 & 3 \\ 1 & 2 & \bullet \\ 1 & 2 & \bullet \\ 1 & \times & \bullet \\ \hline \end{array}$$

It is easy to check that all the second order jets vanish and that the general solution $\left\{\xi^1 = ax^2 + b, \xi^2 = cx^1 + d \mid a + c = 0\right\}$ depends on 3 arbitrary constants. As the non-multiplicative variable written with the sign $\times$cannot be used, the symbol g_1 is not involutive because it is finite type with $g_2 = 0$. This system is trivially FI because it is made by homogeneous PD equations. We have the following commutative diagrams:

$$\begin{array}{ccccccccc}
 & & & & 0 & & 0 & & 0 \\
 & & & & \downarrow & & \downarrow & & \downarrow \\
 & & 0 & \to & S_3T^*\otimes E & \to & S_2T^*\otimes F_0 & \to & h_2 & \to 0 \\
 & & \downarrow & & \downarrow & & \downarrow & & \downarrow & \\
0 & \to & R_3 & \to & J_3(E) & \to & J_2(F_0) & \to & Q_2 & \to 0 \\
 & & \downarrow & & \downarrow \pi_2^3 & & \downarrow \pi_1^2 & & \downarrow & \\
0 & \to & R_2 & \to & J_2(E) & \to & J_1(F_0) & \to & Q_1 & \to 0 \\
 & & \downarrow & & \downarrow & & \downarrow & & \downarrow & \\
 & & 0 & & 0 & & 0 & & 0 &
\end{array}$$

$$\begin{array}{ccccccccc}
 & & & & 0 & & 0 & & 0 \\
 & & & & \downarrow & & \downarrow & & \downarrow & \\
 & & 0 & \to & 20 & \to & 30 & \to & 10 & \to 0 \\
 & & \downarrow & & \downarrow & & \downarrow & & \downarrow & \\
0 & \to & 3 & \to & 40 & \to & 50 & \to & 13 & \to 0 \\
 & & \downarrow & & \downarrow \pi_2^3 & & \downarrow \pi_1^2 & & \downarrow & \\
0 & \to & 3 & \to & 20 & \to & 20 & \to & 3 & \to 0 \\
 & & \downarrow & & \downarrow & & \downarrow & & \downarrow & \\
 & & 0 & & 0 & & 0 & & 0 &
\end{array}$$

$$\begin{array}{ccccccccc}
 & & & & 0 & & 0 & & \\
 & & & & \downarrow & & \downarrow & & \\
0 & \to & S_3T^*\otimes E & \to & S_2T^*\otimes F_0 & \to & h_2 & \to 0 \\
 & & \downarrow \delta & & \downarrow \delta & & \downarrow & \\
0 & \to & T^*\otimes S_2T^*\otimes E & \to & T^*\otimes T^*\otimes F_0 & \to & T^*\otimes h_1 & \to 0 \\
 & & \downarrow \delta & & \downarrow \delta & & \downarrow & \\
0 \to \wedge^2T^*\otimes g_1 & \to & \wedge^2T^*\otimes T^*\otimes E & \to & \wedge^2T^*\otimes F_0 & \to & 0 & \\
\downarrow \delta & & \downarrow \delta & & \downarrow & & & \\
0 \to \wedge^3T^*\otimes E & = & \wedge^3T^*\otimes E & \to & 0 & & & \\
\downarrow & & \downarrow & & & & & \\
0 & & 0 & & & & &
\end{array}$$

$$\begin{array}{ccccccccc}
 & & & & 0 & & 0 & & \\
 & & & & \downarrow & & \downarrow & & \\
 & & 0 & \to & 20 & \to & 30 & \to & 10 & \to 0 \\
 & & & & \downarrow \delta & & \downarrow \delta & & \downarrow & \\
 & & 0 & \to & 36 & \to & 45 & \to & 9 & \to 0 \\
 & & & & \downarrow \delta & & \downarrow \delta & & \downarrow & \\
0 & \to & 3 & \to & 18 & \to & 15 & \to & 0 & \\
 & & \downarrow \delta & & \downarrow \delta & & \downarrow & & & \\
0 & \to & 2 & = & 2 & \to & 0 & & & \\
 & & \downarrow & & \downarrow & & & & & \\
 & & 0 & & 0 & & & & &
\end{array}$$

The next result points out the importance of the Spencer δ-cohomology. Indeed, we shall prove that the last symbol diagram is commutative and exact. In particular, the lower left map δ is surjective and thus the upper right induced map $h_2 \to T^* \otimes Q_1$ is also surjective while these two maps have isomorphic kernels.

For this, we notice that the 3 components of $\wedge^2 T^* \otimes g_1$ are $\left\{v^2_{1,12}, v^2_{1,13}, v^2_{1,23}\right\}$ and the map δ is described by the two linear equations:

$$w^1_{123} \equiv v^1_{1,23} + v^1_{2,31} + v^1_{3,12} = v^2_{1,13} = 0, \quad w^2_{123} \equiv v^2_{1,23} + v^2_{2,31} + v^2_{3,12} = v^2_{1,23} = 0$$

that is to say by two linearly independent equations. Accordingly, in the left column we have:

$$dim\left(H^2\left(g_1\right)\right) = dim\left(Z^2\left(g_1\right)\right) = dim\left(ker\left(\delta\right)\right) = 1$$

An unusual snake-type diagonal chase left to the reader as an exercise proves that the induced map $h_2 \to T^* \otimes Q_1$ is surjective with a kernel isomorphic to $H^2\left(g_1\right)$. This is indeed a *crucial result* because it also proves that the additional CC has only to do with the single second order component of the Riemann tensor in dimension 2, a striking result that could not even be imagined by standard methods. Moreover, we know that if a system $R_q \subset J_q\left(E\right)$ is FI, for example when it is homogeneous like in this case, and its symbol $g_q \subset S_q T^* \otimes E$ is such that s is the smallest integer such that g_{q+s} becomes 2-acyclic (or involutive), then the generating CC are of order at most $s+1$ ([3] [10] [12]).

Collecting the above results, we find the 3 *first order* differentially independent generating CC coming from the Janet tabular and the *additional* single *second order* generating CC describing the 2-dimensional *Riemann* operator, that is the linearized Riemann tensor in the space $\left(x^1, x^2\right)$:

$$\begin{cases} \Psi^4 \equiv d_{22}\Phi^1 + d_{11}\Phi^3 - d_{12}\Phi^2 = 0 \\ \Psi^3 \equiv d_3\Phi^3 - d_2\Phi^5 = 0 \\ \Psi^2 \equiv d_3\Phi^2 - d_2\Phi^4 - d_1\Phi^5 = 0 \\ \Psi^1 \equiv d_3\Phi^1 - d_1\Phi^4 = 0 \end{cases}$$

An elementary computation provides the second order CC:

$$d_{22}\Psi^1 + d_{11}\Psi^3 - d_{12}\Psi^2 - d_3\Psi^4 = 0$$

The corresponding differential sequence written with differential modules over the ring $D = K\left[d_1, d_2, d_3\right] = K\left[d\right]$ is:

$$0 \to D \xrightarrow[2]{} D^4 \xrightarrow[2]{} D^5 \xrightarrow[1]{} D^2 \xrightarrow{p} M \to 0$$

where p is the canonical (residual) projection. We check indeed that $1-4+5-2=0$ but this sequence is quite far from being even strictly exact. Of course, as R_2 is involutive, we may set $C_r = \wedge^r T^* \otimes R_2$ and obtain the corresponding canonical second Spencer sequence which is induced by the Spencer operator:

$$0 \to \Theta \xrightarrow{j_2} C_0 \xrightarrow{D_1} C_1 \xrightarrow{D_2} C_2 \xrightarrow{D_3} C_3 \to 0$$

with dimensions:

$$0 \to \Theta \xrightarrow{j_2} 3 \xrightarrow[1]{D_1} 9 \xrightarrow[1]{D_2} 9 \xrightarrow[1]{D_3} 3 \to 0$$

Proceeding inductively as we did for finding the second order CC, we may obtain by combinatorics the following formally exact sequence:

$$0 \to \Theta \to 2 \xrightarrow[1]{} 5 \xrightarrow[2]{} 13 \xrightarrow[1]{} 19 \xrightarrow[1]{} 12 \xrightarrow[1]{} 3 \to 0$$

with Euler-Poincaré characteristic $2-5+13-19+12-3=0$ but, as before, there is a matrix 260×280 at least and we doubt about the use of computer algebra, even on such an elementary example. With $F_0 = J_1(E)/R_1$, the starting long exact sequence used as a middle row of the first diagram with dimensions:

$$0 \to 3 \to 40 \to 50 \to 13 \to 0$$

and we have $13 = (3+3\times 3)+1$, that is three generating first order CC which are differentially independent, plus their 9 prolongations, plus one second order CC which is nevertheless *not* differentially independent. Hence we have a total number of $3+1=4$ generating CC but this number has nothing to do with any differential transcendence degree because Ψ^4 is differentially algebraic over $\{\Psi^1, \Psi^2, \Psi^3\}$.

We finally compute the corresponding (canonical) Janet sequence by quotient. For this, we must use the trivial second Spencer sequence:

$$0 \to E \xrightarrow{j_2} C_0(E) \xrightarrow{D_1} C_1(E) \xrightarrow{D_2} C_2(E) \xrightarrow{D_3} C_3(E) \to 0$$

namely:

$$0 \to 2 \xrightarrow[2]{} 20 \xrightarrow[1]{} 40 \xrightarrow[1]{} 30 \xrightarrow[1]{} 8 \to 0$$

with $2-20+40-30+8=0$. The (canonical) Janet sequence is thus:

$$0 \to \Theta \to E \xrightarrow[2]{} F_0 \xrightarrow[1]{} F_1 \xrightarrow[1]{} F_2 \xrightarrow[1]{} F_3 \to 0$$

with now $F_0 = J_2(E)/R_2$ and $F_r = C_r(E)/C_r$, $\forall r = 0,1,2,3$ and dimensions:

$$0 \to \Theta \to 2 \xrightarrow[2]{} 17 \xrightarrow[1]{} 31 \xrightarrow[1]{} 21 \xrightarrow[1]{} 5 \to 0$$

so that we have again $2-17+31-21+5=0$ in a coherent way with the fact that $rk_D(M)=0$.

EXAMPLE 2.2: With $n=3, m=1, q=2$ and $K=\mathbb{Q}(x^1,x^2,x^3)=\mathbb{Q}(x)$, let us consider the following linear inhomogeneous system:

$$\begin{aligned} y_{33} - x^2 y_1 &= v, \\ y_{12} &= u \end{aligned}$$

- *Step* 1: The symbol g_2 is defined by $v_{33}=0, v_{12}=0$ may not be involutive *or* the coordinate system may not be δ-regular. However, changing linearly the local coordinates with $x^1 \to x^1, x^2 \to x^2 + x^1, x^3 \to x^3$, we obtain the Janet tabular for g_2:

$$\begin{cases} v_{33} = 0 \\ v_{22} + v_{12} = 0 \end{cases} \qquad \begin{array}{|ccc|} \hline 1 & 2 & 3 \\ 1 & 2 & \bullet \\ \hline \end{array}$$

and thus the Janet tabular for g_3:

$$\left\{\begin{array}{ll} v_{333}=0 & \boxed{\begin{array}{ccc}1&2&3\end{array}}\\ v_{233}=0 & \begin{array}{ccc}1&2&\bullet\end{array}\\ v_{223}+v_{123}=0 & \begin{array}{ccc}1&2&\bullet\end{array}\\ v_{222}+v_{122}=0 & \begin{array}{ccc}1&2&\bullet\end{array}\\ v_{133}=0 & \begin{array}{ccc}1&\bullet&\bullet\end{array}\\ v_{122}+v_{112}=0 & \begin{array}{ccc}1&\bullet&\bullet\end{array}\end{array}\right.$$

We let the reader check as an exercise that g_2 is not 2-acyclic by counting the dimensions in the long sequence:

$$0\to g_4\xrightarrow{\delta}T^*\otimes g_3\xrightarrow{\delta}\wedge^2T^*\otimes g_2\xrightarrow{\delta}\wedge^3T^*\otimes T^*$$

and that g_3 is involutive, thus 2-acyclic, with characters $(0,0,4)$. It follows that $dim(g_2)=6-2=4$, $dim(g_3)=0+0+4=4$, $dim(g_4)=4,\cdots$. We obtain from the main theorem $\rho_r\left(R_2^{(1)}\right)=R_{2+r}^{(1)}$. It is easy to check that $R_2^{(1)}=R_2$ with $dim(R_2)=8$, $dim(R_3)=8+4=12$, $dim(R_4)=11+4=15$, $dim(R_5)=56-39=13+4=17$ but things are changing after that. As such a property is intrinsic, coming back to the original system of coordinates, we have after one more prolongation:

$$\left\{\begin{array}{l} y_{1233}=u_{33}\\ -y_{1233}+x^2y_{112}+y_{11}=-v_{12}\\ -x^2y_{112}=-x^2u_1\end{array}\right.$$

and thus $y_{11}=u_{33}-v_{12}-x^2u_1$. We may thus consider the new second order system $R_2'=R_2^{(2)}\subset R_2$ with a strict inclusion and $dim\left(R_2^{(2)}\right)=7$:

$$y_{33}-x^2y_1=v,\ y_{12}=u,\ y_{11}=w,\ w=u_{33}-v_{12}-x^2u_1$$

We may start again with R_2' and study its symbol g_2' defined by the 3 linear equations with the following Janet tabular obtained after doing the same change of local coordinates as before:

$$\left\{\begin{array}{ll} v_{33}=0 & \boxed{\begin{array}{ccc}1&2&3\end{array}}\\ v_{22}+v_{12}=0 & \begin{array}{ccc}1&2&\bullet\end{array}\\ v_{12}+v_{11}=0 & \begin{array}{ccc}1&\bullet&\bullet\end{array}\end{array}\right.$$

This symbol is neither 2-acyclic nor involutive but its prolongation g_3', defined by the 8 equations:

$$\left\{\begin{array}{ll} v_{333}=0 & \boxed{\begin{array}{ccc}1&2&3\end{array}}\\ v_{233}=0 & \begin{array}{ccc}1&2&\bullet\end{array}\\ v_{223}-v_{113}=0 & \begin{array}{ccc}1&2&\bullet\end{array}\\ v_{222}+v_{111}=0 & \begin{array}{ccc}1&2&\bullet\end{array}\\ v_{133}=0 & \begin{array}{ccc}1&\bullet&\bullet\end{array}\\ v_{123}+v_{113}=0 & \begin{array}{ccc}1&\bullet&\bullet\end{array}\\ v_{122}-v_{111}=0 & \begin{array}{ccc}1&\bullet&\bullet\end{array}\\ v_{112}+v_{111}=0 & \begin{array}{ccc}1&\bullet&\bullet\end{array}\end{array}\right.$$

is involutive with characters $(0,0,2)$ and we may consider again the system:

$$\begin{cases} y_{33} - x^2 y_1 = v \\ y_{12} = u \\ y_{11} = w = u_{33} - v_{12} - x^2 u_1 \end{cases}$$

Instead of doing the same change of variables, writing out the system R_3' and study its formal inegrability with corresponding $9+11=20$ CC for (u,v,w), an elementary but tedious computation, we shall use a trick, knowing in advance that the generating CC *must* be of order $1+1=2$ because g_2' had to get one prolongation in order to become involutive and thus 2-acyclic.

- *Step* 2: It thus remains to find out the CC for (u,v) in the initial inhomogeneous system. As we have used two prolongations in order to exhibit R_2', we have second order formal derivatives of u and v in the right members. Now, from the above argument, we have second order CC for the new right members and could hope therefore for a fourth order generating CC. The trick is to use the three different brackets of operators that can be obtained. We have in a formal way:

$$\begin{aligned} \left[d_{33} - x^2 d_1, d_{12}\right] y &= y_{1233} - x^2 y_{112} - y_{1233} + x^2 y_{112} + y_{11} \\ &= y_{11} \\ &= u_{33} - x^2 u_1 - v_{12} \end{aligned}$$

$$\left[d_2, d_{11}\right] y = 0 = d_2\left(d_{11} y\right) - d_1\left(d_{12} y\right) = \left(u_{233} - v_{122} - x^2 u_{12} - u_1\right) - u_1$$

brings the *third order* CC:

$$A \equiv u_{233} - v_{122} - x^2 u_{12} - 2u_1 = 0$$

$$\begin{aligned} \left[d_{33} - x^2 d_1, d_{11}\right] y &= y_{1133} - x^2 y_{111} - y_{1133} + x^2 y_{111} \\ &= 0 \\ &= \left(d_{33} - x^2 d_1\right) w - v_{11} \\ &= u_{3333} - v_{1233} - 2x^2 u_{133} + x^2 v_{112} - v_{11} + \left(x^2\right)^2 u_{11} \end{aligned}$$

brings the *fourth order* CC:

$$B \equiv u_{3333} - v_{1233} - 2x^2 u_{133} + x^2 v_{112} - v_{11} + \left(x^2\right)^2 u_{11} = 0$$

We have indeed the identity $A_{33} - x^2 A_1 - B_2 = 0$ and thus (A,B) are differentially dependent, that is B is a new generating fourth order CC which is not a consequence of the prolongations of A. Again, the total number of generating CC, that is $1+1=2$, has nothing to do with the differential transcendence degree of the CC differential module which is $dim(F_0) - dim(E) = 2-1=1$.

EXAMLE 2.3: With the same $n=3, m=1, q=2$ and $K = \mathbb{Q}\left(x^1, x^2, x^3\right) = \mathbb{Q}(x)$, we now prove that a slight change of the equations may provide quite important changes in the number and order of the CC. Such an example is the only one that we could have found in more than 40 years of computing CC in mathematics and applications. For this, let us consider the new system:

$$y_{33} - x^2 y_1 = v,\ y_{22} = u$$

Before starting, we first notice that it is a prioiri not evident to discover that $R=R_\infty$ is a finite dimensional vector space over K with $dim_K(R)=6$. However such a result can be obtained by direct integration (Compare to the Janet example treated in the introduction of [12]).

- *Step* 1: The symbol g_2 is defined by $v_{33}=0, v_{22}=0$ may not be involutive *or* the coordinate system may not be δ-regular. However, we obtain the Janet tabular for g_2:

$$\begin{cases} v_{33}=0 \\ v_{22}=0 \end{cases} \begin{bmatrix} 1 & 2 & 3 \\ 1 & 2 & \bullet \end{bmatrix}$$

and thus the Janet tabular for g_3:

$$\begin{cases} v_{333}=0 \\ v_{233}=0 \\ v_{223}=0 \\ v_{222}=0 \\ v_{133}=0 \\ v_{122}=0 \end{cases} \begin{bmatrix} 1 & 2 & 3 \\ 1 & 2 & \bullet \\ 1 & 2 & \bullet \\ 1 & 2 & \bullet \\ 1 & \bullet & \bullet \\ 1 & \bullet & \bullet \end{bmatrix}$$

We let the reader check as an exercise that g_2 is not 2-acyclic by counting the dimensions in the long sequence:

$$0 \to g_4 \xrightarrow{\delta} T^* \otimes g_3 \xrightarrow{\delta} \wedge^2 T^* \otimes g_2 \xrightarrow{\delta} \wedge^3 T^* \otimes T^*$$

and that g_3 is involutive, thus 2-acyclic, with characters $(0,0,4)$ as in the previous example. It follows that $dim(g_2)=6-2=4$, $dim(g_3)=0+0+4=4$, $dim(g_4)=4,\cdots$. We obtain from the main theorem $\rho_r\left(R_2^{(1)}\right)=R_{2+r}^{(1)}$. It is easy to chek that $R_2^{(1)}=R_2$ with $dim(R_2)=8$, $dim(R_3)=8+4=12$, $dim(R_4)=11+4=15$, $dim(R_5)=56-39=13+4=17$, $\cdots$. We have after two prolongation:

$$\begin{cases} y_{2233}=u_{33} \\ -y_{2233}+x^2y_{122}+2y_{12}=-v_{22} \\ -x^2y_{122}=-x^2u_1 \end{cases}$$

and thus $2y_{12}=u_{33}-v_{22}-x^2u_1$. We may thus consider the new second order system $R_2'=R_2^{(2)}\subset R_2$ with a strict inclusion and $dim(R_2')=7$:

$$y_{33}-x^2y_1=v,\ y_{22}=u,\ y_{12}=w,\ 2w=u_{33}-v_{22}-x^2u_1$$

We may start again with R_2' and study its symbol g_2' defined by the 3 linear equations with the following Janet tabular obtained after doing the same change of local coordinates as before:

$$\begin{cases} v_{33}=0 \\ v_{22}=0 \\ v_{12}=0 \end{cases} \begin{bmatrix} 1 & 2 & 3 \\ 1 & 2 & \bullet \\ 1 & \bullet & \bullet \end{bmatrix}$$

This symbol is not involutive but its prolongation g_3', defined by the 8 equations:

$$\begin{cases} v_{333}=0 \\ v_{233}=0 \\ v_{223}=0 \\ v_{222}=0 \\ v_{133}=0 \\ v_{123}=0 \\ v_{122}=0 \\ v_{112}=0 \end{cases} \begin{bmatrix} 1 & 2 & 3 \\ 1 & 2 & \bullet \\ 1 & 2 & \bullet \\ 1 & 2 & \bullet \\ 1 & \bullet & \bullet \\ 1 & \bullet & \bullet \\ 1 & \bullet & \bullet \\ 1 & \bullet & \bullet \end{bmatrix}$$

is involutive with characters $(0,0,2)$ and we may consider again the system:

$$\begin{cases} y_{33}-x^2y_1=v \\ y_{22}=u \\ y_{12}=w \end{cases}$$

with $2w=u_{33}-v_{22}-x^2u_1$. As before, instead of writing out the system R_3' and studying its formal inegrability by an elementary but tedious computation, we shall use a trick, knowing in advance that the generating CC *must* be of order at least $1+1=2$ because g_2' had to get one prolongation in order to become involutive and thus 2-acyclic.

- *Step* 2: It thus remains to find out the CC for (u,v) in the initial inhomogeneous system. As we have used two prolongations in order to exhibit R_2', we have second order formal derivatives of u and v in the right members. Now, from the above argument, we have second order CC for the new right members and could hope therefore for a fourth order generating CC. The trick is to use the three different brackets of operators that can be obtained. We obtain in a formal way:

$$\begin{aligned} \left[d_{33}-x^2d_1,d_{22}\right]y &= y_{2233}-x^2y_{122}-y_{2233}+x^2y_{122}+2y_{12} \\ &= 2y_{12} \\ &= u_{33}-x^2u_1-v_{22} \end{aligned}$$

Then:

$$2\left[d_2,d_{12}\right]y=0=d_2\left(2d_{12}y\right)-2d_1\left(d_{22}y\right)=\left(u_{233}-v_{222}-x^2u_{12}-u_1\right)-2u_1$$

brings the *third order* CC:

$$A\equiv u_{233}-v_{222}-x^2u_{12}-3u_1=0$$

$$\begin{aligned} 2\left[d_{33}-x^2d_1,d_{12}\right]y &= 2y_{1233}-2x^2y_{112}-2y_{1233}+2x^2y_{112}+2y_{11} \\ &= 2y_{11} \\ &= 2\left(d_{33}-x^2d_1\right)w-2v_{12} \\ &= u_{3333}-v_{2233}-2x^2u_{133}+x^2v_{122}-2v_{12}+\left(x^2\right)^2u_{11} \end{aligned}$$

brings the new first order equation:

$$2y_{11}=2\omega=u_{3333}-v_{2233}-2x^2u_{133}+x^2v_{122}-2v_{12}+\left(x^2\right)^2u_{11}=0$$

Accordingly, we may start afresh with the new system $R_2''=R_2^{(4)}\subset R_2'\subset R_2$

which is *surprisingly* of finite type with $dim(R_2'')=10-4=6$, $g_3''=0$ and defined by the 4 second order PD equations:

$$y_{33}-x^2y_1=v,\ y_{22}=u,\ y_{12}=w,\ y_{11}=\omega,\ w\in j_2(u,v),\ \omega\in j_4(u,v)$$

We obtain therefore:

$$2y_{112}=u_{23333}-v_{22233}-2x^2u_{1233}-2u_{133}+x^2v_{1222}-v_{122}+\left(x^2\right)^2u_{112}+2x^2u_{11}$$
$$-2y_{112}=-u_{133}+v_{122}+x^2u_{11}$$

and thus a CC of order 5, namely:

$$B\equiv u_{23333}-v_{22233}-2x^2u_{1233}-3u_{133}+x^2v_{1222}+\left(x^2\right)^2u_{112}+3x^2u_{11}=0$$

However, we have indeed the identity $A_{33}-x^2A_1-B=0$ and thus $B\in j_2(A)$, that is B is a *not* a new generating fifth order CC as it is only a consequence of the prolongations of A. Using now the bracket of operators $[d_{11},d_{33}]=0$ that has not been already used, we get:

$$2y_{1133}=u_{333333}-v_{223333}-2x^2u_{13333}+x^2v_{12233}-2v_{1233}+\left(x^2\right)^2u_{1133}$$
$$-2y_{1133}+2x^2y_{111}=-2v_{11}$$
$$-2x^2y_{111}=-x^2u_{13333}+x^2v_{12233}+2\left(x^2\right)^2u_{1133}-\left(x^2\right)^2v_{1122}+2x^2v_{112}-\left(x^2\right)^3u_{111}$$

We obtain therefore a new sixth order CC:

$$\begin{aligned}C\equiv\ & u_{333333}-v_{223333}-3x^2u_{13333}+2x^2v_{12233}-2v_{1233}+3\left(x^2\right)^2u_{1133}\\ & -\left(x^2\right)^2v_{1122}+2x^2v_{112}-\left(x^2\right)^3u_{111}-2v_{11}\\ =\ & 0\end{aligned}$$

which cannot be a differential consequence of A. After tedious computations, one can find the differential identity:

$$A_{3333}-2x^2A_{133}+\left(x^2\right)^2A_{11}-C_2=0$$

The corresponding simplest free resolution, written with differential modules, is thus:

$$0\to D\xrightarrow[4]{}D^2\xrightarrow[6]{}D^2\xrightarrow[2]{}D\xrightarrow{p}M\to 0$$

Again, the total number of generating CC, that is $1+1=2$, has nothing to do with the differential transcendence degree of the CC differential module which is still $dim(F_0)-dim(E)=2-1=1$ because $rk_D(M)=0$.

3. Mathematical Tools

Instead of starting with a linear system $R_q\subset J_q(E)$ of order q on E, let us start with a bundle map $\Phi:J_q(E)\to F_0$ with $R_q=ker(\Phi)$ and let us consider the linear PD operator $D:E\xrightarrow{j_q}J_q(E)\xrightarrow{\Phi}F_0$. Using the canonical inclusion $J_{q+r}(E)\subset J_r\left(J_q(E)\right)$, let us define the *r- prolongation* $\rho_r(\Phi):J_{q+r}(E)\to J_r\left(J_q(E)\right)\xrightarrow{J_r(\Phi)}J_r(F_0)$. The general case of the successive prolongations with $r\geq 0$ is described by the following commutative and

exact diagram:

$$\begin{array}{ccccccccc}
 & & 0 & & 0 & & 0 & & \\
 & & \downarrow & & \downarrow & & \downarrow & & \\
0 & \to & g_{q+r+1} & \to & S_{q+r+1}T^* \otimes E & \xrightarrow{\sigma_{r+1}(\Phi)} & S_{r+1}T^* \otimes F_0 & \to & h_{r+1} & \to 0 \\
 & & \downarrow & & \downarrow & & \downarrow & & \downarrow & \\
0 & \to & R_{q+r+1} & \to & J_{q+r+1}(E) & \xrightarrow{\rho_{r+1}(\Phi)} & J_{r+1}(F_0) & \to & Q_{r+1} & \to 0 \\
 & & \downarrow & & \downarrow \pi_{q+r}^{q+r+1} & & \downarrow \pi_r^{r+1} & & \downarrow & \\
0 & \to & R_{q+r} & \to & J_{q+r}(E) & \xrightarrow{\rho_r(\Phi)} & J_r(F_0) & \to & Q_r & \to 0 \\
 & & & & \downarrow & & \downarrow & & \downarrow & \\
 & & & & 0 & & 0 & & 0 &
\end{array}$$

with *symbol*-map induced in the upper *symbol sequence* ([19] [20] [21]).

Chasing in this diagram while applying the "*snake*" lemma ([10] [22] [23]), we obtain the *long exact connecting sequence*:

$$0 \to g_{q+r+1} \to R_{q+r+1} \to R_{q+r} \to h_{r+1} \to Q_{r+1} \to Q_r \to 0$$

which is thus connecting in a tricky way FI (*lower left*) with CC (*upper right*). Needless to say that absolutely no classical procedure can produce such a result which is thus totally absent from the GR papers already quoted.

Setting $H\left(R_{q+r}\right) = R_{q+r} \big/ \pi_{q+r}^{q+r+1}\left(R_{q+r+1}\right)$, we have equivalently the shorter long exact sequence:

$$0 \to H\left(R_{q+r}\right) \to h_{r+1} \to Q_{r+1} \to Q_r \to 0$$

As a possible interpretation, $dim\left(Q_r\right)$ is the total number of CC of order $0,1,\cdots$ up to r included. However, the problem to solve is to study the structure of the projective limit of vector bundles made by the induced epimorphisms $Q_{r+1} \to Q_r$. Of course, as it is mostly realized in the examples, we have to suppose that R_q is *sufficiently regular* in such a way that the R_{q+r} are vector bundles $\forall r \geq 0$ *and* that the $R_{q+r}^{(s)} = \pi_{q+r}^{q+r+s}\left(R_{q+r+s}\right)$ are also vector bundles, such a situation being in particular always realized when $R_q \subset J_q\left(E\right)$ or D are defined over a differential field K. In this case, introducing the filtered noetherian ring $D = K\left[d_1,\cdots,d_n\right] = K\left[d\right]$ of differential operators with coefficients in K, we may introduce a differential module M with induced filtration $0 = M_0 \subseteq M_1 \subseteq \cdots \subseteq M_q \subseteq \cdots \subseteq m_\infty = M$ in such a way that the system $R = R_\infty = hom_K\left(M,K\right)$ associated with M with $R_q = hom_K\left(M_q,K\right)$ is of course *automatically* FI (*care*). Following Macaulay in ([24]), we have already proved in many places ([3] [10]) that R is a differential module for the *Spencer operator* $d: R \to T^* \otimes R: f \to dx^i \otimes d_i f$ with $d_i: R \to R: R_{q+1} \to R_q$ defined by the explicit formula:

$$\left(d_i f\right)_\mu^k = \partial_i f_\mu^k - f_{\mu+1_i}^k \in K$$

It is important to notice that such an operator/system is far from being formally integrable because:

$$\partial_i\left(\partial_j f_\mu^k - f_{\mu+1_j}^k\right) - \partial_j\left(\partial_i f_\mu^k - f_{\mu+1_i}^k\right) = \partial_j f_{\mu+1_i}^k - \partial_i f_{\mu+1_j}^k$$

As can be seen from the examples previously presented, starting with Ψ_r for a given r, the main problem is to compare the epimorphism $\Psi_{r+1}: J_{r+1}(F_0) \to Q_{r+1}$ with the morphism $\rho_1(\Psi_r): J_{r+1}(F_0) \to J_1(Q_r)$ in the following commutative diagram *which may not be exact*:

$$\begin{array}{ccccccccc}
 & & 0 & & 0 & & 0 & & 0 \\
 & & \downarrow & & \downarrow & & \downarrow & & \downarrow \\
0 \to & g_{q+r+1} & \to & S_{q+r+1}T^* \otimes E & \xrightarrow{\sigma_{r+1}(\Phi)} & S_{r+1}T^* \otimes F_0 & \xrightarrow{\sigma_1(\Psi_r)} & T^* \otimes Q_r & \\
 & \downarrow & & \downarrow & & \downarrow & & \downarrow & \\
0 \to & R_{q+r+1} & \to & J_{q+r+1}(E) & \xrightarrow{\rho_{r+1}(\Phi)} & J_{r+1}(F_0) & \xrightarrow{\rho_1(\Psi_r)} & J_1(Q_r) & \\
 & \downarrow & & \downarrow \pi_{q+r}^{q+r+1} & & \downarrow \pi_r^{r+1} & & \downarrow & \\
0 \to & R_{q+r} & \to & J_{q+r}(E) & \xrightarrow{\rho_r(\Phi)} & J_r(F_0) & \xrightarrow{\Psi_r} & Q_r & \to 0 \\
 & & & \downarrow & & \downarrow & & \downarrow & \\
 & & & 0 & & 0 & & 0 &
\end{array}$$

where the central row is induced from the long exact sequence:

$$0 \to J_1(R_{q+r}) \to J_1\left(J_{q+r}(E)\right) \to J_1\left(J_r(F_0)\right) \to J_1(Q_r) \to 0$$

and may not be exact.

PROPOSITION 3.1: We have only in general:

$$B_{r+1} = im\left(\rho_{r+1}(\Phi)\right) = ker\left(\Psi_{r+1}\right) \subseteq ker\left(\rho_1(\Psi_r)\right) = \rho_1(B_r)$$

Proof: Denoting the Spencer operator by d in place of the standard notation D of the literature that could be confused with the ring D of differential operators, we have the following commutative diagram:

$$\begin{array}{ccccccccc}
0 \to & R_{q+r+1} & \to & J_{q+r+1}(E) & \xrightarrow{\rho_{r+1}(\Phi)} & B_{r+1} & \subset & J_{r+1}(F_0) \\
 & \downarrow d & & \downarrow d & & \downarrow d & & \downarrow d \\
0 \to & T^* \otimes R_{q+r} & \to & T^* \otimes J_{q+r}(E) & \xrightarrow{\rho_r(\Phi)} & T^* \otimes B_r & \subset & T^* \otimes J_r(F_0)
\end{array}$$

As B_{r+1} projects *onto* B_r and $d_i B_{r+1} \subset B_r$, it follows from ([12], Propositions 10, p 83) or ([10], Remark 2.9, p 315) that $B_{r+1} \subseteq \rho_1(B_r)$. We have thus a projective limit of systems, each one being defined by more equations than the preceding one and such a procedure must finish with a FI system that can even be prolonged, as we shall see in the examples, in order to obtain an involutive system that may be used to start a Janet sequence. The decision to stop is provided by the maximum order of the CC obtained, namely of order bounded by $r+s+1=t$ if the system $R_{q+r}^{(s)}$ is involutive or at least with a 2-acyclic symbol. □

The idea is to use the *composite morphism* $S_r T^* \otimes F_0 \to Q_r$ while chasing in order to prove that any element of $J_{r+1}(F_0)$ killed by $\rho_1(\Psi_r)$ can be decomposed into the sum of an element in $im\left(\rho_r(\Phi)\right)$ plus an element in $S_{r+1}T^* \otimes F_0$ killed by $\sigma_1(\Psi_r)$. With more details, setting for simplicity $S_r T^* \otimes F_0 = S_r(F_0)$, introducing the *coboundary* bundle $B\left(S_{r+1}(F_0)\right) = im\left(\sigma_{r+1}(\Phi)\right)$ and the *cocycle* bundle $Z\left(S_{r+1}(F_0)\right) = ker\left(\sigma_1(\Psi_r)\right)$, we may define the corresponding *coho-*

mology bundle $H\left(S_{r+1}\left(F_0\right)\right)=Z\left(S_{r+1}\left(F_0\right)\right)/B\left(S_{r+1}\left(F_0\right)\right)$. We may also define similarly $H\left(J_{r+1}\left(F_0\right)\right)=ker\left(\rho_1\left(\Psi_r\right)\right)/im\left(\rho_{r+1}\left(\Phi\right)\right)$ and we obtain the following crucial proposition (See [4], Example 2.A.9) through a chase left to the reader as an exercise:

PROPOSITION 3.2: There exists a short exact sequence:

$$0\to H\left(R_{q+r}\right)\to H\left(S_{r+1}\left(F_0\right)\right)\to H\left(J_{r+1}\left(F_0\right)\right)\to 0$$

Let us now deal with the symbol cohomology by chasing in the following commutative diagram:

$$\begin{array}{ccccccc}
 & 0 & & 0 & & 0 & 0 \\
 & \downarrow & & \downarrow & & \downarrow & \downarrow \\
0\to & g_{q+r+1} & \to & S_{q+r+1}T^*\otimes E & \to & S_{r+1}T^*\otimes F_0 & \to T^*\otimes Q_r \\
 & \downarrow\delta & & \downarrow\delta & & \downarrow\delta & \searrow \quad \| \\
0\to & T^*\otimes g_{q+r} & \to & T^*\otimes S_{q+r}T^*\otimes E & \to & T^*\otimes S_rT^*\otimes F_0 & \to T^*\otimes Q_r \\
 & \downarrow\delta & & \downarrow\delta & & \downarrow\delta & \downarrow \\
0\to & \wedge^2T^*\otimes g_{q+r-1} & \to & \wedge^2T^*\otimes S_{q+r-1}T^*\otimes E & \to & \wedge^2T^*\otimes S_{r-1}T^*\otimes F_0 & 0 \\
 & \downarrow\delta & & \downarrow\delta & & & \\
0\to & \wedge^3T^*\otimes g_{q+r-2} & = & \wedge^3T^*\otimes S_{q+r-2}T^*\otimes E & & &
\end{array}$$

where neither the first nor the second upper columns may be exact and where the left column may not be exact, unless g_q is involutive or 2-acyclic. Chasing with the same notations, we obtain:

PROPOSITION 3.3: There exists an exact sequence:

$$0\to H^2\left(g_{q+r-1}\right)\to H\left(S_{r+1}\left(F_0\right)\right)\to T^*\otimes H\left(S_r\left(F_0\right)\right)$$

The upper left arrows are not in general epimorphisms and it may be sometimes useful to consider h_r as a kind of symbol in the more abstract diagram:

$$\begin{array}{ccccccccc}
 & 0 & & 0 & & 0 & & & \\
 & \downarrow & & \downarrow & & \downarrow & & & \\
0\to & g_{q+r+1} & \to & S_{q+r+1}T^*\otimes E & \to & S_{r+1}T^*\otimes F_0 & \to & h_{r+1} & \to 0 \\
 & \downarrow\delta & & \downarrow\delta & & \downarrow\delta & & \downarrow\delta & \\
0\to & T^*\otimes g_{q+r} & \to & T^*\otimes S_{q+r}T^*\otimes E & \to & T^*\otimes S_rT^*\otimes F_0 & \to & T^*\otimes h_r & \to 0 \\
 & \downarrow\delta & & \downarrow\delta & & \downarrow\delta & & \downarrow\delta & \\
0\to & \wedge^2T^*\otimes g_{q+r-1} & \to & \wedge^2T^*\otimes S_{q+r-1}T^*\otimes E & \to & \wedge^2T^*\otimes S_{r-1}T^*\otimes F_0 & \to & \wedge^2T^*\otimes h_{r-1} & \to 0 \\
 & \downarrow\delta & & \downarrow\delta & & \downarrow\delta & & & \\
0\to & \wedge^3T^*\otimes g_{q+r-2} & \to & \wedge^3T^*\otimes S_{q+r-2}T^*\otimes E & \to & \wedge^3T^*\otimes S_{r-2}T^*\otimes F_0 & & & \\
 & \downarrow\delta & & \downarrow\delta & & & & & \\
0\to & \wedge^4T^*\otimes g_{q+r-3} & \to & \wedge^4T^*\otimes S_{q+r-3}T^*\otimes E & & & & &
\end{array}$$

where the rows are now exact. However, understanding the meaning of h_r as a kind of new symbol may not be possible unless $h_{r+1}\to T^*\otimes h_r$ is a monomorphism, that is when g_q is 2-acyclic *and* h_r is 1-acyclic, that is when g_q is *also* 3-acyclic (or involutive). Once more, we understand the crucial importance of 2-acyclicity but we recall that *the only symbol known to be* 2*-acyclic without being involutive is the symbol of the conformal Killing system whenever* $n\geq 4$, *which is also* 3*-acyclic whenever* $n\geq 5$ ([3] [11] [12] [13]).

4. Applications

MACAULAY EXAMPLE REVISITED:

With $m=1, n=3, q=2, K=\mathbb{Q}$, let us introduce two operators $P, Q \in D=K\left[d_1, d_2, d_3\right]$ and consider the second order system $R_2 \subset J_2(E)$ used by Macaulay as early as in 1916 ([4] [24]):

$$Qy \equiv y_{33}=v, \quad Py \equiv y_{13}-y_2=u$$

We have the strict inclusions:

$$R_2^{(2)} \subset R_2^{(1)} \subset R_2 \subset J_2(E) \qquad 6<7<8<10$$

As $g_2^{(2)} \subset g_2^{(1)} \subset g_2$ are involutive, we obtain $\rho_r\left(R_2^{(2)}\right)=R_{r+2}^{(2)}$ by using the *Prolongation/Projection* (PP) procedure. We exhibit the parametric jets of the bundles that will be used in the following diagrams:

$$par_2=\left\{y, y_1, y_2, y_3, y_{11}, y_{12}, y_{22}, y_{23}\right\}$$

$$par_3=\left\{y, y_1, y_2, y_3, y_{11}, y_{12}, y_{22}, y_{111}, y_{112}, y_{122}, y_{222}, y_{223}\right\}$$

$$par_4=\left\{y, y_1, y_2, y_3, y_{11}, y_{12}, y_{111}, y_{112}, y_{122}, y_{222}, y_{1111}, y_{1112}, y_{1122}, y_{1222}, y_{2222}, y_{2223}\right\}$$

and thus $dim\left(R_2\right)=8, dim\left(R_3\right)=12, dim\left(R_4\right)=16$. More generally, we let the reader prove that $dim\left(R_{r+2}\right)=4r+8, \forall r \geq 0$, thus $dim\left(R_{r+4}\right)=4r+16, \forall r \geq 0$ and $dim\left(g_{r+4}\right)=r+6, \forall r \geq 0$.

We have the Janet tabular for $R_2^{(2)}$:

$$\begin{cases} y_{33}=v & \begin{bmatrix} 1 & 2 & 3 \\ 1 & 2 & \bullet \\ 1 & 2 & \bullet \\ 1 & \bullet & \bullet \end{bmatrix} \\ y_{23}=v_1-u_3 & \\ y_{22}=v_{11}-u_{13}-u_2 & \\ y_{13}-y_2=u & \end{cases}$$

The *two* CC are:

$$A \equiv v_{13}-v_2-u_{33}=0, \quad A_1 \equiv v_{113}-v_{12}-u_{133}=0$$

while the other ones are what we called *identity to zero* like:

$$d_2\left(y_{13}-y_2\right)-d_1\left(y_{23}\right)+d_2 y_2=0=u_2-\left(v_{11}-u_{13}\right)+\left(v_{11}-u_{13}-u_2\right)=0$$

There is thus only *one* generating CC of order 2, namely $A=0$, given by the commutation relation $P \circ Q-Q \circ P \equiv 0$ and the corresponding operator D_1 is thus surely formally subjective. Setting $F_1=Q_2$, we obtain the following diagram with exact central and lower rows whenever $r \geq 1$.

$$\begin{array}{ccccccccc} & & 0 & & 0 & & 0 & & 0 \\ & & \downarrow & & \downarrow & & \downarrow & & \downarrow \\ 0 & \rightarrow & g_{r+4} & \rightarrow & S_{r+4}T^* \otimes E & \rightarrow & S_{r+2}T^* \otimes F_0 & \rightarrow & S_rT^* \otimes F_1 & \rightarrow 0 \\ & & \downarrow & & \downarrow & & \downarrow & & \downarrow & \\ 0 & \rightarrow & R_{r+4} & \rightarrow & J_{r+4}(E) & \rightarrow & J_{r+2}(F_0) & \rightarrow & J_r(F_1) & \rightarrow 0 \\ & & \downarrow & & \downarrow & & \downarrow & & \downarrow & \\ 0 & \rightarrow & R_{r+3} & \rightarrow & J_{r+3}(E) & \rightarrow & J_{r+1}(F_0) & \rightarrow & J_{r-1}(F_1) & \rightarrow 0 \\ & & & & \downarrow & & \downarrow & & \downarrow & \\ & & & & 0 & & 0 & & 0 & \end{array}$$

$$\begin{array}{ccccccccc}
 & & 0 & & 0 & & 0 & & 0 \\
 & & \downarrow & & \downarrow & & \downarrow & & \downarrow \\
0 & \to & r+6 & \to & (r+5)(r+6)/2 & \to & \boxed{(r+3)(r+4)} & \to & (r+1)(r+2)/2 & \to 0 \\
 & & \downarrow & & \downarrow & & \downarrow & & \downarrow & \\
0 & \to & 4r+16 & \to & (r+5)(r+6)(r+7)/6 & \to & (r+3)(r+4)(r+5)/3 & \to & (r+1)(r+2)(r+3)/6 & \to 0 \\
 & & \downarrow & & \downarrow & & \downarrow & & \downarrow & \\
0 & \to & 4r+12 & \to & (r+4)(r+5)(r+6)/6 & \to & (r+2)(r+3)(r+4)/3 & \to & r(r+1)(r+2)/6 & \to 0 \\
 & & \downarrow & & \downarrow & & \downarrow & & \downarrow & \\
 & & \boxed{r+2} & & 0 & & 0 & & 0 & \\
 & & \downarrow & & & & & & & \\
 & & 0 & & & & & & &
\end{array}$$

$$\begin{array}{ccccccccc}
 & & 0 & & 0 & & 0 & & 0 \\
 & & \downarrow & & \downarrow & & \downarrow & & \downarrow \\
0 & \to & g_{r+4} & \to & S_{r+4}T^* \otimes E & \to & \boxed{S_{r+2}T^* \otimes F_0} & \to & S_rT^* \otimes F_1 & \to 0 \\
 & & \downarrow \delta & & \downarrow \delta & & \downarrow \delta & & \downarrow \delta & \\
0 & \to & T^* \otimes g_{r+3} & \to & T^* \otimes S_{r+3}T^* \otimes E & \to & T^* \otimes S_{r+1}T^* \otimes F_0 & \to & T^* \otimes S_{r-1}T^* \otimes F_1 & \to 0 \\
 & & \downarrow \delta & & \downarrow \delta & & \downarrow \delta & & & \\
0 & \to & \boxed{\wedge^2 T^* \otimes g_{r+2}} & \to & \wedge^2 T^* \otimes S_{r+2}T^* \otimes E & \to & \wedge^2 T^* \otimes S_rT^* \otimes F_0 & & & \\
 & & \downarrow \delta & & \downarrow \delta & & & & & \\
0 & \to & \wedge^3 T^* \otimes g_{r+1} & = & \wedge^3 T^* \otimes S_{r+1}T^* \otimes E & & & & & \\
 & & \downarrow & & \downarrow & & & & & \\
 & & 0 & & 0 & & & & &
\end{array}$$

where $S_4T^* \otimes E \simeq S_4T^*$ and $F_1 \simeq Q_2$ while $Q_1 = 0$ as there is no CC of order 1. From the snake lemma and a chase, we obtain the *long exact connecting sequence* when $r = 0$:

$$0 \to g_4 \to R_4 \to R_3 \to h_2 \to F_1 \to 0$$

$$0 \to 6 \to 16 \to 12 \to 3 \to 1 \to 0$$

relating FI (*lower left*) to CC (*upper right*). By composing the epimorphism $S_2T^* \otimes F_0 \to h_2$ with the epimorphism $h_2 \to F_1$, we obtain an epimorphism $S_2T^* \otimes F_0 \to F_1$ and the long exact sequence:

$$0 \to g_4 \to S_4T^* \otimes E \to S_2T^* \otimes F_0 \to F_1 \to 0$$

which is nevertheless *not* a long ker/coker exact sequence by counting the dimensions as we have $6-15+12-1=2 \neq 0$.

The above diagrams illustrate perfectly the three propositions of Section 2. We have in particular:

$$H\left(J_{r+2}\left(F_0\right)\right)=0 \Rightarrow H\left(J_{r+1}\left(F_0\right)\right)=0,\ H\left(S_{r+2}\left(F_0\right)\right)=H\left(R_{r+3}\right)\neq 0$$

and the formally exact sequence, which is nevertheless not strictly exact though $1-2+1=0$:

$$0 \to \Theta \to E \xrightarrow{\frac{D}{2}} F_0 \xrightarrow{\frac{D_1}{2}} F_1 \to 0$$

$$0 \to \Theta \to 1 \to 2 \to 1 \to 0$$

We remind the reader that, contrary to the situation met with FI systems where the exactness on the jet level is obtained inductively from the exactness on the symbol level, here we discover that *we may have the exactness on the jet level without having exactness on the symbol level.*

EXAMPLE 2.1 REVISITED:

First of all, let us compute the dimensions and the parametric jets that will be used in the following diagrams.

$$par_1 = par_2 = \left\{ y, y_1, y_2, y_3, y_1^2 \right\},$$

$$n = dim(X) = 3,\ m = dim(E) = 2,$$
$$dim(R_1) = dim(R_2) = 3,\ dim(g_1) = 1,\ g_2 = 0 \Rightarrow g_3 = 0$$

$$\begin{array}{ccccccccccc}
 & & & & 0 & & 0 & & 0 & & \\
 & & & & \downarrow & & \downarrow & & \downarrow & & \\
 & & 0 & \to & S_3T^* \otimes E & \to & S_2T^* \otimes F_0 & \to & T^* \otimes Q_1 & \to & 0 \\
 & & \downarrow & & \downarrow & & \downarrow & \searrow & \downarrow & & \\
0 & \to & R_3 & \to & J_3(E) & \to & J_2(F_0) & \to & J_1(Q_1) & \to & 0 \\
 & & \downarrow & & \downarrow \pi_4^3 & & \downarrow \pi_1^2 & & \downarrow & & \\
0 & \to & R_2 & \to & J_2(E) & \to & J_1(F_0) & \to & Q_1 & \to & 0 \\
 & & \downarrow & & \downarrow & & \downarrow & & \downarrow & & \\
 & & 0 & & 0 & & 0 & & 0 & &
\end{array}$$

$$\begin{array}{ccccccccc}
 & & & & 0 & & 0 & & 0 & \\
 & & & & \downarrow & & \downarrow & & \downarrow & \\
 & & 0 & \to & 20 & \to & 30 & \to & 9 & \to 0 \\
 & & \downarrow & & \downarrow & & \downarrow & \searrow & \downarrow & \\
0 & \to & 3 & \to & 40 & \to & 50 & \to & 12 & \to 0 \\
 & & \downarrow & & \downarrow \pi_2^3 & & \downarrow \pi_1^2 & & \downarrow & \\
0 & \to & 3 & \to & 20 & \to & 20 & \to & 3 & \to 0 \\
 & & \downarrow & & \downarrow & & \downarrow & & \downarrow & \\
 & & 0 & & 0 & & 0 & & 0 &
\end{array}$$

$$\begin{array}{ccccccccccc}
 & & & & & & 0 & & 0 & & 0 & & \\
 & & & & & & \downarrow & & \downarrow & & \downarrow & & \\
 & & 0 & & \to & & S_3T^* \otimes E & \to & S_2T^* \otimes F_0 & \to & T^* \otimes Q_1 & \to & 0 \\
 & & & & & & \downarrow \delta & & \downarrow \delta & & \| & & \\
 & & 0 & & \to & & T^* \otimes S_2T^* \otimes E & \to & T^* \otimes T^* \otimes F_0 & \to & T^* \otimes Q_1 & \to & 0 \\
 & & & & & & \downarrow \delta & & \downarrow \delta & & \downarrow & & \\
0 & \to & \wedge^2 T^* \otimes g_1 & \to & \wedge^2 T^* \otimes T^* \otimes E & \to & \wedge^2 T^* \otimes F_0 & \to & 0 & & & & \\
 & & \downarrow \delta & & \downarrow \delta & & \downarrow & & & & & & \\
0 & \to & \wedge^3 T^* \otimes E & = & \wedge^3 T^* \otimes E & \to & 0 & & & & & & \\
 & & \downarrow & & \downarrow & & & & & & & & \\
 & & 0 & & 0 & & & & & & & &
\end{array}$$

$$\begin{array}{ccccccccccc}
 & & & & 0 & & 0 & & 0 & & \\
 & & & & \downarrow & & \downarrow & & \downarrow & & \\
 & & 0 & \to & 20 & \to & \boxed{30} & \to & 9 & \to & 0 \\
 & & & & \downarrow\delta & & \downarrow\delta & & \| & & \\
 & & 0 & \to & 36 & \to & 45 & \to & 9 & \to & 0 \\
 & & & & \downarrow\delta & & \downarrow\delta & & \downarrow & & \\
0 & \to & \boxed{3} & \to & 18 & \to & 15 & \to & 0 & & \\
 & & \downarrow\delta & & \downarrow\delta & & \downarrow & & & & \\
0 & \to & 2 & = & 2 & \to & 0 & & & & \\
 & & \downarrow & & \downarrow & & & & & & \\
 & & 0 & & 0 & & & & & &
\end{array}$$

It is not at all evident to study these diagrams. We have $dim\left(B\left(S_2\left(F_0\right)\right)\right)=20<dim\left(Z\left(S_2\left(F_0\right)\right)\right)=30-9=21$. We have already proved that $dim\left(H\left(S_2\left(F_0\right)\right)\right)=21-20=1=dim\left(H^2\left(g_1\right)\right)=3-2=1$, a result not evident at first sight explaining why the only second order additional generating CC is nothing else than the Riemann tensor in dimension equal to 2.

We have explained in ([4]) that such a system has its origin in the study of the integration of the Killing system for the Schwarzschild metric, which is not FI. With more details, let us use the Boyer-Lindquist coordinates $\left(t,r,\theta,\phi\right)=\left(x^0,x^1,x^2,x^3\right)$ instead of the Cartesian coordinates $\left(t,x,y,z\right)$ and consider the Schwarzschild metric $\omega=A\left(r\right)dt^2-\left(1/A\left(r\right)\right)dr^2-r^2d\theta^2-r^2\sin^2\left(\theta\right)d\phi^2$ and $\xi=\xi^i d_i\in T$, let us introduce $\xi_i=\omega_{ri}\xi^r$ with the 4 *formal derivatives* $\left(d_0=d_t,d_1=d_r,d_2=d_\theta,d_3=d_\phi\right)$. With speed of light $c=1$ and $A=1-\frac{m}{r}$ where m is a constant, the metric can be written in the diagonal form:

$$\begin{pmatrix} A & 0 & 0 & 0 \\ 0 & -1/A & 0 & 0 \\ 0 & 0 & -r^2 & 0 \\ 0 & 0 & 0 & -r^2\sin^2\left(\theta\right) \end{pmatrix}$$

Using the notations that can be found in the theory of differential modules, let us consider the Killing equations:

$$\Omega\equiv L\left(\xi\right)\omega=0 \quad \Leftrightarrow$$

$$\Omega_{ij}\equiv d_i\xi_j+d_j\xi_i-2\gamma_{ij}^r\xi_r=0$$

where we have introduced the Christoffel symbols γ while setting $A'=\partial_r A$ in the differential field K of coefficients. As in the previous Macaulay example and in order to avoid any further confusion between sections and derivatives, we shall use the sectional point of view and rewrite the previous equations in the symbolic form $L\left(\xi_1\right)\omega=\Omega\in S_2T^*$ where L is the *formal Lie derivative*.

$$\begin{cases} \xi_{3,3}+\sin(\theta)\cos(\theta)\xi_2+rA\sin^2(\theta)\xi_1=\frac{1}{2}\Omega_{33} \\ \xi_{2,3}+\xi_{3,2}-2\cot(\theta)\xi_3=\Omega_{23} \\ \xi_{1,3}+\xi_{3,1}-\frac{2}{r}\xi_3=\Omega_{13} \\ \xi_{0,3}+\xi_{3,0}=\Omega_{03} \\ \xi_{2,2}+rA\xi_1=\frac{1}{2}\Omega_{22} \\ \xi_{1,2}+\xi_{2,1}-\frac{2}{r}\xi_2=\Omega_{12} \\ \xi_{0,2}+\xi_{2,0}=\Omega_{02} \\ \xi_{1,1}+\frac{A'}{2A}\xi_1=\frac{1}{2}\Omega_{11} \\ \xi_{0,1}+\xi_{1,0}-\frac{A'}{A}\xi_0=\Omega_{01} \\ \xi_{0,0}-\frac{AA'}{2}\xi_1=\frac{1}{2}\Omega_{00} \end{cases}$$

This system $R_1\subset J_1(T)$ is far from being involutive because it is finite type with second symbol $g_2=0$ defined by the 40 equations $v_{ij}^k=0$ in the initial coordinates. From the symmetry, it is clear that such a system has at least 4 solutions, namely the time translation $\partial_t\leftrightarrow\xi^0=1\Leftrightarrow\xi_0=A$ and, using Cartesian coordinates (t,x,y,z), the 3 space rotations $y\partial_z-z\partial_y, z\partial_x-x\partial_z, x\partial_y-y\partial_x$.

These results are brought by the formal Lie derivative of the Weyl tensor because the Ricci tensor vanishes by assumption and we have the splitting $Riemann\simeq Ricci\oplus Weyl$ according to the *fundamental diagram II* that we discovered as early as in 1988 ([25]), still not acknowledged though it can be found in ([1] [2] [3]). In particular, as the *Ricci* part is vanishing by assumption, we may identify the *Riemann* part with the *Weyl* splitting part as tensors ([3]) and it is possible to prove (using a tedious direct computation or computer algebra) that there are only 6 non-zero components. It is important to notice that this result, bringing a strong condition on the zero jets because of the Lie derivative of the Weyl tensor and thus on the first jets, involves indeed the first derivative of the Weyl tensor because we have a term in $(A'')'$. When $\Omega=0$, *we obtain after* 2 *prolongations* the additional 5 new first order PD equations:

$$\xi_1=0,\xi_{1,2}=0,\xi_{1,3}=0,\xi_{0,2}=0,\xi_{0,3}=0$$

As we are dealing with sections, $\xi_1=0$ *does imply* $\xi_{1,1}=0$ and $\xi_{0,0}=0$ but *does not imply* $\xi_{1,0}=0$, these later condition being only brought by one additional prolongation and we have the strict inclusions $R_1^{(3)}\subset R_1^{(2)}\subset R_1^{(1)}=R_1$. Hence, it remains to determine the dimensions of the subsystems $R_1'=R_1^{(2)}$ and $R_1''=R_1^{(3)}$ with the strict inclusion $R_1''\subset R_1'$, exactly again like in the Macaulay example. Knowing that $dim(R_1)=dim(R_2)=10$, $dim(R_3)=5$, $dim(R_4)=4$, we have thus obtained the 15 equations defining R_1' with $dim(R_1')=20-15=5$ and the 16 equations defining R_1'' with $dim(R_1'')=20-16=4$, namely:

$$\xi_{3,3}+\sin(\theta)\cos(\theta)\xi_2=0$$
$$\xi_{2,3}+\xi_{3,2}-2\cot(\theta)\xi_3=0$$
$$\xi_{1,3}=0$$
$$\xi_{0,3}=0$$
$$\xi_{2,2}=0$$
$$\xi_{1,2}=0$$
$$\xi_{0,2}=0$$
$$\xi_{3,1}-\frac{2}{r}\xi_3=0$$
$$\xi_{2,1}-\frac{2}{r}\xi_2=0$$
$$\xi_{1,1}=0$$
$$\xi_{0,1}-\frac{A'}{A}\xi_0=0$$
$$\xi_{3,0}=0$$
$$\xi_{2,0}=0$$
$$\xi_{0,1}-\frac{A'}{A}\xi_0=0$$
$$\xi_{3,0}=0$$
$$\xi_{2,0}=0$$

Setting now in an intrinsic way $\xi_0=A\xi^0,\xi_1=-\frac{1}{A}\xi^1,\xi_2=-r^2\xi^2$ and in a non-intrinsic way (*care*) $\xi_3=-r^2\xi^3$, we may even simplify these equations and get a system *not depending on A anymore*:

$$\begin{cases}\xi_3^3+\sin(\theta)\cos(\theta)\xi^2=0\\ \xi_3^2+\xi_2^3-2\cot(\theta)\xi^3=0\\ \xi_3^1=0\\ \xi_3^0=0\\ \xi_1^3=0\\ \xi_1^2=0\\ \xi_1^1=0\\ \xi_1^0=0\end{cases}$$
$$\begin{cases}\xi_0^3=0\\ \xi_0^2=0\\ \xi_0^1=0\\ \xi_0^0=0\\ \xi_2^2=0\\ \xi_2^1=0\\ \xi_2^0=0\\ \xi^1=0\end{cases}$$

It is easy to check that $R_1^{(3)}$, having minimum dimension equal to 4, is formally integrable, though not involutive as it is finite type, and to exhibit 4 solu-

tions linearly independent over the constants. Indeed, we must have $\xi^0 = c$ where c is a constant and we may drop the time variable not appearing elsewhere while using the equation $\xi^1 = 0$. It follows that $\xi^2 = f(\theta,\phi), \xi^3 = g(\theta,\phi)$ while f, g are solutions of the first, second and fifth equations of Killing type wih a general solution depending on 3 constants, a result leading to an elementary probem of 2-dimensional elasticity left to the reader as an exercise. The system $R_1^{(3)}$ is formally integrable while the system $R_2^{(2)}$ is involutive. Having in mind the PP procedure, it follows that the CC could be of order 2, 3 *and even* 4. Equivalently, we may cut the integration of this system into three systems:

1) First of all, we have $\xi^1 = 0$ and thus $\xi_0^1 = 0, \xi_1^1 = 0, \xi_2^1 = 0, \xi_3^1 = 0$.

2) Then, we may consider $\xi_0^0 = 0, \xi_1^0 = 0, \xi_2^0 = 0, \xi_3^0 = 0 \Rightarrow \xi^0 = c$.

3) Finally, we arrive to the FI system with the same properties as the ones found for Example 2.1:

$$\begin{cases} \xi_3^3 + \sin(\theta)\cos(\theta)\xi^2 = 0 \\ \xi_3^2 + \xi_2^3 - 2\cot(\theta)\xi^3 = 0 \\ \xi_1^3 = 0 \\ \xi_1^2 = 0 \\ \xi_2^2 = 0 \end{cases}$$

that is with 3 generating first order CC and 1 additional second order generating CC.

Proceeding like in the motivating examples, we may introduce the inhomogeneous systems:

$$\left\{\xi_1 = U, \xi_{1,2} = V_2, \xi_{1,3} = V_3, \xi_{0,2} = W_2, \xi_{0,3} = W_3\right\} \in j_2(\Omega)$$

and we finally obtain 16 PD equations, namely $\xi_1 = U$ plus the 15 PD equations:

$$\xi_{0,0} = \frac{1}{2}\Omega_{00} + \frac{AA'}{2}U,\ \xi_{0,1} - \frac{A'}{A}\xi_0 = \Omega_{01} - \boxed{d_0 U} \in j_3(\Omega),\ \xi_{0,2} = W_2,\ \xi_{0,3} = W_3$$

$$\xi_{1,0} = \boxed{d_0 U} \in j_3(\Omega),\ \xi_{1,1} = \frac{1}{2}\Omega_{11} - \frac{A'}{2A}U,\ \xi_{1,2} = V_2,\ \xi_{1,3} = V_3$$

$$\xi_{2,0} = \Omega_{02} - W_2,\ \xi_{2,1} - \frac{2}{r}\xi_2 = \Omega_{12} - V_2,\ \xi_{2,2} = \frac{1}{2}\Omega_{22} - rAU$$

$$\xi_{3,0} = \Omega_{03} - W_3,\ \xi_{3,1} - \frac{2}{r}\xi_3 = \Omega_{13} - V_3,\ \xi_{3,2} + \xi_{2,3} - 2\cot(\theta)\xi_3 = \Omega_{23},$$

$$\xi_{3,3} + \sin(\theta)\cos(\theta)\xi_2 = \frac{1}{2}\Omega_{33} - rA\sin^2(\theta)U$$

As a byproduct, we have $dim(R_3) = 5, dim(R_4) = 4$ and we obtain 15 second order CC in $j_2(\Omega)$ along the ker/coker exact sequence:

$$\begin{array}{ccccccccc} 0 \to & R_3 & \to & J_3(T) & \to & J_2(S_2T^*) & \to & Q_2 & \to 0 \\ & & & & \searrow & \nearrow & & & \\ & & & & & B_2 & & & \\ & & & & \nearrow & \searrow & & & \\ & & & 0 & & & 0 & & \end{array}$$

$$0 \to 5 \to 140 \to 150 \to 15 \to 0$$
$$\searrow \quad \nearrow$$
$$135$$

Then, we have identities to zero like $d_0\xi^1 - \xi_0^1 = 0$ but we have also *surely* the three third order CC like $d_1\xi^1 - \xi_1^1 = 0, d_2\xi^1 - \xi_2^1, d_3\xi^1 - \xi_3^1$, then *perhaps* the other third order CC $d_2\xi_3^0 - d_3\xi_2^0 = 0$ and *perhaps* even fourth order CC like $d_0\xi_1^0 - d_1\xi_0^0 = 0$ which is containing the leading term $d_{00}U$ after substitution. However, we have the linearization formulas:

$$\rho_{kl,ij} = \omega_{kr}\rho_{l,ij}^r \Rightarrow R_{kl,ij} = \omega_{kr}R_{l,ij}^r + \rho_{l,ij}^r\Omega_{kr}$$

$$\rho_{ij} = \rho_{i,rj}^r \Rightarrow \omega^{rs}R_{ri,sj} = R_{ij} + \omega^{rs}\rho_{i,rj}^t\Omega_{st} \neq R_{ij}$$

and obtain therefore the formulas:

$$\frac{2r}{3m\sin^2(\theta)}R_{23,30} + \frac{2}{3}\Omega_{02} = \xi_{0,2} = -\frac{2r^3A}{3m}R_{01,12} + \frac{1}{3}\Omega_{02} \Leftrightarrow R_{02} = R_{0,12}^1 + R_{3,32}^3 = 0$$

$$\frac{2r}{3m}R_{23,02} + \frac{2}{3}\Omega_{03} = \xi_{0,3} = -\frac{2r^3A}{3m}R_{01,13} + \frac{1}{3}\Omega_{03} \Leftrightarrow R_{03} = R_{0,13}^1 + R_{0,23}^2 = 0$$

with two similar ones for $\xi_{1,2}$ and $\xi_{1,3}$ showing the unexpected *partition* of the Ricci tensor:

$$\{R_{ij}\} = \{R_{00}, R_{11}, R_{22}, R_{33}\} + \{R_{12}, R_{13}, R_{02}, R_{03}\} + \{R_{01}, R_{23}\}$$

determined by the $15 = 10 + 5 = 4 + 4 + 2$ second order CC that we have exhibited.

Now, after one prolongation, we get:

$$\xi_{1,00} + \left(\frac{AA''}{2} - \frac{(A')^2}{4}\right)\xi_1 + \frac{1}{2}d_1\Omega_{00} - d_0\Omega_{01} - \frac{A'}{2A}\Omega_{00} + \frac{AA'}{24}\Omega_{11} = 0$$

and thus $d_1\xi_{0,0} - d_0\xi_{0,1} = 0$. Similarly, we have:

$$\xi_{1,01} + \frac{A'}{2A}\xi_{1,0} - \frac{1}{2}d_0\Omega_{11} \equiv d_0\left(d_1\xi_1 + \frac{A'}{2A}\xi_1 - \Omega_{11}\right) = 0$$

and thus $d_1\xi_{1,0} - d_0\xi_{1,1} = 0$. It follows that $d_1U + \frac{A'}{2A} - \frac{1}{2}\Omega_{11} = 0$ is a generating CC of order 3 but $d_{01}U - \frac{A'}{2A}d_0U - d_0\Omega_{11} = 0$ is not a generating CC of order 4.

In order to proceed further on, we notice that the generating CC of order 3 already found can be written as:

$$d_1U + \frac{A'}{2A}U - \frac{1}{2}\Omega_{11} = 0, d_2U - V_2 = 0, d_3U - V_3 = 0$$

Using crossed derivatives, we get:

$$d_1V_2 + \frac{A'}{2A}d_2U - \frac{1}{2}d_2\Omega_{11} = 0, d_1V_3 + \frac{A'}{2A}d_3U - \frac{1}{2}d_3\Omega_{11} = 0, d_2V_3 - d_3V_2 = 0$$

and thus $d_1\xi_{1,2} - d_2\xi_{1,1} = 0, d_1\xi_{1,3} - d_3\xi_{1,1} = 0, d_2\xi_{1,3} - d_3\xi_{1,2} = 0$.

However, in order to prove that $d_2\xi_{0,3}-d_3\xi_{0,2}=0$ or equivalently that $d_2W_3-d_3W_2=0$, the previous procedure cannot work but we must never forget that U,V_2,V_3,W_2,W_3 both belong to $j_2(\Omega)$. Introducing the formal Lie derivative $R=L(\xi_1)\rho$, we recall that:

$$W_2=-\frac{2r^3A}{3m}R_{01,12}+\frac{1}{3}\Omega_{02},\quad W_3=-\frac{2r^3A}{3m}R_{01,13}+\frac{1}{3}\Omega_{03}$$

Hence, linearizing the *Bianchi identity*:

$$\nabla_1\rho_{01,23}+\nabla_2\rho_{01,31}+\nabla_3\rho_{01,12}=0\Rightarrow d_1R_{01,23}+d_2R_{01,31}+d_3R_{01,12}+\cdots=0$$

we have proved in ([4]) that the third order CC $d_2W_3-d_3W_2=0$ is not a generating one because it is just a differential consequence of the second order CC $R_{01,23}=0$.

Finally, as already noticed, the symbol $g_1'\subset g_1\subset T^*\otimes T$ is not involutive and even 2-acyclic because otherwise there should only be first order CC for the right members defining the system $R_1'\subset J_1(T)$. As a byproduct, we have, at least on the symbol level, the second order CC:

$$d_{22}\xi_{3,3}+d_{33}\xi_{2,2}-d_{23}\left(\xi_{3,2}+\xi_{2,3}\right)=0$$

and thus:

$$d_{22}\left(\frac{1}{2}\Omega_{33}-rA\sin^2(\theta)\xi_1-\sin(\theta)\cos(\theta)\xi_2\right)$$
$$+d_{33}\left(\frac{1}{2}\Omega_{22}-rA\xi_1\right)-d_{23}\left(\Omega_{23}+2\cot(\theta)\xi_3\right)=0$$

containing surely $d_{22}\xi_1,d_{22}\xi_2,d_{33}\xi_1,d_{23}\xi_3$ and thus surely d_2U,d_2V_2,d_3V_3, producing therefore a third order CC that cannot be reduced by means of any Bianchi identity, that is we finally have 15 generating second order CC and 4 new generating third order CC, in a manner absolutely similar to that of all the motivating examples of this paper.

As shown in ([4]), the study of the Killing system for the Kerr metric is even more difficult because the space of solutions is reduced from 4 already given to the 2 infinitesimal generators $\{\partial_t,\partial_\phi\}$ only. Accordingly, we discover that the Schwarzschild and the Kerr metrics do behave quite differently and *there is thus no hope at all for selecting specific solutions of the Einstein equations in vacuum*. We consider this result as a key challenge when questioning the origin and existence of gravitational waves in general relativity and believe this problem has never been pointed out clearly for the very simple reason that the underlying mathematics are not known by physicists.

EXAMPLE 2.2 REVISITED:

Coming back to the system $R_2'=R_2^{(2)}\subset R_2$ with a strict inclusion and second members $\left(u,v,w=u_{33}-v_{12}-x^2u_1\right)$, let us exchange x^1 with x^2 in order to have an involutive third order symbol g_3' in δ-regular coordinates and consider the system R_3' with now $w=u_{33}-v_{12}-x^1u_2$ in the new coordinates:

$$\left\{\begin{array}{ll} y_{333}-x^1y_{23}=v_3 & 1\ 2\ 3 \\ y_{233}-x^1y_{22}=v_2 & 1\ 2\ \bullet \\ y_{223}=w_3 & 1\ 2\ \bullet \\ y_{222}=w_2 & 1\ 2\ \bullet \\ y_{133}-x^1y_{12}=v_1 & 1\ \bullet\ \bullet \\ y_{123}=u_3 & 1\ \bullet\ \bullet \\ y_{122}=u_2 & 1\ \bullet\ \bullet \\ y_{112}=u_1 & 1\ \bullet\ \bullet \\ y_{33}-x^1y_2=v & \bullet\ \bullet\ \bullet \\ y_{22}=w & \bullet\ \bullet\ \bullet \\ y_{12}=u & \bullet\ \bullet\ \bullet \end{array}\right.$$

This new system is easily seen to be involutive and we have $3+8+9=20$ first order CC if we consider the second members as just simple notations. Substituting and taking now into account that we have in fact $u_2=d_2u$ formally and so on, all these CC reduce to identities to zero of the form $0=0$ but, using again the original coordinates, $A\equiv w_2-u_1=0, A_2=0, A_3=0, B\equiv w_{33}-v_{11}-x^2w_1=0$, a system which is *not* FI. Accordingly, the generating CC are described by A of order 3 and B of order 4 with $A_{33}-x^2A_1-B_2=0$. I remain to check that this result is coherent with the diagrams of the previous section.

For this, we let the reader compute by hands or with computer algebra the following dimensions $dim(R_2)=1+3+4=8$,
$dim(R_3)=dim(J_3(E))-dim(J_1(F_0))=12$ because there is no CC of order 1,
$dim(R_4)=15$
$\Rightarrow dim(Q_2)=dim(R_4)-dim(J_4(E))+dim(J_2(F_0))=15-35+20=0$ because there is no CC of order 2, $dim(R_5)=17$
$\Rightarrow dim(Q_3)=dim(R_5)-dim(J_5(E))+dim(J_3(F_0))=17-56+40=1$ because there is only 1 CC of order 3. We have therefore the long sequence:

$$0\to R_6\to J_6(E)\to J_4(F_0)\to J_1(Q_2)\to 0$$

$$0\to 19\to 84\to 70\to 4\to 0$$

and obtain $dim(H(J_4(F_0)))=(70-4)-(84-19)=66-65=1$ both with $dim(Q_4)=5$, in a coherent way with the only CC A of order 3. We let the reader prove that we have similarly $dim(Q_5)=13$ by taking into account the fact that $B_2=A_{33}-x^2A_1$. In order to take into account the existence of a new generating CC of order 4, we let the reader check that $dim(Q_4)=5$ and set $F_1=Q_4$ in order to define a fourth order operator $\mathcal{D}_1:F_0\to F_1$ by the involutive system:

$$\left\{\begin{array}{ll} B\equiv u_{3333}+\cdots=0 & 1\ 2\ 3 \\ A_3\equiv u_{2333}+\cdots=0 & 1\ 2\ \bullet \\ A_2\equiv u_{2233}+\cdots=0 & 1\ 2\ \bullet \\ A_1\equiv u_{1233}+\cdots=0 & 1\ \bullet\ \bullet \\ A\equiv u_{233}+\cdots=0 & \bullet\ \bullet\ \bullet \end{array}\right.$$

Starting anew from this operator, we obtain the first order involutive system:

$$\begin{cases} d_3A_3 - x^2A_1 - B_2 = 0 \\ d_3A_2 - d_2A_3 = 0 \\ d_3A_1 - d_1A_3 = 0 \\ d_3A - A_3 = 0 \\ d_2A_1 - d_1A_2 = 0 \\ d_2A - A_2 = 0 \\ d_1A - A_1 = 0 \end{cases} \begin{array}{|ccc|} \hline 1 & 2 & 3 \\ 1 & 2 & 3 \\ 1 & 2 & 3 \\ 1 & 2 & 3 \\ 1 & 2 & \bullet \\ 1 & 2 & \bullet \\ 1 & \bullet & \bullet \\ \hline \end{array} \Rightarrow \begin{array}{|ccc|} \hline 1 & 2 & 3 \\ 1 & 2 & 3 \\ 1 & 2 & 3 \\ 1 & 2 & \bullet \\ \hline \end{array} \Rightarrow \boxed{1\ 2\ 3}$$

where each Janet tabular is induced from the preceding one till the end of the procedure as in ([12], p 153, 154 for details). We also notice that this system brings *automatically* the Spencer operator.

We obtain therefore the following differential sequence:

$$0 \to \Theta \to E \xrightarrow[2]{\mathcal{D}} F_0 \xrightarrow[4]{\mathcal{D}_1} F_1 \xrightarrow[1]{\mathcal{D}_2} F_2 \xrightarrow[1]{\mathcal{D}_3} F_3 \xrightarrow[1]{\mathcal{D}_4} F_4 \to 0$$

$$0 \to \Theta \to 1 \xrightarrow[2]{} 2 \xrightarrow[4]{} 5 \xrightarrow[1]{} 7 \xrightarrow[1]{} 4 \xrightarrow[1]{} 1 \to 0$$

which is formally exact on the jet level, even if it is not strictly exact because the first operator is not FI, and we check that $1-2+5-7+4-1=0$. We notice that the part between F_0 and F_4 is typically a Janet sequence for $\mathcal{D}_1$.

It follows that we have the following long exact sequence on the level of jets, $\forall r \geq -5$:

$$0 \to R_{r+9} \to J_{r+9}(E) \to J_{r+7}(F_0) \to J_{r+3}(F_1) \to J_{r+2}(F_2)$$
$$\to J_{r+1}(F_3) \to J_r(F_4) \to 0$$

a result leading to:

$$\begin{aligned} dim(R_{r+9}) &= 1(r+10)(r+11)(r+12)/6 - 2(r+8)(r+9)(r+10)/6 \\ &\quad + 5(r+4)(r+5)(r+6)/6 - 7(r+3)(r+4)(r+5)/6 \\ &\quad + 4(r+2)(r+3)(r+4)/6 - 1(r+1)(r+2)(r+3)/6 \\ &= 2r+25 \end{aligned}$$

and thus to $dim(R_{r+4}) = 2r+15, \forall r \geq 0$, a result not evident to grasp at first sight because it comes from the lack of formal integrability of R_2 and the strict inclusion $R_2^{(2)} \subset R_2$.

EXAMPLE 2.3 REVISITED:

Coming back to the systems R_2 with second members (u,v) and $R_2' = R_2^{(2)} \subset R_2$ with a strict inclusion and second members $(u,v,2w = u_{33} - v_{22} - x^2u_1)$, let us exchange x^1 with x^2 in order to have an involutive third order symbol g_3' in δ-regular coordinates but the system R_3', with now $w = u_{33} - v_{12} - x^1u_2$ in the new coordinates, is *not* FI. Hence, we must start anew with the system $R_2'' = R_2^{(4)} \subset R_2'$ with a strict inclusion, described by the 4 PD equations:

$$\begin{cases} y_{33} - x^2y_1 = v \\ y_{22} = u \\ y_{12} = w \\ y_{11} = \omega \end{cases}$$

where $2\omega = u_{3333} - v_{2233} - 2x^2 u_{133} + x^2 v_{122} - 2v_{12} + \left(x^2\right)^2 u_{11}$. Using one prolongation, we get the third order PD equations:

$$\left\{\begin{array}{ll} y_{333} - x^2 y_{13} = v_3 & 1\ 2\ 3 \\ y_{233} - y_1 = v_2 + x^2 w & 1\ 2\ \bullet \\ y_{223} = u_3 & 1\ 2\ \bullet \\ y_{222} = u_2 & 1\ 2\ \bullet \\ y_{133} = v_1 + x^2 \omega & 1\ \bullet\ \bullet \\ y_{123} = w_3 & 1\ \bullet\ \bullet \\ y_{122} = u_1 = w_2 \Rightarrow A & 1\ \bullet\ \bullet \\ y_{113} = \omega_3 & 1\ \bullet\ \bullet \\ y_{112} = w_1 = \omega_2 \Rightarrow B & 1\ \bullet\ \bullet \\ y_{111} = \omega_1 & 1\ \bullet\ \bullet \end{array}\right.$$

and we discover that the symbol g_2'' is finite type because $g_3'' = 0$. As we had to use one prolongation in order to get a 2-acyclic symbol, we obtain *sixth* order CC $(A, B, C) \in j_2(u, v, w, \omega)$. We refer the reader to ([10], p 315) or ([13], p 83) for more details on this delicate result.

Using the notations of the last section, we now provide the systems B_2, B_3, B_4, B_5, B_6 together and we notice the following striking results:

$$B_2 = J_2(F_0), B_3 \subset \rho_1(B_2) \subset J_3(F_0), B_4 = \rho_1(B_3) \subset J_4(F_0),$$

$$B_5 = \rho_1(B_4) \subset J_5(F_0), B_6 \subset \rho_1(B_5) \subset J_6(F_0)$$

reaching therefore the following involutive system of order 6 where we did not quote $B = 0$ because we already proved that $B = A_{33} - x^2 A_1$:

$$\left\{\begin{array}{ll} C \equiv u_{333333} + \cdots = 0 & 1\ 2\ 3 \\ A_{333} \equiv u_{233333} + \cdots = 0 & 1\ 2\ \bullet \\ A_{233} \equiv u_{223333} + \cdots = 0 & 1\ 2\ \bullet \\ A_{223} \equiv u_{222333} + \cdots = 0 & 1\ 2\ \bullet \\ A_{222} \equiv u_{222233} + \cdots = 0 & 1\ 2\ \bullet \\ A_{133} \equiv u_{123333} + \cdots = 0 & 1\ \bullet\ \bullet \\ A_{123} \equiv u_{122333} + \cdots = 0 & 1\ \bullet\ \bullet \\ A_{122} \equiv u_{122233} + \cdots = 0 & 1\ \bullet\ \bullet \\ A_{113} \equiv u_{112333} + \cdots = 0 & 1\ \bullet\ \bullet \\ A_{112} \equiv u_{112233} + \cdots = 0 & 1\ \bullet\ \bullet \\ A_{111} \equiv u_{111233} + \cdots = 0 & 1\ \bullet\ \bullet \\ A_{33} \equiv u_{23333} + \cdots = 0 & \bullet\ \bullet\ \bullet \\ A_{23} \equiv u_{22333} + \cdots = 0 & \bullet\ \bullet\ \bullet \\ A_{22} \equiv u_{22233} + \cdots = 0 & \bullet\ \bullet\ \bullet \\ A_{13} \equiv u_{12333} + \cdots = 0 & \bullet\ \bullet\ \bullet \\ A_{12} \equiv u_{12233} + \cdots = 0 & \bullet\ \bullet\ \bullet \\ A_{11} \equiv u_{11233} + \cdots = 0 & \bullet\ \bullet\ \bullet \\ A_3 \equiv u_{2333} + \cdots = 0 & \bullet\ \bullet\ \bullet \\ A_2 \equiv u_{2233} + \cdots = 0 & \bullet\ \bullet\ \bullet \\ A_1 \equiv u_{1233} + \cdots = 0 & \bullet\ \bullet\ \bullet \\ A \equiv u_{233} + \cdots = 0 & \bullet\ \bullet\ \bullet \end{array}\right.$$

Starting anew from this operator providing 46 CC, we obtain the first order involutive system:

$$\left\{\begin{array}{l} d_3A_{333}-2x^2A_{133}+\left(x^2\right)^2A_{11}-C_2=0 \\ d_3A_{233}-d_2A_{333}=0 \\ d_3A_{223}-d_2A_{233}=0 \\ d_3A_{222}-d_2A_{223}=0 \\ \quad\vdots \\ d_3A_1-d_1A_3=0 \\ d_3A-A_3=0 \\ d_2A_{133}-d_1A_{233}=0 \\ \quad\vdots \\ d_2A_1-d_1A_2=0 \\ d_2A-A_2=0 \\ d_1A_{33}-A_{133}=0 \\ \quad\vdots \\ d_1A_1-A_{11}=0 \\ d_1A-A_1=0 \end{array}\right. \quad \begin{array}{|ccc|} \hline 1&2&3\\ 1&2&3\\ 1&2&3\\ 1&2&3\\ \vdots&\vdots&\vdots\\ 1&2&3\\ 1&2&3\\ 1&2&\bullet\\ \vdots&\vdots&\vdots\\ 1&2&\bullet\\ 1&2&\bullet\\ 1&\bullet&\bullet\\ \vdots&\vdots&\vdots\\ 1&\bullet&\bullet\\ 1&\bullet&\bullet\\ \hline \end{array}$$

with 20 equations of class 3, 16 equations of class 2 and 10 equations of class 1. There are 36 CC providing an involutive system with 26 equations of class 3, 10 equations of classs 2 but no equation of class 1. We get a final system of 10 CC of class 3 without any CC. Like in the preceding application, we have thus obtained the following formally exact sequence:

$$0\to\Theta\to E\xrightarrow[2]{\mathcal{D}}F_0\xrightarrow[6]{\mathcal{D}_1}F_1\xrightarrow[1]{\mathcal{D}_2}F_2\xrightarrow[1]{\mathcal{D}_3}F_3\xrightarrow[1]{\mathcal{D}_4}F_4\to 0$$

$$0\to\Theta\to 1\xrightarrow[2]{}2\xrightarrow[6]{}21\xrightarrow[1]{}46\xrightarrow[1]{}36\xrightarrow[1]{}10\to 0$$

with $1-2+21-46+36-10=0$, a part of it being a Janet sequence as before. Similarly, we get:

$$\begin{aligned} dim\left(R_{r+11}\right) &= 1(r+12)(r+13)(r+14)/6-2(r+10)(r+11)(r+12)/6 \\ &\quad +21(r+4)(r+5)(r+6)/6-46(r+3)(r+4)(r+5)/6 \\ &\quad +36(r+2)(r+5)(r+6)/6-10(r+1)(r+2)(r+3)/6 \\ &= 18 \end{aligned}$$

or even $dim\left(R_{r+6}\right)=18,\forall r\geq 0$ as a striking result indeed that can be checked directly through the exact sequences:

$$0\to R_8\to J_8(E)\to J_6(F_0)\to F_1\to 0$$

$$0\to 18\to 165\to 168\to 21\to 0$$

$$\cdots$$

$$0\to R_6\to J_6(E)\to J_4(F_0)\to Q_4\to 0$$

$$0\to 18\to 84\to 70\to 4\to 0$$

$$0\to R_5\to J_5(E)\to J_3(F_0)\to Q_3\to 0$$

$$0\to 17\to 56\to 40\to 1\to 0$$

and comes from the fact that $dim_K(R)=6<\infty$ or, equivalently, $dim_K(M)=6<\infty$.

The reader not familiar with the formal theory of differential systems or modules may be surprised by the fact the two dimensions just found do not coincide at all because $6<18$. However, we have indeed $dim(R_3'')=dim(R_2'')=dim(R_2^{(4)})=6$ and the exact sequence:

$$0\to g_4\to R_4\to R_3\to R_3/R_3^{(1)}\to 0$$

$$0\to 4\to 15\to 12\to 1\to 0 \quad\Rightarrow\quad dim(R_3^{(1)})=12-1=11$$

showing that $dim(R_3^{(1)})<dim(R_3)<dim(R_4)$ with $11<12<15$. However, we have the general Theorem 2.A.7 in ([20]) providing the useful *prolongation/projection* (PP) procedure, namely that we have $\rho_r(R_q^{(1)})=R_{q+r}^{(1)},\forall r\geq 0$ whenever the symbol g_q of R_q is 2-acyclic. In the present case, we have indeed $\rho_r(R_3^{(1)})=R_{r+3}^{(1)},\forall r\geq 0$ because g_3 is known to be involutive, and the final system $R_3^{(4)}$ is involutive with zero symbol, providing $R_2^{(4)}$ which is only FI but with dimension 6. This situation is quite tricky indeed because prolongations are filling up successively the PD equations of order 2, then 3 and so on, adding therefore:

$$\{y_{12}=0\},\{y_{123}=0,y_{122}=0,y_{112}=0\},\{y_{11}=0\},\{y_{113}=0,y_{112}=0,y_{113}=0\},\cdots$$

5. Conclusions

When a differential operator $\mathcal{D}$ of order q is given, the problem of finding its *compatibility conditions* (CC) is to look for a new operator $\mathcal{D}_1$ of a certain order s such that $\mathcal{D}_1\eta=0$ *must* be satisfied in order to be able to solve the inhomogeneous system $\mathcal{D}\xi=\eta$. This is an old problem first solved as a footnote by M. Janet in 1920 ([10] [11] [12] [17]) and finally studied by D.C. Spencer with collaborators around 1970 ([19] [20] [21]). The main idea is to construct a *finite length differential sequence* by repeating this procedure anew with $\mathcal{D}_1$ and so on till one eventually ends with $\mathcal{D}_n$ according to Janet when n is the number of independent variables. It soon became clear that constructing $\mathcal{D}_1$ is largely depending on various intrinsic properties of $\mathcal{D}$.

- If $\mathcal{D}$ is *involutive*, then $\mathcal{D}_1,\cdots,\mathcal{D}_n$ are first order involutive operators in the corresponding *Janet sequence* that can be constructed "*step by step*" as above but also "*as a whole*" like in the Poincaré sequence for the exterior derivative.
- If $\mathcal{D}$ is only *formally integrable* (FI), that is *all* the equations of order $q+r$ of the corresponding homogeneous system can be obtained by *only* r prolongations, then the order of $\mathcal{D}_1$ is $s+1$ when s is the smallest integer such that the symbol of order $q+s$ becomes 2-acyclic. Such a result is still not acknowledged today by physicists even though it is essential for studying the conformal Killing system of space-time in general relativity.
- If $\mathcal{D}$ is not even FI, not only the construction of $\mathcal{D}_1$ may become very difficult but also a *strange phenomenon* may appear, namely one can start to

find CC of order s_1, then no new CC other than the ones generated by *these* CC up to order $s_2 > s_1$ when *suddenly* new generating CC may appear, generating all the CC up to order $s_3 > s_2$ and so on till the procedure ends.

This delicate question has been recently raised by physicists in order to study the system of Killing equations for certain useful metrics solutions of the Einstein equations in vacuum (Minkowski gives $s = 2$ while Schwarzschild gives $s_1 = 2, s_2 = 3$). Needless to say that computer algebra is of quite a poor help in this case because the dimensions of the jet spaces and the size of the matrices involved (up to 420×460 for $r = 0$ in the last example) may increase drastically ([26]).

The aim of this paper has been first to provide illustrating examples of the above situations and one of them with $s_1 = 3, s_2 = 6$ seems to be the only one known in the literature today. In addition, we have solved the (general) generating problem by using new differential homological algebraic methods, with the hope that computer algebra will soon become of some help in a near future.

Conflicts of Interest

The author declares no conflicts of interest regarding the publication of this paper.

References

[1] Pommaret, J.-F. (2013) *Journal of Modern Physics*, **4**, 223-239. https://doi.org/10.4236/jmp.2013.48A022

[2] Pommaret, J.-F. (2017) *Journal of Modern Physics*, **8**, 2122-2158. https://doi.org/10.4236/jmp.2017.813130

[3] Pommaret, J.-F. (2018) New Mathematical Methods for Physics. NOVA Science Publisher, New York.

[4] Pommaret, J.-F. (2018) *Journal of Modern Physics*, **9**, 1970-2007. https://doi.org/10.4236/jmp.2018.910125 https://arxiv.org/abs/1805.11958v2

[5] Andersson, L. (2015) Spin Geometry and Conservation Laws in the Kerr Spacetime. https://arxiv.org/abs/1504.02069

[6] Shah, A.G., Whitting, B.F., Aksteiner, S., Andersson, L. and Bäckdahl, T. (2016) Gauge Invariant perturbation of Schwarzschild Spacetime. https://arxiv.org/abs/1611.08291

[7] Khavkine, I. (2017) *Journal of Geometry and Physics*, **113**, 131-169. https://arxiv.org/abs/1409.7212 https://doi.org/10.1016/j.geomphys.2016.06.009

[8] Aksteiner, S. and Bäckdahl, T. (2018) All Local Gauge Invariants for Perturbations of the Kerr Spacetime. https://arxiv.org/abs/1803.05341 https://doi.org/10.1103/PhysRevLett.121.051104

[9] Khavkine, I. (2018) Compatibility Complexes of Overdetermined PDEs of Finite Type, with Applications to the Killing Equations. https://arxiv.org/abs/1805.03751

[10] Pommaret, J.-F. (2001) Partial Differential Control Theory, Kluwer, Dordrecht (1000 p).

[11] Pommaret, J.-F. (1978) Systems of Partial Differential Equations and Lie Pseudogroups, Gordon and Breach, New York. Russian Translation: MIR, Moscow, 1983.

[12] Pommaret, J.-F. (1994) Partial Differential Equations and Group Theory. Kluwer. https://doi.org/10.1007/978-94-017-2539-2

[13] Pommaret, J.-F. (2016) Deformation Theory of Algebraic and Geometric Structures. Lambert Academic Publisher (LAP), Saarbrucken, Germany. https://arxiv.org/abs/1207.1964

[14] Cartan, E. and Einstein, A. (1979) Letters on Absolute Parallelism. Princeton University Press, Princeton.

[15] Kashiwara, M. (1995) Algebraic Study of Systems of Partial Differential Equations, Mémoires de la Société Mathématique de France 63 (Transl. from Japanese of His 1970 Master's Thesis).

[16] Schneiders, J.-P. (1994) *Bulletin de la Societe Royale des Sciences de Liege*, **63**, 223-295.

[17] Janet, M. (1920) *Journal de Mathématiques*, **8**, 65-151.

[18] Pommaret, J.-F. (2013) *Multidimensional Systems and Signal Processing*, **26**, 405-437. https://doi.org/10.1007/s11045-013-0265-0

[19] Spencer, D.C. (1965) *Bulletin of the American Mathematical Society*, **75**, 1-114.

[20] Goldschmidt, H. (1968) *Annales scientifiques de l'École normale supérieure*, **4**, 417-444. https://doi.org/10.24033/asens.1168

[21] Goldschmidt, H. (1968) *Annales scientifiques de l'École normale supérieure*, **4**, 617-625. https://doi.org/10.24033/asens.1173

[22] Northcott, D.G. (1966) An Introduction to Homological Algebra. Cambridge University Press, Cambridge.

[23] Rotman, J.J. (1979) An Introduction to Homological Algebra, Pure and Applied Mathematics. Academic Press, Cambridge.

[24] Macaulay, F.S. (1916) The Algebraic Theory of Modular Systems, Cambridge.

[25] Pommaret, J.-F. (1988) Lie Pseudogroups and Mechanics. Gordon and Breach, New York.

[26] Quadrat, A. and Robertz, R. (2014) *Acta Applicandae Mathematicae*, **133**, 187-234. https://hal-supelec.archives-ouvertes.fr/hal-00925533 https://doi.org/10.1007/s10440-013-9864-x

Journal of Modern Physics, 2019, 10, 402-421
http://www.scirp.org/journal/jmp
ISSN Online: 2153-120X
ISSN Print: 2153-1196

Quantization of Hubble's Law and the Emergence of Classical Localization in a Quantum World

G. R. Harp

SETI Institute, Mountain View, CA, USA
Email: gerryharp@gmail.com

How to cite this paper: Harp, G.R. (2019) Quantization of Hubble's Law and the Emergence of Classical Localization in a Quantum World. *Journal of Modern Physics*, **10**, 402-421.
https://doi.org/10.4236/jmp.2019.103026

Received: January 28, 2019
Accepted: March 16, 2019
Published: March 19, 2019

Abstract

We apply a canonical transformation Hubble's law to turn it into a quantum equation and derive its solutions in a homogenous universe (assumptions analogous to the FLRW universe). The eigenfunctions of Hubble's law are also stationary states (eigenfunctions of the Hamiltonian). The study of these solutions reveals many striking results, including: 1) By enforcing boundary conditions at the cosmic horizon, we derive a fundamental lower limit to the uncertainty in any rest mass (or measurement thereof) $\delta m_{\min} = 2\pi H_0 \hbar^2 c^{-2}$. This implies a lower limit also to the mean particle mass which we call the mass quantum $\bar{m}_H \equiv \delta m_{\min}/2 = 5.1\times 10^{-68}$ kg. 2) We postulate that particles with finite mass can be regarded as a composition of a large number of mass quanta and deduce a relation between mass uncertainty δm_0 and mass m_0: $\delta m_0 \doteq \sqrt{m_0/\bar{m}_H}\,\delta m$. 3) This uncertainty leads naturally to localization of the composite mass, with the radius of localization proportional to the inverse square root of mass $r_{loc} = \sqrt{\pi\hbar\left(m_0 H_0\right)^{-1}}$. We associate this localization with the classical localization of a massive particle. 4) We derive an expression for the critical mass where there is a crossover from quantum behavior to classical behavior $m_{\text{crossover}} = (16/9)^{1/5}\,\pi\rho^{2/5}\hbar^{3/5}H_0^{-3/5}$, where ρ is the material mass density. The classical sizes derived in 4) are consistent with empirical results for our universe. We note the theory described here has no free parameters, hence it points to a new fundamental equation of the universe, essentially defining the mass quantum. It is a pure quantum theory that does not invoke general relativity at any stage, and the derivation uses mathematics accessible to an upper level undergraduate student in physics.

Keywords

Quantum Cosmology, Hubbles Law, Canonical Quantization, Quantum Theory

1. Introduction

Why do ordinary objects appear to follow classical space-time trajectories but very small objects follow quantum (wavelike) trajectories? Here we derive a quantitative theory that provides one answer to this question. Generally, this paper is motivated by topics of great current interest at the very foundations of physics: Is quantum theory (QT) applicable not only at microscopic length scales but also at large, even cosmological length scales? Does the expansion of the universe have any implications for microscopic particles?

Regarding length scale, in a recent review article [1] Legget writes, "as pointed out by Schrödinger in 1935 in his famous 'cat' paper [2], there is no good reason to accept (the) division of the world into a microscopic regime where QT reigns and a macroscopic one governed by classical physics." On the other hand, [3] reminds us, "it is safe to state, in any case, that quantum superpositions of truly massive, complex objects are *terra incognita*". Whether or not QT prevails at all length scales is now a topic of intense interest, motivating experimental tests of quantum mechanics at mesoscopic scales [1] [3] [4] [5]. In this paper, we take the rule that QT applies at all length scales as a premise of the theory.

Whether or not the Hubble expansion has an impact at microscopic scales is another area of controversy. According to Nobelist Leon Lederman, "The expansion of the universe doesn't actually affect the spaces between particles. The universe's expansion is not a force that will rip particles, molecules, or even objects apart [6]." Meanwhile, theories of "phantom energy" predict precisely the opposite [7]. This paper takes the latter view as a premise of the theory, which we paraphrase, in a universe where the Hubble parameter $H_0 > 0$, the stationary states of all massive free particles are modified compared to stationary states in flat space $(H_0 = 0)$. Some other works assuming cosmological expansion affecting quantum systems are found in [8] [9] [10]. Outside the domain of general relativity, C. L. Herzenberg has developed a theory that predicts classical localization from the universe' expansion [11] [12]. The mechanism of Herzenberg's theory is unrelated to the theory presented here.

The single-particle theory presented here approximates a more general quantum field theory whose derivation we leave for the future. We consider spin-zero bosons and quasi-particles on any length scale, from elementary Higgs bosons, to composite bosons such as the ground state ^{1}H atom, to very large spin zero quasiparticles such as nonrotating stars.

Another important feature is what this theory leaves out. This is a pure quantum theory that makes no reference to General Relativity (GR) or even the concept of gravity. Again, we view this work as an approximation of a complete theory

including GR that can be addressed in future work. We emphasize that our theory does not change or overturn GR; it simply ignores it. At first this might appear to be inconsistent with our use of Hubble's natural law in the derivation. But Hubble's law (redshift increases with distance) is an empirical result from astronomical observations, and its validity is independent of whatever theory is used to explain it. We are therefore justified in our use of Hubble's law without reference to gravity. However, we shall sometimes borrow colloquial terminology from GR (e.g. "flat space") when it improves flow and creates no ambiguities.

To the best of our knowledge, this derivation of free particle states in expanding space is new. To make this paper accessible to the widest possible audience, we try to keep the mathematics and framework as simple as possible. This single-particle derivation is accessible to the student with only an undergraduate level understanding of QT[1] and avoids potential conflicts between QT and GR as those theories are known to be incompatible.

A unique feature of this derivation is how the stationary states are derived by enforcing consistency with observational evidence, without resorting to Hamiltonian or Lagrangian mechanics. As we shall see, this is a useful trick since we do not know how to model expanding space with an exact pseudo-potential energy function. Instead, the results of our theory permit derivation of an exact pseudopotential that, when applied to flat space, results in the same stationary states as for an expanding universe.

Outline of the Rest of the Paper

In Section 2, we apply the canonical substitutions to turn Hubble's law into a quantum operator equation, and then present its eigenfunctions. We follow a straightforward path to determination of the time part of the wavefunctions, their energies and momenta. For example, we find that two co-moving observers may measure different values for the energy and momentum for the same particle. We then show the correspondence between our stationary states and the stationary states in flat space, *i.e.* plane waves.

In part 3, we apply the boundary condition that the wavefunctions must vanish at the cosmic horizon. This boundary condition places a lower limit on the uncertainty of the particle rest mass, and implies the existence of a mass quantum, which is the smallest particle rest mass allowed by the theory. The mass quantum and its uncertainty point to a simple method to estimate the mass uncertainty δm_0 for an arbitrary rest mass m_0. We see how the mass uncertainty leads to a natural localization of the particle, which we identify with (a lower limit to) the classical localization of the particle. For macroscopic objects, localization radii are very small compared to the object size, and so their trajectories take on classical behavior. For convenience of reference we call this new theory, "localization theory".

[1]Besides new physics, we suggest that this derivation is a topic suitable for undergraduate or graduate courses in QT as an example of how to bring one of the major principles of cosmology into QT.

We derive an expression for the critical mass where we predict a crossover from quantum behavior to classical behavior, and it depends on material density. These results are in broad agreement with the observed universe.

In the discussion section, we show the close relationship between localization theory and the very successful theory of quantum decoherence as competing explanations for classical localization. We note that in the non-relativistic regime, our results agree with a particular version of decoherence theory called "spontaneous quantum collapse."

Finally, we consider how localization theory may impact gravitational attraction and measurements of the gravitational constant G in some limiting situations. Here and at various points in the paper we make predictions for the outcomes of a variety of real experiments that could support or conflict with the theory. The main part of the paper ends with some concluding remarks.

We move several of the less critical sections of the derivation into appendices. In Appendix 2, we list a set of criticisms of the derivation and provide some initial responses. We consider normalization, completeness and orthogonality of our wavefunctions. In Appendix 3 we outline the derivation of a pseudopotential that can be used in flat space calculations which has stationary states have the same form as those in expanding space.

Appendix 1 presents an alternative derivation for the value of the mass quantum that takes a very different approach than that in the main text. The coarse agreement between the two derivations lends further support to our conclusion that the classical localization arises from the finite size and finite age of our universe.

2. Quantization of Hubble's Law

Hubble's natural law, $\boldsymbol{v}(\boldsymbol{r}) = H_0\boldsymbol{r}$, is an interpretation consistent with electromagnetic observations of distant galaxies. It states that distant bodies are receding from any observer with a radial velocity equal to the distance of separation multiplied by the Hubble constant H_0 (neglecting proper motion). Although H_0 is known to vary slowly with time, we approximate it with a constant $H_0 = 2.2\times10^{-18}$ Hz (except in Appendix 1). To describe the expansion of the universe, this paper uses only Hubble's natural law, and does not appeal to the theory of general relativity (GR).

To begin, we consider finite set of noninteracting classical test particles[2] (mass density~0, temperature = 0, pressure = 0) in a large empty void between galaxies.[3] The condition for a stationary particle configuration is evidently: If each test particle p has an inwardly directed velocity

$$\boldsymbol{v}_p = -H_0\boldsymbol{r}_p, \tag{1}$$

[2]Test particles have such small mass that the gravitational influence of those particles can be neglected. For a cloud of test particles, we require that the cloud's density is small enough so that the gravitational effect of the particle swarm is also negligibly small.

[3]Although we do not refer to general relativity, our assumptions are quite similar to those for a Friedmann-Lemaître-Robertson-Walker Universe. We shall ignore any the gravitational effects caused by inhomogeneities in the rest of the mass in the universe.

then the Hubble expansion is cancelled exactly and the particle configuration is time independent. This condition for stationarity is key to the derivation that follows.

We quantize Equation (1) for a single particle (instead of a set) with arbitrary rest mass m_0, where it's probability density is spread out over a large region in the void. The vector $\boldsymbol{r}_p$ is now interpreted as the center of mass position for the wavefunction. We multiply through Equation (1) by the relativistic mass γm_0 (Lorentz factor $\gamma^{-1} \equiv \sqrt{1-v^2c^{-2}}$) and rearrange to obtain

$$0 = \boldsymbol{p}_r + \gamma H_0 m_0 \boldsymbol{r}. \tag{2}$$

where $\boldsymbol{r} \to \left(\boldsymbol{r} - \boldsymbol{r}_p\right)$.

We make the canonical substitution $\boldsymbol{p}_r = -i\hbar\nabla_r$, and multiply on the right by the particle wavefunction $\Psi(r,t)$ to obtain the quantum equivalent of Equation (2)

$$0 = \left[-i\hbar\nabla_r + \frac{\gamma m_0 H_0 r}{\hbar}\right]\Psi(r,t) = \left[-i\hbar\nabla_r + \frac{m_0 c}{\hbar}\frac{H_0 c^{-1} r}{\sqrt{1-\left(H_0 c^{-1} r\right)^2}}\right]\Psi(r,t) \tag{3}$$

In (3) we have put the particle center of mass at the origin ($\boldsymbol{r}_p = 0$) and replaced the velocity in γ using Equation (1). Equation (3) is the quantum version of Hubble's law, and it is consistent with special relativity.

2.1. Solution

Equation (3) is a first-order differential equation. It was constructed using the assumption that its solutions are stationary states, which implies that the wavefunction is separable and for some time-independent function $\omega(\boldsymbol{r})$

$$\Psi(r,t) = \mathrm{e}^{-i\omega(r)t}\psi(r). \tag{4}$$

Our path to Equation (4) is novel because at no point did we employ Hamiltonian mechanics. Direct substitution into Equation (3) verifies the solution

$$\psi(r) = A\mathrm{e}^{-i\phi}\exp\left[i\frac{m_0 c r_H}{\hbar}\left(1-\frac{r^2}{r_H^2}\right)^{1/2}\right] \tag{5}$$

where the Hubble distance $r_H \equiv H_0^{-1}c$ and the normalization constant $A = \sqrt{3r_H^{-3}}$. For convenience, we set the global phase offset $\phi = m_0 c r_H \hbar^{-1}$ so that the wavefunction is real at $r = 0$. To be a stationary state we must choose the positive value of the square root for $\left(1-r^2/r_H^2\right)^{1/2}$. Put another way, there is no solution where the momentum points away from the origin. That there is no sign ambiguity arises directly from the fact that Equation (3) is a *first-order* differential equation.

The distance r_H is also called the "cosmic horizon," because classical particles beyond this distance are moving with speed greater than *c*, hence may have no interaction with a particle centered at the origin. The cosmic horizon is a dividing line between two regions of the wavefunction. Inside the horizon the wavefunction has the expected form of an oscillating exponential (**Figure 1(a)**, blue

solid). As $r \to r_H$, the particle momentum tends to infinity. This does not imply that the wavefunction undergoes an infinite number of phase cycles while approaching the horizon, as is evident in Figure 1(a). Instead, the total number of phase cycles $N_{\text{cycles}} \equiv m_0 c r_H \left(2\pi\hbar\right)^{-1}$ executed between $0 \le r \le r_H$ is a finite number proportional to the rest mass. For a hydrogen atom, $N_{\text{cycles,H atom}} = 1.0 \times 10^{41}$.

In Figure 1(b), our analysis shows the surprising fact that a quantum particle can tunnel a short distance beyond the cosmic horizon with an evanescent decay. In the evanescent region the particle has imaginary velocity, while a classical particle in the same region would have a velocity greater than the speed of light.

In section 3 we deal with the momentum singularity at $r \to r_H$ by requiring the wavefunction vanishes at the cosmic horizon and in the evanescent region. However, under certain extreme initial conditions at the time of the big bang, the evanescent solution could be nonzero. For the sake of conciseness, we do not consider such cases here.

2.2. Energies of Stationary States

For an observer at any position $\boldsymbol{r}$, the stationary state of a particle centered at

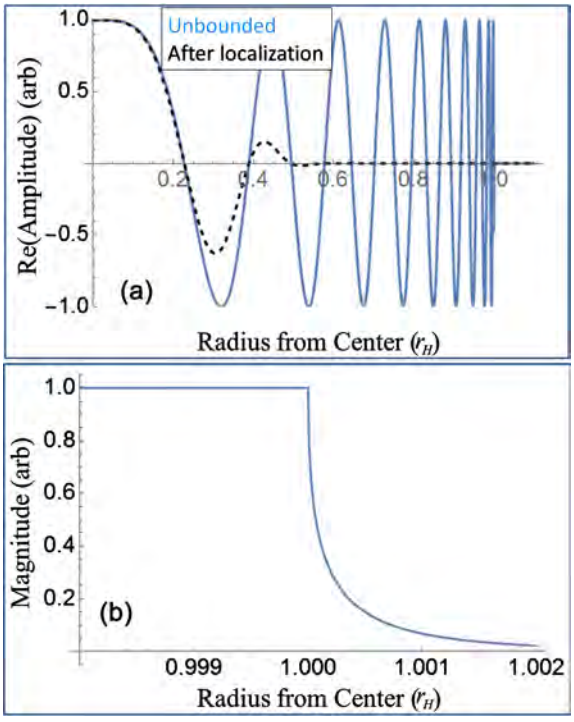

Figure 1. Example plots of the real part of the amplitude (a)-blue solid line and magnitude (b)-blue solid line of Equation (5). The horizontal axis is plotted in units of r_H. These plots assume a tiny particle mass with $\left(m_0 c r_H \hbar^{-1}\right) = 60$. The black dashed line in (a) shows the corresponding wavefunction after application of boundary conditions. The boundary conditions require the wavefunction to be localized at the origin, as discussed in Section 3.

$\boldsymbol{r}_p$ including time dependence is, from Equation (4)

$$\Psi(\boldsymbol{r},t) \equiv \psi(\boldsymbol{r}-\boldsymbol{r}_p)\mathrm{e}^{-i\omega(\boldsymbol{r}-\boldsymbol{r}_p)t}. \tag{6}$$

We now compute the value of ω that is consistent with our spatial wavefunctions. Einstein's equation from Special Relativity (SR) states

$$\hbar^2\omega^2(\boldsymbol{r}-\boldsymbol{r}_p) = m_0^2c^4 + \hbar^2k^2(\boldsymbol{r}-\boldsymbol{r}_p). \tag{7}$$

where the expression for the momentum $\hbar\boldsymbol{k}$ can be read directly from Equation (3)

$$k(\boldsymbol{r}-\boldsymbol{r}_p) = \frac{m_0c}{\hbar}\frac{(\boldsymbol{r}-\boldsymbol{r}_p)/r_H}{\sqrt{1-\left(|\boldsymbol{r}-\boldsymbol{r}_p|/r_H\right)^2}}. \tag{8}$$

It is important to notice that SR is a local theory, and Equation (7) applies only if the energy, momentum, and mass are measured at the same space-time position or event. In flat space, stationary states have the same momentum everywhere, and all observers measure the same particle energy. Here, the stationary states have a momentum ($\hbar\boldsymbol{k} = \hbar\boldsymbol{k}(\boldsymbol{r})$) that varies depending on the observer's relative position. The same is true for the energy. For example, consider the stationary state $\Psi(r,t)$ with both the particle and the observer at $r=0$. Here $k(r\to 0)=0$ and we recover the Compton frequency

$$\omega(r\to 0) = \frac{m_0c^2}{\hbar} \tag{9}$$

We consider a second observer at distance r' with zero velocity relative to the first.[4] the second observer measures a different energy:

$$\omega(r') = \frac{m_0c^2}{\hbar}\sqrt{1+\frac{\hbar}{m_0^2c^2}k(r')^2}. \tag{10}$$

This leads to an important result of this paper: though the states $\Psi(r<r_H,t)$ are stationary by construction hence have a *time-independent* energy, their apparent energy depends on observer position even for co-moving observers. A similar result is obtained in the classical case and the position dependence of energy derives from the locality of SR and not specifically from QT.

2.3. Comparison to Free Particle States in Flat Space

In flat space vacuum, the stationary states are plane waves

$$\psi_{PW}(\boldsymbol{r},t) \propto \exp\left[i\boldsymbol{k}\cdot\boldsymbol{r} - i\omega t\right]. \tag{11}$$

In this section we compare and draw analogies between these and our stationary states $\Psi(\boldsymbol{r},t)$ for expanding space. Firstly, both ψ_{PW} and Ψ oscillate periodically with time (*c.f.* Equation (4)), everywhere. In this section we approximate $\Psi(r,t)$ in a small region with extent $a \ll r_H$, and see that $\Psi(r,t)$

[4]The zero-velocity condition is defined by and can be checked by the two observers through the exchange of a laser beam with known frequency. Zero velocity implies the laser has the same photon energy for both observers.

reduces to the form of a plane wave.

Consider a cubical volume of space with side a and centered at the position $\boldsymbol{r}_0$. The distance a is assumed to be but small compared to r_H: $0 < a \ll r_H$. We define the offset coordinate $\delta\boldsymbol{r} = \boldsymbol{r} - \boldsymbol{r}_0$ with $0 \le \delta r \le a$. Substituting into Equation (8), expanding in a Taylor's series about $\delta\boldsymbol{r} = 0$, and keeping only the lowest order term in $\delta\boldsymbol{r}$ we find

$$\boldsymbol{k}(\boldsymbol{r}_0) \cong \frac{m_0 c}{\hbar} \frac{\boldsymbol{r}_0 / r_H}{\sqrt{1-(\boldsymbol{r}_0 / r_H)^2}}. \tag{12}$$

Equation (12) is *independent of observer position* within the cube and defines a 1:1 correspondence between the stationary states $\Psi(\boldsymbol{r},t)$ in expanding space and $\psi_{PW}(\boldsymbol{r},t)$ in flat space; the former converges to the latter as $H_0 \to 0$.

Equation (12) is helpful for applications where we wish to propagate a given initial state forward in time. Suppose at $t = 0$ we are given an arbitrary wavefunction $\phi(r,0)$ with support only a local region of space. To propagate this wavefunction forward in time, we perform the following transformations at $t = 0$:

$$\begin{aligned} \phi(\boldsymbol{r},0) = \int_{-\infty}^{\infty} \tilde{\phi}(\boldsymbol{k}) \mathrm{e}^{i\boldsymbol{k}\cdot\boldsymbol{r}} \mathrm{d}\boldsymbol{k} &\xrightarrow{k_{PW} \to k(r_0)} \int_{-\infty}^{\infty} \tilde{\phi}(\boldsymbol{k}(\boldsymbol{r}_0)) \mathrm{e}^{i\boldsymbol{k}(r_0)\cdot\boldsymbol{r}} \mathrm{d}\boldsymbol{k} \\ &\xrightarrow{\mathrm{e}^{ikr} \to \psi(r)} \int_{r_0=0}^{r_H} \tilde{\phi}(\boldsymbol{r}_0) \Psi(\boldsymbol{r} - \boldsymbol{r}_0, 0) \mathrm{d}\boldsymbol{r}_0 \end{aligned}. \tag{13}$$

The expansion on the right hand side can be propagated forward using the time dependence in Equation (6). Notice that this transformation takes an integral over momentum space and replaces it will an integral over real space. This is possible because there is a 1:1 correspondence between a specific momentum in flat space and the position of the center of mass in expanding space.

3. The Emergence of Spontaneous Localization

3.1. Quantization of Mass Uncertainty $\sigma_{\min}$

The crucial element to complete this theory is to apply the boundary condition that the wavefunction must go to zero at the cosmic horizon. This condition is satisfied in the usual way: by constructing linear combinations of the unbounded wavefunctions that have the desired property. For example, the wavefunctions for a particle in a box are constructed by combining pairs of oppositely directed travelling waves into standing waves, enforcing nodes at the box edges.

Similarly, we demand that $\Psi(\boldsymbol{r},t)$ must go to zero at the cosmic horizon. If this were not the case, then an observer approaching the cosmic horizon (from the inside) would measure a divergent momentum and energy, $p, E \to \infty$.[5] The behavior of the unbounded states Equation (5) at the cosmic horizon ($r \to r_H$)

[5]This assumption is equivalent to enforcing a soft upper limit to particle kinetic energy. This is exactly what is observed for the most energetic particles (i.e. cosmic rays) in our universe. Although other processes such as scattering from cosmic microwave background photons place even more stringent limits on the maximum observed kinetic energy.

gives

$$\psi\left(r \to r_H\right) = A\mathrm{e}^{-i\phi} = A\exp\left[-\frac{m_0 c r_H}{\hbar}\right] \tag{14}$$

The only non-constant factor in the exponential is the rest mass. Thus, an integral over a range of rest masses achieves our boundary condition

$$\psi\left(r, m_0\right) \to \int_0^\infty a(m)\psi(r, m)\mathrm{d}m, \tag{15}$$

where $a(m)$ represents the particle probability distribution as a function of rest mass. Because the mean rest mass $\bar{m}_0$ of elementary particles are fixed, for such particles we infer that $a(m)$ has a strong narrow peak at $m = m_0$. For the sake of this discussion, the detailed functional form of $a(m)$ is important to the exact value of δm result within a factor of order 1, and this factor is not important for the main conclusions of this paper. As an example we choose $a(m)$ to be a top hat function centered at m_0 and having width δm:

$$a(m) = \frac{1}{\delta m} \quad \text{for } \left[\left(m_0 - \delta m/2\right) < m < \left(m_0 + \delta m/2\right)\right], \tag{16}$$

and zero otherwise. Putting (16) into (15) and setting the result equal to zero at the cosmic horizon we obtain a quantization condition on the distribution parameter δm

$$\delta m = \frac{2\pi\hbar}{c r_H} n, \quad n = 1, 2, 3, \cdots \tag{17}$$

which has a minimum value $\delta m_{\min}$ when $n = 1$. Later we will need the standard deviation of the distribution in (16), which is easily computed: $\sigma_{\min} \equiv \sqrt{1/12}\,\delta m_{\min}$.

3.2. The Mass Quantum $\bar{m}_H$ and Its Uncertainty

Because the universe has finite extent, Equation (17) shows that the mass distribution width is $\delta m_{\min}$. This does not necessarily imply that the actual rest mass is quantized, as postulated below. But it does imply that no mass may be smaller than a minimum $\bar{m}_H$, dependent on the Hubble parameter. If we try to create a particle with nominal zero mass, its mass is still uniformly distributed over the range $\delta m_{\min}$, and the mean value of the smallest mass is

$$\bar{m}_H \equiv \delta m_{\min}/2 = \frac{\pi\hbar H_0}{c^2} = 5.1\times10^{-68}\ \mathrm{kg} \tag{18}$$

We shall call $\bar{m}_H$ the mass quantum and identify its "uncertainty" with the standard deviation $\sigma_H = \sqrt{1/12}\delta m_{\min} = 3^{-1/2}\bar{m}_H$. *This is perhaps the most important result of this paper.*

To further motivate the concept of a minimum mass, we turn to a semiclassical argument based on quantization of angular momentum. Consider a classical particle with relativistic mass $\gamma m_0 \equiv m_{SR}$ executing circular motion with radius $r_{\max}$. We set the angular momentum of this particle equal to the minimum, Planck's value: $m_{SR} v r_{\max} = h$. Given the maximum velocity is c, the minimum

value of the mass is $m_{SR,\min} = h\left(cr_{\max}\right)^{-1}$. Letting $r_{\max} \to r_H$, we recover Equation (18) to within a factor of two. This argument reinforces the result of Equation (17). We see that the two ingredients for the existence of a mass quantum are 1) the quantization of angular momentum and 2) that the accessible universe has finite volume.

3.3. Uncertainty in Larger Masses

In the next step, we introduce a new theory postulate:

Postulate: every mass m_0 and its uncertainty can be modeled as the superposition of many mass quanta and their uncertainties.

We do not propose that particles are composed of many very small particles, only that mass is quantized. However, because the quanta are bosons, there is no conflict with multiple quanta residing in the same place at the same time.

We model any mass m_0 as a superposition of $m_0/\bar{m}_H$ individual quanta all with the same center of mass. What uncertainty is associated with m_0? To model uncertainty, we treat the mass of any individual quantum m_q as a random variable uniformly distributed in the range ($0 \le m_q \le \delta m_{\min}$) with mean value $\bar{m}_H$. The central limit theorem [13] then provides an estimate of the uncertainty in m_0 [6]

$$\sigma_{m_0} = \sqrt{N_{quanta}}\,\sigma_H = 3^{-1/2}\sqrt{m_0\,\bar{m}_H}\,. \tag{19}$$

When $N_{quanta} \gg 1$, the central limit theorem also gives us the shape of the probability distribution around the nominal mass m_0,

$$P_{m_0}(m) \propto \pi^{-1/2} \exp\left[-\left(m-m_0\right)^2 \Big/ \sigma_{m_0}^2\right] \tag{20}$$

Equations (19) and (20) are another important result. They derive from the postulate that large masses can be treated as a superposition of mass quanta with known uncertainty.

3.4. Greater Localization for Larger Uncertainties

Because the value of σ_H is inversely proportional to the maximum allowed (Hubble) radius r_H, it may be intuited that masses with larger uncertainty will be confined to smaller radii, hence smaller volumes. Inverting Equation (17) and replacing $\delta m \to \sqrt{12}\sigma$, the radius of localization r_{loc} for a mass m_0 takes a particularly simple form[7]

[6]We note that for Equation (19) to be consistent with Equation (17), the number of quanta must be a perfect square, $N_{quanta} = n^2$, where n is an integer. This has no practical significance because ordinary masses are comprised of a very large number of quanta so a nearby perfect square value will always be well within the mass uncertainty.

[7]It is notable that Herzenberg (Herzenberg 2006, 2009) derived a very similar localization distance with the same functional form as presented here:

$$r_{loc,\text{Herzenberg}} \approx \sqrt{\frac{\pi\hbar}{2m_0 H_0}},$$

despite the fact that Herzenberg used a derivation quite distinct from ours. This "coincidence" may be explained, since the geometry of expanding space is essentially the same in both papers.

$$r_{loc}(m_0) \equiv \frac{2\pi\hbar}{\sqrt{12}\sigma_{m_0} c} = \sqrt{\frac{\pi\hbar}{m_0 H_0}} \tag{21}$$

As expected, the localization radius becomes infinite as $H_0 \to 0$, and it is inversely proportional to the square root of the rest mass. This means that the particle wavefunction is confined to a volume $\Omega(m_0)$ approximately equal to that of a sphere with radius r_{loc}: $\Omega(m_0) \cong \frac{4}{3}\pi r_{loc}^3$. Below, we identify $\Omega(m_0)$ with the classical localization volume of macroscopic particles, from raindrops to stars. An example of the wavefunction post localization is found in Figure 1(a), indicated by a black dashed curve. To reveal the localization behavior in more detail, Figure 2 plots the envelope function multiplying the wavefunction in Figure 1 after the boundary condition has been met.

Statement (21) is quite general, and can be recovered exactly by reversing the derivation leading to Equation (17). *Equation* (21) *has no free parameters*, meaning that if it does not approximate observed reality, then the only option is to abandon it. There is no ambiguity. Comparisons of r_{loc} (column 5) and estimates of the classical radius (column 4) for representative masses are given in Table 1.

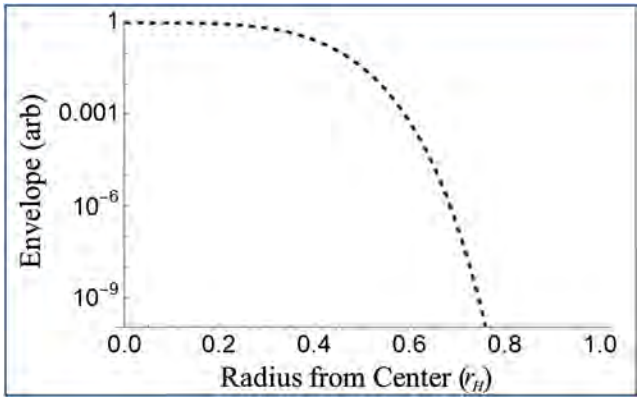

Figure 2. Plot of the enveloping function that multiplies the wavefunction in Figure 1 after localization has been applied. The curve at small radius has a Gaussian-like shape.

Table 1. Estimates of the classical radius and localization parameter r_{Loc} for various (elementary or composite) bosons.

Particle type	Mass m_0 (kg)	Density (kg/m^3)	Classical Radius (meters)	r_{Loc} in steady-state universe $H_0 = 2.2\times10^{-18}$ s (meters)
Mass quantum $\bar{m}_H \equiv \frac{\pi\hbar H_0}{c^2}$	5.1×10^{-68}	-	-	1.4×10^{26}
"Dark matter particle" see text	3×10^{-58}	-	-	(200,000 LY) 1.9×10^{21}
Hydrogen atom	1.67×10^{-27}	-	-	750,000
Higgs boson	2.2×10^{-25}	-	-	65,000
Mass for $r_{loc} = 1$ cm (Lead)	9.5×10^{-12}	11,340	5.8×10^{-7}	0.01
1 kg water	1	1000	0.062	3.08×10^{-8}
Total mass of universe	1.99×10^{30}	3×10^{-28}	7.0×10^{8}	2.2×10^{-23}

Assuming a spherical shape, we can invert Equation (21) to express the critical mass for crossover from quantum to classical behavior as a function of the material density ρ

$$m_{0,\text{crossover}} = (16/9)^{1/5} \pi \rho^{2/5} \hbar^{3/5} H_0^{-3/5} \tag{22}$$

The values of critical mass for a variety of materials are shown in Table 2.

4. Discussion and Conclusions

Ask a physicist about the size of an atom and she would probably describe the boundaries of the diffuse electron cloud surrounding the nucleus. But this is only half of the story. From another perspective, the atom is a point-like composite particle whose center of mass is described by another, different wavefunction. To obtain a complete description of the spatial distribution of just one of the bound electrons, we must convolve the atom's center of mass wavefunction with the internal wavefunction of the electron about the nucleus. This paper focuses on the often-neglected center of mass wavefunction, specifically for a point-like composite boson with arbitrary mass.

This theory offers one explanation for why large objects appear to be perpetually localized in space. At this point we take a step back and consider the successes of localization theory.

We have quantized Hubble's law and computed the stationary state wavefunctions in a steady-state universe that obeys Hubble's law. We characterized those states for their position-dependent momentum and energy. We show how the limits of a finite universe give rise to a fundamental uncertainty in particle masses. We make quantitative predictions about spontaneous localization of massive particles which we associate with classical localization. We perform these tasks with a pure quantum theory that does not rely on general relativity. Localization theory is purely based on standard quantum mechanics and has no free parameters.

In further support of our theory that mass is quantized, we offer a second derivation of the mass quantum based on the Heisenberg uncertainty principle (Appendix 1).

Table 2. Estimates of the critical mass and critical radius for various materials. The critical mass is crossover point from quantum behavior (for smaller mass) and classical behavior (for larger mass).

Material	Mass m_0 (kg)	Density (kg/m^3)	Classical Radius (meters)	r_{loc} in steady-state universe $H_0 = 2.2\times10^{-18}$ (meters)
Critical mass for average density of universe	1.7×10^{-20}	3×10^{-28}	350	350
Critical mass for Air	1.86×10^{-9}	1.225	1.04×10^{-3}	1.04×10^{-3}
Critical mass for a Styrofoam ball	8.20×10^{-9}	50	5×10^{-4}	5×10^{-4}
Critical mass for interstellar dust grain (amorphous SiO_2)	3.59×10^{-8}	2000	2.4×10^{-4}	2.4×10^{-4}
Critical mass for neutron star density	0.01	10^{17}	4×10^{-7}	4×10^{-7}

As an aside, we note the existence of a pseudopotential in flat space that reproduces the same stationary states as described here (outline of derivation presented in Appendix 3).

4.1. Consistency with Decoherence Theories of Spontaneous Quantum Collapse

The physical problem of classical localization in a quantum world has long been recognized as demonstrating an incompleteness of quantum theory. Most physicists would agree that the best current theory for classical localization comes from decoherence theory. Decoherence has been described as resulting from the inter-connectedness of all matter in the universe through the fundamental forces. No particle can ever be considered completely isolated, as illustrated by Zeh in [14] p. 27. "*Borel* (*Borel* 1914, *pp.* 27-35) *showed long ago that even the gravitational effect resulting from shifting a small piece of rock as distant as Sirius by a few centimeters would completely change the microscopic state of a gas in a vessel here on earth within seconds after the retarded field of force had arrived*."

Connectedness means that the Hamiltonian of any subsystem expressed in terms of subsystem coordinates (q, p), also depends on the actual state of the entire universe or environment. That is, $H_{\text{subsystem}} \to H_{\text{subsystem}}\left(q, p; q_{env}(t), p_{env}(t)\right)$, after Joos in [14] p. 35. It is as if the system under study is constantly perturbed by collisions with a large number of very small virtual particles such as gravitons [15], generated by the finite temperature of the quantum vacuum state.

Some theories of spontaneous wavefunction collapse [16] address connectedness by adding a space- and time-dependent random factor to the Hamiltonian. We argue that the model presented here is consistent with such models, albeit with a different interpretation. We begin with a generalized Hamiltonian including spontaneous collapse

$$H_{\text{General}}\left(q_i, p_i, t\right) \approx H_{\text{subsystem}}\left(q_{sub}, p_{sub}, t\right) + T_{env}\left(q_{env}, p_{env}, t\right) \tag{23}$$

where T_{env} represents random perturbations in space and time. Averaging over many position and time realizations, we may replace T_{env} with its expectation value $\left\langle T_{env}(q, p, t)\right\rangle$. Assuming these perturbations δE_T are small and linear, it is reasonable to assume their probability distribution [14] [17]

$$P\left(\delta E_T\right) \approx \exp\left[-t^2/\sigma_t\right] \times \prod_i \exp\left[-q_i^2/\sigma_{q_i}^2\right] \propto \pi^{-1/2} \exp\left[-\delta E_T^2/\sigma_{E_T}^2\right] \tag{24}$$

In our localization theory, we find that the particle rest mass has an intrinsic uncertainty which can be described with additive term describing the distribution of possible rest masses (20). In the non-relativistic case these distributions have the same form as Equation (24) (referencing Equation (20)):

$$P\left(\delta E_T\right) \propto P_{m_0}\left(mc^2\right) \tag{25}$$

and the distributions remain similar even at relativistic energies. *We conclude that in* (*some*) *decoherence theories of spontaneous collapse, the full Hamilto-*

nian including system and environment will induce particle localization essentially indistinguishable from that of localization theory presented here.

While spontaneous collapse theory and the present theory can give rise to almost indistinguishable results, they derive from very different physics. The present theory has no free parameters while decoherence theory is adjusted to fit reality by careful choice of the free parameter σ_{E_T} (Equation (24)). Decoherence theory does not yet have a model to predict σ_{E_T} from first principles.

The present theory assumes a steady-state universe and does not address the very real mystery of wavefunction collapse. Conversely, spontaneous collapse theories presume that wavefunction collapse is the chief ingredient for particle localization.

Although the interpretation is different, we emphasize that our theory in no way invalidates the results of decoherence theory; the two theories can be made to be consistent. With the acceptance of our localization theory, the vast literature and most if not all the deductions of decoherence theory remain viable.

4.2. Blurring of Gravity

In a more speculative vein, we consider the potential effects of localization theory on gravitational interactions. Some theories of quantum gravity begin by assuming that a mass whose wavefunction is dispersed in space can be treated by classical general relativity with a continuous mass spatial distribution proportional to the probability density of the wavefunction. Not all theories include this assumption, but it seems like a reasonable place to start.

For small particles, localization theory also assumes a dispersed center of mass wavefunction with the localization radius of Equation (21). Consulting Table 1 for a solitary hydrogen atom isolated in vacuum, we predict its center of mass wavefunction is dispersed over a region ~10^6 meters in diameter. If this estimate is correct, then we expect the gravitational force between two hydrogen atoms to be essentially nil at microscopic distances. Hence the question, "what is the gravitational contribution to the binding energy of an isolated H_2 molecule in vacuum?" is answered by "none at all." The gravity from a hydrogen atom can be approximated as that of a point particle only at distances greater than the radius of localization.

Indeed, suppose a scientist wishes to repeat Cavendish's measurement of the gravitational constant G using a tiny torsion balance and very small lead spheres, of order 1 micron in diameter. In Table 1 we see that the sphere's radius of localization on the order of 1 centimeter. Thus, in very sensitive measurements where the spheres are separated by distances less than 1 cm, the apparent value of G will be substantially smaller than its accepted value. Thus, localization theory makes a quantitative prediction of reduced gravitational attraction for very small separations which can, in principle, be compared with laboratory observations.

4.3. Final Remarks

This paper finds that classical localization of large masses is a direct result of the

expansion of space and is inversely related to the Hubble constant. This means that in a flat universe ($H_0 = 0$) classical localization does not occur, in conflict with the predictions of decoherence theory. Localization theory and decoherence theory may both be true at once, but contemplation of this difference may lead to experiments that distinguish the two theories.

The original impetus for our development of localization theory was the intuition that Hubble expansion must have some detectable effect on the interaction between microscopic particles. We were further motivated by the intuitive conviction that quantum theory (QT) applies even to large "particles" like planets, and there should be a detectable effects of ordinary QT even over cosmological distances.

In a lighthearted closing, we note that localization theory may have something to say about dark matter. Observations show that dark matter tends to be confined on galactic scales, say 200,000 light years. If this confinement were explained by localization theory, it is possible to estimate the mass of a typical "dark matter particle," and we do this in Table 1. The mass of such a small particle is on the order of 10^{-58} kg.

Acknowledgements

The author gratefully acknowledges Stu Pilorz, Laurance Dolye, and David Carico for many useful discussions and critiques.

Conflicts of Interest

The author declares no conflicts of interest regarding the publication of this paper.

References

[1] Legget, A.J. (2008) *Rep Prog Phys*, **71**.

[2] Schrödinger, E. (1935) *Naturwissenschaften*, **23**, 807-812. https://doi.org/10.1007/BF01491891

[3] Arndt, M. and Hornberger, K. (2014) *Nature Physics*, **10**, 271.

[4] Kurizki, G., Bertet, P., Kubo, Y., Mølmer, K., Petrosyan, D., Rabl, P. and Schmiedmayer, J. (2015) *Proceedings of National Academy of Sciences of the United States of America*, **112**, 3866-3873. https://doi.org/10.1073/pnas.1419326112

[5] Robens, C., Alt, W., Meschede, D., Emary, C., Alberti, A., Physik, A., Bonn, U. and Bonn, D. (2015) *Physical Review X*, **5**, 011003. https://doi.org/10.1103/PhysRevX.5.011003

[6] https://van.physics.illinois.edu/qa/listing.php?id=1120

[7] Caldwell, R.R., Kamionkowski, M. and Weinberg, N.N. (2003) *Physical Review Letters*, **91**, 071301. https://doi.org/10.1103/PhysRevLett.91.071301

[8] Bonnor, W.B. (1996) *Monthly Notices of the Royal Astronomical Society*, **282**, 1467-1469. https://doi.org/10.1093/mnras/282.4.1467

[9] Bonnor, W.B. (1999) *Classical and Quantum Gravity*, **16**, 1313. https://doi.org/10.1088/0264-9381/16/4/020

[10] Carrera, M. and Giulini, D. (2010) *Reviews of Modern Physics*, **82**, 169.

https://doi.org/10.1103/RevModPhys.82.169

[11] Herzenberg, C.L. (2006) *Physics Essays*, **19**, 634-637. https://doi.org/10.4006/1.3028869

[12] Herzenberg, C.L. (2009) ArXiv:0912.1158 1.

[13] Billingsley, P. (1995) Probability and Measure. Third Edition, John Wiley & Sons, Inc., Hoboken, 357.

[14] Giulini, D.J.W., Joos, E., Kiefer, C., Kupsch, J., Stamatescu, I.-O. and Zeh, H.D. (2013) Decoherence and the Appearance of a Classical World in Quantum Theory. 2nd Edition, Springer, Berlin.

[15] Melkikh, A.V.A. (2013) ArXiv Prepr. 1311.0205, 1.

[16] Bassi, A., Lochan, K., Satin, S., Singh, T.P. and Ulbricht, H. (2013) *Reviews of Modern Physics*, **85**, 471. https://doi.org/10.1103/RevModPhys.85.471

[17] Joos, E. (2013) Decoherence and the Appearance of a Classical World in Quantum Theory. In: Giulini, D.J.W., Joos, E., Kiefer, C., Kupsch, J., Stamatescu, I.-O. and Zeh, H.D., Eds., 2nd ed., Springer, Berlin, 35-136.

Appendix 1: Alternative Derivation/Extension of the Steady-State Theory to a Dynamic Universe

A1. Mass Uncertainty Based on Duration of Measurement

In very precise mass measurements, the energy-time uncertainty principle plays an important role. We consider a thought experiment where a scientist with a perfect scale wishes to weigh (find mass of) a single muon[8]. After placing the muon and releasing the scale, she must wait a finite time for the scale to settle, and the accuracy of her measurement improves with increasing wait time. Even a perfect scale can never display the exact particle mass in a finite amount of time, because of Heisenberg's uncertainty principle for time and energy, usually expressed as $\Delta E \Delta t \geq \hbar/2$. Since rest energy is proportional to mass, we may write

$$\sigma_{\min} \Delta t \geq \frac{\hbar}{2c^2} \approx 5.87 \times 10^{-52} \text{ kg} \cdot \text{s} \tag{26}$$

Equation (25) is relevant to our thought experiment because the muon is unstable and spontaneously decays into lighter particles with an average lifetime of 2.2 μs. As she pursues higher accuracy, Equation (25) and muon decay places a fundamental limit on the uncertainty in her measurement; in this case $\sigma_\mu m_\mu^{-1} \approx 1.4 \times 10^{-18}$. Even idealized mass measurements of single muons will show statistical fluctuations about the nominal muon mass with an uncertainty of σ_μ. A simplistic interpretation of the uncertainty is that muons come in a random distribution of different mass values centered on the mean value.

This argument applies at all mass scales, from elementary particles to planets. Because no particle has ever existed longer than the age of the universe (T = thirteen point eight billion years), Equation (25) predicts that no particle mass may have an uncertainty smaller than $\sigma_{\min} = 1.3 \times 10^{-69}$ kg. This is a lower limit for the mass indeterminacy since Equation (25) is an inequality.

In the theory of the main text, we computed the minimum mass uncertainty to be $\sigma_H = 2.94 \times 10^{-68}$ kg. In other words, the uncertainty σ_H is indeed larger than the lower limit set by the uncertainty principle, by a factor of 22. We consider this level of agreement to be a success, and the result from the uncertainty principle supports the result from localization theory.

A2. Model of a Dynamic Universe

A still better estimate of $\sigma_{\min}$ is derived for the dynamic universe in **Figure 3**. We model the dynamic universe as a homogeneous spherical region bounded on all sides by the comic horizon. This horizon is expanding at the speed of light and within its bounds the Hubble parameter is time dependent $H_0 \to H\left(t = T_0\right)$. The origin of the time axis is taken to be the time of the big bang and T_0 refers to the current epoch.

In the real universe, the value of the mass quantum might depend on the un-

[8]The fact that the muon is a Fermion has no relevance to this part of the discussion. The accepted muon mass is 1.88×10^{-18} kg.

iverse' peculiar expansion history. However, we model the passage of time as a Markov chain of events, where the observed properties at time t depend only on the properties at the time t' immediately preceding t. Since the separation between t and t' is infinitesimal, our model assumes that the current states of matter can be predicted using only current physics and current values of physical constants and their time derivatives. The Markov assumption is justified by its common usage in most domains of physics including pure quantum field theory and all classical physics.

Our perspective is that the dynamic properties of the universe can be modeled *as if* it was a linear extrapolation of current dynamics. Figure 3 makes a schematic comparison of our models of the steady-state and dynamic universe. In our dynamic universe, the Hubble parameter is equal to the inverse of the effective age of the universe; $H\left(T_0+\Delta t\right)=\left(T_0+\Delta t\right)^{-1}$.

The time derivative of the Hubble parameter is only one part in 10^{-18} per second. We assume that this may be neglected over short periods of time, and the wavefunctions describing matter in the dynamic universe can be well approximated by the wavefunctions of the steady-state universe (Equations (4) and (5)), except with a time-dependent Hubble parameter. This permits us to carry over most of the results of the steady state theory.

Using $H_0=T_0^{-1}$ we may rewrite Equation (26)

$$\sigma_{\min}\geq\frac{\hbar H_0}{2c^2} \tag{27}$$

And with the replacement $\sigma_{\min}\to\sigma_H$, we write down the equation for the localization radius, $r_{loc,dynamic}$ corresponding to Equation (21)

$$r_{loc,dynamic}\left(m_0,T_0\right)\leq\sqrt{\frac{4\pi^2\hbar}{m_0H_0}}\,. \tag{28}$$

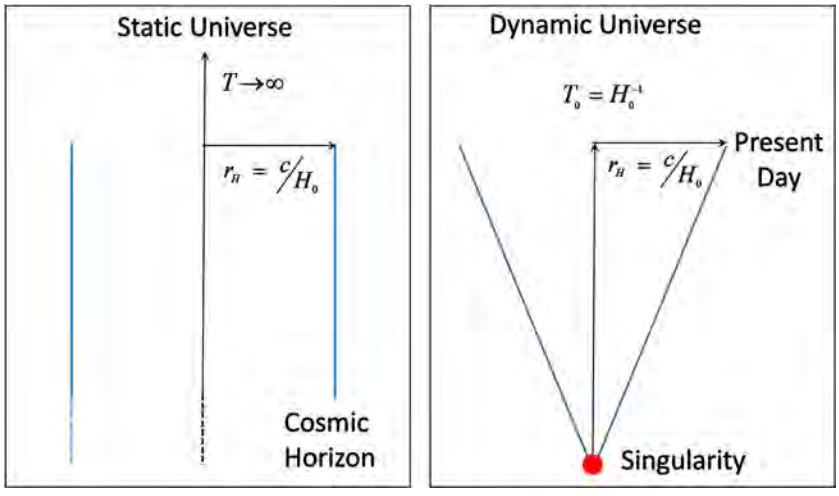

Figure 3. Schematic comparison of the two models of the universe discussed in this paper. On the left we have a steady-state universe where the cosmic horizon does not move with time. On the right, the universe comes into existence as a singularity and the cosmic horizon moves outward from that time at the speed of light.

The right hand side of Equation (27) is larger than the steady state localization radius by a factor of $\sqrt{4\pi}$. Since Equation (27) is an *inequality*, the results for the dynamic universe are entirely consistent with those of the steady-state universe. Therefore, Equation (27) provides further support for localization theory as derived in the main paper.

Appendix 2: Criticisms of the Derivation and Initial Responses

Single particle theory

This theory describes only isolated particles and the concept of multi-particle interactions is not addressed. A quantum field version of the theory may solve this problem. For now, it is at least plausible to approximate particle-particle gravitational interactions assuming the particles are localized to begin with (see 4.2).

Ambiguity in value of δm

We remind the reader that in Equation (17) the width of the mass distribution δm that satisfies the boundary condition is multi-valued, depending on the quantum number *n*. To estimate the minimum permitted mass, it is reasonable to choose the lowest quantum number $n=1$. But other values are permissible for δm and we ignore those solutions here. We note that with increasing quantum number, the value of δm becomes more and more dependent on the exact choice of mass distribution function $a(m)$, and such ambiguities are minimized when $n=1$.

Ambiguity between Hubble constant and age of universe

In our primary derivation, the universe is ageless, and localization derives from a nonzero Hubble constant. In our secondary derivation (Appendix 1), localization derives from the finite age of the universe. It is no coincidence that our dynamic universe' age is equal to H_0^{-1}, but even so there is an ambiguity about the origins of mass quantization for the two models. In the steady-state model, mass uncertainty is caused by spatial localization of particles within cosmic horizon. In the dynamic theory, mass uncertainty comes from time localization inferred from the singularity of the big bang. A more complete theory will combine both effects.

Choice of basis set for wavefunction expansion

We have chosen to express generic particle states with a Huygens-like basis set of spherically symmetric functions $\Psi(\boldsymbol{r}_{cm})$ with variable center of mass positions. We choose this basis for convenience of comparison with the $H_0=0$ plane wave states. However, direct integration shows that two functions $\Psi(\boldsymbol{r}_1)$ and $\Psi(\boldsymbol{r}_2)$ centered at different positions $\boldsymbol{r}_1 \neq \boldsymbol{r}_2$ are only approximately orthogonal.

A more natural basis would be a set of functions all centered at the same point and distinguished by three quantum numbers: $\Psi(n,l,m)=R_n(r)Y_l^m(\vartheta,\phi)$. The $Y_l^m(\vartheta,\phi)$ are spherical harmonics and the radial functions $R_n(r)$ are determined by boundary conditions. However correct this basis set may be, it is not so useful as a tool for understanding the stationary states. We leave the more exact derivation of a basis containing spherical harmonics to future work.

Use of Central Limit Theorem

The central limit theorem of statistics was derived for classical particles. Hence its application in Equation (19) relating to quantum particles may be dubious. We justify its use here based on an intuitive sense that it predicts the right behavioral trend, and in the end it provides a useful result that is consistent and explanatory for our universe. If nothing else, the comparison of theoretical predictions and experiments will either support or discredit our choice.

Wavefunction outside the cosmic horizon

Localization theory admits the possibility of a particle being detected at a point beyond the cosmic horizon r_H. Yet we focus only on particle states confined within the cosmic horizon and negligible amplitude outside. The form of the wavefunction beyond r_H derived from Equation (3) is given numerically by $A\mathrm{e}^{-3.67\times10^{102}m_0\sqrt{2\delta+\delta^2}}$ where δ is the radial distance beyond r_H. Even for the hydrogen atom, the e^{-1} decay distance is $4.7\times10^{-112}/m_0^2 = 1.7\times10^{-58}$ m, which can be compared to the localization radius of the total mass of the universe, which is much larger 2.2×10^{-23} m.

This provides some justification for neglecting the wavefunction outside, but the real particle distribution is entirely dependent on the initial conditions. These initial conditions were set at the moment of the big bang hence we know nothing about them. Thus, a fraction of the particles in the universe may lie outside (have support only outside) their own cosmic horizons. We intend to investigate this situation in a future paper, but we emphasize one key point. At the cosmic horizon, the wavefunction energy is infinite, and this acts as an impenetrable barrier for particles caught outside the horizon at $t=0$. No physical interaction can push a particle from outside to inside, or *vice versa*. Thus, outside particles comprise a different state of matter as compared with inside particles. We conjecture that the (strong force, weak force) interactions between outside particles and inside particles are highly constrained. Only electronic and gravitational interactions would not suffer this restriction.

Appendix 3: Modeling $H_0 > 0$ with an Effective Potential

With an expression for $\Psi(r,t)$ (Equations (4) and (5)), it is straightforward to derive an effective potential $V(r,t)$ for a particle in flat space that gives the same solution as $\Psi(r,t)$ when $H_0 > 0$. In flat space, the free states of a spin-zero boson are solutions of the Klein Gordon equation, to which we add a fictitious potential

$$\left[\left(i\hbar\frac{\partial}{\partial t}-V(r,t)\right)^2+\hbar^2c^2\left(r^{-2}\frac{\partial}{\partial r}r^2\frac{\partial}{\partial r}\right)-m_0^2c^4=0\right]\Psi(r,t). \tag{29}$$

Plugging the desired solution $\Psi(r,t)$ into Equation (29) gives a second-order differential equation containing only derivatives of $V(r,t)$, and where most of the terms are algebraic. This shows another advantage of our novel deduction of stationary states in expanding space: with an expression for the wavefunction, the derivation of effective potential is straightforward.

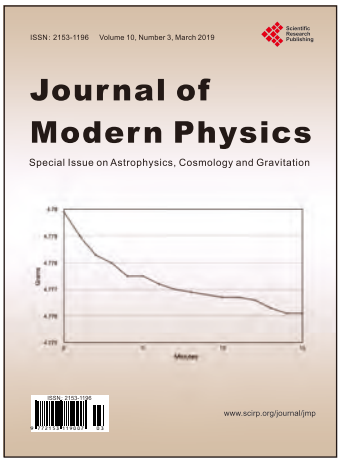

Call for Papers

Journal of Modern Physics

ISSN: 2153-1196 (Print) ISSN: 2153-120X (Online)
http://www.scirp.org/journal/jmp

Journal of Modern Physics **(JMP)** is an international journal dedicated to the latest advancement of modern physics. The goal of this journal is to provide a platform for scientists and academicians all over the world to promote, share, and discuss various new issues and developments in different areas of modern physics.

Editor-in-Chief

Prof. Yang-Hui He City University, UK

Subject Coverage

Journal of Modern Physics publishes original papers including but not limited to the following fields:

Biophysics and Medical Physics
Complex Systems Physics
Computational Physics
Condensed Matter Physics
Cosmology and Early Universe
Earth and Planetary Sciences
General Relativity
High Energy Astrophysics
High Energy/Accelerator Physics
Instrumentation and Measurement
Interdisciplinary Physics
Materials Sciences and Technology
Mathematical Physics
Mechanical Response of Solids and Structures
New Materials: Micro and Nano-Mechanics and Homogeneization
Non-Equilibrium Thermodynamics and Statistical Mechanics
Nuclear Science and Engineering
Optics
Physics of Nanostructures
Plasma Physics
Quantum Mechanical Developments
Quantum Theory
Relativistic Astrophysics
String Theory
Superconducting Physics
Theoretical High Energy Physics
Thermology

We are also interested in: 1) Short Reports—2-5 page papers where an author can either present an idea with theoretical background but has not yet completed the research needed for a complete paper or preliminary data; 2) Book Reviews—Comments and critiques.

Notes for Intending Authors

Submitted papers should not have been previously published nor be currently under consideration for publication elsewhere. Paper submission will be handled electronically through the website. All papers are refereed through a peer review process. For more details about the submissions, please access the website.

Website and E-Mail

http://www.scirp.org/journal/jmp **E-mail: jmp@scirp.org**

What is SCIRP?

Scientific Research Publishing (SCIRP) is one of the largest Open Access journal publishers. It is currently publishing more than 200 open access, online, peer-reviewed journals covering a wide range of academic disciplines. SCIRP serves the worldwide academic communities and contributes to the progress and application of science with its publication.

What is Open Access?

All original research papers published by SCIRP are made freely and permanently accessible online immediately upon publication. To be able to provide open access journals, SCIRP defrays operation costs from authors and subscription charges only for its printed version. Open access publishing allows an immediate, worldwide, barrier-free, open access to the full text of research papers, which is in the best interests of the scientific community.

- High visibility for maximum global exposure with open access publishing model
- Rigorous peer review of research papers
- Prompt faster publication with less cost
- Guaranteed targeted, multidisciplinary audience

Scientific Research Publishing

Website: http://www.scirp.org

Subscription: sub@scirp.org

Advertisement: service@scirp.org